

**Experience-Dependent Structural Rearrangements  
of Synaptic Connectivity  
in the Adult Central Nervous System**

**Inauguraldissertation**

zur

Erlangung der Würde eines Doktors der Philosophie

vorgelegt der

Philosophisch-Naturwissenschaftlichen Fakultät

der Universität Basel

von

**Nadine Gogolla**

aus Deutschland

Basel, 2007

Genehmigt von der Philosophisch-Naturwissenschaftlichen Fakultät

auf Antrag von

**PD. Dr. Pico Caroni**  
(Dissertationsleitung)

**Prof. Dr. Andreas Lüthi**  
(Korreferat)

**Prof. Dr. Silvia Arber**  
(Fakultätverantwortliche)

**Prof. Dr. Heinrich Reichert**  
(Vorsitz)

Basel, den 26. Juni 2007

**Prof. Dr. Hans-Peter Hauri**  
(Dekan)

## *Acknowledgements*

In the first place I would like to thank Pico Caroni for giving me the opportunity to do my PhD in his group and under his supervision. I thank you Pico, for sharing your enthusiasm for science with me, teaching me to see and to make me believe. Thank you for all the interesting, challenging and stimulating discussions. Your critique and support, as well as your keen mind were an invaluable aid to learn and to develop. I appreciate very much all your help and advice. Danke für alles, Pico.

I would like to thank Ivan Galimberti. Above all, for being a true friend to me and for the fun and happiness we shared at work and outside the lab. Your indestructible optimism and calmness helped me to overcome and forget the troubles and to enjoy the many happy moments. You made me see how going slow makes you advance fast. Grazie mille, Ivan, for just being as you are and for so much more.

I would like to thank the members of my thesis committee, Silvia Arber and Andreas Lüthi. Thank you for always being available, all the friendly and spontaneous support and your willingness to help, on the bench and in discussions.

Special thanks goes to ALL the members of the Caroni group, past and present, for the scientific discussions, help and input, but above all for the good time and the fun I had to work amongst you. Special thanks to Tami, Alex, Smita and Claudia, Ewa, Mike and Yuichi, as well as Sarah, Dominique, Lan and Kerstin.

I would like to thank Cyril Herry for his enthusiasm and investment in 'our' project, for teaching me so many things and for being my friend. I also thank Claudia Vittori. It was fun to work and discuss with you, Claudia, thanks for joining the lab and 'enriching' the cerebellum project. I am grateful to both of you for the nice time we had working together and discussing results and life.

I would like to thank many extraordinary and interesting people I met throughout my time at the FMI. I am grateful for the many friendly contacts that made the time I spent here such an enjoyable and rich experience.

Finally and most importantly, I would like to say thank you to my family and to Frédérique. Danke and merci! Your constant presence and love are the basis for the things I do.

## TABEL OF CONTENTS

<i>Abbreviations</i> .....	5
<b>1. INTRODUCTION</b>	
<i>Overview</i> .....	6
<b>1.1. Experience-dependent plasticity</b> .....	6
1.1.1. Potentiation and depression of synaptic strength .....	8
1.1.2. Key molecular pathways involved in plasticity .....	9
1.1.3. Structural plasticity .....	10
1.1.4. Impact of age on neuronal plasticity .....	12
1.1.5 The capacity to adapt is influenced by the life-style.....	15
<b>1.2. Hippocampus</b>	
1.2.1. The hippocampus as a model system to study neuronal circuit plasticity .....	16
1.2.2. Hippocampal functions .....	17
1.2.3. Anatomy of the hippocampus .....	19
1.2.4. Basic hippocampal circuits .....	21
1.2.5. The dentate gyrus and the mossy fiber pathway .....	21
<b>2. RESULTS</b>	
<b>2.1. Long-term rearrangements of hippocampal mossy fiber terminal connectivity in the adult regulated by experience</b> .....	24
2.1.1. Summary .....	25
2.1.2. Introduction .....	25
2.1.3. Results .....	29
2.1.4. Discussion .....	52
2.1.5. Acknowledgements .....	57
2.1.6. Experimental procedures .....	58
<b>3. SUPPLEMENTARY RESULTS</b>	
<b>3.1. Experience-dependent structural plasticity of neuronal circuit connectivity in the adult cerebellar cortex</b> .....	64
3.1.1. Summary .....	65
3.1.2. Introduction .....	65
3.1.3. Results .....	68
3.1.4. Discussion .....	79
3.1.5. Materials & Methods .....	82

<b>3.2. Wnt signaling regulates experience-related rearrangements of hippocampal mossy fiber terminal connectivity in the adult</b> .....	83
3.2.1. Summary .....	84
3.2.2. Introduction .....	84
3.2.3. Results .....	88
3.2.4. Discussion .....	103
3.2.5. Materials & Methods .....	107
<b>3.3. Lack of Rab3a affects mossy fiber terminal morphology but not experience-related rearrangements of their connectivity</b> .....	108
3.3.1. Summary .....	109
3.3.2. Introduction .....	109
3.3.3. Results .....	111
3.3.4. Discussion .....	117
3.3.5. Materials & Methods .....	120
<b>4. GENERAL DISCUSSION</b>	
<i>Overview</i> .....	121
4.1. Rewiring of neuronal circuits in the adult CNS .....	121
4.1.1 Learning versus life-style .....	122
4.1.2. Aging versus experience .....	122
4.1.3. Roles for Rab3a and Wnt in structural plasticity in the adult CNS.....	123
<i>Conclusion</i> .....	124
<b>5. SUPPLEMENTARY PROTOCOLS</b>	
5.1. Preparation of organotypic hippocampal slice cultures for long-term live imaging .....	125
5.2. Long-term live imaging of neuronal circuits in organotypic hippocampal slice cultures .....	145
5.3. Staining protocol for organotypic hippocampal slice cultures .....	156
<b>6. REFERENCES</b> .....	168
<i>Curriculum vitae</i> .....	190
<i>Erklärung</i> .....	192

## ***Abbreviations***

<b>AMPA</b>	$\alpha$ -amino-3-hydroxy-5-methyl-4-isoazolepropionic acid
<b>AMPA-R</b>	AMPA-receptor
<b>BDNF</b>	brain derived neurotrophic factor
<b>BIO</b>	6-bromoindirubin-3'-oxime (specific GSK3 $\beta$ inhibitor)
<b>CA</b>	corpus ammonis (hippocampal region)
<b>CNS</b>	central nervous system
<b>DG</b>	dentate gyrus (hippocampal region)
<b>DIV</b>	day in vitro
<b>Dvl</b>	Disheveled
<b>EE</b>	enriched environment
<b>Fz</b>	Frizzled receptor
<b>GABA</b>	$\gamma$ -amino butyric acid
<b>GC</b>	granule cell
<b>GSK3<math>\beta</math></b>	glycogen synthase kinase 3 beta
<b>KO</b>	knock-out
<b>LMT</b>	large mossy fiber terminal
<b>LMT-C</b>	local mossy fiber terminal arborization complex
<b>LTD</b>	long-term depression
<b>LTP</b>	long-term potentiation
<b>mfLTP</b>	mossy fiber long-term potentiation
<b>MEF2</b>	myocyte enhancer factor 2
<b>MFT</b>	mossy fiber terminal
<b>NMDA</b>	N-methyl-D-aspartate
<b>NMDA-R</b>	N-methyl-D_aspartate receptor
<b>PFB</b>	parallel fiber bouton
<b>PSD</b>	postsynaptic density
<b>PDS-95</b>	postsynaptic density protein-95
<b>Rab3a</b>	family member of the Ras small GTPase superfamily
<b>sFRP-1</b>	secreted Frizzled related protein-1
<b>Wnt</b>	composite from the gene names <i>Wingless</i> and <i>Int-1</i>
<b>Wnt7b</b>	Wnt protein 7b
<b>Wnt3</b>	Wnt protein 7b
<b>TrkB</b>	tyrosine kinases receptor B
<b>WT</b>	wild-type

# 1. INTRODUCTION

## *Overview*

The functioning of the brain critically relies on its capacity to adapt and respond to its environment. The brain's ability to change in response to experience is called plasticity and underlies principal brain functions, such as learning and memory.

My thesis work investigated the ability of the brain to structurally remodel upon altered experiences, and changes that occur during normal aging. Furthermore, I addressed what might be the molecular mechanisms regulating such remodeling.

I will therefore start by introducing the term of experience-dependent plasticity and exemplify the brain's capacity to adapt to changes in experience and usage.

I will then attempt to describe mechanisms of experience-dependent plasticity on the functional, molecular and structural level. Furthermore, I will discuss the impact of age and life-style on the brain's capacity for plasticity.

Finally, I will close the introduction by outlining the function and anatomy of the brain region that was the main subject of our investigations, namely the hippocampus, and specifically the mossy fiber pathway.

## ***1.1. EXPERIENCE-DEPENDENT PLASTICITY***

As we live, we experience consciously and unconsciously the world around and inside of us. Each piece of information reaching our brain will affect its future functioning and will influence our behavior. The capacity of the brain to change in response to experience is called plasticity. Such experience-dependent plasticity occurs throughout the brain and is essential for brain function.

Plasticity within the neuronal network of the brain manifests in many different ways such as in structural, physiological and molecular changes (Gilbert, 1998).

The ability of the brain to adapt becomes very obvious when external events robustly alter experience and force the brain to adjust in order to regain certain functionalities. Many studies of brain plasticity therefore use lesions as well as deprivation of sensory organs to study the adaptations of the brain to these modifications of experience.

Merzenich and colleagues in the early 1980s showed that peripheral nerve lesions in a monkey can lead to changes in the so-called cortical maps, for instance the topographic cortical representation of the skin of a hand. The cortex areas corresponding to the denervated skin were reoccupied by nerves serving the neighboring hand areas within a few months (Merzenich et al., 1983a, 1983b, 1984). A variety of studies demonstrated such changes in cortical mapping upon lesions of sensory organs or amputations of digits. Similarly, changes in the receptive field properties of sensory neurons, as well as structural rearrangements of axons and dendrites have been reported (Calford & Tweedale, 1991a, 1991b; Kalaska & Pomeranz, 1979; Kelahan & Doetsch, 1984; Rasmussen et al. 1982, 1986, 1988; Turnbull & Rasmussen, 1990, 1991, Darian-Smith & Gilbert, 1994). These modifications represent the attempts of the brain to recover functionality and demonstrate the immense capacity of the adult brain to adapt.

Importantly, changes upon modified experience not only occur upon insults and large-scale alterations of sensory input, but also underlie many physiological brain functions such as learning and memory.

This idea has been well studied in the context of perceptual learning. The ability to discriminate between similar sensory stimuli can be trained and improved by repeated exposure. The paradigm of perceptual learning turned out to be very useful to study the cellular and molecular underpinnings of experience-dependent plasticity, as the places where to expect changes are very well understood and the gain in functionality can be easily measured. These facts facilitate the correlations between functionality and plastic changes in the nervous tissue.

Many studies using functional magnetic resonance imaging (fMRI) demonstrated that perceptual learning boosts specific activity in the involved brain regions (Furmanski et al., 2004; Li et al., 2006). Alterations underlying such changes in broad network activity on the cellular level have been identified. They can consist of the specific potentiation of individual neurons involved in processing the trained stimulus (Schoups et al., 2001; Frenkel et al., 2006) or an increase in the number of neurons representing the trained input (Recanzone et al., 1992, 1993). Interestingly, significant changes in neuronal responses were not always detected in the classical receptive field for a given stimulus

but often involved neurons neighboring the representation of the trained stimulus through a phenomenon called contextual modulation (Crist & Gilbert, 2001; Li et al., 2004).

How are these changes in network and cellular activities achieved? The answers are plentiful. They can be the result of changes in synaptic strength, adaptations of cellular input responsiveness, and structural changes including changes in absolute synapse numbers and remodeling of neuronal circuit connectivity. It is likely that many if not all of these mechanisms underlie experience-dependent plasticity in several systems and that they mutually influence and regulate each other. I will discuss these mechanisms in greater detail in the following sections of my introduction.

### ***1.1.1. Potentiation and depression of synaptic strength***

Most of the excitatory and many inhibitory synapses in the adult brain exhibit various forms of use- and activity-dependent synaptic plasticity. These are defined as changes in the amplitude of synaptic potentials in response to an otherwise unchanged input as a result of synapse modifications. Especially long-lasting forms of such synaptic plasticity are thought to be a cellular basis for the encoding of experience and storing of information in neuronal networks.

There are several forms of long-term synaptic plasticity, affecting both excitatory and inhibitory synapses in the CNS. They usually occur after repetitive trains of synaptic activity or upon specific pairings of pre- and postsynaptic firings described below. Collectively they are called long-term potentiation (LTP) and long-term depression (LTD).

The first to describe LTP were Bliss and his colleagues (Bliss & Gardner-Medwin, 1973; Bliss & Lomo, 1973) and since then LTP has been intensely studied because of its presumed role in learning and memory (Bliss & Collingridge 1993; Bennett, 2000; Malenka & Nicoll, 1999). LTP can be induced by a single high-frequency stimulus train as well as by short, repetitive trains, such as in theta burst stimulations, which are more reminiscent of activity patterns recorded in awake-behaving animals. LTD on the other hand can be induced by low frequency stimulation (Mulkey & Malenka, 1992; Dudek &

Bear, 1993; Goda & Stevens, 1996). In addition to the temporal proximity, the sequence of pre- and postsynaptic spiking also plays a key role in synaptic modifications. In spike timing-dependent plasticity (STDP), presynaptic spiking shortly before postsynaptic spiking leads to LTP, whereas the opposite order leads to LTD (Levy & Steward, 1983; Markram et al., 1997; Dan & Poo, 2004). The effects of STDP were already predicted by Donald Hebb in his famous postulate in the late 1940s that states (Hebb, 1949):

*“Let us assume that the persistence or repetition of a reverberatory activity (or "trace") tends to induce lasting cellular changes that add to its stability.... When an axon of cell A is near enough to excite a cell B and repeatedly or persistently takes part in firing it, some growth process or metabolic change takes place in one or both cells such that A's efficiency, as one of the cells firing B, is increased.”*

Evidence that mechanisms of this so called Hebbian plasticity play a crucial role in experience-dependent plasticity *in vivo* comes from studies in sensory cortices showing that correlated neuronal firing can induce receptive field and map plasticity (Clark et al., 1988; Maffei & Galli-Resta, 1990; Schuett et al., 2001; Fu et al., 2002; Allen et al., 2003; Dan & Poo, 2006).

### ***1.1.2. Key molecular pathways involved in plasticity***

Changes in activity drive molecular mechanisms that alter synaptic properties and render them persistent. Activity-dependent signaling cascades have been subject of intense investigations and there is an enormous list of signal transduction molecules implicated in synaptic plasticity. It should be noted that long-term synaptic modifications like LTP or LTD are not unitary phenomena, but rather a family of processes that vary in their cellular and molecular mechanisms. Most consistently, synaptic plasticity involves the increase in pre- and/or postsynaptic calcium levels through NMDA receptors or voltage-sensitive calcium channels (Malenka & Bear, 2004).

This local calcium increase triggers calcium sensitive molecules to start signaling cascades that result in the potentiation of the synapse. Many of these signaling cascades

are regulated by the calcium binding protein calmodulin, which seems to be a key regulator of synaptic plasticity (Xia & Storm, 2005).

The lists of "plasticity molecules" are long. Many of the earliest changes that occur during synaptic plasticity are mediated by kinases and phosphatases. Outstanding roles have been attributed especially to PKA (cyclic adenosine 3', 5'-monophosphate (cAMP)-dependent protein kinase A) and  $\alpha$ -CamKII (alpha-calcium/calmodulin-dependent protein kinase II). For example,  $\alpha$ -CamKII has been found essential in LTP induction and experience-dependent plasticity *in vivo* (Glazewski et al., 1996, 2000). Similarly, PKA regulates the calcium permeability of NMDA receptors, and thus is crucial for many different forms of LTP and LTD, and is required for plasticity, e.g. in the visual cortex (Fischer et al. 2004; Huang et al., 2005; Skerberdis et al., 2006). Other work also suggests crucial roles for PKC (protein kinase C), the tyrosine kinase Src, and MAPK (mitogen-activated protein kinase).

Furthermore, gene expression analyses upon paradigms of plasticity induction revealed several common plasticity "pathways" involving MAPK, as well as other kinases and phosphatases (Ossipow et al., 2004; Majdan & Shatz, 2006).

### ***1.1.3. Structural plasticity***

In addition to changes in synaptic strength, structural alterations of cellular connectivities provide another or complementary mechanism to encode experience in the brain.

Through the specific loss and gain of synapses or the remodeling of existing ones, alterations in connectivity and thus neuronal circuits change the properties of neuronal networks and their functional output.

Interestingly, some of the principal molecular regulators of synaptic plasticity discussed above have also been implicated in regulating structural remodeling of synapses.

In this way, dynamics of pre- and postsynaptic structures can be stimulated by neurotransmitters or changes in calcium concentrations (Korkotian & Segal, 1999; Bonhoeffer & Yuste, 2002; Tashiro et al., 2003; DePaola et al., 2003; Brunig et al., 2004; Segal, 2005). Synaptically released glutamate, for instance, was reported to result in spine

growth via NMDA receptors (Engert & Bonhoeffer, 1999) and several studies have demonstrated a clear correlation between alterations of synaptic strength and the turnover of dendritic spines (Yuste & Bonhoeffer, 2001, 2004). Likewise, electrical stimulations that induce LTP and LTD lead to dendritic spine formation and elimination, respectively (Toni et al., 1999; Nägerl et al., 2004). Notably, many forms of dendritic structural plasticity as well as LTP induction require NMDA receptor activation (Nägerl et al., 2004; Datwani et al., 2002; Sin et al., 2002).

Evidence that such activity-dependent structural remodeling of synapses also plays a crucial role in experience-dependent plasticity is abundant. Many studies, using fixed tissue preparations, demonstrated that average spine densities and morphologies can be altered upon learning, age or other changes in experience, such as sensory stimulation, deprivation, stress or enriched environment (e.g. Globus & Scheibel, 1967; Globus et al. 1973; Parnavelas et al., 1973; Moser et al., 1994; Stewart et al., 2005, Kozorovitskiy et al. 2005, Tailby et al., 2005).

More recently, *in vivo* imaging studies of identified dendrites and axons have provided additional evidence that dendritic spines as well as presynaptic boutons exhibit structural plasticity in the adult CNS (Trachtenberg et al., 2002; De Paola et al., 2006; Majewska et al., 2006; Stettler et al., 2006), and that spine growth and loss *in vivo* can be modified by experience (Holtmaat et al., 2006). Although the formation of a new spine does not automatically mean the formation of a functional synapse, recent evidence suggests that only about 4% of cortical spines do not bear synapses and another study shows that spine growth precedes synapse formation *in vivo* (Knott et al., 2006; Arellano et al., 2007). Therefore, the assumption that the formation of new spines equals the appearance of new synapses seems generally valid.

Another means of exploring how experience affects synaptic dynamics is by mapping the distribution of pre- and postsynaptic markers. This was for instance done in an elegant *in vivo* study showing that the postsynaptic density (PSD) protein-95 readily redistributes

within neighboring spines and that the time of retention at individual PSDs was affected by their size, by animal's age, as well as by sensory experience (Gray et al. 2006).

#### ***1.1.4. Impact of age on neuronal plasticity***

Anybody who thinks about brain functions in the context of different ages must immediately realize that our brain does not work the same at all ages. Young babies are born lacking many abilities that become common during the next years such as walking, precise motor skills, language, acute sight and many more skills that are governed by the brain. On the other hand, children have an immense capacity to learn and adapt to their environment, and in this capacity they surpass adults by far. Although there is a considerable age-related decline in many cognitive functions, increasing experience and proficiency of routine tasks can make adults and also elderly people be advantaged in many all day situations and challenges.

What are the physiological mechanisms that underlie those age-related differences of brain functioning?

It has been long appreciated that during specific, early postnatal phases experience has a much bigger impact on behavior and brain function than at any other time in life. These phases were called critical (or sensitive) periods. Quickly it became clear that brain circuits subserving a given function are not only particularly sensitive to changes in experience related to this function during the critical period, but also need certain kinds of information as instructive signals for their continued normal development (Berardi et al. 2000; Hensch, 2005). In general one could say that critical periods are used to shape genetically inherited basic structures and functions of the brain and adapt them to the environmental and physical characteristics of the individual.

Critical periods have been very well documented for sensory systems. Mechanisms that allow for heightened plasticity during critical periods but also mechanisms that restrict plasticity before and after these phases have been described in much detail (Hensch, 2003). It may be important to note that there is not only one general critical period for the brain but rather one critical period with unique timing and duration for each functional

system. Common characteristics of all critical periods are that they have an onset and an end. This timing and duration is not only a question of age but is usage dependent, as it can be delayed by a lack of appropriate experience (Mower, 1991) or it can be started earlier and last for longer when experience is rich (Cancedda et al. 2004, Brainard & Knudsen 1998).

It is important to emphasize in this context that the ability to adapt to the environment is never lost throughout life. Although the extent and the readiness at which adaptations take place are reduced later on, similar adjustments as during critical periods can be induced in adults but seem to require either longer, repeated or incremental presentation of stimuli (Linkenhoker & Knudsen 2002, Sawtell et al. 2003, Hofer et al. 2006). Therefore, critical period research has led to important insights into adult experience-dependent plasticity by the direct comparison of adult and juvenile reactions towards the same stimuli.

It is still not clear whether adaptations in the adult are achieved through the same plasticity mechanisms as in the juvenile. However, studies on critical period plasticity have provided a detailed body of mechanisms that permit plasticity in the juvenile and restrict but also enable it later in life.

It is generally believed that adult neurons are morphologically much more stable than during the critical period. Several recent *in vivo* imaging studies demonstrated that dendritic arbors and spines are much more constant in adults than in juveniles and that spine motilities decrease with age (Lendvai et al., 2000; Gan et al., 2003; Majewska et al., 2003; Konur & Yuste 2004).

In agreement with these findings, many lines of evidence suggest that the extracellular matrix (ECM) in the adult CNS is much denser and less permissive for growth processes. Consequently, removal of certain ECM components allows for heightened functional and morphological plasticity in the adult (Pizzorusso et al., 2002, 2006; Berardi et al., 2004). Furthermore, extracellular proteolysis by tissue-type plasminogen activator (tPA) declines with age and increases upon plasticity induction during the critical period.

Disruption of tPA release prevents plasticity and its structural consequences on dendritic spines (Mataga et al., 2002, 2004).

Also myelination seems to play an important role in reducing plasticity after the critical period. Blocking signaling of myelin-derived Nogo by knockout of the Nogo-66 receptor leads to a lifelong heightened plasticity and thus a never-ending critical period (McGee et al., 2005).

In addition to the decreased structural plasticity in the adult compared to juveniles, several studies also revealed molecular mechanisms to be differently recruited in critical period and adult plasticity. These mechanisms for instance include differential epigenetic regulations, like histone acetylation and phosphorylation, and CREB regulated gene expression (Suzuki et al., 2004; Pham et al., 2004; Putignano et al., 2007). Interestingly, pharmacological stimulation of histone acetylation promoted plasticity in the adult (Putignano et al., 2007).

In contrast to the particularities of brain function early in life, the effects of normal aging on brain function are much less understood. However, it has become obvious that changes at all levels of neuronal function occur continuously throughout life. For instance, changes in neuronal morphologies, such as in dendritic trees or spine densities (Turner & Deupree, 1991; Markham & Juraska, 2002), gene expression (Jiang et al. 2001; Lee et al., 2000), electrophysiological properties (Barnes et al., 1983) as well as in network activities (Wilson et al., 2005) occur throughout life and may contribute to the differences in learning, memory and cognition at different ages.

There is much evidence that many cognitive abilities as well as the ability to process sensory information decline with age (Burke & Barnes, 2006). At the same time, some studies report profound compensations and adaptations in aged subjects. For instance, it was shown that older adults have increased multisensory integration capabilities than younger adults and in this way by far overcome their disadvantage in unisensory perception (Laurienti et al. 2006).

In conclusion, it seems that the brain remains plastic and retains an immense potential for adaptation throughout the entire life even if the strategies to adapt might be distinct at different ages.

#### ***1.1.5. The capacity to adapt is influenced by the life-style***

Interestingly, not only the age of an animal but also its life-style and -situation have important impacts on the plastic abilities of its nervous system.

A large variety of life conditions have been implicated in influencing experience-dependent plasticity. Amongst many other factors, the animal's gender, hormone status, stress level, social behavior, hibernation, parental behavior, and rearing conditions have been reported to influence plasticity (Rollenhagen & Bischof, 1994; Silva-Gomez et al., 2003; Kozorovitskiy et al., 2006; Vyas et al., 2006; von der Ohe, 2007).

Likewise, housing animals in environments that are “enriched” in comparison to their regular housing conditions induces a large variety of cellular, molecular and behavioral changes (van Praag et al., 2000; Nithianantharajah & Hannan, 2006) .

Although the enriched environment conditions vary from laboratory to laboratory, they most often consist of the possibility for social interaction, increased motor and exploratory activities as well as enrichment in sensory stimuli, such as objects of different colors, materials and odors. Even if the “enriched” environment of a laboratory cage is still very poor in comparison to the natural environment, the difference to the regular housing conditions is apparently already big enough to produce many consistent and robust effects on learning and memory performance and is thus a useful model to study experience-dependent plasticity.

Early studies investigating the effects of differential housing showed that enrichment altered cortical weight and thickness (Bennett et al., 1969; Diamond et al., 1972, 1976). Subsequent and more detailed studies have shown that in some neuronal populations enrichment can increase dendritic branching, length and spine numbers, as well as synapse numbers and sizes (Greenough & Volkmar, 1973a, 1973b; Greenough et al., 1985; Connor et al., 1982; Turner et al., 1985; Faherty et al., 2003; Leggio et al., 2005).

Consistent with enrichment-induced synaptogenesis, increases in levels of pre- and postsynaptic proteins, such as PSD-95 and synaptophysin, have been found (Frick & Fernandez, 2003; Nithianantharajah et al., 2004; Kozorovitskiy et al., 2005; Lambert et al., 2005).

Furhermore, genes involved in synaptic function and cellular plasticity are altered upon enriched environment (Rampon et al., 2000). For instance, enrichment induces alterations in the expression of NMDA and AMPA receptor subunits. These findings go in line with evidence for increased synaptic strength, including specific forms of synaptic plasticity such as LTP, upon enriched environment (Foster et al., 1996, Foster & Dumas, 2001; Duffy et al., 2001; Artola et al., 2006).

Enrichment can also increase levels of neurotrophins, such as brain-derived neurotrophic factor (BDNF) and nerve growth factor (NGF) (Torasdotter et al., 1998; Pham et al., 1999; Ickes et al., 2000).

At the behavioural level, enrichment enhances learning and memory (Moser et al., 1997; Schrijver et al., 2002; Lee et al., 2003), reduces memory decline in aged animals (Bennett et al., 2006), decreases anxiety and increases exploratory activity (Chappillon et al., 1999; Roy et al., 2001; Benaroya-Milshtein et al., 2004, Friske & Gammle, 2005).

Interestingly, enriched environment leads to increased hippocampal neurogenesis and the newly born granule cells have been demonstrated to be integrated into functional circuits (Kempermann et al., 1997, 1998a, 1998b, 2002) Still, whether or not these newborn cells contribute and in which ways to the improved performance in learning and memory is still a matter of debate (Bruehl-Jungerman et al., 2005; Meshi et al., 2006)

## ***1.2. HIPPOCAMPUS***

### ***1.2.1. The hippocampus as a model system to study neuronal circuit plasticity***

We have chosen the hippocampus as a model system to study morphological, neuronal circuit plasticity because of its unique anatomy and roles in learning and memory. A rich amount of indispensable knowledge is available concerning hippocampal functioning,

anatomy and physiology and has been invaluable to put our findings into context. Furthermore, many imaging, electrophysiological and behavioral tools have been developed by others and exploited in our work to study the hippocampus' plasticity *in vitro* and *in vivo*. The basic features of the hippocampus are described in the following paragraphs.

### ***1.2.2. Hippocampal functions***

Maybe the earliest recognized and most widely accepted role of the hippocampus is its role in memory (Eichenbaum 2000, Milner 1998). Damage to the hippocampus causes anterograde amnesia, the incapacity to store new memories, and defective declarative memory, e.g. the failure to recall everyday facts and events. Perceptual and cognitive abilities are usually unaffected, as are the capacities for working memory and retrieval of remote memories. In addition to the inability to convert new information into stable memories, patients with bilateral hippocampal damage also suffer from a temporally graded retrograde amnesia, with recent retrograde memory being impaired while remote memories remain intact (Zola-Morgan & Squire, 1990, Teng & Squire, 1999).

This indicates that the hippocampal formation has a time-limited role in memory storage and is not necessary for storage or retrieval of remote memories. This temporal limitation of memory storage in the hippocampus was further investigated in animal studies and it was shown that the brain activity during memory performance was shifted with time from the hippocampus to cortical areas indicating that the memory 'trace' moves from a primary hippocampal to a later cortical location (Bontempi et al. 1999).

The common observation of temporally graded retrograde amnesia has led to the prevalent hypothesis that memories undergo consolidation, an extended process through which memories become more permanent (Polster et al. 1991).

There are several mechanisms thought to underlie consolidation and to make memories long-lasting. Modifications of synaptic efficacy, like long-term potentiation (LTP), structural changes of synapses (Dudai, 1996; McGaugh, 2000; Lamprecht & LeDoux,

2004), as well as interactions between different brain regions, such as between hippocampus and cortical areas, are believed to be essential for memory consolidation (Dudai, 2004, Frankland et al. 2004, Ross & Eichenbaum 2006).

Another but closely related functional characteristic of the hippocampus is the occurrence of cells that fire in a location-specific manner, the so called place cells. The discovery of place cells led to the suggestion that the hippocampus is involved in generating a mental representation of the outside world and its spatial organization, known as the “cognitive map” (O’Keefe and Dostrovsky, 1971). This discovery led to the formulation of the ‘cognitive map theory’ of memory formation (O’Keefe and Nadel, 1978).

The cognitive map theory states that the hippocampus is essentially a spatial mapping system that is used to organize and remember the items and events of experience. In contrast to this idea, a second theory states that the hippocampus is a more general learning system important for encoding relationships between environmental stimuli and creating episodic memories independent of spatial context. This alternative theory is called the ‘relational learning’, ‘declarative memory’ or ‘episodic memory’ theory.

Recent evidence suggests that these two theories may not be mutually exclusive as there are many examples of hippocampal cells encoding either spatial or nonspatial information. At the same time there are cells that code nonspatial information coupled to spatial correlates. Thus, for many experimental data both theories could hold true (O’Keefe & Nadel, 1978; Wood et al., 1999; Moita et al., 2003; Knierim, 2003). Since episodic memories, by definition, include information about the time and place where the episode occurred, contextual information is a necessary prerequisite for any episodic memory. Thus, place fields seem to contribute importantly to episodic memory as part of the needed context representations. (Smith & Mizumori, 2006)

Interestingly, during sleep place cells have a tendency to fire in the same sequence as they did during the actual movement in an earlier awake state (Skaggs & McNaughton, 1996; Qin et al. 1997) and it has been suggested that sleep plays an important role in

memory consolidation (Stickgold, 2005). According to the ‘trace reactivation’ theory, memory traces stored during the wake state are reactivated during slow-wave sleep and thus consolidated and bound to other traces (Hoffman & McNaughton, 2002).

Thus, although it is widely accepted that the hippocampus plays a critical role in learning and memory, there are contrasting views and many ideas of how the hippocampus achieves these functionalities.

Interestingly, the hippocampus displays two characteristic and mutually exclusive brain-wave activities that may be associated with learning and memory. During exploration the hippocampus exhibits theta activity and is thought to acquire new representations of its environment, whereas during quiet wakefulness and slow-wave sleep, it displays sharp wave activities that are thought to facilitate the consolidation of the information (Buzsaki, 2002; Sutherland & McNaughton 2000).

Taken together, an immense richness of information has become available about hippocampal features and function. Still, it remains a major and challenging task to combine knowledge about activities of cells and networks with functionalities achieved by the hippocampus, such as the encoding of memories.

### ***1.2.3. Anatomy of the hippocampus***

The hippocampus is located in the temporal lobe of each brain hemisphere. From outside it appears as an elongated, banana-shaped structure with its long axis extending in a “C”-shaped fashion throughout the temporal lobe. The long-axis of each hippocampus is referred to as the septotemporal axis; the orthogonal axis is referred to as the transverse axis.

The hippocampus is one part in a group of structures within the limbic system usually called the hippocampal formation comprising the dentate gyrus, hippocampus, subiculum, pre- and parasubiculum, and the entorhinal cortex.

When cut transversely, the hippocampus has a very distinctive and readily identifiable structure due to its clear lamination: both the neuronal cell bodies and the zones of connectivity are arranged in orderly layers. The hippocampus proper consists of two crescent-like regions, the Ammon's horn or "CA" region (short for "Cornu Ammonis" due to its resemblance to the ram's horn carried by the Egyptian god Ammon), and the dentate gyrus (DG). The CA region can be further subdivided into three subregions called CA1, CA2 and CA3 that are distinct with respect to their connectivity and to the size of their pyramidal cell bodies. CA3 and CA2 pyramidal cell bodies are larger than those of CA1. CA3 is the only region receiving input from the dentate gyrus. Together the hippocampus resembles in shape that of a seahorse which led to its name (from the Greek words for horse "hippo" and "kampos" meaning sea monster).

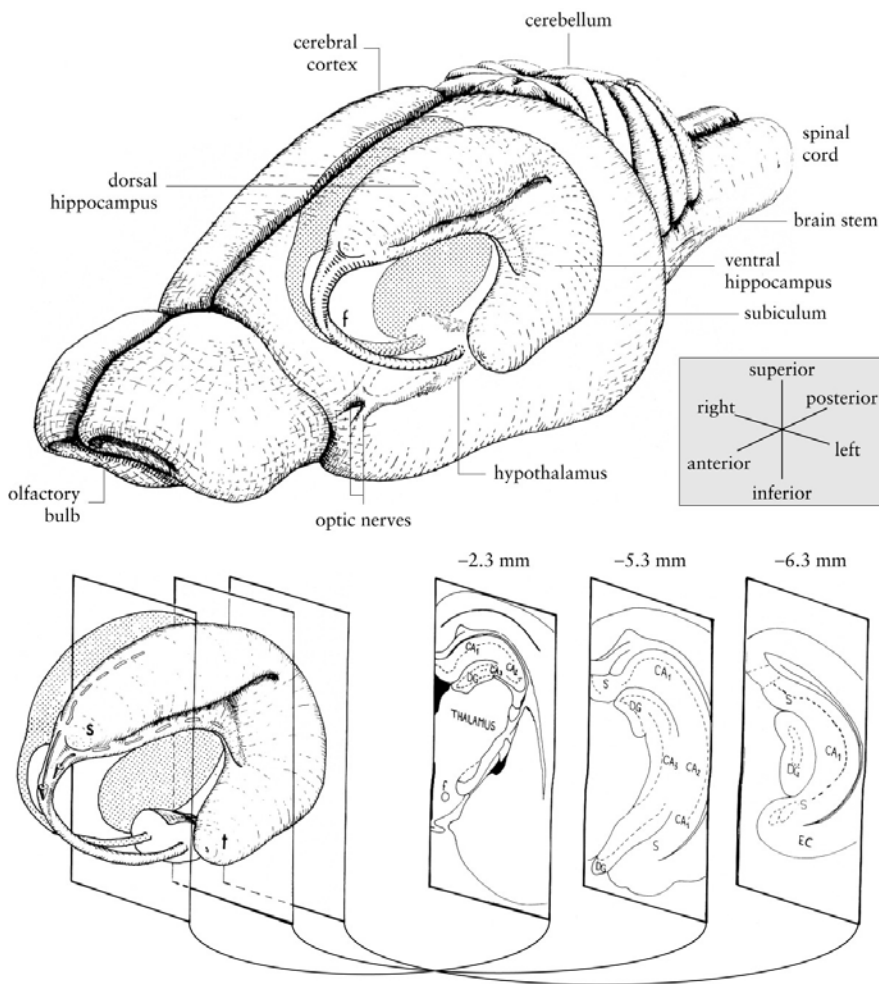


Figure 1. Three dimensional representation of the rat hippocampus (modified from Amaral & Whitter, 1995)

#### ***1.2.4. Basic hippocampal circuits***

The basic circuitry of the hippocampus is often simplified as a unidirectional excitatory pathway linking consecutively the main hippocampal regions in a closed circuit. It is important to note that this is a simplistic view of a much more complex circuitry leaving out numerous important recurrent, associative as well as commissural and interneuronal components.

For simplicity, the entorhinal cortex is considered to be the starting point giving rise to the perforant path that projects through or “perforates” the subiculum and terminates both in the dentate gyrus and in the CA3 field of the hippocampus. Entorhinal cortex also connects directly to CA1, generating a shorter loop that synapses DG and CA3. The next step in the circuitry is the dentate gyrus giving rise to the mossy fibers that terminate in the stratum lucidum on the proximal dendrites of the CA3 pyramidal neurons. The CA3 pyramidal cells, in turn, project heavily to other levels of CA3 by associational connections, as well as to CA1, as the so called Schaffer collaterals. Schaffer collaterals innervate both, the apical and basal dendrites of CA1 pyramidal cells. CA1 in contrast to CA3 pyramidal cells do not give rise to a major set of collaterals and has very few associational connections, instead it projects to the subiculum and to the deep layers of the entorhinal cortex. The subiculum itself also originates a projection to the deep layers of the entorhinal cortex. Finally, the deep layers of the entorhinal cortex, project to many of the same cortical areas that originally projected to the entorhinal cortex. Thus, information entering the entorhinal cortex from a particular cortical area can traverse the entire hippocampal circuit and ultimately be returned to the cortical area from which it originated (Amaral & Witter, 1989; Johnston & Amaral, 2004).

#### ***1.2.5. The dentate gyrus and the mossy fiber pathway***

The dentate gyrus consists of three layers: the principle or granule cell layer; the largely acellular molecular layer, above the granule cell layer; and the hilus, or polymorphic cell layer, located below the granule cell layer. The granule cells have small (about 10  $\mu\text{m}$  in diameter) cell bodies arranged in a densely packed cell layer shaped like a “U” or “V” surrounding the hilus.

The dentate gyrus granule cells are monopolar neurons; their dendrites emerge only from one side of the neuron and extend perpendicularly to the cell layer into the overlying molecular layer where they receive their synaptic inputs. The unmyelinated axons of the granule cells are called mossy fibers and originate from the opposite site of the cell body. They extend towards the hilus where they establish several collaterals. Through numerous small and fewer big varicosities these collaterals contact hilar interneurons that can be excitatory and inhibitory. A particular excitatory interneuron type of the hilus contacted by the mossy fibers is the mossy cell. Mossy cells are innervated by granule cells of the same septotemporal level but themselves project to distant levels located both septally and temporally from the level of their cell bodies as well as to the dentate gyrus of the other hemisphere. Their projections occupy almost exclusively the inner third of the molecular layer of the dentate gyrus and are called *ipsilateral associational-commissural projections*. In addition to contacting granule cells, these projections also synapse onto GABAergic interneurons of the dentate gyrus and thus provide feedforward excitatory as well as inhibitory pathway to distant septotemporal levels. At the same time, mossy fiber collaterals also contact GABAergic, inhibitory interneurons that are more locally limited in their projections and thus inhibit granule cell activity at the same septotemporal levels.

The mossy fibers next exit the hilus as a coalesced bundle of fibers and enter the stratum lucidum of CA3 where they synapse onto CA3 pyramidal neurons.

Once the mossy fibers leave the hilus they have very few collaterals and establish very large and characteristic presynaptic terminals, the so-called large mossy fiber terminals (LMTs). Each mossy fiber establishes about 10-15 LMTs at 80-150  $\mu\text{m}$  intervals contacting very large and complex dendritic spines, the thorny excrescences of postsynaptic CA3 pyramidal neurons. The great majority of mossy fibers contact the proximal part of the apical dendrite of CA pyramidal cells in the stratum lucidum. Only in the part of CA3 located closest to the dentate gyrus (CA3c), some mossy fibers extend deep to the pyramidal cell layer in what has been called the infrapyramidal bundle. Only in this region, the mossy fibers innervate both, the apical and basal dendrites of pyramidal

cells. Interestingly, the extent of the infrapyramidal projection varies across species and even across strains within species and seems to correlate with behavioral performance in spatial tasks (Schwegler & Crusio, 1995).

Each CA3 pyramidal neuron has been estimated to be contacted by 30-50 LMTs (Henze et al. 2000). A single LMT contains many active zones and thus establishes many synaptic contacts with a single CA3 pyramidal neuron. The LMT is an exceptionally strong synapse, also described as a “detonator synapse” because of its ability to elicit as a single synaptic connection action potentials in postsynaptic pyramidal cells (Reid et al. 2001, Henze et al. 2002). In addition to these powerful excitatory connections, mossy fibers establish synapses with inhibitory interneurons through en-passant varicosities and LMT filopodia. These connections provide effective feed-forward inhibition, especially at low-frequency firing (Acsady et al., 1998).

For most of its course through area CA3, the mossy fiber pathway can be considered the only true lamellar fiber system of the hippocampal formation as it shows only a very limited degree of septotemporal divergence. However, near the CA3-CA2 border the mossy fibers make an abrupt turn temporally and project in a significant way (1-2 mm) longitudinally towards the temporal pole of the hippocampus (Amaral & Witter, 1998).

This lamellar organization together with the stereotyped and sparse excitatory connectivity makes the mossy fiber and its LMTs an ideal system to study circuit rearrangements.

## 2. RESULTS

### 2.1. LONG-TERM REARRANGEMENTS OF HIPPOCAMPAL MOSSY FIBER TERMINAL CONNECTIVITY IN THE ADULT REGULATED BY EXPERIENCE

Ivan Galimberti<sup>1,2</sup>, Nadine Gogolla<sup>1,2</sup>, Stefano Alberi<sup>3</sup>, Alexandre Ferrao Santos<sup>2</sup>,  
Dominique Muller<sup>3</sup>, and Pico Caroni<sup>2</sup>

<sup>1</sup>Equal contribution

<sup>2</sup>Friedrich Miescher Institut, Maulbeerstrasse 66, CH-4058 Basel, Switzerland

<sup>3</sup>CMU, University of Geneva, Geneva, Switzerland

**Neuron**

2006 (Vol. 50: 749-763)

### **2.1.1. SUMMARY**

We investigated rearrangements of connectivity between hippocampal mossy fibers and CA3 pyramidal neurons. We find that mossy fibers establish 10-15 local terminal arborization complexes (LMT-Cs) in CA3 exhibiting major differences in size and divergence in adult mice. LMT-Cs exhibited two types of long-term rearrangements in connectivity in the adult: progressive expansion of LMT-C subsets along individual dendrites throughout life, and pronounced increases in LMT-C complexities in response to enriched environment. In organotypic slice cultures, subsets of LMT-Cs also rearranged extensively and grew over weeks and months, altering the strength of preexisting connectivity, and establishing or dismantling connections with pyramidal neurons. Differences in LMT-C plasticity reflected properties of individual LMT-Cs, not mossy fibers. LMT-C maintenance and growth were regulated by spiking activity, mGluR2-sensitive transmitter release from LMTs, and PKC. Thus, subsets of terminal arborization complexes by mossy fibers rearrange their local connectivities in response to experience and age throughout life.

### **2.1.2. INTRODUCTION**

Sustained rearrangements of synaptic connections can provide mechanisms to alter connectivity in neuronal circuits, and encode experience in the brain (Lichtman and Colman, 2000; Poirazi and Mel, 2001; Chklovskii et al., 2004). It is well established that local rearrangements of circuitry driven by experience play prominent roles in the fine-tuning of neuronal circuits during postnatal development (Lichtman and Colman, 2000; Linkenhoker and Knudsen, 2002; Gan et al., 2003; Linkenhoker and Knudsen, 2005). In contrast, although there is abundant evidence for pronounced physiological plasticity in the adult, evidence that structural rearrangements of circuitry also take place in the adult has been scarce (but see Knott et al., 2002). Recent *in vivo* time-lapse imaging studies in neocortex have reported appearance and disappearance of postsynaptic dendritic spine subpopulations, and shown that the frequency of these events can be influenced by sensory experience (Lendvai et al., 2000; Trachtenberg et al., 2002; Holtmaat et al., 2005). These remodeling events were more frequent in younger mice, but turnover was

also detected in older adults (Holtmaat et al., 2005; Lee et al., 2006; but see Zuo et al., 2005). In addition, a study using long-term organotypic hippocampal slice cultures showed that subsets of presynaptic terminals can undergo comparable balanced turnover, and that the extent of this turnover is again enhanced by synaptic activity (De Paola et al., 2003). Finally, recent studies of adult mouse barrel and visual cortex have provided evidence for such structural plasticity of presynaptic terminals *in vivo* (De Paola et al., 2006; Stettler et al., 2006). However, these studies imaged groups of either pre- or postsynaptic elements within small regions of neuropil, and could thus not assign complete sets of synapses by individual identified presynaptic neurons to their postsynaptic targets. Consequently, it has remained unclear to what extent synapse rearrangement processes in the adult produce net alterations in the numbers of synaptic connections between identified synaptic partners. For the same reasons, it has also remained unclear whether, and under what circumstances, repeated rearrangement processes can lead to incremental shifts of connectivity in the adult. To address these questions, we looked for simple and well-characterized circuitry that had been implicated in experience-related anatomical plasticity, and which was accessible to large-scale repeated imaging during long periods of time.

The mossy fiber projection by dentate gyrus granule cells onto hippocampal pyramidal neurons in CA3 (Johnston and Amaral, 1998; Henze et al., 2000) is an attractive system to investigate patterns of synaptic connection rearrangements on a comprehensive scale. First, most of the mossy fiber projection in CA3 is lamellar with respect to the hippocampal long axis, and exhibits stereotype and simple relationships with respect to the number of its postsynaptic partners. Each mossy fiber establishes 10-15 large mossy fiber terminals (LMTs) at 80-150  $\mu\text{m}$  intervals along its projection in CA3 that can be unambiguously identified anatomically (Johnston and Amaral, 1998). The average number of distinct mossy fiber inputs per pyramidal neuron in CA3 has been estimated at about 30-45 (Henze et al., 2000), suggesting that the probability for random pairs of mossy fibers to synapse onto the same pyramidal neuron is very low. These low synapse numbers stand in sharp contrast to the very high degree of connectivity among pyramidal neurons in CA3, and from CA3 to CA1. Second, mossy fibers in stratum lucidum

establish well-characterized and powerful excitatory synaptic connections with pyramidal cells through LMTs, and with inhibitory interneurons through en-passant varicosities and LMT filopodia (Acsady et al., 1998; Geiger and Jonas, 2000; Reid et al., 2001; Henze et al., 2002; Engel and Jonas, 2005; Nicoll and Schmitz, 2005). The latter provide efficient feed-forward inhibition, and mediate the predominant outcome of mossy fiber activation when these spike at low frequencies (Lawrence and McBain, 2003; Mori et al., 2004). In contrast, mossy fibers elicit increasing excitation of CA3 pyramidal neurons when firing at higher frequencies (Geiger and Jonas, 2000; Henze et al., 2002; Mori et al., 2004). As a consequence, and probably depending on spiking frequency, one or a small number of converging LMTs can be sufficient to elicit action potentials in a postsynaptic pyramidal cell, assigning a major instructional role to this synapse in triggering network activity in the hippocampus (Henze et al., 2002). In addition, postsynaptic spiking induced by LMTs also serves as a powerful trigger to induce LTP at co-active weaker associational synapses onto the distal sections of the same pyramidal neuron dendrites (Kobayashi and Poo, 2004). A third key feature is that individual mossy fibers only fire rarely during hippocampal recruitment (sparse code), suggesting that small ensembles of co-active granule cells as such convey information to the hippocampal network, and that the precise outcome of the firing for each of these cells might be functionally important (Johnston and Amaral, 1998; Henze et al., 2002).

Several lines of evidence have implicated the mossy fiber projection in anatomical plasticity related to experience. Neuroanatomical analyses using Timm staining in mice and rats have suggested that mossy fiber projection sizes are correlated to performance in hippocampal-dependent tasks (e.g. Schopke et al., 1991; Pleskacheva et al., 2000), and that experience can lead to significant alterations in the size of the mossy fiber projection (Schwegler et al., 1991; Ramirez-Amaya et al., 2001). Furthermore, long-term stress can lead to reductions in spatial learning performance and in the average density of mossy fiber synapses as determined by electron microscopy, and these impairments can be reversed through training for spatial tasks (McEwen, 1999; Sandi et al., 2003). Finally, independent studies have revealed that the dendrites and dendritic spines of CA3 pyramidal neurons are particularly sensitive to stress-inducing treatments and stress-

related hormones (e.g. McEwen, 1999), suggesting that both the pre- and postsynaptic elements of mossy fiber synapses are subject to experience-related anatomical plasticity in the adult. Taken together, these findings from distinct species and experimental approaches support the notion that the mossy fiber projection and its LMT synapses in CA3 provide a promising system to investigate persistent rearrangements of synaptic circuitry influenced by experience in the adult brain.

Here we exploited transgenic mice expressing membrane-targeted GFP in only few neurons (*Thyl-mGFP<sup>s</sup>*) (De Paola et al., 2003), and high-resolution imaging to investigate the connectivity of LMTs in fixed mouse tissue and organotypic slice cultures. We find that LMTs are highly heterogeneous in vivo and in slice cultures, and that many of them are connected through 10-200  $\mu\text{m}$  processes to “satellite LMTs” that can contact distinct pyramidal neurons in CA3. LMTs are thus components of local presynaptic terminal arborization complexes (LMT-Cs) by mossy fibers, exhibiting varying degrees of divergence with respect to their local targets in CA3. We then show that LMT-Cs exhibit pronounced long-term rearrangements in the adult. We provide evidence for two distinct types of rearrangements: 1) a life-long gradual growth of the largest LMT-Cs along pyramidal cell dendrites; 2) a dramatic increase in the complexity of many LMT-Cs in mice housed in an enriched environment. We finally show that subsets of LMT-Cs exhibit comparable rearrangements and growth over weeks and months in slice cultures, that these anatomical rearrangements reflect functional rearrangements in the local connectivity of LMT-Cs with pyramidal neurons, that heterogeneities in plasticity and growth reflect local properties of individual LMT-Cs, and that LMT-C maintenance and growth are regulated by synaptic activity, mGluR2-sensitive transmitter release from LMTs, and PKC. Taken together, these results demonstrate the existence of sustained local rearrangements of connectivity by defined terminal arborization structures regulated by activity in the adult.

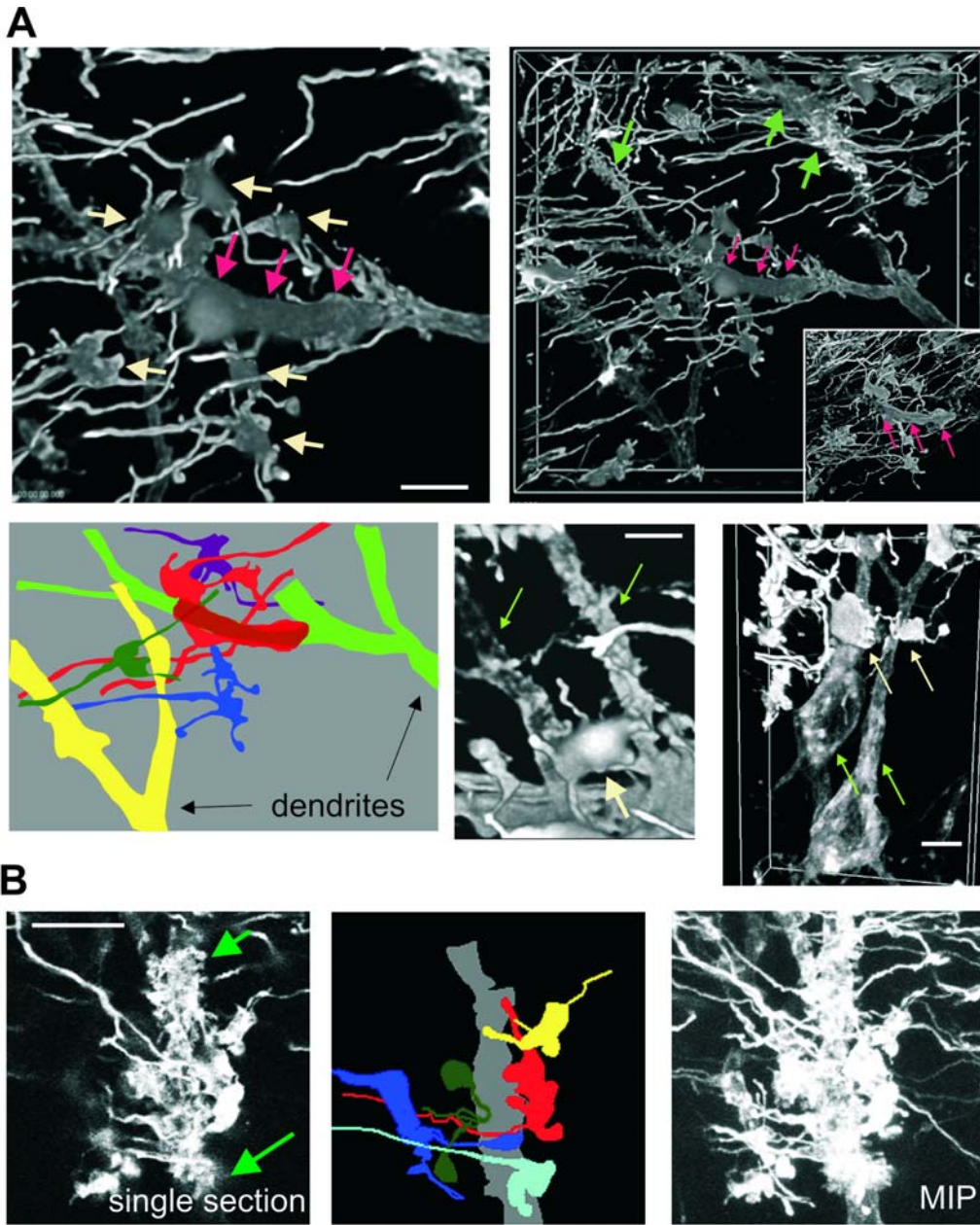
### 2.1.3. RESULTS

#### **Divergence and convergence of LMT complex connectivities onto pyramidal neurons**

As a prerequisite to investigate the anatomical plasticity of LMTs, we analyzed their morphologies and connectivities, using *Thy1-mGFP<sup>s</sup>* transgenic mouse lines expressing membrane-targeted GFP in only few neurons (De Paola et al., 2003), high-resolution light microscopy of perfused brain tissue, and 3D image processing. The degree of anatomical resolution conferred by the mGFP marker allowed us to provide views of hippocampal LMTs at a very high level of overall organization and resolution (Fig. 1). We found that in addition to core terminal regions with filopodia adjacent to the main axon, which had been described in previous studies, LMTs frequently exhibited processes of 10-200  $\mu\text{m}$  in length, which emerged from the core LMT and terminated at “satellite LMTs” (Fig. 1A, Suppl. Fig. 1; range of 0-5 satellites per LMT; depending on age, 38% (2.5 months), 58% (6 months), and 70% (16 months) of all LMTs exhibited satellites; see Fig. 3C). Like core LMTs, satellites were larger than 2.5  $\mu\text{m}$  in diameter, exhibited filopodia, and contacted pyramidal neurons (see below). To rule out the possibility that some of the structures might be due to the mGFP marker itself, we also acquired images from mice expressing cytosolic YFP (*Thy1-cYFP<sup>s</sup>*) (Feng et al., 2000). Although the resolution was substantially inferior, the cytosolic marker revealed the same types of subcomponents and arrangements, including core regions and satellites, as detected with the mGFP marker (Suppl. Fig. 1B). For the sake of clarity, we therefore introduce the term “LMT complex” (LMT-C) to designate a local presynaptic terminal arborization structure consisting of a core LMT, its filopodia, its satellite LMTs, and their filopodia. Accordingly, mossy fibers establish 10-15 LMT-Cs in CA3, and some of these LMT-Cs exhibit satellites.

A comparison among large sets of LMT-Cs within small regions of hippocampus revealed pronounced variations among these presynaptic terminal complexes, which ranged from small core terminal regions to very large and highly complex structures consisting of LMTs with multiple subunits, and of several satellites (Fig. 1; see also Figs.

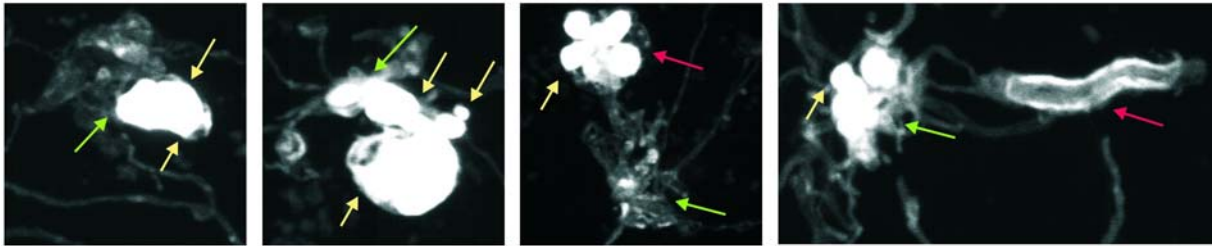
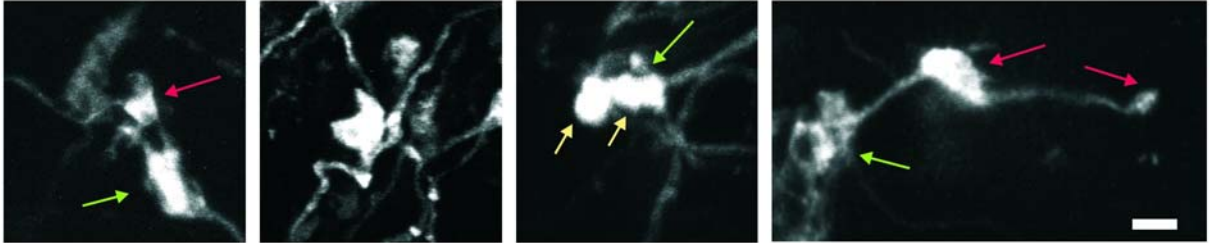
2A, 2C, 3C). Reconstruction of three LMTs from serial EM sections of non-transgenic hippocampi provided independent evidence that individual LMTs can consist of multiple interconnected subunits (Suppl. Fig. 2). The very large sizes of some LMT-Cs, and the presence of satellites at many of them suggested that many of these terminal structures might establish synaptic contacts with more than one postsynaptic CA3 pyramidal neuron. Indeed, a detailed analysis provided clear evidence of individual LMT-Cs in contact with more than one CA3 pyramidal neuron (Fig. 1A, Suppl. Videos 1, 2). This was not only true for the different LMTs belonging to an LMT-C, but also for large individual LMTs (Fig. 1A). In addition to this unexpected local divergence of the outputs by one LMT-C onto distinct pyramidal neurons, we also found clear evidence for extensive convergence of distinct LMT-C inputs onto individual thorny excrescence clusters (Fig. 1B). We conclude that LMT-Cs are local terminal arborization structures of mossy fibers exhibiting dramatic differences in their sizes, complexities, and divergence onto CA3 pyramidal neurons in adult mice.



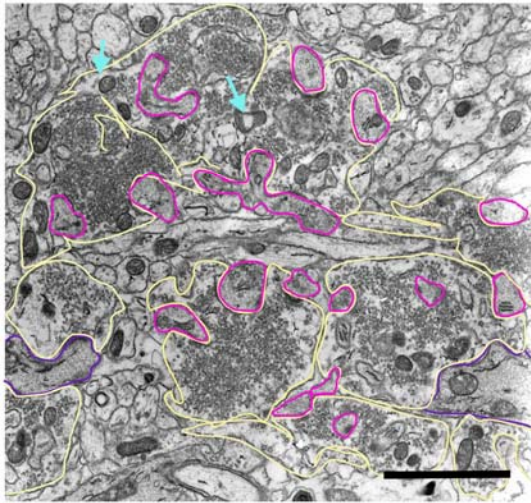
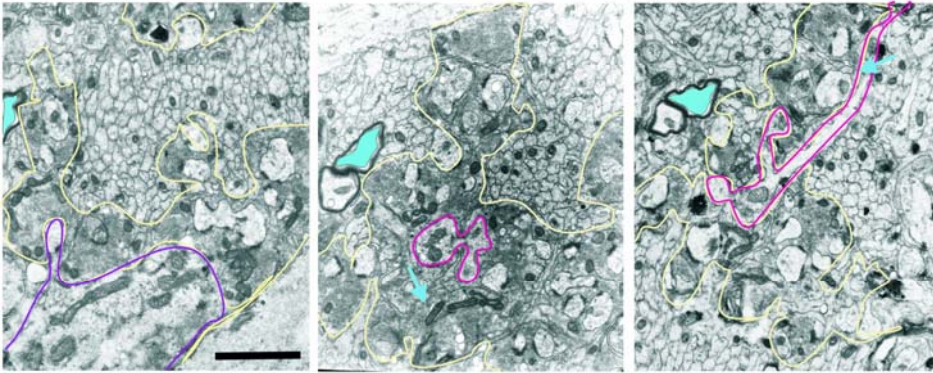
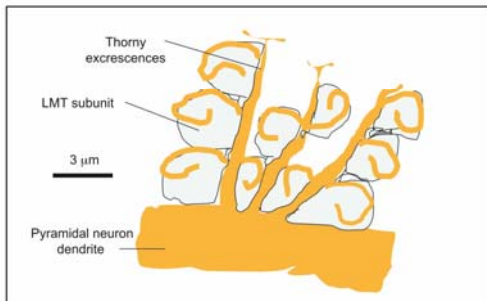
**Figure 1. Divergence and convergence of LMT-C connectivity onto pyramidal neurons in CA3.**

**A:** Complexity and divergence of LMT-Cs. Individual mossy fibers and pyramidal neurons in CA3a/b (6-months *Thy1-mGFP<sup>s</sup>* mouse); Imaris volume projections (high-intensity mode acquisition). Upper panel, left: cream arrows: LMTs, red arrows: one LMT covering a long segment of pyramidal neuron dendrite. Upper panel right: lower magnification image of field shown on the left. Green arrows: two examples of thorny excrescence clusters. The inset shows the same field, but seen from behind (mirror image to facilitate orientation); proximal sections were excluded to reveal the dendrite-facing surface of the elongated LMT (red arrow). Lower panel left: camera lucida drawing of CA3 field shown above. LMTs belonging to the same complex (3D-analysis) are in the same color. Lower panels center and right: Examples of LMT-Cs (cream arrows) each contacting two distinct pyramidal neurons (green arrows); right: LMT and one satellite (to the right).

**B:** Convergence of LMT-Cs belonging to distinct mossy fibers at the same thorny excrescence cluster of a pyramidal neuron dendrite in CA3 stratum lucidum (2.5-months *Thy1-mGFP<sup>s</sup>* mouse). Left: single confocal section (green arrows delineate the outline of the thorny excrescence cluster); center: camera lucida drawing, including LMTs from 5 distinct mossy fibers converging onto the thorny excrescence cluster; right: MIP of stacks including the cluster and its mGFP-positive LMT inputs. The LMT-Cs belonging to the dark blue and green mossy fibers both include satellites, and converge on a second dendrite on the left. Bars: 5  $\mu$ m.

**A****B**

**Supplementary Figure 1. Comparison of LMT-Cs in vivo, as visualized using *Thy1-mGFPs* or *Thy1-cYFPs* mice.** Image settings (MIP of raw data) comparable to those shown in Fig. 2A for LMT-Cs in slice cultures. Arrows: original LMT (green; next to mossy fiber), satellites (red), beady subunits (yellow). A: Examples of LMT-Cs in 15 Mo, *Thy1-mGFPs* mice. Note how the LMT structures are comparable to those detected in slice cultures. B: Examples of LMT-Cs in 4 Mo, *Thy1-cGFPs* mice. Note how complex arrangements, including beaded subunits and satellites are also visualized with cytosolic YFP. Bar: 5  $\mu$ m.

**A****B****C**

**Supplementary Figure 2. Ultrastructural analysis of complex LMTs.**

Electron micrographs of CA3a LMTs in 3 months wild-type mice. Blue arrows: regions where connection between subunits is included in the section. A: A complex LMT consisting of multiple interconnected subunits (cream outlines; verified by consecutive sections). Note arrangement of many thorny excrescences (red outlines) around the edge of LMT subunits. B: Serial sections of one complex LMT. Outlines: interconnected subunits (cream), base of dendrite (violet, left panel) and examples of postsynaptic thorns interconnecting LMT subunits (red); for orientation, a myelinated axonal profile is filled in blue. C: Partial reconstruction of LMT complex shown in (B). The schematic is based on 65 consecutive sections, and outlines the main topographic relationships included in the sections (axonal elements in blue, dendritic elements in yellow); it indicates the arrangement of thorny excrescence main branches (three of them), and their secondary branches extending around the edges of LMT subunits, but does not include tertiary side-branches into LMT subunits and their synaptic complexes. LMT subunits were interconnected along thorn main branches. Bars: 2  $\mu$ m.

### **Life-long expansion of hippocampal LMT subsets along pyramidal dendrites**

We next wondered whether the dramatic complexities and differences among LMT-Cs are present to a similar extent throughout life, or whether LMT-Cs might undergo systematic alterations with maturation and during adulthood. A comparison of LMTs from the same regions of hippocampal CA3, but from mice of different ages, revealed clear differences in the size distributions of these presynaptic terminal structures, and a selective shift to larger sizes with increasing age (Fig. 2A-C). The mGFP construct labeled mossy fibers and LMT-Cs with remarkable and comparable homogeneity throughout life (Suppl. Fig. 3), arguing against the possibility that these LMT size shifts might reflect systematic distortions of the imaging data set. Interestingly, the shifts in LMT sizes did not affect all LMT size groups equally: while a large fraction (50-80%, depending on the age) of LMTs was relatively small (volumes equivalent to 1-3 subunits of 3  $\mu\text{m}$  diameter) at any age, the remaining LMTs shifted to larger sizes, and the average sizes of the largest 5-10% among them grew dramatically with age (Fig. 2B).

Remarkably, this gradual age-related growth of larger LMTs was not confined to any particular period of life, but instead continued throughout life, including old age (Fig. 2B). This was not accompanied by a corresponding decrease in the average density of LMTs (average densities of LMTs per  $(92 \times 92 \times 7.5 \mu\text{m})$  volumes of CA3a, normalized per mGFP-positive granule cell on the same section were:  $1.14 \pm 0.12$  (3 months),  $1.18 \pm 0.20$  (6 months),  $1.37 \pm 0.15$  (16 months),  $1.34 \pm 0.18$  (22 months);  $N=8$  sections, 16 volumes, from 2 mice each; range of 21-42 LMTs per volume), arguing against the possibility that the higher contribution of the larger LMTs to the total volume of LMTs with increasing age was due to a corresponding loss of smaller LMTs.

A detailed comparison of larger LMTs at different ages revealed that the predominant contributions to their increase in size were longitudinal extensions, which were oriented transversal to the mossy fiber projection (Fig. 2C). This was reflected in a gradual increase in LMT long-to-short axis ratio values with increasing age (Fig. 2C). High-resolution analysis suggested that this reflected an expansion of the stretch of CA3 pyramidal neuron dendrite occupied by individual larger LMTs (Fig. 2C). Taken together, these results provide evidence that, in the mouse, there is a continuous net

growth of the largest subpopulations of LMTs throughout life, and that this growth mainly involves the expansion of LMT subsets along pyramidal neuron dendrites in CA3. This relationship between age and LMT size distributions was detected consistently among BalbC x C57/Bl6 mice grown under standard housing conditions, suggesting that it reflects the impact of a life-long developmental mechanism in the hippocampus.

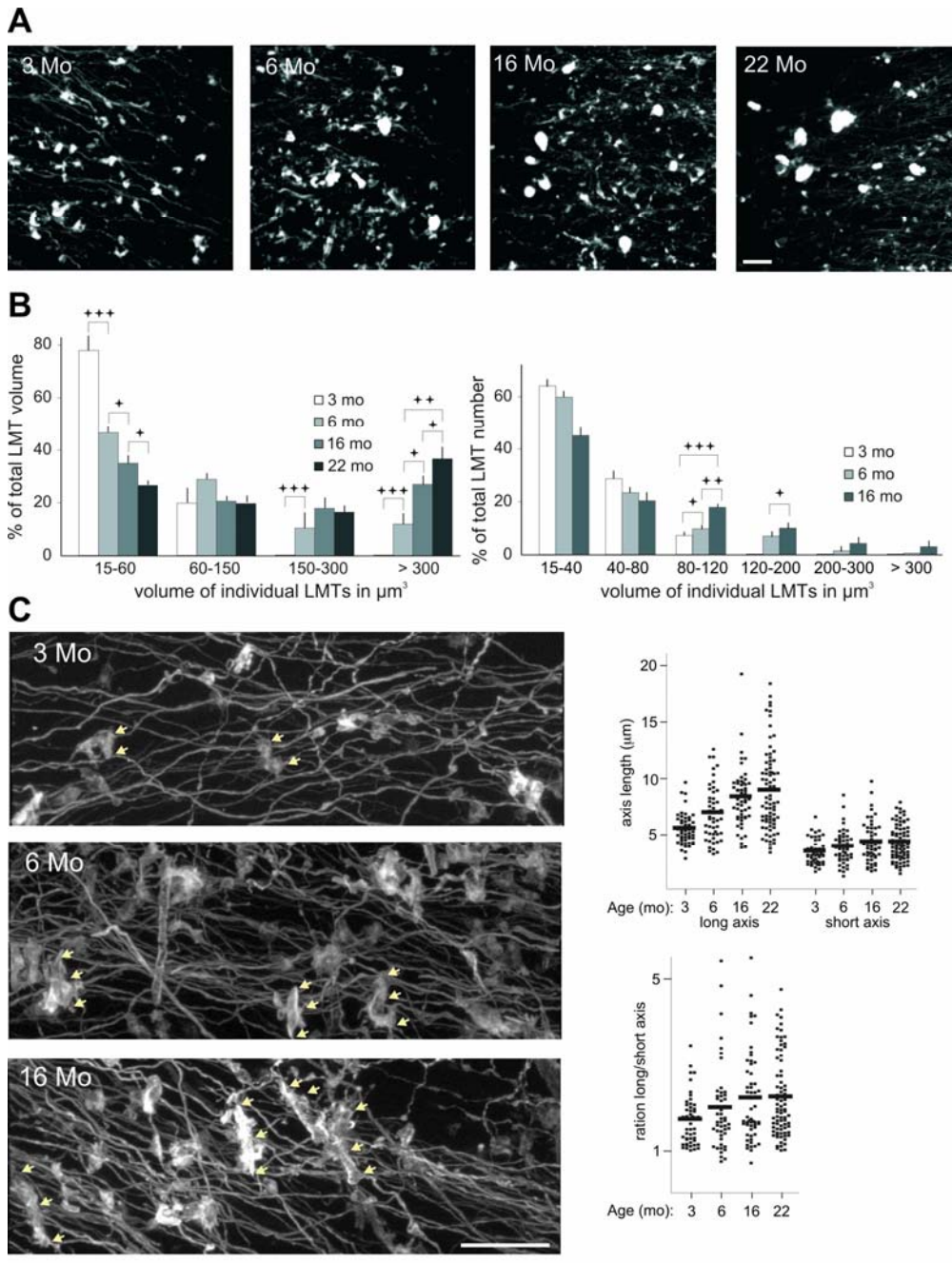
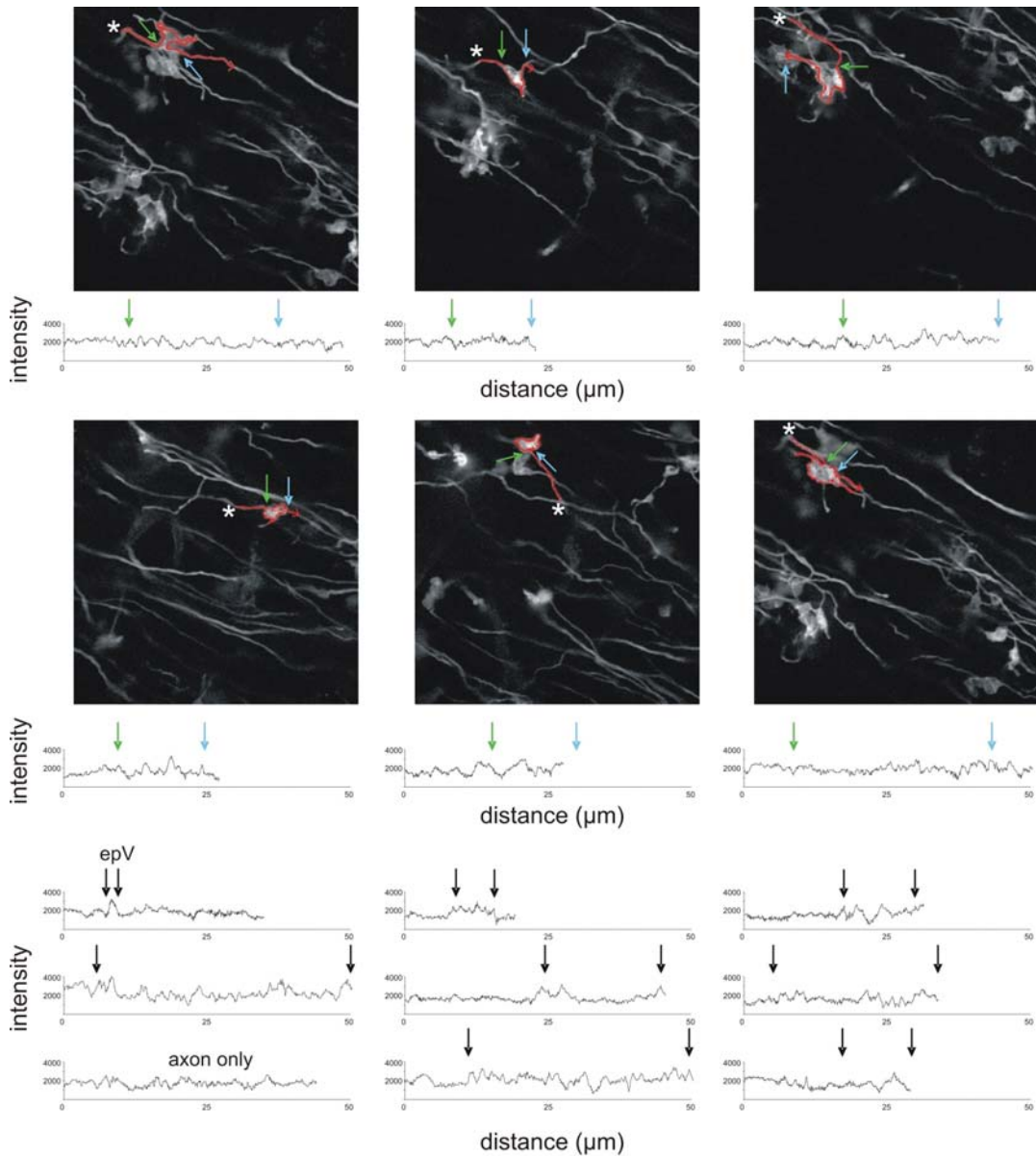


**Figure 2. Life-long expansion of hippocampal LMT subsets along pyramidal dendrites.**

**A:** Overview of LMT distributions in CA3a in male mice of different ages. Note higher incidence of large and very large LMTs in older mice. **B:** Quantitative analysis of LMT size distributions as a function of age (CA3a). Left: Overall contributions of LMTs grouped by volume to the total volume of LMTs in the sample. Note gradually increasing contribution of the larger LMTs (150-300, and > 300  $\mu\text{m}^3$ ) with increasing age. N= 9 cubes (from 3 male mice per age). One-way ANOVA:  $p < 0.001$  (15-60  $\mu\text{m}^3$ ),  $p = 0.45$  (60-150  $\mu\text{m}^3$ ),  $p < 0.05$  (150-300  $\mu\text{m}^3$ ),  $p < 0.001$  (>300  $\mu\text{m}^3$ ). Right: Relative prevalences of LMTs of different sizes as a function of age. N= 9 cubes (from 3 male mice per age). Post-hoc Student's t-test (left and right):  $p < 0.05$  (\*),  $p < 0.01$  (\*\*),  $p < 0.001$  (\*\*\*). A Tukey HSD post-hoc test confirmed these significance relationships. **C:** LMT arrangements in CA3a as a function of age. Note longitudinal expansions of larger LMTs parallel to pyramidal neuron dendrites. Cream arrows delineate the longitudinal extension of some of the largest LMTs in each panel (3 Mo: 2 LMTs; 6 and 16 Mo: 3 LMTs each). Quantitative analysis: N= 80 LMTs, 3 mice per age; bars: median values; short axis perpendicular to longest axis; one-way ANOVA:  $p < 0.01$  (ratio long/short). Scale bars: 25  $\mu\text{m}$ .



**Supplementary Figure 3. Homogeneity of axonal and LMT labeling by mGFP construct.**

Upper six panels: examples of confocal images and corresponding signal intensity plots for the membrane stretches indicated

by the red lines (6 months mouse). The following positions are indicated along the line, and again along the intensity plot: beginning of the trace (asterisk), beginning of LMT (green arrow), end of LMT (blue arrow). Lower nine histograms: more examples of membrane stretch intensities (mice: 6 months (first three), 16 months, and 22 months (last three)). Note that the signal intensity fluctuations do not change in amplitude or frequency along the membrane of axons or within LMTs. LMTs of different sizes, either from the same or distinct mice, and at different ages exhibited comparable intensity fluctuations, suggesting that mGFP did not accumulate selectively at LMT subsets. The variations in signal intensity appeared on a scale that was substantially smaller than the size of LMTs. Furthermore, changing thresholds in the volume rendering software, altered the sizes of individual objects to a comparable extent, without modifying the relative size differences of LMTs. Occasional areas of higher signal intensities within LMTs reflect highly convoluted membrane formations, which can be revealed by non-saturating imaging conditions (see Fig2A lower panels), and were also detected in the electron micrographs. Small areas of high membrane density and high signal intensity were detected at comparable frequencies at LMTs of different sizes, and from mice of different ages.

### **Experience-related increase of LMT-C complexities in adult mice**

To investigate the possibility that experience might influence LMT-C size distributions and/or complexities, we analyzed LMTs of mice housed under enriched environment (EE) conditions known to promote brain and hippocampal plasticity (van Praag et al., 2000), and compared them to those of littermates kept under standard housing (Ctrl) conditions (see Experimental procedures). We carried out three types of EE experiments: 1) in the main set of experiments, mice were kept in EE from P40 to P80, and analyzed at P80 (EE-P40/P80); 2) in a second set of experiments aimed at comparing the effects of age and EE on LMT morphologies, mice were kept in EE from 4 months to 15 months, and analyzed at 15 months (EE-4Mo/15Mo); 3) the third set of experiments was aimed at determining whether changes due to EE (from 1 month to 4.5 months) might be maintained when mice were returned to standard conditions (from 4.5 months to 6 months; EE-1Mo/4.5Mo-Ctrl6Mo). As shown in Fig. 3A, all three experimental conditions produced a significant shift in the prevalence of larger LMT sizes compared to controls. At first approximation, EE thus appeared to accelerate the effects of age on LMT size distributions. However, a more detailed analysis revealed that the effects of EE and age on LMT-C morphologies were qualitatively different. Thus, EE conditions did not produce a corresponding net elongation of LMTs (Fig. 3B), and specifically induced a pronounced increase in the complexity of LMT-Cs, as revealed by the higher incidence of LMT-Cs with satellites, and the higher numbers of satellites per LMT-C (Fig. 3C). This specific increase in LMT size and satellite numbers was accompanied by a specific increase in the length and complexity of postsynaptic thorny excrescences upon EE (Fig. 3D). Significantly, increasing age did not lead to a comparable increase in postsynaptic thorn lengths (Fig. 3D), and LMTs of EE-4Mo/15Mo mice exhibited more satellites and complex outlines than those of corresponding Ctrl mice (not shown). Taken together, these results provide strong evidence for the existence of experience-related rearrangements of LMT-C connectivity *in vivo*, and suggest that EE conditions and age exert distinct influences on LMT-C rearrangement processes.

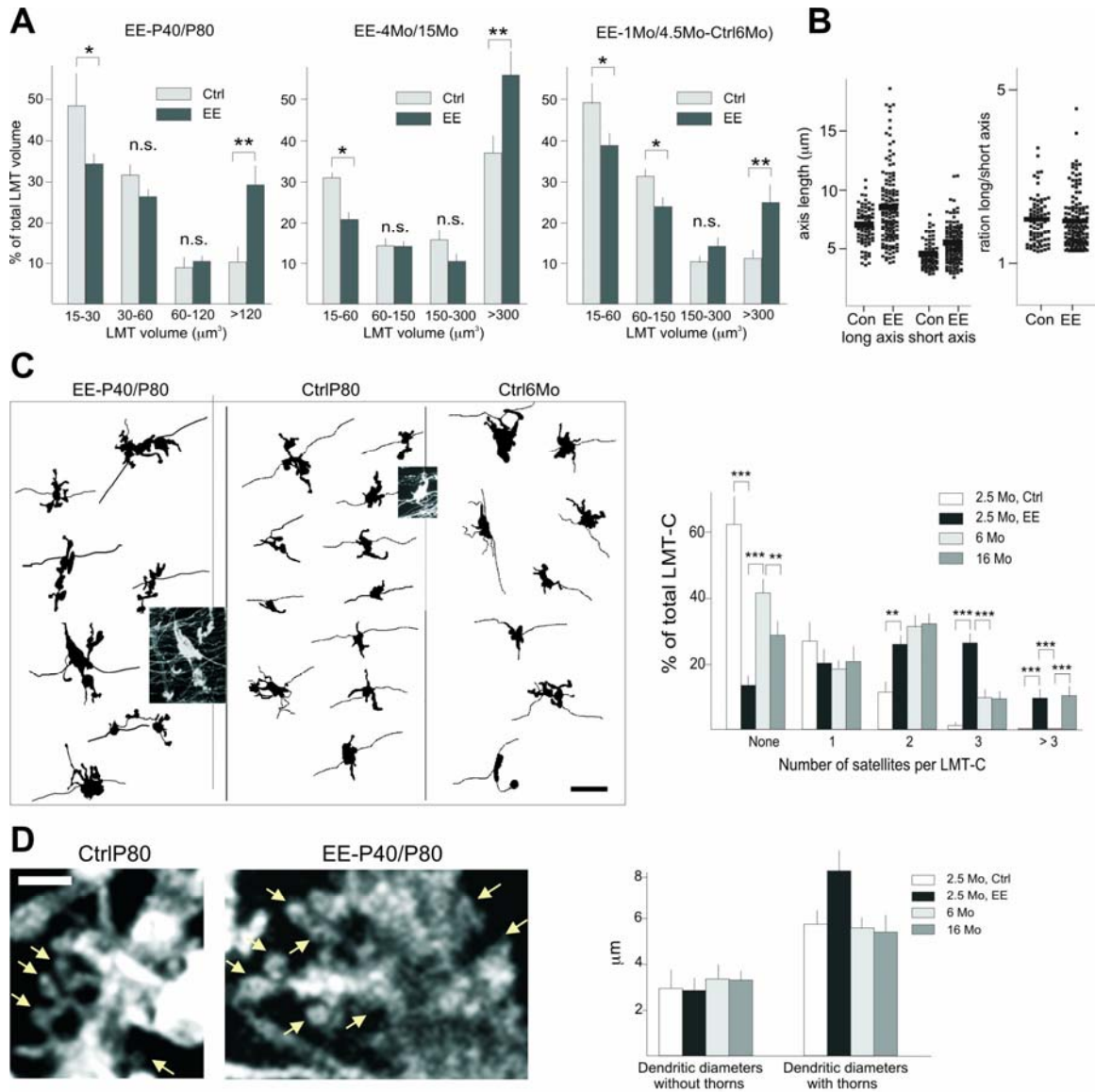


**Figure 3. Experience-related increase in the complexity of LMT-Cs.**

**A:** Quantitative analysis of LMT size distributions in the different EE protocols. Overall contributions of LMTs grouped by volume to the total volume of LMTs in the sample. Note how all EE experiments led to size distribution shifts resembling those induced by increasing age (compare to Fig. 2B, left). N=6 cubes (from 4 female mice each). Post hoc Student's t-test:  $p < 0.05$  (\*),  $p < 0.01$  (\*\*).

**B:** Quantitative analysis of long/short axis ratios in EE-P40/P80 versus control P80 mice. N=80 LMTs, 3 mice per condition; bars: median values; one-way ANOVA: non significant (ratio long/short).

**C:** Specific increase in the complexity of LMT-Cs induced by EE in vivo. Left: Camera lucida drawings of representative LMT-Cs (CA3a) from P80 mice, kept under EE (left) or Ctrl (center) conditions, and comparison to LMT-Cs from 6 months control mice. Note higher frequencies of satellites upon EE conditions. Right: Relative prevalences of LMT-Cs without and with satellites as a function of enriched environment and age. N=120 LMTs, from 3 female mice each.

**D:** Specific increase in thorny excrescence lengths and complexities upon EE conditions (CA3a). Left: High-magnification examples of thorny excrescences (mGFP signal; arrows point to some of the thorns). Right: Quantitative analysis of dendrite diameters excluding or including thorny excrescences (at clusters) as a function of EE and age. N=40 dendrites, from 2 female mice each. Bars: 15 (B), and 2 (C)  $\mu\text{m}$ .

### **Long-term rearrangements and growth of LMT-C subsets in slice cultures**

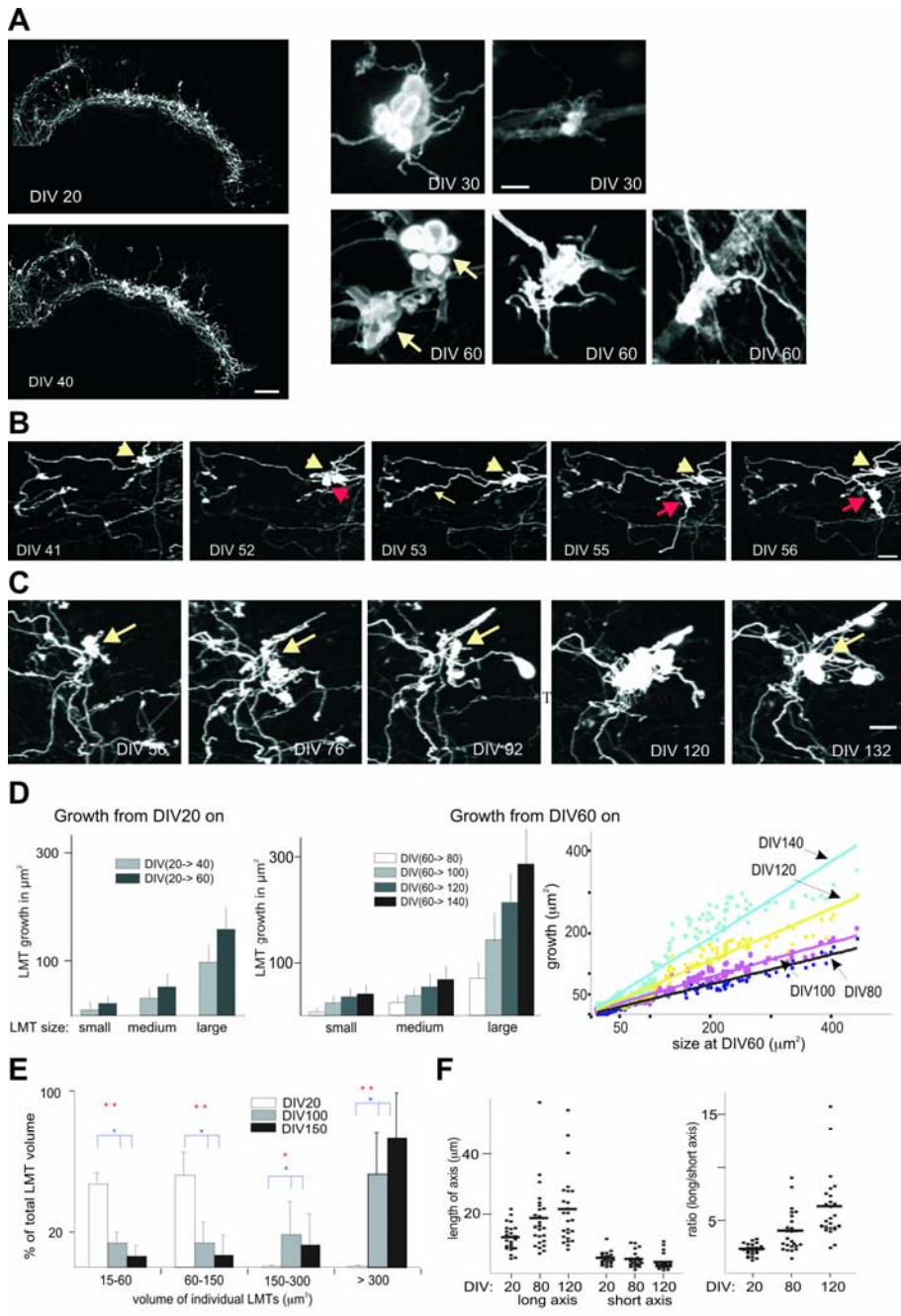
To investigate LMT-C rearrangements and their regulation in a more experimentally accessible system, we analyzed organotypic slice cultures from *Thy1-mGFP<sup>s</sup>* mice, where LMT-Cs can be imaged and treated in situ. The slices also allowed us to analyze entire sets of LMTs belonging to individual axons. In these cultures, LMT-Cs exhibited subcomponent arrangements, satellites and diversities comparable to those detected in vivo (Fig. 4A-C). Since we found that neurogenesis was extremely rare under our culture conditions (a total of 2 BrdU/calretinin double-positive cells out of 8 slices; BrdU labeling at day in vitro (DIV) 6, analysis at DIV9 or DIV16), age differences among individual granule cells could not account for the dramatic differences in LMT-C morphologies. Furthermore, comparable LMT-C diversities, including satellites were also detected when non-transgenic slice cultures were transfected with a cytosolic RFP construct (cRFP, see Fig. 6A), ruling out the possibility that the LMT-C morphologies were a property of transgene positive granule cells in *Thy1-mGFP<sup>s</sup>* mice, or due to the activity of the Thy1 promoter in granule cells.

In order to capture any type of morphological plasticity by mossy fibers, we acquired high-resolution images of entire mossy fiber projections in CA3a-c (Fig. 4A) during periods ranging from a few days to several (up to 5) months. We found that when viewed at intervals of 3-5 days and more, many LMT-Cs exhibited dramatic alterations in their morphology (Fig. 4B, C). In contrast, even when mossy fibers were imaged for up to 3-4 months, we did not detect new process outgrowths from the mossy fiber axon itself. Instead, axonal dynamics was confined to remodeling and outgrowth events from LMT-Cs (the only exceptions were occasional short filopodial outgrowths from en-passant varicosities (De Paola et al., 2003), which are presynaptic terminals by mossy fibers onto inhibitory interneurons). In addition to changes in the shape and size of individual LMTs, we noticed that a fraction of LMT-Cs exhibited dramatic large-scale structural plasticity (Fig. 4B); this plasticity included process outgrowth or retraction events of up to more than 120  $\mu\text{m}$  per day, and the rapid formation or loss of satellite LMTs (Fig. 4B). These satellite rearrangements frequently led to the establishment or dismantling of contacts

with distinct CA3 pyramidal neurons (Suppl. Fig. 4; in 5/5 investigated cases, the new contacts exhibited Bassoon-positive clusters (not shown, but see Fig. 5D)).

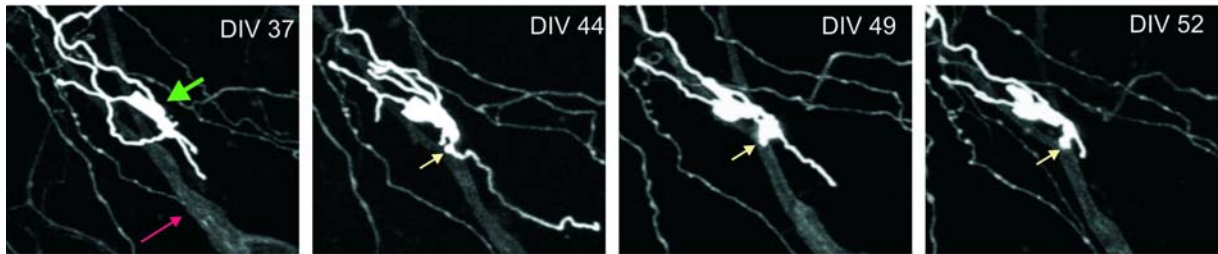
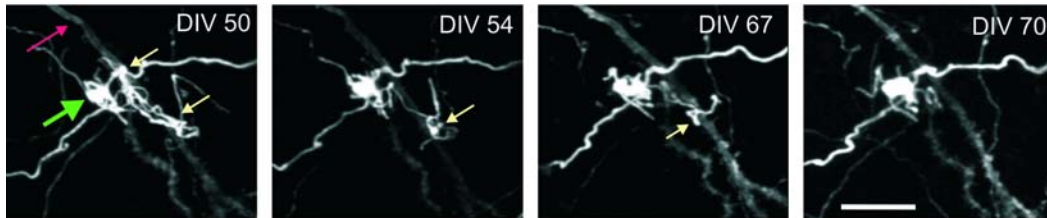
To determine whether LMT-C remodeling might lead to sustained changes in the arrangement and/or sizes of LMT-Cs in CA3 as a function of time, we repeatedly imaged the same mossy fibers and their identified individual LMT-Cs at 20 days intervals for periods of up to 4 months. We found that disappearance or appearance events, in which an entire LMT-C could either not be detected anymore at two subsequent imaging sessions, or appeared after DIV20, were not frequent (disappearances: 76/1500; appearances: 58/1500 LMT-Cs). Instead, many preexisting LMT-Cs grew in size during many months in slice cultures (Fig. 4C, D). To analyze the growth properties of LMT-Cs, we computed size differences for large sets of individual LMT-Cs as a function of time. Only LMT-Cs detectable throughout the entire experimental period were included in the analysis. Grouping of the results according to the absolute sizes of LMT-Cs at the first observation time revealed a net and sustained increase in the average sizes of persisting LMT-C over time in the slices, which was much more pronounced for larger LMT-Cs (Fig. 4D). A regression analysis revealed that the absolute magnitudes of LMT-C growth were strongly correlated to the initial sizes of individual LMT-Cs, but not to the actual sizes of LMT-Cs at successive imaging sessions (Fig. 4D). In a way strikingly reminiscent to the shifts of LMT sizes in vivo, LMT-C rearrangements in slices led to a gradual increase in the contribution by the largest LMT-Cs to total LMT-C volume (Fig. 4E). In further analogy to LMTs in vivo, LMT growth in slices mainly involved elongation, leading to a significant increase in the long-to-short axis ratio of LMTs with time in vitro (Fig. 4F). The fastest growing LMT-Cs also remodeled on a larger scale than the smaller LMT-Cs (not shown), suggesting that they exhibited stronger anatomical plasticity properties. LMT-C growth was not a consequence of the live imaging procedure, since slice cultures imaged for the first time at ages ranging from 20 days to 4 months in vitro exhibited average LMT-C sizes that were comparable to those that had been determined when following identified LMT-Cs longitudinally for a corresponding period of time in vitro (not shown). In addition to this presynaptic growth, and consistent with a net increase in active zone numbers (see Fig. 5D, E), we also detected remodeling,

growth and increased complexity of individual thorny excrescences (see Suppl. Fig. 5 for an example). We conclude that subsets of LMT-Cs rearrange extensively in organotypic slice cultures, altering the sets of pyramidal neurons with which they establish contacts through satellites, and consistently growing in size over many months. The arrangements and heterogeneities of LMT-Cs in slice cultures thus closely resemble those in vivo, and their remodeling and expansion properties exhibit features consistent with those inferred from comparing mice of different ages or housing conditions.



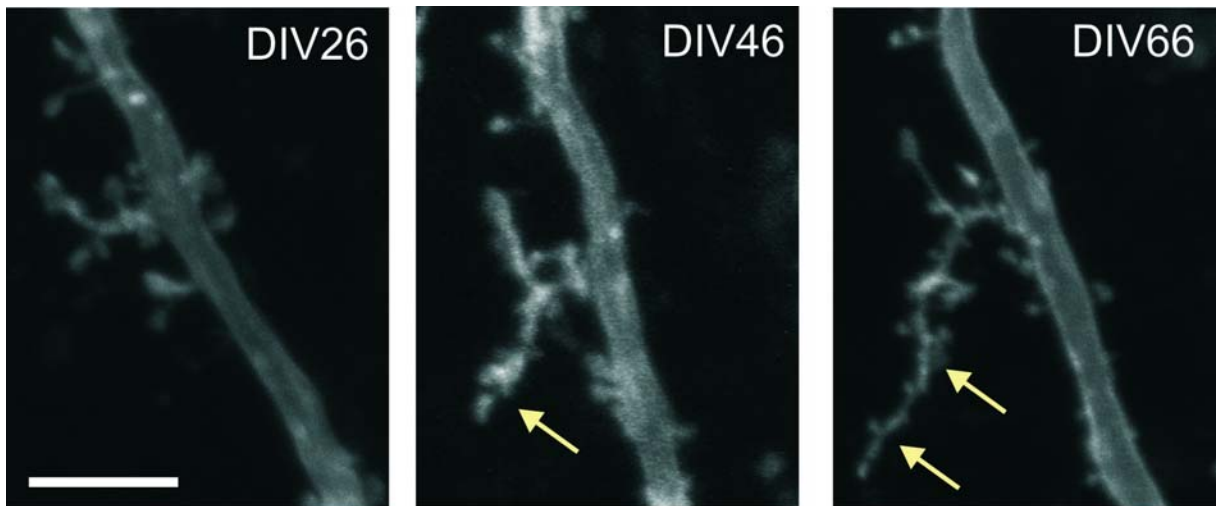
**Figure 4. Rearrangements and growth of LMT-C subsets in organotypic slice cultures.**

**A:** Left: Overview of an entire mossy fiber projection at DIV20 and DIV40. The dentate gyrus is to the left. Note growth of several LMTs. Right: Complexity and diversity of LMT-Cs in slice cultures. The images are maximum intensity projections (MIP), or raw data. The two LMTs in the lower left panel (DIV60, arrows) belong to the same complex. **B:** Large-scale anatomical plasticity at one LMT-C in CA3a (cream arrow). Note outgrowth of a long process within one day (DIV52 to DIV53; thin cream arrow), and formation of satellite LMTs (red arrows). **C:** Rearrangements and growth of a large LMT-C (cream arrow) from DIV56 to DIV132. **D:** Quantitative analysis of LMT-C growth in slice cultures. Left, and middle panel: Sizes of individual identified LMT-Cs that persisted throughout the analysis were compared at the indicated times, and LMT-Cs were then grouped into small ( $< 30 \mu\text{m}^2$ ), medium ( $< 60 \mu\text{m}^2$ ) and large ( $\geq 60 \mu\text{m}^2$ ), according to their sizes at DIV20.  $N=50$  identified LMT-Cs each, from 5 slice cultures. Right: Linear regression analysis of identified LMT-C sizes between DIV60 and DIV140. Linear correlation values ( $R^2$ ): 0.95 (DIV80), 0.95 (DIV100), 0.92 (DIV120), 0.88 (DIV140). **E:** LMT-C volume distribution as a function of age. Contribution of LMT-C size groups to the total volume of LMT-Cs in slice cultures (comparable to the data of Fig. 2B).  $N=5$  cubes, from 5 slices. One-way ANOVA (orange asterisk):  $p<0.05$  (\*),  $p<0.01$  (\*\*). Post-hoc t-test (blue):  $p<0.05$  (\*). **F:** Quantitative analysis of long/short LMT axis as a function of age in vitro.  $N=20$  LMTs, from 5 slices; bars: median values; one-way ANOVA:  $p<0.001$  (ratio long/short). Bars: 100 (A, left), 5 (A, right), and 10  $\mu\text{m}$  (B, C).

**A****B**

**Supplementary Figure 4. Examples of LMT-C outgrowths establishing satellites on distinct pyramidal neurons in CA3a stratum lucidum.**

Green arrows: main LMT; red arrows: mGFP-positive pyramidal neuron dendrite. Physical contacts were analyzed using Imaris (3D) software. A: Example of new contact. This LMT-C did not contact the mGFP positive dendrite at DIV37. A contact was detectable at DIV44 (cream arrow), and a distinct LMT subunit (cream arrows) was maintained beyond DIV52. This LMT-C is linked to its mossy fiber (short segment just visible at upper left corner, DIV52 panel) through a ca. 35  $\mu$ m side-branch. B: Example of contact loss. The LMT-C contacts the mGFP positive dendrite at two positions (cream arrows) through satellites at DIV50. One of the contacts has been lost at DIV54, and the second one is lost between DIV67 and DIV70. Bar: 15  $\mu$ m.



**Supplementary Figure 5. Elongation and increased complexity of a large thorny excrescence in slice culture (mGFP signal).** Note how the thorny excrescence has elongated at DIV46 and DIV66 (arrows). Shorter thorny excrescences along this pyramidal neurons dendrite in CA3 exhibit smaller changes. Bar: 10  $\mu$ m.

### **Larger LMTs produce a stronger excitation of postsynaptic pyramidal neurons**

Do LMT-C rearrangements and growth lead to changes in the functional connectivity of individual LMT-Cs? To determine whether larger LMTs might differ from smaller LMTs with respect to the strength of their output onto pyramidal neurons in CA3, we carried out intracellular pair recording experiments in slice cultures (DIV20-30). One mGFP-positive granule cell was recorded and stimulated under current-clamp mode and a second electrode filled with sulforhodamine or Lucifer-yellow was used to label CA3 pyramidal cell dendrites present in the close vicinity of one of its core LMTs (either its largest core LMT, or a smaller core LMT; see Experimental procedures). These CA3 neurons were then recorded under voltage clamp, and tested for monosynaptic connectivity to the mGFP-positive granule cell. In this way, we achieved intracellular pair-recordings among synaptically connected granule cells and pyramidal neurons in about 10% of the attempts (Fig. 5A; see Methods). We found that DCG-IV-sensitive (Ishida et al., 1993) excitatory postsynaptic responses evoked by granule cell stimulation were substantially stronger at larger LMTs than at the smaller LMTs (Fig. 5A). Significantly, the paired-pulse facilitation and frequency-dependent facilitation properties of large and small LMTs were not detectably different (Fig. 5B, C), suggesting that smaller (weaker) and larger (stronger) LMTs exhibit proportional short-term presynaptic plasticity, and that the greater synaptic strength might reflect a larger number of active zones in larger LMTs. To determine whether and how differences in the sizes of LMTs might reflect differences in numbers of synaptic release sites, we analyzed Bassoon-positive active zones (tom Dieck et al., 1998) in individual LMTs (Fig. 5D, E). We found that all elements of LMTs contained numerous active zones (Fig. 5D, see also Suppl. Fig. 2), and that LMT sizes and active zone numbers were closely correlated independent of time in culture (Fig. 5E). We found comparable correlations between LMT volumes and active zone numbers for LMTs and their satellites in vivo (N.G. and P.C., unpublished results). We conclude that the large variations among LMT sizes reflect corresponding variations in active zone numbers, that the expansion of LMT-Cs over time reflects an increase in the number of release sites at those LMT-Cs, and that the establishment of satellites reflects the addition of release sites by the LMT-C onto the same or new postsynaptic pyramidal neurons in CA3. Taken together, the results thus suggest that the profound anatomical

rearrangements of individual LMT-Cs in slice cultures reflect corresponding rearrangements of their local connectivities onto pyramidal neurons in CA3.

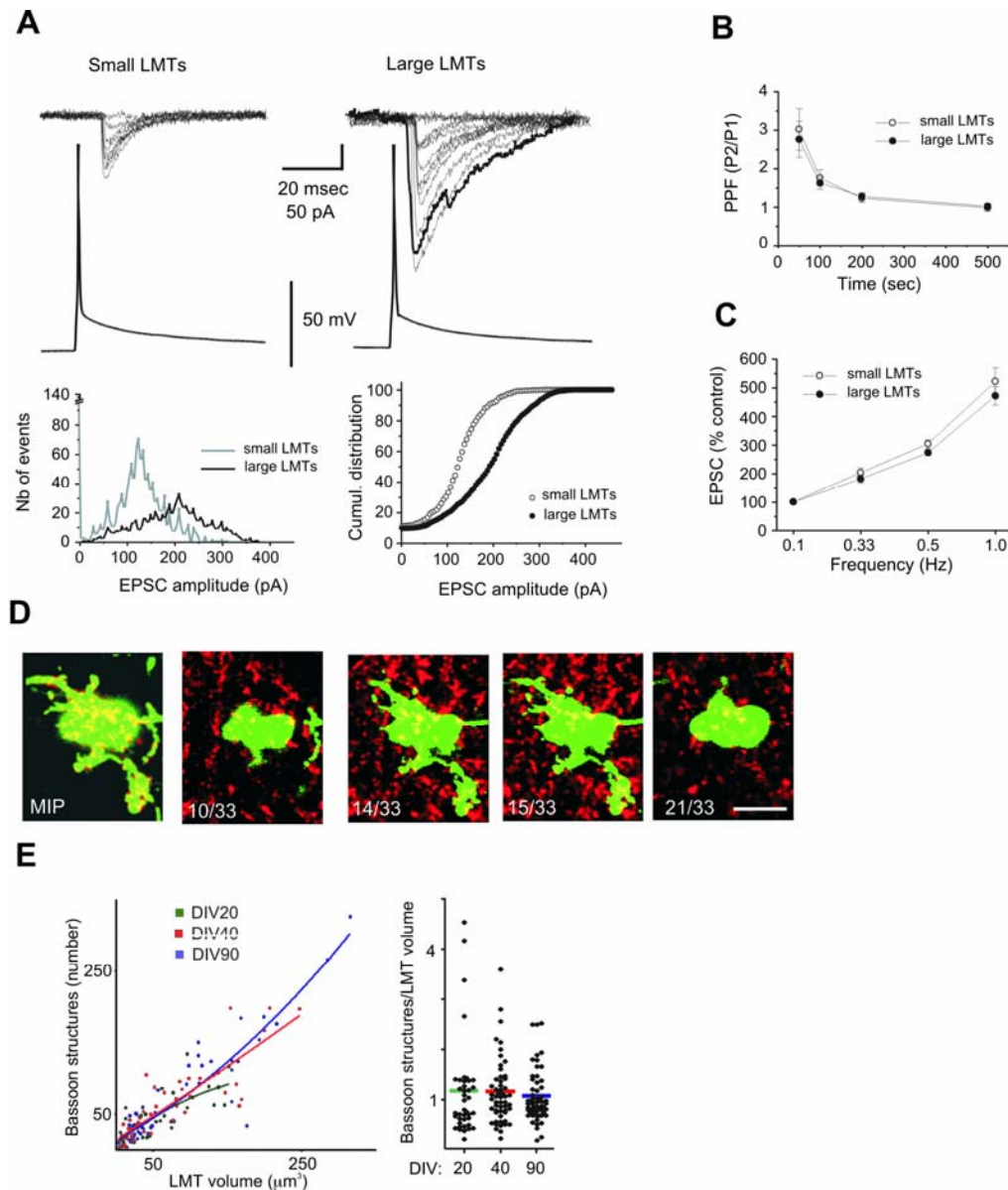


**Figure 5. Larger LMTs elicit stronger postsynaptic responses in pyramidal neurons and have more active zones.**

**A:** Monosynaptic CNQX-sensitive responses recorded in CA3 pyramidal neurons upon intracellular stimulation of mGFP-positive granule cells in DIV20-30 slice cultures. Top: ten superimposed recordings for small and large LMTs. Bottom: Amplitude distribution histogram (left) and cumulative plot of evoked amplitudes for the same set of data. Holding potential:  $-70\text{mV}$ ; Bicuculine  $10\ \mu\text{M}$ , D-AP5  $80\ \mu\text{M}$ . Small LMTs:  $8\text{-}25\ \mu\text{m}^2$ ; large LMTs:  $80\text{-}150\ \mu\text{m}^2$ . Total of evoked currents: 1264 (small LMTs) and 923 (larger LMTs). **B:** Paired-pulse facilitation does not differ when recorded in large or small LMTs.  $N=5$ ,  $p>0.1$ . **C:** Frequency-dependent facilitation does not differ in small and large LMTs. Data normalized to  $0.1\text{Hz}$  values. Averages of 15 traces each;  $N=5$ ,  $p>0.1$ . **D:** Distribution of active zones within an LMT-C with a satellite (DIV80); Bassoon immunocytochemistry red; mGFP green. Left: MIP; Bassoon labeling outside the LMT was cropped out. Right panels: single confocal planes (33 planes total; plane distance  $0.3\ \mu\text{m}$ ). Note presence of active zones throughout the LMT and in its satellite. Bar:  $5\ \mu\text{m}$ . **E:** Contents of Bassoon-positive structures (active zones) as a function of LMT volume and age in vitro. Left: regression analysis; the lines are polynomial fits. Note comparable, and near to linear relationships between LMT volume and active zone contents at DIV20, 40 and 90. Right: Active zone number/LMT volume ratios; bars: median values;  $N=80$  LMTs per condition. One-way ANOVA:  $p=0.76$  (i.e. no differences as a function of age).

### **Different LMT-Cs belonging to the same mossy fiber exhibit distinct plasticity properties**

What underlies the dramatic differences in LMT-C arrangements, sizes and anatomical plasticity in slice cultures? One possibility was that differences in LMT sizes might reflect differences among granule cells and their mossy fibers. Alternatively, LMT-Cs belonging to the same mossy fiber might differ among each other. To address this issue, we first analyzed a large set of individual mossy fibers, focusing on the relative sizes of their LMT-Cs, and on whether or not they established satellites. To our surprise, we found that for the majority of mossy fibers (34/40) one LMT-C was at least three times as large as any of the remaining LMT-Cs along the same mossy fiber, which tended to exhibit more comparable sizes (Fig. 6A-C). These size relationships among the LMT-Cs of a given mossy fiber were detectable for slice cultures of any age beyond 5DIV (not shown), and were not restricted to granule cells exhibiting Thy1-driven mGFP expression (Fig. 6A).

We next reasoned that mossy fibers might exhibit some larger LMT-Cs at any given time, but that their position might change with time, in parallel with LMT-C remodeling and growth; alternatively, individual “plastic LMT-Cs” might maintain their growth properties and augment their relative sizes over time. We therefore carried out longitudinal studies, in which we followed all individual LMT-Cs of identified mossy fibers over months in slice cultures. We found that individual “plastic LMT-Cs” maintained this distinguishing property over months in culture, when they kept growing more than the smaller LMT-Cs (Fig. 6B, C). This led to a gradual shift of the total presynaptic volume of individual axons towards the largest LMT-C (Fig. 6E). Since “plastic LMT-Cs” also recovered more effectively from treatments that reversed LMT-C growth (see below; Fig. 6D), we concluded that the large differences in the plasticity and growth of LMT-Cs reflect local properties of individual LMT-Cs.

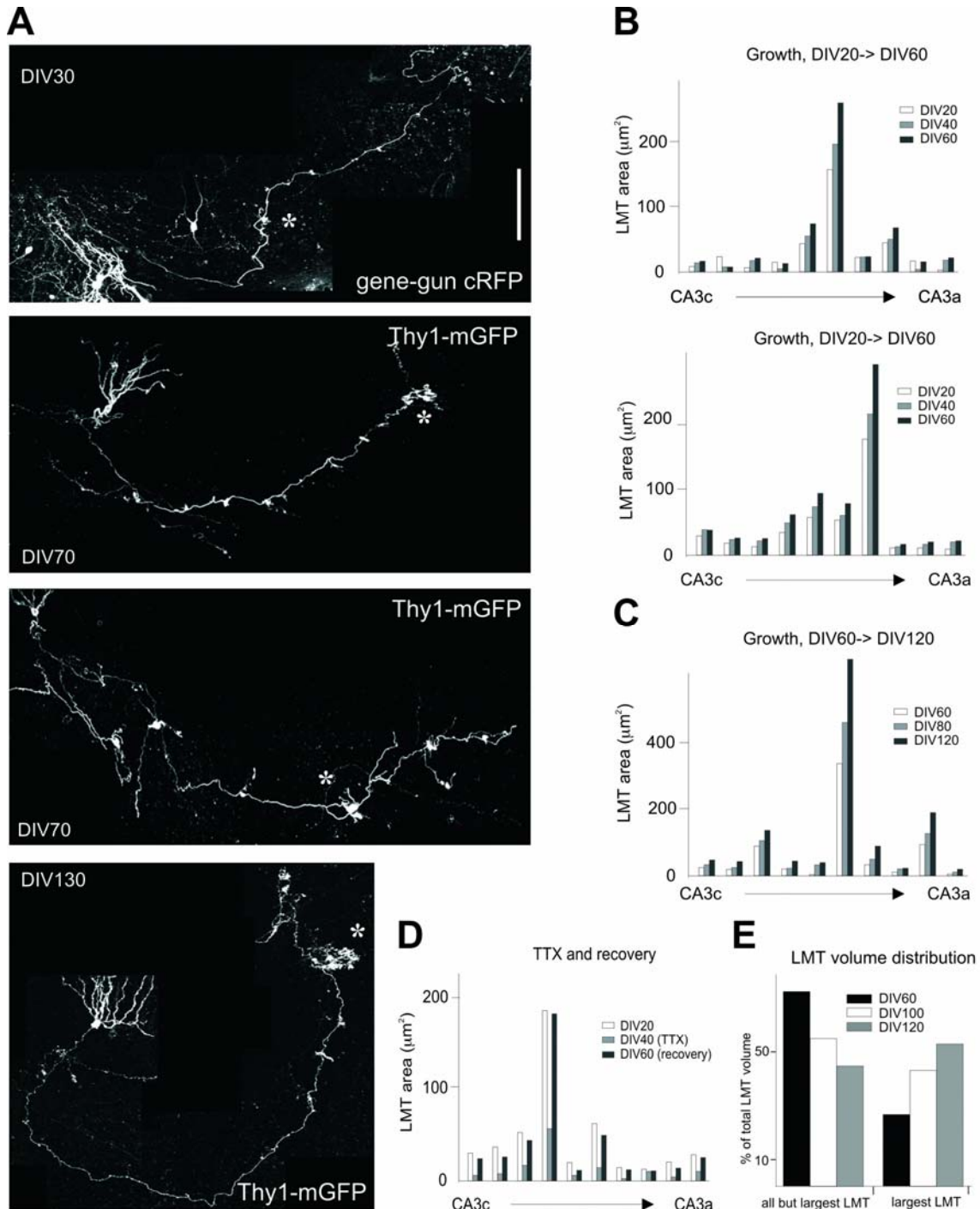


**Figure 6. Plasticity and growth are specific properties of individual LMT-Cs, not mossy fibers.**

**A:** Top: Example of mossy fiber from non-transgenic DIV30 slice expressing cRFP (gene-gun transfection); Middle and bottom: examples of DIV70 (two of them) and DIV130 (one) slice cultures, each with one well-labeled mGFP-positive granule cell. Cell bodies and dendrites are to the left; asterisk: position of the largest LMT-C. The cRFP expressing mossy fiber exhibits its largest LMT-C within the infrapyramidal projection; as expected, the largest LMT-C at DIV30 is smaller than those at DIV70, which are smaller than that at DIV130. **B-C:** Growth of individual LMTs between DIV20 and DIV60 (b), or DIV60 and DIV120 (c). Each graph represents one mossy fiber and its individual LMTs (CA3c to the left). **D:** Larger LMTs maintain this distinction when recovering from shrinkage induced by TTX, Experimental conditions as described for Fig. 7. **E:** Redistribution of total LMT volume as a function of age in vitro between largest LMT-C, and remaining LMT-Cs belonging to the same axon. Median values from 3 individual axons. Bar: 140  $\mu\text{m}$ .

### **Local, activity-dependent regulation of LMT-C maintenance and growth**

To investigate the mechanisms regulating LMT-C remodeling and growth, we carried out pharmacological experiments in slice cultures. Experimental conditions consisted of acquiring one set of images at DIV20 (control conditions), of including pharmacological agents to the culture medium during the next 20 days, of a second imaging session at 40DIV, followed by returning slices to control medium conditions. Further imaging at 60DIV and 80DIV was carried out to verify that any drug effect was reversible. In additional experiments aiming at excluding effects restricted to comparatively young slice cultures, we also carried out treatment experiments starting at 60DIV.

Under control conditions, current-clamp recordings of granule cells in slice cultures showed a level of background firing activity in the range of 3-3.5 Hz with occasional bursts of action potentials very much consistent with the firing properties reported in vivo (e.g. Penttonen et al., 1997). We found that the inclusion of a TTX dose sufficient to completely and reversibly block spiking activity in the slices (not shown) not only blocked LMT-C growth, but led to a substantial reduction in LMT-C average sizes in both, young (DIV20) and more mature (DIV60) slices (Fig. 7A, B). This reduction affected both the sizes of individual LMTs and the number of satellites by LMT-Cs (not shown). It was accompanied by a corresponding reduction in the number of active zones per LMT (i.e. average numbers of active zones per LMT volume were not affected by TTX; Fig. 7C), indicating that it reflected a net decrease in the number of release sites in the slices. The inhibitory neurotransmitter GABA also induced LMT-C shrinkage (Fig. 7B). The absolute extent of LMT-C shrinkage in the presence of TTX or GABA (or DCG-IV, see below) was closely correlated to LMT-C size (Fig. 7B), suggesting that both growth and maintenance of “plastic LMT-Cs” depend on spiking activity. Shrinkage of LMT-Cs in the presence of TTX was reversible (Fig. 7B). Significantly, larger LMT-Cs resumed growth at higher rates than smaller LMT-Cs when recovering from the TTX treatment, and this again applied to both populations of identified LMT-Cs (Fig. 7B), and the individual LMT-Cs of identified mossy fibers (Fig. 6D).

To determine whether transmitter release from LMTs is required to sustain LMT-C growth, we carried out experiments in the presence of the mGluR2 agonist DCG-IV (Ishida et al., 1993), which produces a specific and complete blockade of evoked transmitter release from LMTs in hippocampal slices (Kamiya et al., 1996). We found that DCG-IV was as effective as TTX in reversibly suppressing LMT-C growth and inducing LMT shrinkage (Fig. 7A, B). Interestingly, and unlike TTX, DCG-IV produced an over-proportional decrease in the number of active zones per LMT (Fig. 7C). We conclude that LMT-C growth and maintenance depend on spiking activity in the slices, and on the local release of transmitter from LMTs.

Long-term potentiation at mossy fiber to pyramidal neuron synapses in CA3 is NMDA receptor independent, PKC dependent, and predominantly controlled presynaptically. To determine whether signaling pathways related to the induction of LTP at these synapses might influence LMT growth and maintenance in slices, we carried out experiments in the presence of the specific inhibitor of PKC Chelerythrine. We found that the PKC inhibitor augmented growth at small LMTs, but caused shrinkage at large LMTs (Fig. 7D). At closer inspection, the growth of small LMTs was not distributed equally among many small LMTs, but instead led to the emergence of 1-2 larger LMTs, concomitant with shrinkage of the original large LMTs (not shown). In contrast, and in keeping with its lack of effect on synaptic plasticity at mossy fiber to pyramidal neuron synapses, the NMDA receptor antagonist APV did not significantly affect LMT growth (Fig. 7D). We conclude that differences among the growth properties of individual LMT-Cs are maintained across conditions allowing or preventing growth at all LMTs, suggesting that the relative extent of LMT growth is regulated locally at individual LMTs. However, this maintenance of LMT asymmetry depends on PKC activity, suggesting that whether a particular LMT grows over-proportionally might be affected by conditions influencing functional plasticity at these synapses.

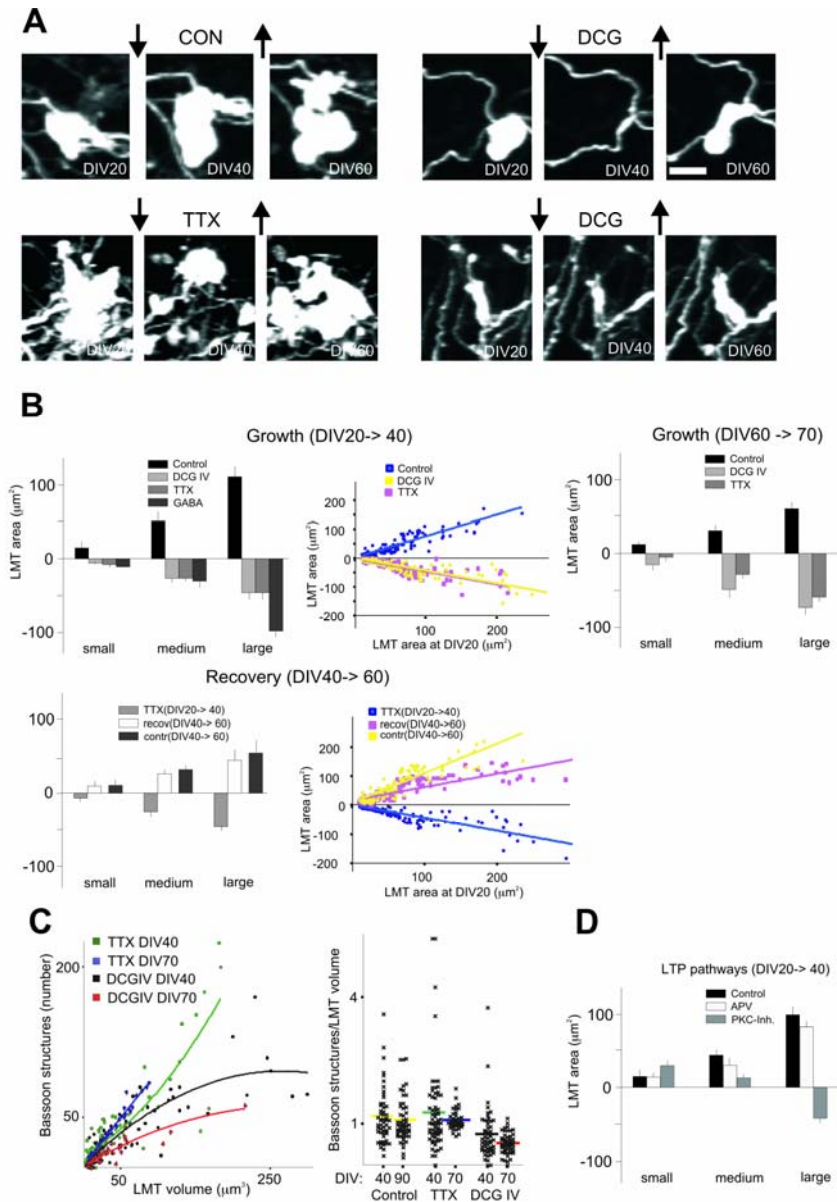


**Figure 7. Regulation of LMT-Cs maintenance and growth by spiking activity, mGluR2 and PKC.**

**A:** Reversible shrinkage of LMT-Cs in the presence of either TTX, or the mGluR2 agonist DCG-IV. Drugs were added to the slice medium just after the first imaging session at DIV20 (arrows pointing down), and washed out just after the second session at DIV40 (arrows pointing up). CON: medium change without added drugs. **B:** Quantitative analysis of LMT growth in the presence or absence of TTX, DCG-IV or GABA. Upper row: Shrinkage of LMT-Cs in the presence of drugs. Left and middle: Experimental conditions as in (A). Left: grouping of identified LMT-Cs according to sizes as described for Fig. 4. Middle: regression analysis of LMT-C growth versus LMT size at DIV20. Linear regression correlations ( $R^2$ ): 0.85 (control), 0.81 (TTX), 0.86 (DCG-IV). Right: Drug-induced shrinkage of LMT-Cs in 2-months cultures. TTX or DCG-IV were added at DIV60, and their effects were analyzed at DIV70. Grouping of identified LMT-Cs as described for Fig. 4. Lower row: Recovery of LMT-C growth upon washout of TTX. Left and middle panel as described above. Linear regression correlations ( $R^2$ ): 0.80 (DIV40, TTX), 0.78 (recovery TTX, DIV60), 0.78 (control DIV60). Growth values for control conditions are included for comparison (dark bars). N=50 LMT-Cs per size group, from 5 slice cultures. **C:** Active zone contents of LMTs in the presence of TTX or DCG-IV, as a function of LMT volume and age in vitro. Values are for 20 days (DIV40) or 10 days (DIV70) in the presence of drug. Left: regression analysis of LMT volume versus active zone numbers for different experimental conditions. The curves are polynomial fits. Right: distribution of active zone per LMT volume values. Note how DCG-IV induces an over-proportional reduction in the numbers of active zones per LMT volume. N=50 LMT-Cs per size group, from 5 slice cultures. One-way ANOVA for TTX versus DCG-IV:  $p < 0.01$ . **D:** Effect of PKC inhibitor Chelerythrine and NMDA receptor antagonist APV on LMT maintenance and growth. Experimental conditions and grouping of data as described in (B, upper row, left). N=50 LMT-Cs per size group, from 5 slice cultures. The effects of the PKC inhibitor (see text) were significant for all LMT size categories:  $p < 0.01$  (small),  $p < 0.05$  (medium),  $p < 0.001$  (large); Student's t-test. Bar: 10  $\mu\text{m}$ .

#### **2.1.4. DISCUSSION**

In this study we provide evidence that functionally important presynaptic complexes in the hippocampus rearrange their local connectivities throughout life, and that these rearrangements are influenced by experience and age. We first show how LMT-Cs are local presynaptic terminal arborizations of mossy fibers, exhibiting large differences in the magnitude and divergence of their local connectivities with pyramidal neurons in CA3. We then provide two independent lines of evidence that LMT-Cs rearrange their connectivities in the adult: we show that subsets of LMT-Cs expand along CA3 dendrites throughout life, and that the complexities of LMT-Cs are dramatically enhanced by housing mice in an enriched environment. We then analyze identified LMT-Cs longitudinally in organotypic slice cultures, and show that: 1) the arrangements and heterogeneities of LMT-Cs in slice cultures resemble closely those in vivo; 2) subsets of LMT-Cs rearrange their connectivities, and grow over weeks and months in slice cultures in patterns resembling those detected in vivo; 3) the anatomical rearrangements reflect corresponding rearrangements in functional connectivity; 4) the marked differences with respect to plasticity and growth reflect local properties of individual LMT-Cs, not their mossy fibers; 5) LMT-C growth and maintenance require spiking activity in the slices, and mGluR2-sensitive transmitter release from LMTs; 6) the stable maintenance of LMT-C size heterogeneities involves PKC activity. Below, we discuss the implications of these findings and their relationship to those from previous studies, focusing on the rearrangements of LMT-C connectivity, the regulation of these processes by synaptic activity and experience, and their possible impact on hippocampal network activity.

##### **Rearrangements of LMT-C connectivity in the adult**

Our results provide novel insights into the organization of mossy fiber terminals in CA3. While the complexity of LMTs had been documented by previous studies (Chicurel and Harris, 1992; Danzer and McNamara, 2004; Gonzales et al., 2001), imaging using *Thy1-mGFP<sup>s</sup>* mice has revealed unsuspected further features, including the existence of satellite LMTs, a great diversity of sizes and morphologies, and the massive sizes of some of these terminals. It does not seem surprising that the satellites have been missed by previous studies, as they would have been very difficult to detect using electron

microscopy or traditional fill methods. Furthermore, most previous studies have focused on LMTs from young animals (ca. 3 weeks), when diversity and complexity are less pronounced. In a further departure from the results of previous studies, we provide evidence that individual LMT-Cs can contact several distinct pyramidal cells in CA3. Based on these results, we propose that instead of terminal boutons, LMTs should be considered as local terminal arborization complexes of mossy fibers (LMT-Cs), exhibiting great diversity in their sizes, and in their degrees of divergence onto pyramidal neurons in CA3. Although the satellites can clearly contact distinct pyramidal neurons, do exhibit numerous Bassoon-positive active zones, and are highly enriched in Synapsin I and synaptic vesicle markers (not shown), their functional status remains to be investigated. The recent demonstration that LMT membranes contain voltage-gated Na-channels and amplify action potentials (Engel and Jonas, 2005) is certainly consistent with the notion that the interconnected compartments of LMT-Cs can be efficiently triggered to release transmitter. Detailed functional investigations of these compartments should yield valuable novel insights into the function of these complex terminal structures.

We provide evidence that subsets of hippocampal LMT-Cs are sites of considerable anatomical plasticity in adult mice. This is consistent with results from recent studies, which have provided evidence for structural plasticity of presynaptic terminals in hippocampal slice cultures (De Paola et al., 2003), and in adult mouse barrel and visual cortex in vivo (De Paola et al., 2006; Stettler et al., 2006). A critical advance over previous studies is, however, that the structural plasticity of LMT-Cs leads to long-term rearrangements of local connectivity, suggesting that it might be an important aspect of hippocampal circuit plasticity in the adult. The rearrangements affected LMT-C connectivity in two distinct ways: 1) expansions along dendrites from the same pyramidal neuron added transmitter release sites, presumably altering the functional impact of mossy fiber spiking onto that particular postsynaptic pyramidal neuron in CA3; 2) the establishment of satellite LMTs onto distinct pyramidal neurons added and/or removed postsynaptic targets to individual LMT-Cs, altering the extent and quality of local divergence of pyramidal neuron innervation by individual LMT-Cs (Fig. 8).

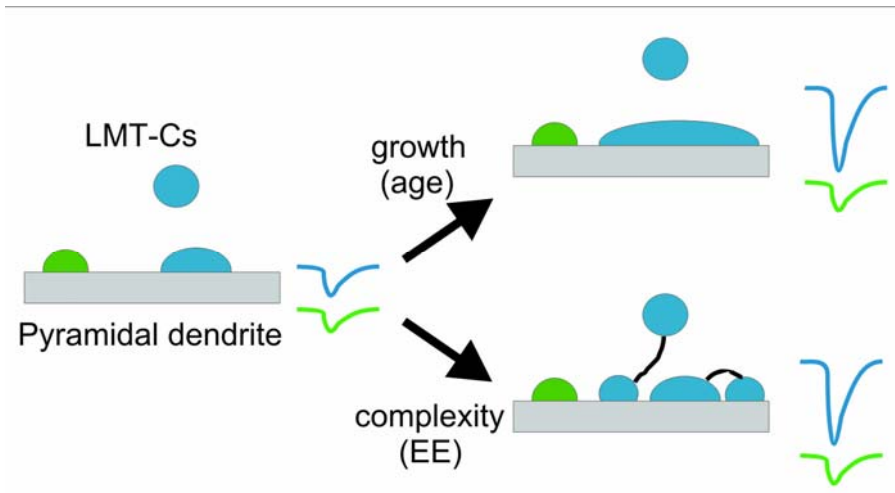


**Figure 8. Schematic of how local anatomical rearrangements can lead to changes in the functional connectivity between mossy fiber LMT-Cs and CA3 pyramidal neurons in the adult.**

Grey box: pyramidal neuron dendrite in stratum lucidum; blue and green ovals: individual LMT-Cs. The two blue LMT-Cs belong to distinct granule cells that are sometimes active at the same time (blue pattern of activation); green and blue are not recruited at the same time. The blue and green traces to the right indicate the postsynaptic excitatory responses of this dendrite at equal mossy fiber firing frequencies. Left: blue and green activation patterns elicit comparably weak postsynaptic responses. Right, upper part: lower blue LMT-C has expanded along the pyramidal dendrite (higher number of active zones), leading to potentiation of the blue postsynaptic response (e.g. age-related growth). Right, lower part: both blue LMT-Cs have established satellites onto the pyramidal dendrite (higher convergence of active zones), leading to potentiation of the blue postsynaptic response (e.g. enriched environment).

### Regulation of LMT-C rearrangements

Having uncovered evidence for long-term rearrangements of hippocampal LMT-C connectivity influenced by experience in adult mice, we turned to organotypic slice cultures to investigate mechanisms controlling LMT-C remodeling. As outlined above, LMT-Cs in slices exhibited arrangements, heterogeneities, and remodeling properties consistent with the notion that regulation of their anatomical plasticity underlies principles comparable to those *in vivo*. Since the functional properties of hippocampal slice cultures and resemble those of acute slices (e.g. Gahwiler et al., 1997), it seems unlikely that principles underlying LMT-C rearrangements *in vivo* would be fundamentally different from those in slice cultures. On the other hand, slices cultures do lack inputs from entorhinal cortex and neuromodulatory systems, suggesting that important aspects of connectivity and network activity in slices might be significantly different from *in vivo*. Investigations in slice cultures thus provide valuable insights into mechanisms controlling LMT-C rearrangements, but the actual impact of these principles for hippocampal plasticity and their age-related properties will eventually need to be verified *in vivo*.

This study provides evidence that anatomical plasticity and rearrangements of connectivity by LMT-Cs in slice cultures are controlled by local factors. The results suggest that “plastic LMT-Cs” differ stably from less plastic ones with respect to some property affecting anatomical growth, either intrinsically, or in response to graded signals from their local environment. Interestingly, maintenance of the original set of “plastic LMT-Cs” depended on PKC activity, suggesting that synaptic plasticity might have a significant impact on the outcome of LMT-C rearrangements. That in the presence of the PKC inhibitor new growth and shrinkage of LMT-Cs appeared to be balanced suggest that in addition to local factors, LMT-C rearrangements might also be influenced by the allocation of synaptic resources within individual axons. The finding that conditions affecting synaptic plasticity influenced synaptic turnover is reminiscent of several recent studies relating LTP and LTD to spine density and growth (e.g. Muller et al., 2000; Nagerl et al., 2004; Zhou et al., 2004). We find that larger LMT-Cs can be detected at all positions along individual mossy fibers in slices, and along the mossy fiber projection in CA3 in vivo. It is well established, that there is topography with respect to connectivity in the hippocampus, and that pyramidal neurons at distinct positions along CA3 project to different regions along CA1 (Johnston and Amaral, 1998). Our results thus raise the possibility that individual mossy fibers might exhibit topographical preferences with respect to the anatomical plasticity and strength of their outputs along CA3 in the adult; such preferences might contribute to topography in the flow of information from the dentate gyrus to CA1.

In addition to uncovering a requirement for synaptic activity in LMT-C maintenance and growth, the pharmacological experiments in slice cultures have provided insights into how LMT-C plasticity might be regulated locally. The finding that LMT-C growth was reversed by an mGluR2 agonist known to specifically block transmitter release from LMTs suggests that local release is important to promote growth. Released transmitter might act on presynaptic receptors (Nicoll and Schmitz, 2005), to promote growth. In addition, several studies have provided evidence that the thorny excrescences of pyramidal cell dendrites in CA3 are particularly sensitive to experience, and can expand

or shrink in response to learning, stress and hormones (e.g. McEwen 1999; Kavalali et al., 1999; Sandi et al., 2003). A second, non-exclusive possibility is thus that synaptic activity might influence LMT growth indirectly, by regulating thorny excrescence growth. This might involve activation of AMPA receptors, since their blockade counteracts growth by individual LMTs in slices (I.G. and P.C., unpublished results). The high affinity of mGluR2 for glutamate, and the peripheral presynaptic distribution of mGluR2 at LMT synapses (Nicoll and Schmitz, 2005) suggest a further mechanism through which stronger LMTs could destabilize neighboring weaker LMTs via ambient glutamate. Such a mechanism might mediate competitive interactions between LMTs converging within thorny excrescence clusters in a way reminiscent of the role of activity in synapse elimination processes (Lichtman and Colman, 2000). It had long been appreciated that in addition to stretches of pyramidal cell dendrite in stratum lucidum exhibiting thorny excrescences distributed in a scattered manner, thorny excrescences can be clustered locally, and many of these clusters can extend for very long distances (>20-30  $\mu\text{m}$ ) along pyramidal neuron dendrites in CA3 (Gonzales et al., 2001; Qin et al., 2001; Kavalali et al., 1999). We find that LMTs from several distinct mossy fibers can converge at such clusters (Fig. 1B), and that postsynaptic territories at the clusters expand upon enriched environment through elongation and increased complexity of thorny excrescences. We further find a great degree of heterogeneity in the density and distribution of thorny excrescences among pyramidal neuron dendrites in stratum lucidum. The clusters might thus reflect specialized postsynaptic territory sites for competitive interactions among convergent LMTs regulated by experience.

### **Functional significance of LMT-C rearrangements in the adult**

What could be the functional significance of the long-term rearrangements of LMT-C connectivity in the adult? Both, the rearrangements related to age and those induced by EE conditions led to a net growth in size by the fraction of larger LMTs, and thus to a net local increase in the numbers of active zones onto pyramidal neurons in CA3 by “plastic LMT-Cs”. Since larger LMTs with higher numbers of active zones elicit stronger excitatory responses in postsynaptic pyramidal neurons (Fig. 5), the growth of individual LMTs would lead to a greater frequency-dependent impact of their activation onto their

postsynaptic pyramidal neurons in CA3. This might, for example, lead to supra-threshold activation of pyramidal neurons by individual LMT-Cs at lower spiking frequencies, and/or to more effective synergisms by small numbers of synchronously active converging LMTs (Fig. 8). Accordingly, the expansion and activity-regulated divergence of LMT-C subsets along pyramidal cell dendrites in CA3 throughout life might result in an increasing focusing of information flow from individual spiking mossy fibers, selectively to a local segment of the associative network in CA3. This focusing might mediate the emergence of microcircuits of preferentially interconnected neurons (Chklovskii et al., 2004; Ikegawa et al., 2004; Yoshimura et al., 2005; Song et al., 2005). In addition to its effects on LMT size distributions, EE specifically increased the frequency of satellites by LMT-Cs, and the lengths and complexities of thorny excrescences. Since LMTs from several distinct mossy fibers intermingle at thorny excrescence clusters (Fig. 1B), the larger and more complex thorns at individual pyramidal neuron dendrites likely accommodate terminals and satellites from a larger number of distinct mossy fibers under EE conditions, reflecting an increase in local divergence and convergence driven by experience. The outcome of LMT rearrangements at thorny excrescence clusters might then involve activity-dependent growth, mGluR2-dependent inhibition of growth, and PKC-mediated competition among LMT-Cs. In this way, the increased complexity of LMT-Cs and thorns under enriched environment conditions might support hippocampal learning by providing more opportunities for local convergence of co-active terminals onto pyramidal neurons in CA3.

#### **2.1.5. Acknowledgments**

We are particularly grateful to Patrick Schwarb and Thierry Laroche for competent and extensive help with the imaging experiments. We thank Lan Xu (FMI, Basel) for excellent assistance with the electron microscopy data, and Yan-Ping Zhang (FMI, Basel) for help with the gene-gun experiments; we thank Andreas Luthi (FMI, Basel) and Silvia Arber (FMI and Biozentrum, Basel) for valuable comments on the manuscript. The Friedrich Miescher Institut is part of the Novartis Research Foundation.

## 2.1.6. EXPERIMENTAL PROCEDURES

### **Mice and reagents**

Transgenic mice expressing membrane-targeted GFP in only few (*Thy1-mGFP<sup>s</sup>*, L21 and L15) or most neurons (*Thy1-mGFP<sup>mu</sup>*, L17) were as described (De Paola et al., 2003). Transgenic males were crossed over more than 10 generations with non-transgenic F1 offsprings from C57Bl6 x BalbC crosses, so that the genetic background of the mice was 50% each of C57Bl6 and BalbC. For enriched environment experiments, sets of female littermates (3-4 mice each) were either kept in normal-sized cages without additional objects (1 mouse per cage; Ctrl conditions), or in large (rat) cages with running wheels and several objects for exploration (3-4 mice per cage; EE conditions). Transgenic mice expressing cytosolic YFP in few neurons (*Thy1-cYFP*) (Feng et al., 2000) were obtained from Jackson Laboratories. Drugs and their final concentrations in the culture medium were as follows: TTX (Latoxan, 1  $\mu$ M, stock in acetate buffer), DCG-IV (Tocris, Bristol, 1  $\mu$ M), GABA (Fluka Biochemica, 100  $\mu$ M), Chelerythrine (Sigma, 1  $\mu$ M), APV (Sigma, 100  $\mu$ M). Antibodies: Bassoon (monoclonal IgG2a, Stressgen, 2  $\mu$ g/ml), anti-mouse Alexa-Fluor-546 (Molecular Probes).

### **Slice cultures**

The slice cultures were established according to the procedure described by Stoppini and colleagues (Stoppini et al., 1991). Brains of P6-P9 transgenic mice were dissected in MEM (GIBCO)-based ice-chilled medium, and hippocampal coronal sections of about 400  $\mu$ m were produced with a tissue chopper (McIlwain). Slices were selected, placed on Millicell (Millipore, PICM03050) and cultured in 6-well dishes at 35°C and 5% CO<sub>2</sub> in the presence of 1ml of medium. The entire slice isolation procedure took about 30 min. The culture medium was exchanged every third day, and drugs were added in fresh culture medium. For drug wash-out, individual slices were placed in 35 mm Petri dishes, washed twice with 1 ml of Tyroid's buffer, returned to 6-well dishes, and washed again twice with 1 ml culture medium during the next 10 min. For all drug treatments, control slices were treated in the same way, except for the absence of the drug.

For some experiments, DIV10-15 slice cultures from non-transgenic mice were transfected with cRFP cDNA under the control of the hSynapsin1 promoter (pMH4-pSYN-tdimer RFP, generous gift from Thomas Oertner (FMI, Basel)). Gene gun transfection was performed according to the instructions of the manufacturer (Bio-Rad, Hercules, CA), except for a 100  $\mu\text{m}$  nylon mesh which was inserted as a pressure-deflecting screen. Slices were imaged 10-15 days after transfection.

### **Imaging**

For time-lapse imaging, slices were placed in 2 ml of physiological Tyrode solution at 37°C, and imaged under controlled temperature conditions (either incubation chamber (in most cases), or heating plate). For routine imaging of the entire mossy fiber projection and its LMTs, we used an Olympus set-up consisting of a Bx61 LSM Fluoview confocal microscope, a 40X/0.75W water immersion objective, and the following settings: PMT 653, Gain 2.4, pinhole 105  $\mu\text{m}$ , 0.62  $\mu\text{m}$ /stack in the z-dimension, 512x512 pixels, and fast scan rate at 9% laser intensity. High-resolution imaging was carried out using a Zeiss set-up consisting of an Axioplan2 LSM 510 Meta Zeiss confocal microscope. In either case, all focal planes within the slice were acquired and analyzed. All slices and structures included in the analysis were examined 5, 10 and 20 days after the last imaging session to verify that no signs of phototoxicity could be detected (e.g. swelling and beading of axons, blurring of the fluorescence signal due to membrane damage). We found that in most cases (more than 98% of the slices), if cell bodies were only imaged at the first session, slices could be imaged repeatedly for at least 8 times without any sign of phototoxicity. For imaging of LMTs from mice of different ages, male transgenic mice were perfused transcardially with 100 ml ice-chilled 4% paraformaldehyde in PBS, and brains were kept in fixation solution over-night at 4°C. Vibratome coronal sections (60  $\mu\text{m}$ ) were then cut using a LEICAVT 100S vibratome (Leica), and mounted in Airvol for fluorescence imaging. Highresolution images were acquired on an upright Zeiss Axioplan2 LSM510 Meta confocal microscope, using a Plan-Neofluar 40x/1.3 oil immersion objective (pinhole size of 65  $\mu\text{m}$ ), or a 100x/1.4 oil immersion objective (pinhole sizes between 100-150  $\mu\text{m}$ ). Images were opened and processed using Imaris 4.2 (Bitplane AG) and Image Access (IMAGIC) softwares. Deconvolution was performed

with Huygens Deconvolution Software from Scientific Volume Imaging SVI (Hilversum, Netherlands). The iterative Maximum Likelihood Estimation (MLE) algorithm was used with the computed Point Spread Function (PSF). For 3D analysis of LMT-Cs, images were opened in Imaris 4.2, smoothed by the Gaussian filter and Background subtraction tools of the software, cropped in 3D to reveal the regions of interest; 300 frames movies were then produced in the animation mode.

### **Immunocytochemistry and histology**

Slice cultures were fixed for 10 min in ice-chilled 20% methanol in PBS, rinsed 3 times with PBS, and post-fixed for 10 min at 4°C in 4% paraformaldehyde, PBS. Tissues were then washed in PBS, solubilized in 0.4% triton X-100, PBS (over-night at 4°C), blocked in the presence of PBS and 20% BSA (4h, RT), and incubated with primary, and then secondary antibody (over-night at 4°C, each).

For electron microscopy, mice were perfused with buffered 2.5% glutaraldehyde, followed by fixation in buffered 2.5% glutaraldehyde (2h), post-fixation in buffered 2% Osmium tetroxide (2h), and dehydration through alcohol, followed by propylene oxide. Fixed brain material (hippocampal CA3a) was embedded in Docupon, stained with uranyl acetate and lead hydroxide, and sectioned with a diamond knife. Complete serial sections (75-85 nm each; total of 8-10 µm) were deposited on slot grids with formvar. Sections were recorded on Kodak electron image plates using a Zizze EM900 at 100 kV.

### **Analysis of imaging data**

We defined LMTs as mossy fiber terminal regions of > 2.5 µm diameter in CA3a-c, which were arranged either en-passant, or as side structures connected to the mossy fiber projection by short (in most cases less than 10 µm) side-branches. As expected, individual LMTs exhibited highly complex morphologies (Chicurel and Harris, 1992; Danzer and McNamara, 2004). We found that they could be further subdivided into three subcomponents: 1) core terminal regions consisting of flattened domains of greatly varying sizes, and of beaded subunits of 2.5-3.5 µm diameter, arranged in grape-like arrays (range of 0-25 bead subunits per LMT), 2) filopodia tipped by swellings of 1-2 µm diameter (range of 2-10 filopodia per LMT; lengths of 5-15 µm), 3) processes of 10-200

$\mu\text{m}$  length, emanating from LMTs and terminating in “satellite LMTs” (range of 0-5 satellites per LMT) (Fig. 1a; Suppl. Fig. 1).

For the quantification of LMT sizes in slice cultures, images were all acquired using the same settings, and processed using Imaris 4.2 and Image Access software.

Acquisition settings (see above) were selected to minimize phototoxicity, but at the same time allow visualization of the thin axonal processes connecting LMTs to their satellites. The latter were defined as terminal structures of more than  $2.5 \mu\text{m}$  in diameter, which were unambiguously connected to the main LMT as confirmed by a 3D analysis using Imaris software. Mossy fibers running deep in the slices exhibited thinner axons, and some of them were lost when cultures were kept for more than 4-5 weeks, possibly due to suboptimal access to oxygen. These deeper fibers could also be recognized by their weaker GFP signals, and were excluded from the analysis. LMT areas were derived from z-projections using ImageJ software. When LMT complexes unambiguously included satellites (about 10-20% of all LMTs), their terminal areas were included in the total size of the LMT complex. Sizes of individual identified LMTs were compared at the indicated times, and LMTs were subsequently grouped and analyzed according to their sizes at DIV20 (small  $< 30 \mu\text{m}^2$ ; medium  $< 60 \mu\text{m}^2$ ; large  $> 60 \mu\text{m}^2$ ). For the quantification of LMT volumes at different ages, at least three confocal 3D stacks (total volume of  $230 \mu\text{m} \times 230 \mu\text{m} \times 40 \mu\text{m}$ ) were acquired in CA3a for each preparation (three mice per age), and analyzed using Imaris 4.2 software. Individual LMT volumes contained in these cubes were measured using the Surpass/ Isosurface function of the software. Non-saturating imaging conditions were chosen for all size analyses. An intensity threshold of 300 was chosen to selectively analyze LMTs (excluding axons and other smaller objects). All identified objects were verified by eye inspection. Generally, the settings for the analysis were identical for all samples of all ages, but in some cases we verified the settings through internal calibration using the diameters and signal intensities of axons. After these measurements, LMTs were grouped according to their volumes. The volumes of all LMTs in one group were added up, and expressed as percentage of the total volume of all LMTs measured per cube. For the quantification of LMT subunit compositions as a function of age, samples were processed as described above ( $230 \mu\text{m} \times 230 \mu\text{m} \times 40 \mu\text{m}$ ). Image settings were then chosen to emphasize the beaded subunit compositions of

individual LMTs. To analyze labeling homogeneities by the mGFP construct, 3D images (voxel sizes of 0.09 x 0.09 x 0.49  $\mu\text{m}$ ) were acquired using LSM510 Meta (100x/1.4 oil objective, 150  $\mu\text{m}$  pinhole size), and opened in Zeiss LSM 510 Image examiner software. Membrane outlines of axons and LMTs included in one confocal plane were followed manually, and light intensities were plotted against distance. To determine numbers of Bassoon-positive structures per individual LMTs, 3D images of Bassoon stained slice cultures were acquired (LSM 510 Meta, 100x/1.4 oil, voxel sizes: 0.09 x 0.09 x 0.28  $\mu\text{m}$ , 150  $\mu\text{m}$  pinhole size for both channels), and LMT volumes were derived as described above. Bassoon-positive structures were defined as single spots of 0.2 - 0.3  $\mu\text{m}$  in diameter. Double counting of active zones was avoided by comparing adjacent confocal planes.

### **Electrophysiology**

Slice cultures (DIV20-30) were transferred to a submerged recording chamber mounted on an upright microscope (BX50WI, Olympus, Germany), and continuously perfused (2-2.5 ml/min) using a solution containing (in mM): NaCl 142, KCl 1.6, CaCl<sub>2</sub> 2.5, MgCl<sub>2</sub> 1.5, NaHCO<sub>3</sub> 24, KH<sub>2</sub>PO<sub>4</sub> 1.2, bicuculline methochloride 0.02, D-AP5 0.08, NBQX 0.0003, glucose 10, ascorbic acid 2; saturated with 95% O<sub>2</sub> and 5% CO<sub>2</sub> (pH 7.4; temperature 34°C). To establish pair recordings, a pipette supplemented with sulforhodamine (1%) or Lucifer Yellow (1%) was closely approached to a small (8-25  $\mu\text{m}^2$ ) or large LMT (80-150  $\mu\text{m}^2$ ) and gentle, positive pressure applied in order to stain juxtaposed CA3 pyramidal neuron dendrites. As soon as dendrites adjacent to the LMT were visible, the pipette was moved along the dendrites to the soma, and the cell was recorded under whole cell patch conditions. Granular cells were recorded under current-clamp mode with pipettes (3-5 M $\Omega$ ) filled with a solution containing (in mM): K-gluconate 135, HEPES 10, EGTA 0.4, MgCl<sub>2</sub> 10, phosphocreatine 14, Mg-ATP 2, Na<sub>2</sub>-GTP 0.2 (pH 7.2-7.3; osmolarity 295-310 mosm). CA3 pyramidal cells were recorded under voltage-clamp mode with pipettes filled with a solution containing (in mM): Cs-methanesulfonate 130, HEPES 10, EGTA 10, MgCl<sub>2</sub> 5, phosphocreatine 14, QX-314 5, picrotoxin 1, Na<sub>2</sub>-ATP 2 and Na<sub>2</sub>-GTP 0.2 (pH 7.2-7.3 adjusted with CsOH; osmolarity: 295- 310 mosm). Current and voltage recordings were obtained using an

Axoclamp-2A and an Axopatch 200B amplifier respectively (Axon Instruments, Union City, CA., USA). Membrane potentials were corrected for liquid junction potentials. Series resistance was compensated up to 50-80 % in order to avoid unstable recordings. Series and input resistances of voltage-clamp recordings were monitored throughout experiments, and data were discarded if they varied by more than 20%. Presynaptic action potentials were evoked by injecting depolarizing current pulses (1-1.5 nA for 2 ms) at 0.5 Hz unless otherwise stated. Signals were filtered at 2 kHz, digitized at 5-10 kHz and stored on hard disk. Data acquisition and analysis were performed using homemade A/D converter and software. The standard deviation of the latencies was used to calculate the jitter. Average values are expressed as mean  $\pm$  S.E.M. Statistical differences were assessed by Student's *t*-test.

### **3. SUPPLEMENTARY RESULTS**

#### **3.1. EXPERIENCE-DEPENDENT STRUCTURAL PLASTICITY OF NEURONAL CIRCUIT CONNECTIVITY IN THE ADULT CEREBELLAR CORTEX**

Nadine Gogolla, Claudia Vittori and Pico Caroni  
*unpublished results*

### **3.1.1. SUMMARY**

Previously, we reported that subsets of hippocampal mossy fiber terminal complexes rearrange their local connectivities with CA3 pyramidal neurons in response to experience throughout life. Here we addressed the question whether such experience-related rearrangements of connectivity are a more general phenomenon and do also occur in other parts of the adult brain. We investigated structural rearrangements of two different axon types and their presynaptic terminals upon environmental enrichment (EE) in the cerebellar cortex. We found that parallel fiber boutons (PFBs) as well as mossy fiber terminals (MFTs) grow in size upon EE in cerebellar lobule V. Differences in average sizes of MFT were specific to small subregions of this lobule. Tracing of individual axon segments revealed that branching and terminal densities were increased on mossy fibers, while parallel fibers exhibited a higher frequency of complex PFBs upon EE. Our data indicate that the cerebellar cortex displays anatomical plasticity and rearrangements of neuronal connectivity at multiple sites and in various forms upon EE experience.

### **3.1.2. INTRODUCTION**

Dynamic changes in axonal arbors and their presynaptic terminals lead to altered connectivity in neuronal circuits and underlie several forms of experience-dependent plasticity. For example, experience-dependent, functional changes in receptive fields of cortical neurons are often accompanied by structural remodeling of axonal arbors (Darian-Smith & Gilbert, 1994, Antonini & Stryker, 1993; Antonini et al., 1999; Trachtenberg & Stryker, 2001). Furthermore, we have previously shown that EE experience and age robustly alter hippocampal mossy fiber connectivity throughout life (Galimberti et al., 2006).

Thus, it is well established that altered experience can induce changes in neuronal circuit connectivity. In contrast, it remains unknown how specific experience-related alterations in connectivity are.

For instance, does general experience affect all or just some functional circuits specifically? Do structural modifications occur at several or even at all sites along a given

circuit? Are all neurons of a given type equally affected? And do different axon types display different plasticity responses to the same stimulus?

To address these questions we looked for a relatively simple neuronal circuitry, with well-characterized topographic and functional organization, that had been implicated in functional and anatomical plasticity.

The cerebellum exhibits a rather simple anatomy with stereotyped connectivity between few, readily identifiable neurons and therefore allows the investigation of synaptic connectivity rearrangements on a comprehensive scale.

The cerebellar cortex contains four major neuron types: the granule and Purkinje cells, as well as the GABAergic, Golgi and stellate/basket interneurons. The cortex receives two major inputs, the mossy and the climbing fibers and sends one single output via the Purkinje cell axon. One of the two major afferents, the mossy fibers, arise from different sources in the brainstem and the spinal cord. They enter the cerebellum rostrally; many of them cross the midline in the cerebellar commissure and distribute bilaterally. Mossy fibers terminate in lobule-specific patterns of discontinuous patches or zones in the granule cell layer. Their presynaptic terminals, the 'rosettes' or mossy-fiber terminals (MFTs), contact the short, claw-like dendrites of several granule cells in complex synapse arrangements, called glomeruli (Voogd & Glickstein 1998). The granule cells are small, densely packed and extremely numerous glutamatergic neurons. Each granule cell gives rise to a single, unmyelinated axon that ascends within the plane of a Purkinje cell towards the surface of the molecular layer. Here, the axon bifurcates into two parallel fibers running perpendicularly to the ascending branch and in parallel to the cerebellar surface. Due to the orthogonal relationship between the parallel fibers and the dendritic structures of the Purkinje cells, each parallel fiber can synaptically contact hundreds of Purkinje cells (Ito, 1984). A single parallel fiber, however, can contact a given Purkinje cell only once or twice (Napper & Harvey, 1988a-c). Most parallel fiber presynaptic terminals or boutons (PFBs) innervate the Purkinje cells (~94%), and only very few contact interneurons (Palkovitz et al., 1971; Napper & Harvey 1991). Most often one PFB contacts one postsynaptic spine but rarely multi-spine boutons, with one bouton contacting two spines, can be observed (Pichitpornchai et al., 1994). Purkinje cells are

large, GABAergic neurons located in a single row at the border of the granular and the molecular layer. Their myelinated axons, the sole output of the cerebellar cortex, terminate on neurons of cerebellar- and brainstem-nuclei. Their dendritic trees are flattened and oriented perpendicular to the parallel fibers. The proximal parts of the dendritic tree are relatively smooth and innervated by multiple synapses from a single climbing fiber; the distal parts are closely covered with spines that get contacted by PFBs.

The cerebellar cortex is organized in a mosaic-like ‘fractured somatotopy’, with multiple representations of the same receptive fields in which the topography is preserved in patches but not in a continuous manner. Those patches display synchronized activity upon mossy fiber stimulation throughout all cortical layers, from the granular- over the Purkinje- to the molecular layer (Cohen & Yarom, 1998), suggesting a columnar or modular functional organization of the cerebellar cortex (Bower & Woolston, 1983). Such repetitive and fragmented representation may allow the cerebellum to integrate the complex combinations of incoming sensory information obtained by different body parts and different sensory organs.

Several lines of evidence have implicated the cerebellar cortex in anatomical plasticity. For instance, it has been shown that climbing fiber and parallel fiber axons, both innervating the Purkinje cell dendritic tree, rapidly remodel if one of the two inputs is absent or changes its activity. This activity-dependent axonal remodeling also induces rearrangements of the dendritic spines on the Purkinje cell (Cesa et al., 2005, 2007; Cesa & Strata, 2005; Morando et al., 2005). Furthermore, upon motor skill acquisition, synaptogenesis and changes in dendritic trees of interneurons have been observed (Black et al., 1990; Kleim et al., 1997). Moreover, the fraction of presynaptic terminals associated with the ascending branch of the granule cell axon increases upon age (Huang et al., 2006). Interestingly, studies in human beings indicate that certain forms of life-long sensory-motor exercise, such as for instance playing an instrument, can specifically increase the volume of the cerebellum. In these studies, the intensity of training correlated with the cerebellar volume increase, indicating that the long-term motor

training coupled to auditory perception is sufficient to increase cortical volume of the cerebellum (Hutchinson et al., 2003).

Taken together, these findings from different species and experimental approaches support the notion that the cerebellar cortex provides a promising system to study the specificity and localization of experience-related synaptic circuit rearrangements.

Here we used the paradigm of EE combined with high-resolution imaging in transgenic mice, expressing membrane-targeted GFP in only a few neurons, in order to investigate sustained rearrangements of neuronal circuit connectivity influenced by experience in the cerebellar cortex of adult mice. We find that experience-related rearrangements of neuronal circuit connectivity in the cerebellar cortex of adult mice occur at several synapses along the same neuronal circuit and affect distinct neuron types in different ways. Furthermore, we demonstrate that anatomical reorganizations are subregion specific, reminiscent of the functional mosaic-like organization of the cerebellar cortex.

### **3.1.3. RESULTS**

#### **Heterogeneity of cerebellar mossy fiber terminal and granule cell morphologies**

In order to investigate anatomical plasticity in the cerebellar cortex, we first analyzed patterns and distribution of neuronal labeling in the cerebella of different *Thy1-mGFP<sup>s</sup>* mouse lines expressing membrane-targeted GFP in only a few neurons (De Paola et al., 2003) as well as the morphologies of the labeled structures.

We found that in the mouse lines used, GFP was expressed almost exclusively in small subsets of mossy fibers and granule cells. Occasionally Bergman glia and very rarely single Purkinje cells were labeled (see Figures 1A and 1B).

Labeling was detected in all cerebellar lobules, but showed a clear anterior to posterior gradient with higher expression in the anterior cerebellum, especially in front of the primary fissure (lobules I-V), and a gradual decrease of labeled structures towards lobule X, which contained only very few labeled mossy fibers and granule cells (Figures 1A and 1B). Often, labeled mossy fibers and granule cells lay next to each others in the same

fields of view (Figure 1C). Rarely, labeled granule cell dendrites were contacted by labeled mossy fibers, or granule cell claws belonging to distinct cells innervated the same glomerulus (not shown).

Interestingly, labeled mossy fibers followed very distinct axonal trajectories within the same lobule, displayed different axonal calibers, as well as distinct presynaptic terminal sizes and morphologies (Figures 1B and 1D). Most probably, many of these differences were due to the different origins of mossy fibers, arising from different brainstem or spinal cord related nuclei. However, even MFTs belonging to the same axon frequently exhibited substantial differences in morphology and size (Figure 1C; see also Figure 4B). Differences in morphology between different MFTs consisted of diversity of their surfaces, ranging from smooth to very convoluted, and their coverage with filopodia. Some terminals exhibited many filopodia giving them a “hairy” appearance while others bore just a few or no filopodia. The filopodia length was found to vary substantially. A subset of MFTs exhibited very long filopodia-like processes that terminated at satellite MFTs.

Similarly, granule cells showed substantial heterogeneities in the length and number of their dendrites as well as in the size and complexity of their dendritic claws. Again, dendrites of the same granule cell often displayed large differences amongst each others, with respect to their length and claw complexity (Figure 1E). Interestingly, the size and complexity of dendritic claws seemed to increase with age (not further investigated yet). Also the granule cell axons, the parallel fibers, showed substantial differences with respect to the presynaptic terminals they established. Marked heterogeneities existed in the spacing as well as in the sizes and shapes of individual PFBs. Differences in all parameters were frequently found amongst PFBs belonging to the same parallel fiber (Figure 1F; see also Figure 2A).

We conclude that pre- as well as postsynaptic structures of the same kind within the same region of the cerebellar cortex exhibit marked morphological differences amongst each others.

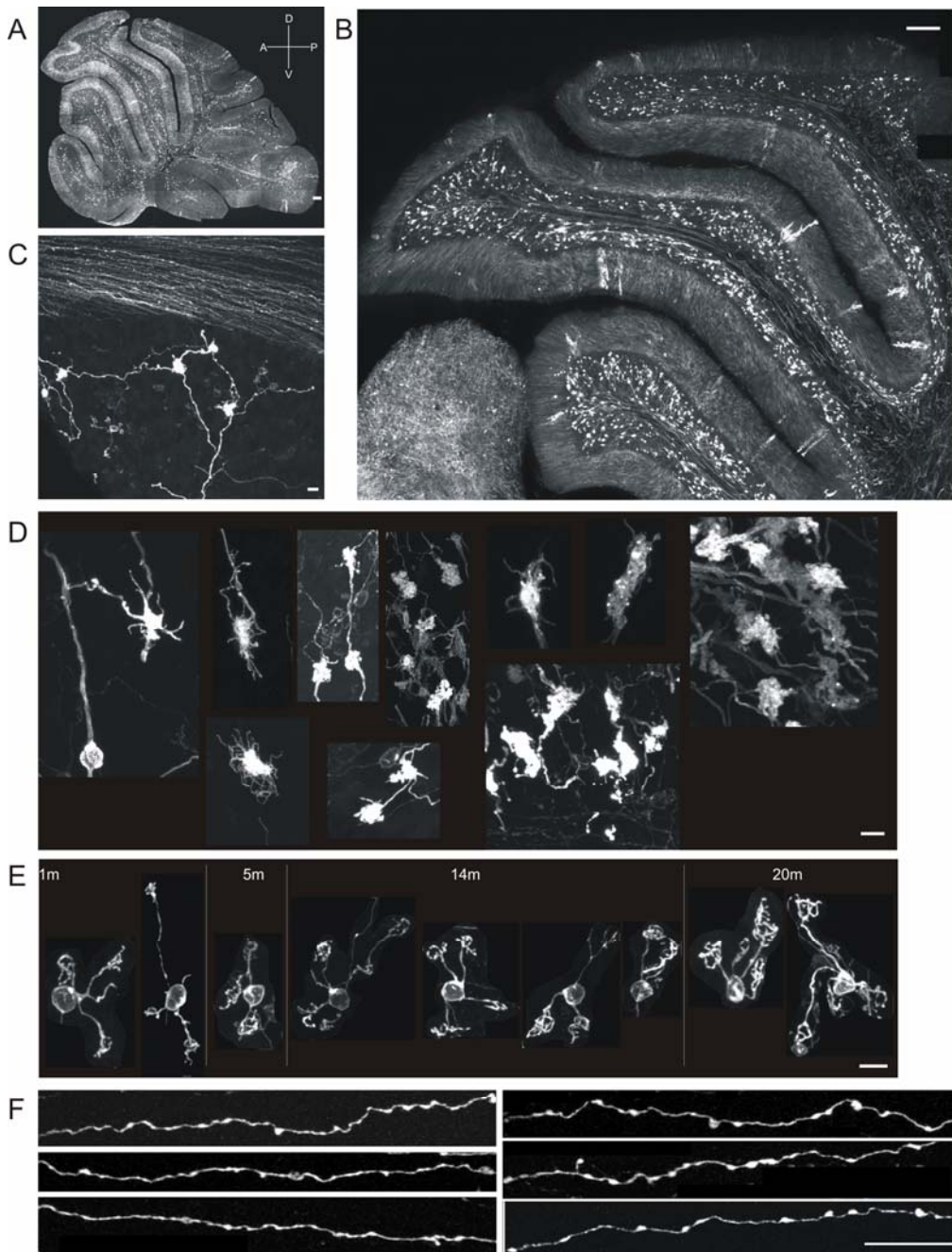


**Figure 1. Morphological heterogeneity of cerebellar mossy fibers and granule cells**

Labeling of small subsets of cerebellar granule cells and mossy fibers reveals their morphological heterogeneity and allows for detailed anatomical analysis of pre- and postsynaptic arrangements in the cerebellar cortex. **(A)** GFP expression in single neurons in the cerebellar cortex. Sagittal section of the cerebellum near the midline of a 1 year old, Thy1-mGFP mouse. Note the decreasing expression intensities from anterior to posterior (A→ P). **(B)** Higher magnification of lobules III-VI in a sagittal midline section. Note the regional heterogeneity of MFT sizes. **(C)** Zoom into a coronal section revealing the arrangements of granule cells and MFTs in the granular cell layer, and parallel fibers in the molecular layer. Purkinje cells are not labeled in this transgenic line. **(D)** Heterogeneity of MFT in a one year old mouse. Note the different MFT sizes and morphologies, from “hairy” (many filopodia) over “glomeruli” (convoluted outline) to “smooth” shapes. **(E)** Complexity and heterogeneity of granule cell dendrites and dendritic claws. Granule cells from animals of different ages (1-20 months). Note the complexity and size of claws especially at older ages. **(F)** Heterogeneity of PFB distribution and size on individual PF. Scale bars: 100  $\mu$ m (A) and (B); 10  $\mu$ m (C-F).

### **Experience-related increase in PFB complexity and size in adult mice**

In order to investigate the possibility that experience might affect synaptic arrangements and structure in the cerebellar cortex, we first analyzed presynaptic terminal distribution on individually traced parallel fiber segments in lobule V of mice housed under EE or standard (CTRL) conditions (see Experimental Procedures). As shown in Figure 2A, PFBs in both conditions were very heterogeneously distributed along the axons.

Additionally, their sizes varied substantially (Figure 2A; see also Figure 1F). A quantitative analysis revealed that the average PFB sizes increased significantly upon EE in general and on individual axons (Figure 2B), while the average density on individual stretches did not change between the two conditions (Figure 2C).

Interestingly, a small subset of PFBs in both conditions displayed a complex morphology consisting of a core bouton on the axon and an enlargement building a second bouton connected to the core by a small process (see Figure 2A, red arrowheads). Remarkably, the frequency of such complex PFBs was more than twice as high under EE than under CTRL conditions (Figure 2D).

Taken together these results provide evidence that parallel fibers exhibit experience-related alterations of their presynaptic terminals.

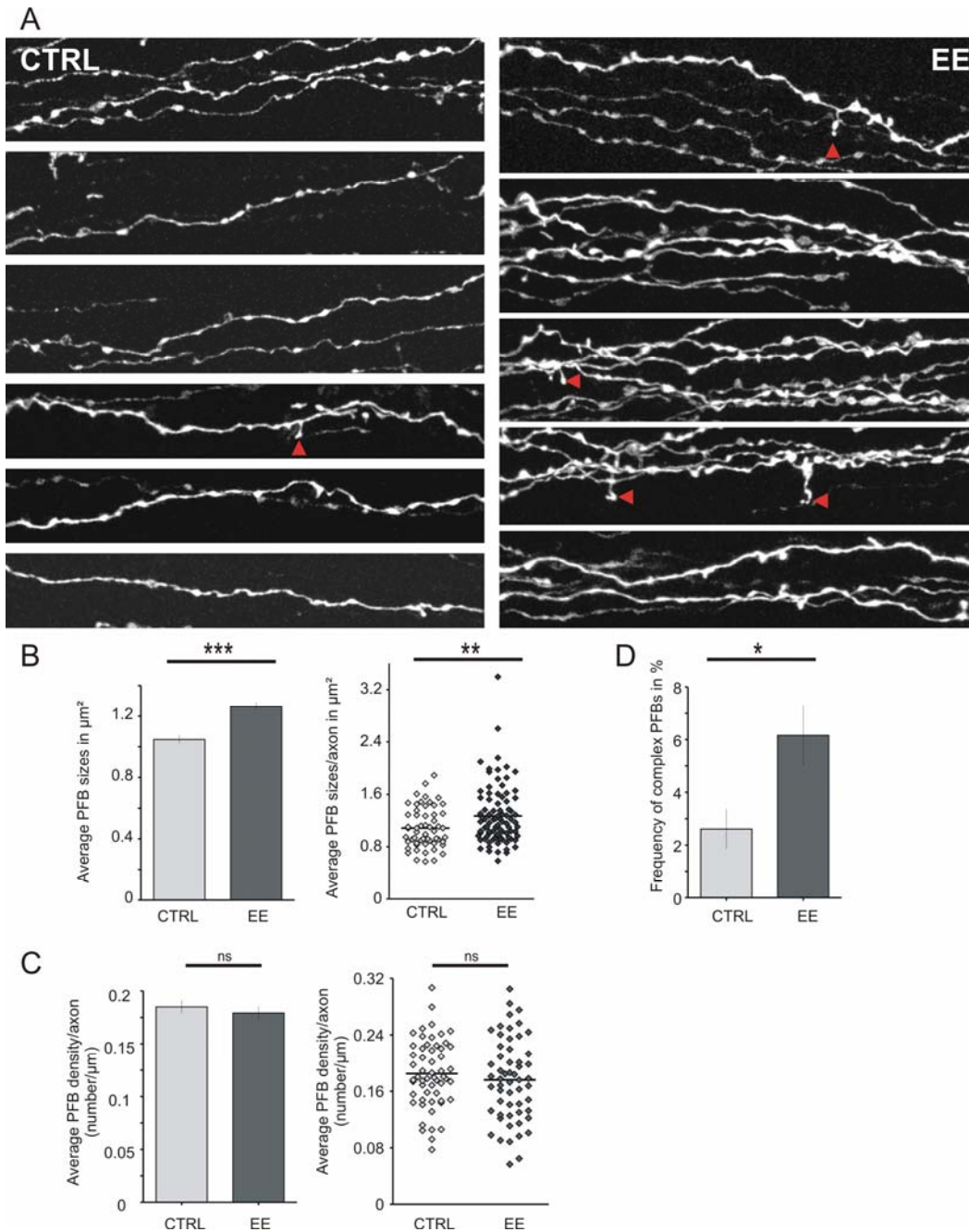


**Figure 2. Experience-related increase in PFB sizes and complexities**

**(A)** Parallel fibers in lobule V of control (left) and enriched (right) mice. A subset of PFBs displays a complex morphology consisting of a core bouton on the axon and an enlargement building a second bouton connected to the core by a small process (red arrowheads). Scale bar: 4  $\mu\text{m}$  **(B)** Quantitative analysis of average PFB sizes in control and enriched mice. (Left) Overall average PFB sizes (N= 750 PFBs). Note the significant increase in PFB sizes upon EE. Post-hoc student's t test: \*\*\* $p < 0.0001$ . (Right) Average PFB sizes on individual axons (N=60). Note the shift of average PFB sizes on individual axons towards larger sizes upon EE. Post-hoc student's t test: \*\* $p < 0.001$ . **(C)** Quantitative analysis of PFB densities on average in the whole population (left) and on individual axons (right). N=60 axons from three animals for each condition. Post-hoc student's t test: non significant for both analysis **(D)** Relative prevalence of complex PFBs in control and enriched mice.  $2.61 \pm 0.76\%$  of control and  $6.16 \pm 1.148\%$  of enriched PFBs exhibit a complex morphology.  $n=750$  PFB on 60 axons from three animals for each condition. Post-hoc student's t test \* $p = 0.02$

### **Experience-related and subregion-specific growth of MFTs**

We next examined whether MFTs exhibited similar experience-related anatomical plasticity as parallel fibers. In order to quantify and compare MFT sizes, we analyzed small subregions (“3D crops”) randomly distributed in lobule V and determined the volumes of individual MFTs included in these subregions. This analysis revealed that the housing under EE conditions produced a significant shift in the prevalence of larger MFT sizes compared to controls (Figures 3A and 3B). At first approximation, EE thus appeared to increase MFT sizes homogeneously. However, a more detailed analysis revealed that the effects of EE were not equally distributed in all analyzed subregions. A detailed analysis of the individual crops demonstrated that only about half of all EE subregions contained terminals that were on average larger than the largest averages found in CTRL regions (Figure 3C). In addition, the EE regions contained MFT of more heterogeneous sizes as indicated by the error bars (Figure 3C). These results indicate that not all MFT and not all subregions of the cerebellar cortex respond equally to EE.

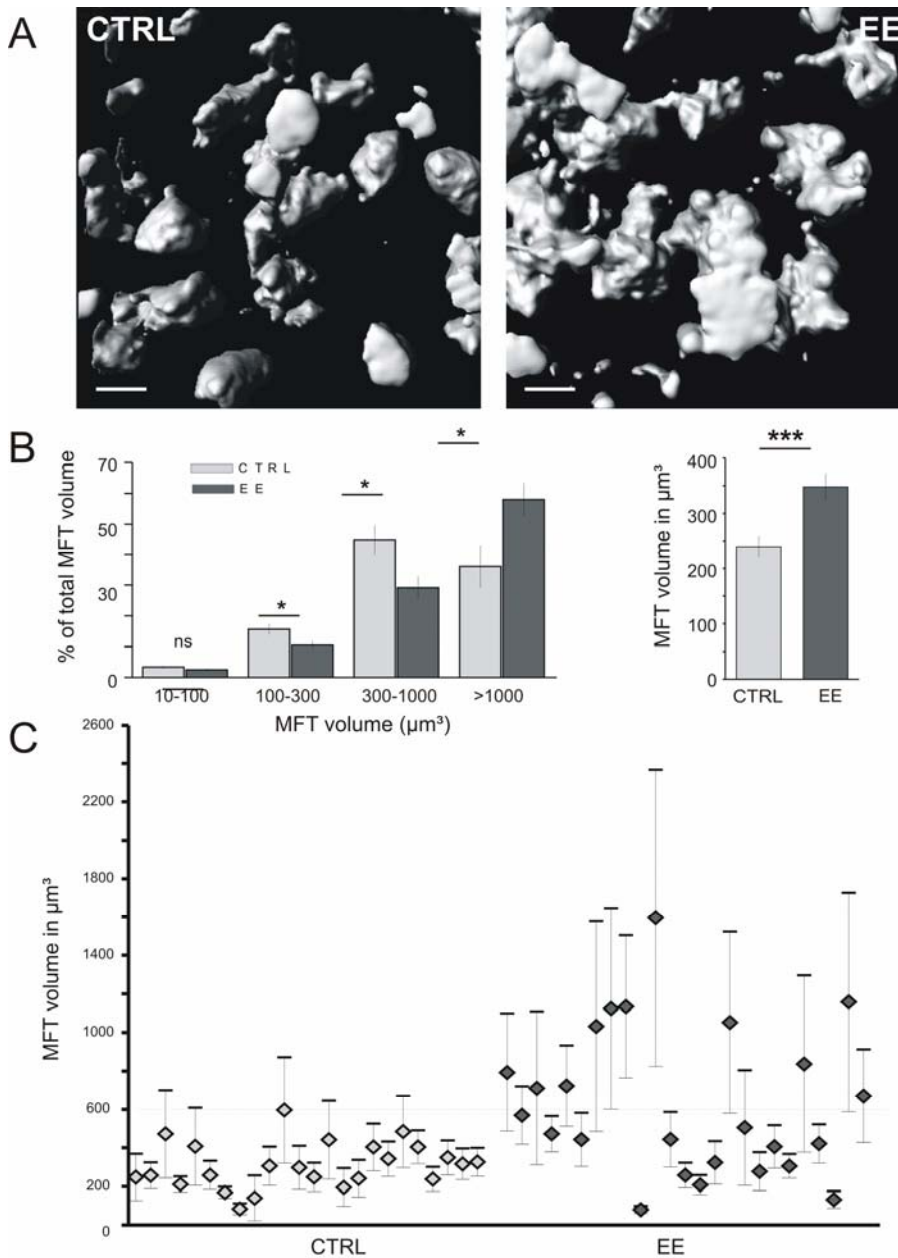


**Figure 3. Experience-dependent and region-specific growth of MFT subsets in the adult *in vivo*.**

(A) Examples of MFT volume calculation in Imapris from CTRL (left) and EE (right) mice. Images show a zoom into a subregion crop. Isosurfaces were built over the MFT in a dimensional Imapris volume projection. These isosurfaces are used for the volume calculation of each MFT. Scale bars: 10  $\mu\text{m}$ . (B) (Left) Overall contributions of LMTs grouped by volume to the total volume of LMTs in the sample. EE leads to significant in size distributions contributing to the three largest size groups. Post hoc student's t test for all three largest size groups  $*p < 0.03$ . (Right) Quantification of average MFT sizes in lobule V in control versus enriched animals. Post-hoc student's t test:  $***p = 0.0006$ . Average sizes of LMTs were  $239.3 \pm 19.97 \mu\text{m}^3$  for control and  $347.9 \pm 24.26 \mu\text{m}^3$  for enriched animals. (C) Effect of enriched environment on MFT size is subregion-specific within lobule V. Displayed are average MFT sizes  $\pm$  SEM for each individual 3D crop analyzed. 24 crops were analyzed for the CTRL and 25 for the EE condition. 3D crops were randomly distributed all over the granule cell layer of lobule V. Only in a subset of the analyzed regions MFTs are larger in EE than in CTRL animals. 100% (24/24) of the control crops contain MFTs that are in average smaller than  $600 \mu\text{m}^3$  (indicated as a dashed line). 44% (11/25) of the crops from enriched animals contain on average larger MFTs, while 56% (14/25) show similar averages as in the control ( $< 600 \mu\text{m}^3$ ).

## **Experience induces rearrangements of mossy fiber terminal connectivity in the adult**

We next wondered whether environmental enrichment in addition to the presumable strengthening of a subset of synapses would also induce substantial rearrangements of neuronal connectivity similar to those observed in the hippocampal mossy fiber pathway (see previous chapter).

In order to address this question we traced stretches of individual mossy fiber axonal arbors innervating lobule V and compared their branching patterns as well as the density of MFT on these individual axons (Figures 4A and 4B). This analysis revealed that mossy fiber axons of EE mice exhibited a higher branch point- and MFT- frequency than those of CTRL animals (Figures 4C and 4D). Interestingly, the increase in branching and MFT densities appeared to occur at specific, concentrated sites and not homogenously throughout the length of the traced stretch (Figure 4C). These sites of enhanced plasticity tended to be found at granule cell layer “shoulders”. These findings provide strong evidence that mossy fiber to granule cell connectivity is considerably rearranged upon EE and that it occurs in ‘preferred regions’.

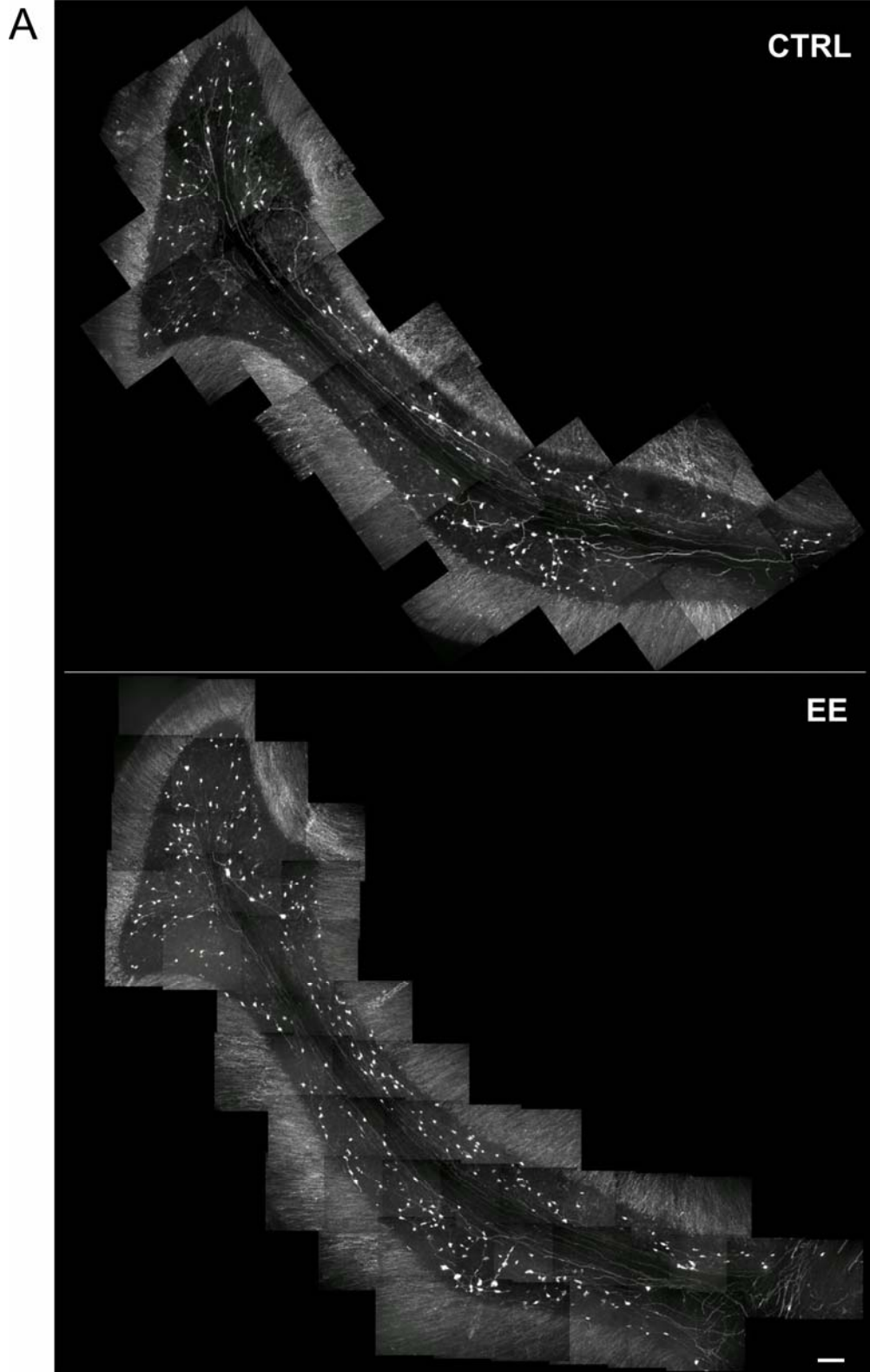


**Figure 4 A. Experience induces rearrangements of mossy fiber connectivity in the adult.** Overviews of lobule V of one enriched (bottom) and one control (top) animal. The whole lobule was stitched together from several MIPs of individual three dimensional stacks. Scale bar: 100 $\mu$ m.

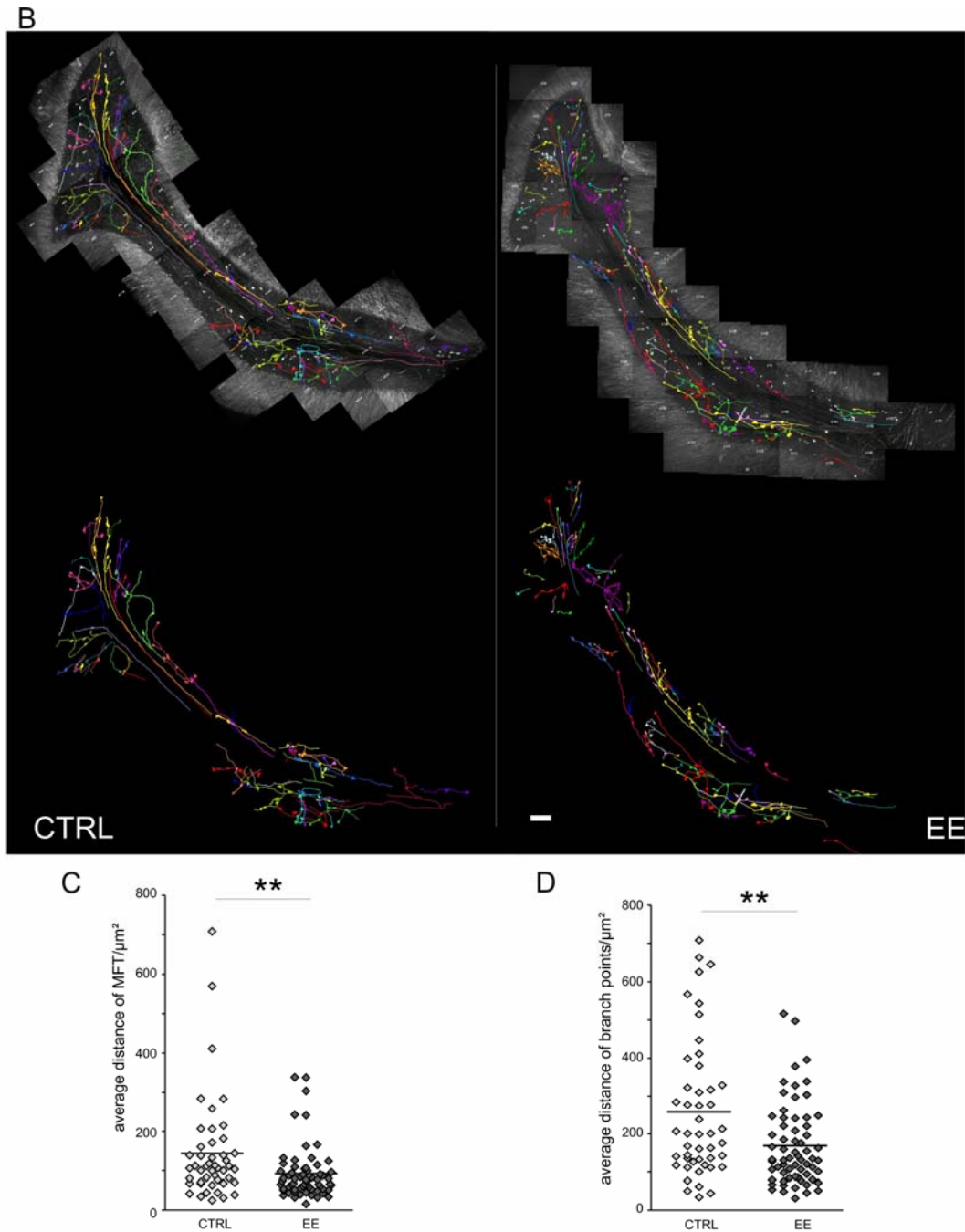


**Figure 4 B-D. Experience induces rearrangements of mossy fiber connectivity in the adult.** Tracing of individual mossy fiber axons in lobule V of enriched and control animals. **(B)** Top panels: Mossy fibers traced and drawn on the MIPs. Bottom panels: Drawings of the mossy fibers without the real image. Scale bar: 100  $\mu\text{m}$  **(C)** Quantitative analysis of the distance of MFT on individual axons from control and enriched mossy fibers. Post-hoc student's t test:  $**p=0.0081$ . In control animals MFT were in average spaced by  $143.1 \pm 19.1 \mu\text{m}$  ( $n=47$  axon stretches), in enriched animals by  $92.02 \pm 8.3 \mu\text{m}$  ( $n=65$  axon stretches). **(D)** Quantitative analysis of the distance of branch points on individual axons from control and enriched mossy fibers. Post-hoc student's t test:  $**p=0.0014$ . In control animals branch points were in average spaced by  $257.7 \pm 26.3 \mu\text{m}$  ( $n=47$  axon stretches), in enriched animals by  $168.5 \pm 13.35 \mu\text{m}$  ( $n=65$  axon stretches).

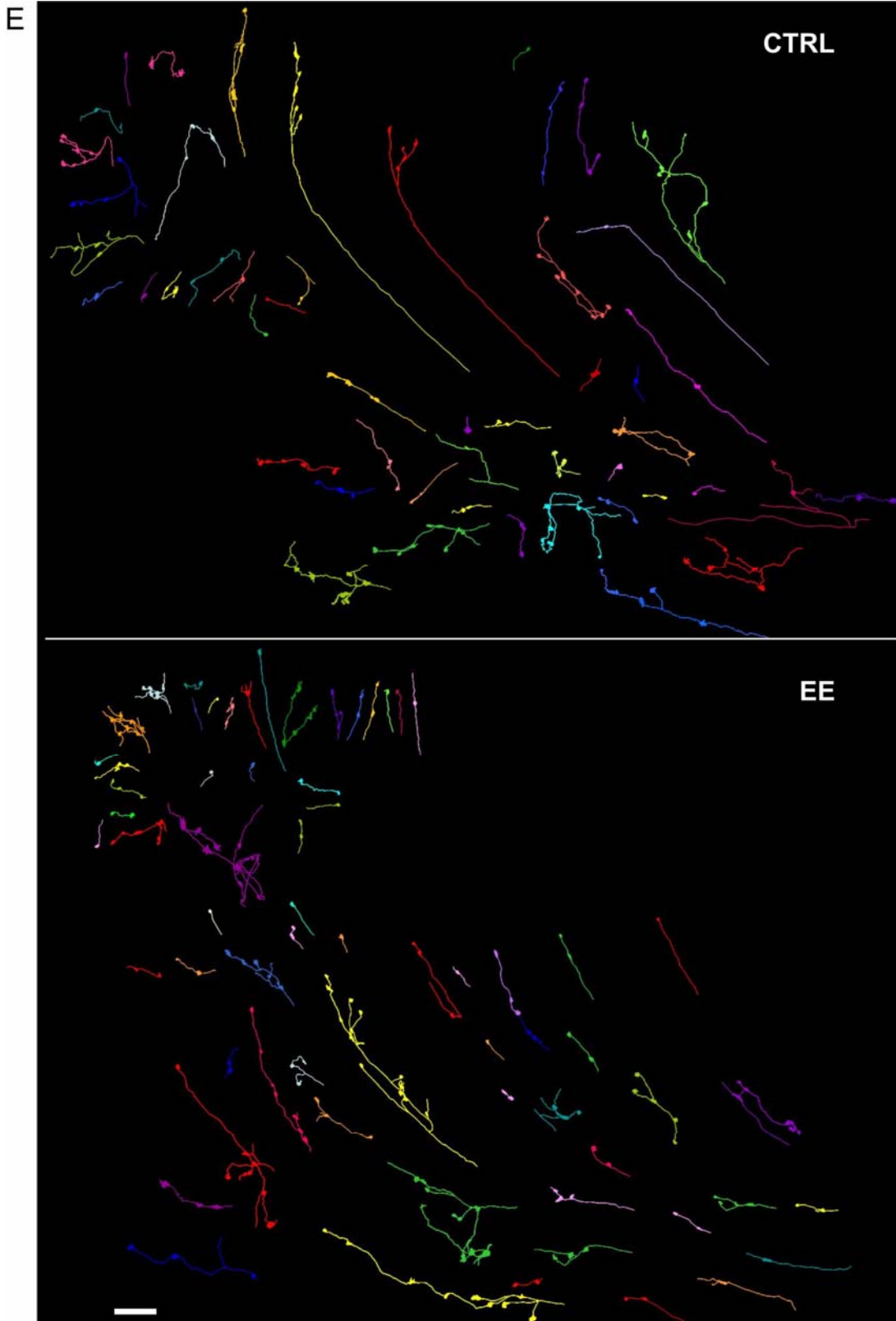


**Figure 4 E. Experience induces rearrangements of mossy fiber connectivity in the adult.** Detailed overview of the individual mossy fiber drawings of control (top) and enriched (bottom) mice. Scale bar: 100  $\mu$ m

### **3.1.4. DISCUSSION**

In this study we provide evidence that experience-related rearrangements of neuronal circuits manifest at different sites in the cerebellar cortex.

We first show that experience increases average PFB sizes and the incidence of complex PFBs on parallel fiber axons. We then provide evidence that subsets of MFTs grow in a region-specific manner. Finally, we demonstrate that mossy fibers exhibit marked rearrangements of their axonal arbors by increased branching and addition of presynaptic terminals. Taken together these findings suggest that both mossy fiber to granule cell as well as parallel fiber to Purkinje cell connectivities are altered upon EE.

Below, I will discuss the possible implications of these findings and suggest possible future directions.

#### **Increased sizes and complexities of PFBs upon EE**

Our results provide evidence that many PFBs grow upon EE. This result is reminiscent of previous studies of structural plasticity upon EE indicating that synapses are strengthened and newly formed resulting in an overall increase of synaptic densities (Turner et al., 1985; Faherty et al., 2003; Leggio et al., 2005). In addition, we found that a subset of PFBs displays a complex morphology consisting of a core bouton on the axon and an enlargement building a second bouton connected to the core by a small process and that this conformation was by far more abundant under EE conditions. This finding suggests the specific strengthening of some individual synapses and is likely to result in shifts of the overall output of a given parallel fiber. This in turn would lead to rearrangements of the relative weights of synaptic connectivity between granule and Purkinje cells.

In order to further investigate the possible impact of these rearrangements it would be crucial to reconstruct entire granule cell axons and compare the distribution and morphology of PFBs on entire axonal arbors.

Additionally, it would be interesting to compare structural plasticity of parallel fibers with the underlying mossy fiber terminals and granule cells, as several lines of evidence suggest a modular functioning of the cerebellar cortex with co-active synapses that lie in vertical columns or patches (see also discussion of microzones below).

## Experience-related, subregion-specific growth of MFTs and rearrangements of mossy fiber terminal connectivities in the adult cerebellar cortex

In this study we demonstrate that EE induces region-specific growth of MFT subsets. This result is interesting with respect to the functional organization of the cerebellar cortex in co-active patches or ‘microzones’ (Oscarsson, 1976). Microzones are defined as functional units of the cerebellar cortex that combine with a small set of subcortical structures to form a cortico-nuclear microcomplex, which is a unitary neuronal complex devoted to a specific function (Ito, 2001, see also Figure 5). For instance, the human cerebellum was estimated to contain approximately 5000 microcomplexes, each of which is thought to play a specific role via its connections with functional systems in the spinal cord, brainstem, and cerebral cortex (Ito, 1984). Several microcomplexes have been associated unequivocally with specific reflexes in mice (see e.g. Tan et al., 1995a, 1995b; Graf et al., 2002) and have been determined to be as small as 50-150  $\mu\text{m}$  wide. Purkinje cells and inhibitory interneurons in each microzone receive climbing fiber inputs from the same receptive field and determine the firing of a small set of Purkinje cells, and thus the output of the zone.

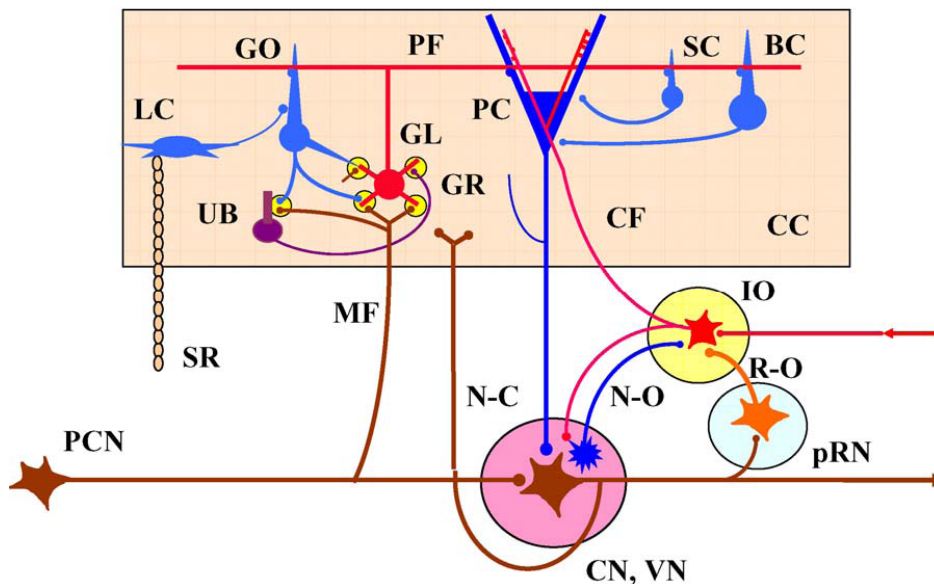


**Figure 5. Wiring diagram for a cerebellar corticonuclear microcomplex.**

The abbreviations stand for: BC, basket cell; CC, cerebellar cortical microzone; CF, climbing fiber; CN, cerebellar nucleus; GR, granule cell; GL, glomeruli; GO, Golgi cell; IO, inferior olive; LC, Lugo cell; MF, mossy fiber; N-C, nucleocortical mossy fiber projection; N-O, nucleo-olivary inhibitory projection; PC, Purkinje cell; PCN, precerebellar neuron; PF, parallel fiber; pRN, parvicellular red nucleus; R-O, rubro-olivary excitatory projection; SC, stellate cell; SR, serotonergic fiber; UB, unipolar brush cell; VN, vestibular nucleus (adapted from Ito, 2006).

The concept of a cortical microzone is very appealing with respect to our findings of subregion specific effects of EE on MFT growth. The analyzed crops in our study were not much larger than 1-2 microzones. It is tempting to speculate that EE specifically recruits some microzones that react with an increase in MFT sizes, while other microzones do not show alterations. In order to test this hypothesis, one could utilize one of the well-studied reflexes and study the MFT and perhaps also parallel fiber plasticity within the microzone characterized to underlie this given reflex.

Likewise, it would be important in further analysis of our data, to investigate whether parallel fibers as well as underlying mossy fiber patches display correlated structural rearrangements.

The idea of microzones is also interesting with respect to the increases in branching and MFT densities upon EE on single axonal arbors traced in lobule V. Increased branching and MFT densities seemed to occur at “hot spots” or in clusters along the projection. Such “spots” could reflect the innervation of a specific microzone and could thus reveal the identity of zones implicated in EE experiences. Again, it would be helpful to repeat similar experiments in animals trained for a well-studied reflex and investigate possible structural rearrangements in a zone known to be implicated in a certain trained task.

Such an experiment would at the same time address another interesting question, namely whether specific learning induces rearrangements of connectivity in implicated neuronal circuits in the adult.

So far we have provided strong evidences that rearrangements of neuronal circuit connectivity occur upon a complex paradigm including many factors, such as increased motor-, social and sensory- activities, that have been previously involved in inducing changes of several kinds, such as hormonal, metabolic, neuro-modulatory. Thus, it is not clear whether the observed changes are a direct effect of the training and learning occurring during EE, or whether they reflect general changes induced by the above mentioned systemic influences. A marked alteration of experience, such as provided by environmental enrichment, could lead to an overall increase in trophic factors or stimulate molecular mechanisms that generally increase synaptic strength and result in

global effects on all neuronal circuits. Alternatively, the induced changes could be usage-specific and involve only actively recruited neuronal circuits. Our data indicate so far that although many brain regions and synapses are affected by EE, we always observed region- and cell-specific differences, arguing for a predominant usage-dependent and against a systemic effect of EE. However, future studies would be necessary to narrow down the effects of EE by investigating which parts within the complex environment lead to changes in which circuits. Maybe more straightforward would be the already above mentioned exploitation of a well-studied learning paradigm, such as the vestibule-ocular reflex (VOR) or the eye-blink conditioning paradigms. The neuronal circuits and plasticity mechanisms underlying these two learning paradigms have been characterized in detail and would thus allow a focused analysis of potential structural rearrangements correlated to a specific learning event.

In summary, we have provided evidence for experience-related rearrangements of neuronal circuit connectivities in the adult cerebellar cortex. The rearrangements were observed at consecutive steps within a neuronal pathway and affected only subsets of the observed neurons and structures. Future studies would be useful to reveal the correlations between the observed changes and the behavioral changes that induced them. For this it would be necessary to reduce the complexity of the experience used to stimulate the plasticity response and to identify the neurons involved in the used task. The cerebellum seems an attractive candidate to make such correlations possible, due to the well-characterized anatomy and the implication of the cerebellum in simple associative learning tasks. Furthermore, due to its superficial localization, the cerebellar cortex is an attractive system to perform *in vivo* imaging upon specific learning, such as classical eye-blink conditioning. Therefore, the results presented here are a first step towards future studies to investigate the potential correlation between learning and structural changes in neuronal connectivity *in vivo*.

### **3.1.5. MATERIALS & METHODS**

The experimental procedures used in this part were the same as those described in the previous chapter. Age of mice in EE: 2 month + 1 month in EE.

3.2. WNT SIGNALING REGULATES EXPERIENCE-RELATED  
REARRANGEMENTS OF HIPPOCAMPAL MOSSY FIBER TERMINAL  
CONNECTIVITY IN THE ADULT

Nadine Gogolla & Pico Caroni

*unpublished results*

### 3.2.1. SUMMARY

Wnt signaling has important roles in structural remodeling of neurons and the establishment of neuronal circuit connectivity during development. Recently, a role for Wnt signaling in activity-dependent synaptic plasticity has been suggested.

Here we investigated the role of Wnt signaling in experience-related rearrangements of hippocampal mossy fiber terminal connectivity in the adult *in vivo*. We found that Wnt7b is expressed in the adult hippocampus *in vivo*, as well as in mature hippocampal slice cultures. Wnt7b expression was strongly upregulated in CA3 pyramidal neurons upon enriched environment (EE) experience. Inhibition of Wnt signaling by the secreted Frizzled related protein 1 (sFRP-1) resulted in marked remodeling of hippocampal large mossy fiber terminals (LMTs) in the adult *in vivo* and in mature slices, and prevented the effects of EE on mossy fiber terminal connectivity.

### 3.2.2. INTRODUCTION

Wnts are a family of secreted glycoproteins that regulate many cell behaviors including proliferation, differentiation, survival, polarity and movement. Wnts play essential roles in embryonic and postnatal development in various systems, including the nervous system. In addition, they have a critical role in the development and progression of many types of cancer (Nusse, 2005). Wnts can act locally, in an auto- or paracrine manner, or at distance, by generating gradients across tissues. Importantly, Wnt signaling plays a key role in diverse aspects of the establishment of neuronal circuit connectivity by regulating axon guidance, dendritic development, axon remodeling and synapse formation (Ciani & Salinas, 2005; Fradkin et al., 2005).

Wnts are, as a prerequisite to their proper functioning, post-translationally palmitoylated. Their binding to seven-pass transmembrane receptors of the Frizzled (Fz) family, leads to activation of disheveled (Dvl), a cytoplasmatic scaffolding protein, and the start of diverse and complex signaling cascades (Cadigan and Liu, 2006).

Downstream of Dvl, the Wnt pathway diverges into at least three branches: the canonical or Wnt/ $\beta$ -catenin pathway; the planar cell polarity pathway and the Wnt/calcium pathway. Additionally, all these pathways might still bifurcate further (Ciani et al. 2004).

Activation of the the canonical/  $\beta$ -catenin pathway results in inhibition of glycogen synthase kinase 3  $\beta$  (GSK3 $\beta$ ), which leads to an increase in the levels of  $\beta$ -catenin in the cytoplasm, its translocation to the nucleus, and the formation of  $\beta$ -catenin-T-cell specific transcription factor (TCF) complex that activates the transcription of target genes (Logan & Nusse 2004). For instance, Wnt signaling has been shown to regulate the cytoskeleton through a branch of the canonical pathway that diverges downstream of GSK3 $\beta$ . Dvl binds to microtubules and, through inhibition of GSK3 $\beta$ , changes the organization of microtubules and increases their stability. Dvl signals locally to regulate the phosphorylation of GSK3 $\beta$  targets, such as microtubule-associated protein 1B (MAP1B), a protein that regulates microtubule dynamics (Ciani et al., 2004).

In an alternative pathway, the planar cell polarity pathway, activated Fz signals to Dvl, which in turn, activates the small GTPases Rho and c-Jun amino (N)-terminal kinase (JNK), indicating that both the actin cytoskeleton and microtubules are likely to be affected. It is important to note that this pathway, despite its name, might affect several cellular behaviors without affecting cell polarity.

Finally, in the Wnt/calcium pathway, binding of specific Wnts to Fz receptors and activation of Dvl leads to calcium influx, and activation of protein kinase C (PKC) and calcium/calmodulin dependent protein kinase II (CamKII) (Logan & Nusse, 2004; Ciani & Salinas, 2005).

Which Wnt signaling pathway will be engaged is determined by the combination of Wnt ligands and Fz receptors. There are many Wnts and Fz receptors in the genome of many species. In the mouse genome, for instance, 19 Wnt and 9 Fz genes have been identified. One Fz can bind many Wnts, and one Wnt can bind several Fz receptors. Additionally, their signaling often involves co-receptors, e.g. low density lipoprotein-receptor related proteins (LRPs), and is modified by agonist and antagonists of Wnt signaling, such as Dickkopf (Dkk), secreted Frizzled related proteins (sFRPs) or Dally. In this way, the same Wnt can signal through several pathways, depending on the cellular environment and developmental stage, e.g. different Fz receptors are expressed by the same cells at different developmental stages.

In conclusion, the Wnt signaling system is highly regulated and particularly sophisticated (Gordon & Nusse 2006).

It is well established that Wnt signaling is crucial for the proper development of the nervous system. Critical roles for Wnts have been identified in neural patterning, axon guidance and remodeling, dendrite morphogenesis, as well as synaptogenesis and synaptic maturation.

Likewise, during development, Wnt signaling is essential for the proper formation of many brain structures. For instance, the canonical Wnt pathway, starting with Wnt3a, has been demonstrated to regulate hippocampus formation, and Wnt3a knockout mice lack the hippocampal region (Lee et al., 2000). Interestingly, Wnt signaling continues to play an important role in the adult hippocampus as it is required for proper adult neurogenesis (Lie et al., 2005).

Wnts have also been described as repulsive and attractive signals during axon guidance in *Drosophila* and in vertebrates (Yoshikawa et al., 2003; Fradkin et al., 2004, 2005; Lyuksyutova et al., 2003), and studies in the cerebellum and spinal cord have revealed a role for Wnt proteins as target-derived signals that regulate the terminal arborization of axons (Hall et al., 2000; Krylova, 2002). Interestingly, Wnts were shown to induce axon remodeling by changing the organization and dynamics of the cytoskeleton, especially microtubules (Ciani et al. 2004, Ciani & Salinas, 2005).

Furthermore, Wnt/ $\beta$ -catenin signaling was identified as a critical mediator of dendritic morphogenesis in hippocampal neurons. During dendritogenesis, Wnt7b has been shown to signal via Dvl, Rac and JNK, through a non-canonical pathway, which does not require Wnt/ $\beta$ -catenin-dependent transcription, but increased Wnt release. Inhibition of the Wnt pathway by sFRP-1 decreases Rac activation and blocks the effect of Wnt7b on dendrite development. Conversely, pharmacological activation of JNK enhances dendrite development (Yu & Malenka 2003, Rosso et al. 2005).

Moreover, studies on the cerebellar mossy fiber to granule cell synapse have revealed a role for the canonical Wnt pathway in synaptogenesis. Wnt7a is expressed in granule cells during synapse formation with mossy fibers, where it increases synapsin I clustering. Consistent with these findings, Wnt7a knockout mice have defects in mossy fiber remodeling and in synapsin I and Bassoon clustering (Lucas & Salinas, 1997; Hall et al. 2000, Ahmad-Annur, 2006). Similarly, at the NMJ, Dvl regulates agrin-mediated AChR

clustering and was identified in a yeast two-hybrid screen to directly interact with MUSK (Luo et al. 2002).

Taken together, these findings provide evidence that Wnt signaling plays multiple and important roles in the development of the nervous system, including the establishment of neuronal circuit connectivity.

At developing central synapses, Wnt proteins function as retrograde signals to regulate axonal and synaptic remodeling as well as maturation.

Interestingly, recent evidences suggest that Wnt proteins might play crucial roles beyond development by affecting synaptic plasticity in the adult. It was shown in acute mouse hippocampal slices (3-4 wks old) that tetanic stimulation of the perforant path induces NMDA receptor dependent Wnt3a release and nuclear  $\beta$ -catenin accumulations in postsynaptic dentate granule cells. Importantly, suppression of this activity-dependent synaptic Wnt release impaired LTP (Chen et al., 2006) demonstrating a role for Wnt signaling in activity-dependent synaptic plasticity in the adult.

Consequently, Wnt signaling is an attractive candidate mechanism to regulate experience-dependent rearrangements of neuronal circuits in the adult brain.

Previously, we have shown that subsets of hippocampal large mossy fiber terminal complexes (LMT-Cs) rearrange their local connectivities with CA3 pyramidal neurons in response to experience and age throughout life (Galimberti et al., 2006).

Here we investigate the possibility that Wnt signaling might mediate mossy fiber connectivity remodeling in response to experience.

### 3.2.3. RESULTS

#### **Wnt7b expression in the adult hippocampus is regulated by experience**

As a prerequisite to study the role of Wnt signaling in anatomical plasticity in the adult hippocampus, we analyzed the expression patterns of Wnt protein expression in this region *in vivo*. We found that Wnt7b protein is expressed in dentate gyrus granule cells as well as in CA3 pyramidal neurons in the hippocampus of adult mice (Figures 1A and 1B). Importantly, despite the presence of Wnt7b in granule cell bodies, mossy fibers did not contain detectable amounts of Wnt7b.

In order to address a potential role for Wnt proteins in experience-related plasticity in the hippocampus we investigated whether Wnt protein expression was influenced by housing mice under EE conditions. Comparison of Wnt7b staining intensities in mice housed under EE and control (CTRL) conditions revealed a substantial increase in Wnt7b protein in CA3 pyramidal neuron cell bodies, and specifically in their apical dendrites. The dendritic staining was particularly increased in large puncta forming lines in direction of the apical pyramidal dendrites within stratum lucidum suggesting that Wnt7b might accumulate in thorny excrescences upon EE (Figure 1C).

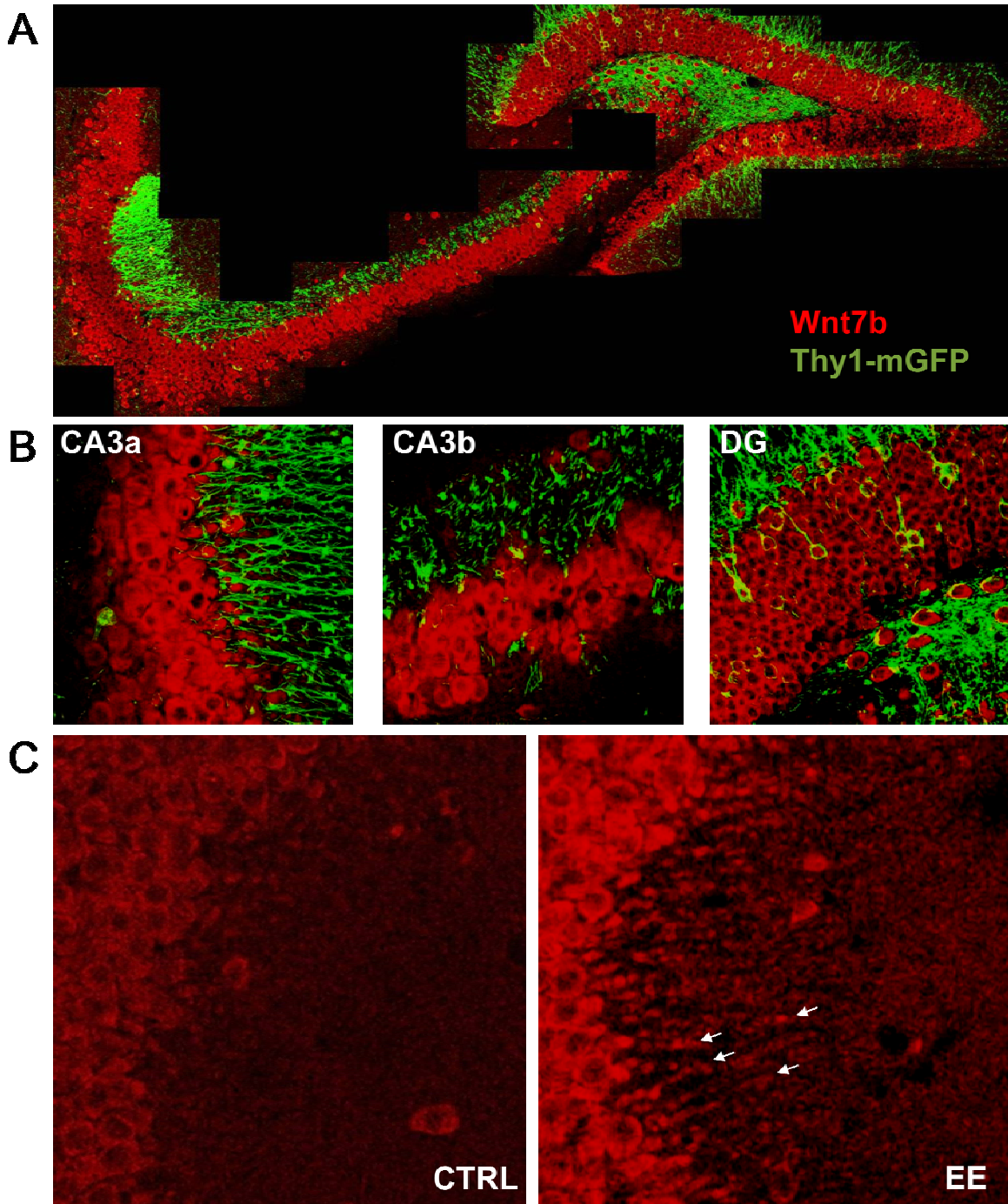


**Figure 1. Wnt7b expression in the adult hippocampus is regulated by experience**

(A) Expression of Wnt7b and Thy1-mGFP in the dentate gyrus and CA3 region of the hippocampus of a 3 month old CTRL mouse. Wnt7b is mostly expressed in the cell bodies of principal cells, but not in axons or dendrites (B) Higher magnifications of the CA3a, CA3b and dentate gyrus (DG) regions. (C) Experience-related increase in Wnt7b protein levels in the CA3 region of mice housed under EE (right) compared to CTRL (left) conditions. Note the marked increase in the levels of Wnt7b in the cell bodies of pyramidal cells, but also in dotted lines in the stratum lucidum (right from cell body layer). The Wnt7b positive puncta in stratum lucidum most likely represent Wnt accumulations in thorny excrescences.

### ***In vivo* inhibition of Wnt signaling by sFRP-1 remodels hippocampal large mossy fiber terminals (LMTs) in the adult**

We next addressed the question whether the sustained Wnt7b expression in adult CA3 pyramidal neurons influenced LMT morphologies. During development, Wnt proteins function as retrograde signals to regulate presynaptic assembly and maturation as well as terminal arborization of axons (Hall et al., 2000). We have demonstrated previously that LMTs undergo life-long systematic alterations in their morphologies, expanding continuously along CA3 pyramidal dendrites (Galimberti et al., 2006). We therefore wondered, whether Wnt signaling might play a role in synapse maintenance and remodeling in the adult hippocampus.

We blocked Wnt signaling by *in vivo* injections of the endogenous Wnt inhibitor sFRP-1 into the hippocampal CA3 region of adult mice (Figure 2A; see also Experimental procedures). We found that two weeks of chronic Wnt inhibition were sufficient to substantially remodel LMT morphologies throughout the CA3 region (Figures 2B-E). At first glance, the LMTs in the sFRP-1 treated hippocampi appeared larger than in the CTRLs and displayed elongated shapes along the direction of CA3 pyramidal dendrites, transversally to the mossy fiber projection. Interestingly, large changes in LMT morphologies seemed to involve groups of LMTs arranged in clusters, which were surrounded by less- or unaffected LMTs (Figures 2B-D). A detailed three-dimensional analysis at higher magnification revealed that Wnt inhibition leads to substantially elongated and flattened shapes of subsets of LMTs. These shapes were strikingly reminiscent of the shapes observed in aged animals (Galimberti et al., 2006; see also the following discussion).

Taken together, these results suggest that Wnt signaling is still active in the adult hippocampus, and that it regulates LMT maintenance and/or remodeling.

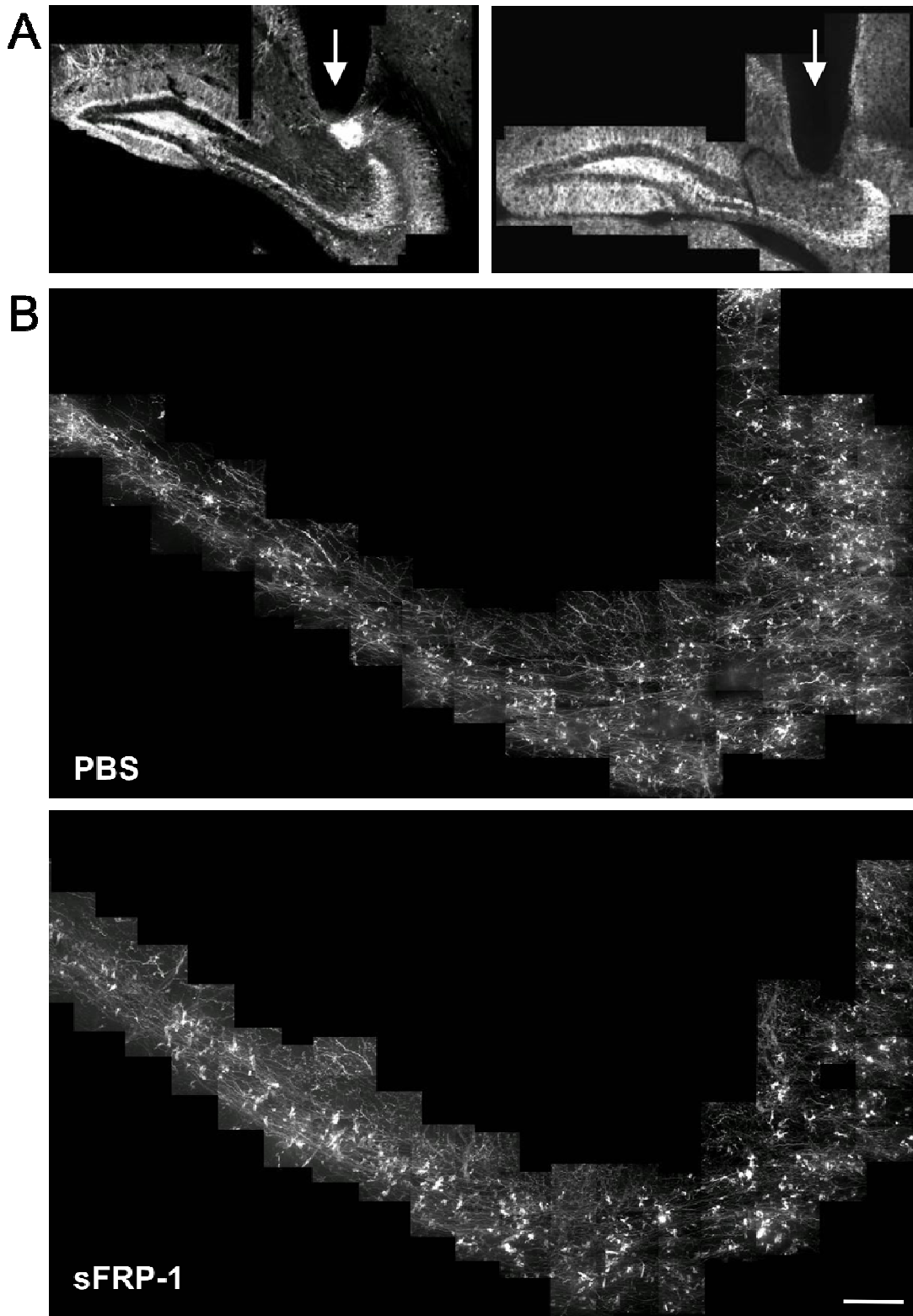


**Figure 2A-B. *In vivo* inhibition of Wnt signaling by sFRP-1 produces a remodeling of hippocampal large mossy fiber terminals (LMTs) in the adult**  
(A) Injection sites (see also Experimental Procedures) in two randomly chosen animals injected with PBS (left) and sFRP-1 (right). (B) The entire mossy fiber projection within CA3 of one CTRL (PBS injected) and one sFRP-1 injected mouse (both 3 months old). Scale bar: 100  $\mu$ m

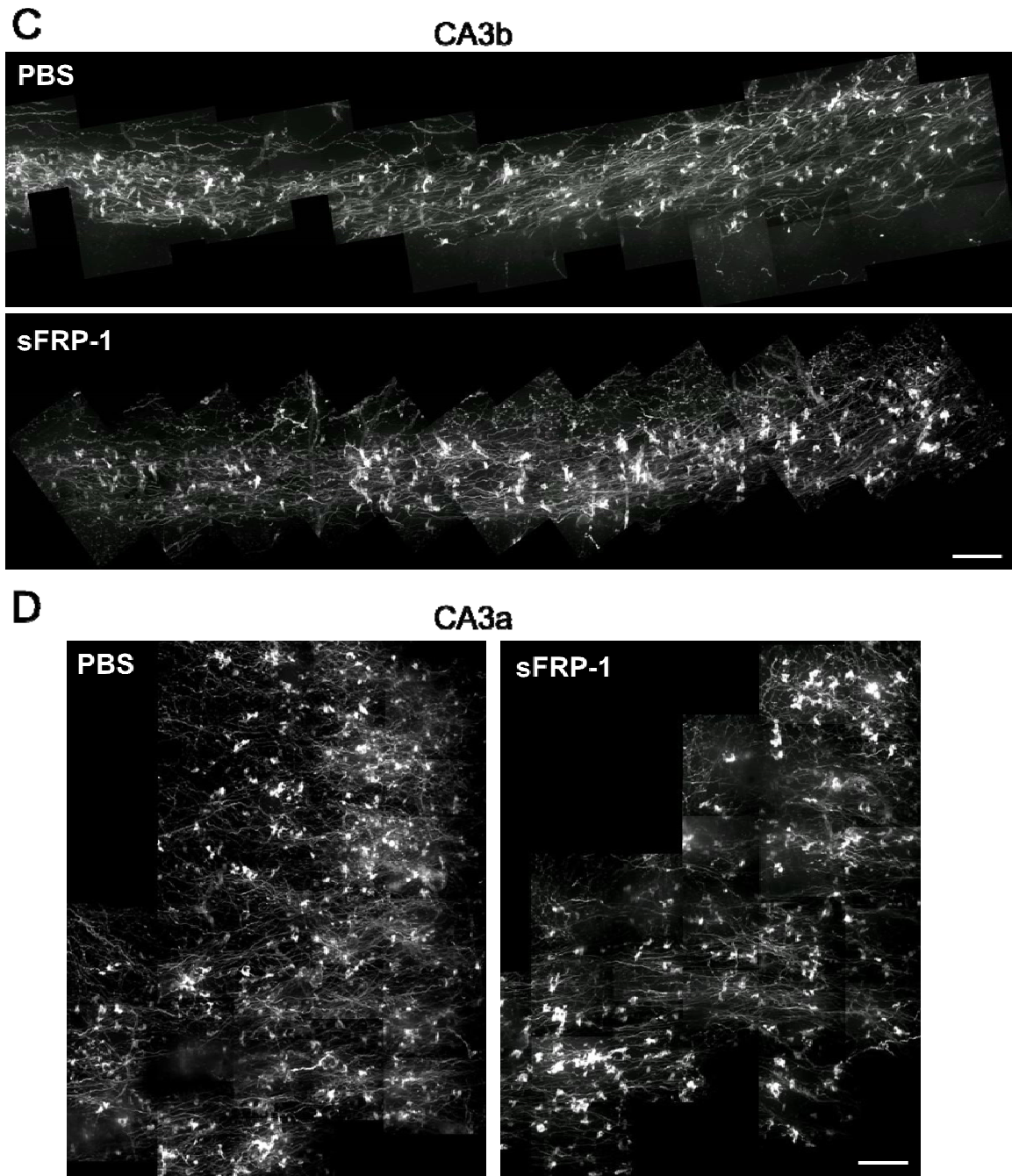


**Figure 2C-D. *In vivo* inhibition of Wnt signaling by sFRP-1 remodels hippocampal large mossy fiber terminals (LMTs) in the adult**

**(C)** Higher magnification of CA3b region of a CTRL and a sFRP-1 treated hippocampus. Note the longitudinal expansion of many LMTs transversally to the mossy fiber axons and along the CA3 pyramidal dendrites (not stained).

**(D)** Higher magnification of CA3a region of a CTRL and a sFRP-1 treated hippocampus. Note the clusters of highly affected LMTs in the sFRP-1 treated CA3a region (top and bottom of right image) in comparison to less affected terminals in the middle of the image.

Scale bars: 50  $\mu$ m.

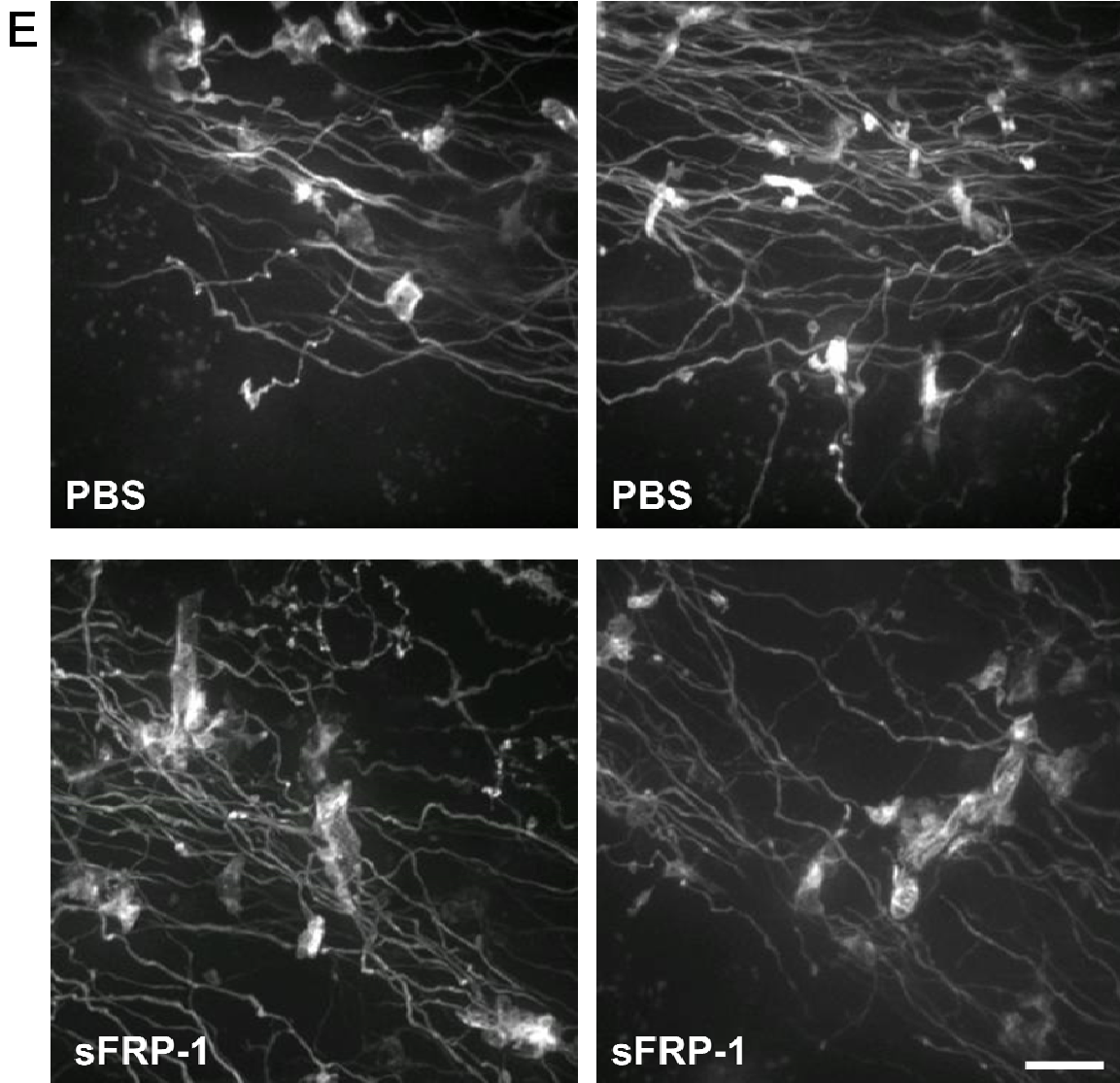


**Figure 2E. *In vivo* inhibition of Wnt signaling by sFRP-1 remodels hippocampal large mossy fiber terminals (LMTs) in the adult**  
(E) High magnification images of two CTRL and two sFRP-1 treated crops within CA3b. Note flattened (grey) and longitudinally expanded shapes of sFRP-1 treated LMTs in comparison to the small and round shapes of CTRL LMTs. Scale bar: 10  $\mu$ m.

All images in this panel are maximum intensity projections of 3D confocal stacks that were analysed in 3D.

**Inhibition of Wnt signaling by sFRP-1 suppresses experience-related rearrangements of mossy fiber terminal connectivity in the adult *in vivo***

We have shown previously that environmental enrichment leads to the rearrangement of mossy fiber terminal connectivity in the adult *in vivo* by inducing a pronounced increase in the complexity of LMT-Cs (Galimberti et al., 2006).

We now found that the inhibition of Wnt signaling throughout the phase of enrichment in a standard EE experiment (1 month of enrichment, 3 month old mice, see Experimental Procedures for further details) led to a suppression of the effects of EE on LMT-C connectivity. sFRP-1 treatment led to changes in LMT morphologies comparable to those observed under CTRL conditions, namely an expansion of LMT subsets along pyramidal neuron dendrites, and a flattening of LMTs (Figures 3A and 3B). On the other hand, no signs of typical EE effects were detected in a first analysis, i.e. LMTs did not grow substantially in all dimensions, but rather elongated and flattened, reminiscent of the changes observed upon aging and similar to the changes induced by sFRP-1 injected animals of the same age housed under CTRL conditions. Moreover, while EE in untreated animals leads to an increase in the number of satellite LMTs per LMT-C, here, in a first analysis we could not detect a similar change upon EE in sFRP-1 treated animals (Figures 3A and 3B). A detailed analysis involving the tracing of single axons and LMT-Cs, as well as the quantitative analysis of LMT sizes will, however, be necessary in order to determine the qualitative and quantitative extent of the inhibiting effects of sFRP-1 on EE-mediated LMT rearrangements (see Discussion).

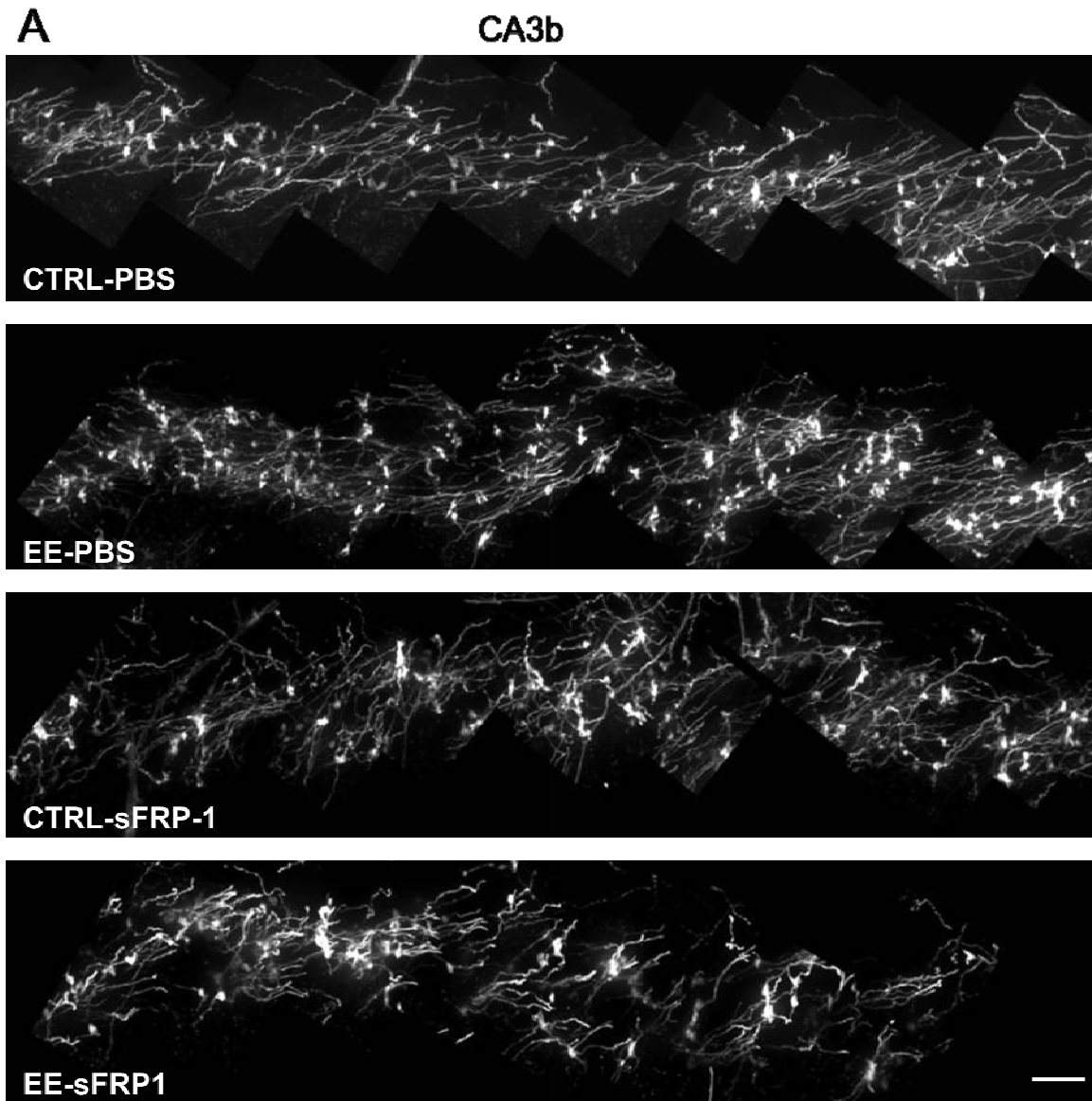


**Figure 3A. Inhibition of Wnt signaling by sFRP-1 suppresses experience-related rearrangements of mossy fiber terminal connectivity in the adult *in vivo***

(A) Mossy fiber projection in CA3b. Note the increase in size and complexity of LMTs (increase in number of LMTs is likely due to satellite addition) in PBS injected animal housed under EE conditions compared to CTRLs. LMTs treated from sFRP-1 treated animals display elongated shapes under both, EE and CTRL housing conditions, but no specific increases in complexity related to the EE condition.

Scale bar: 50  $\mu$ m.

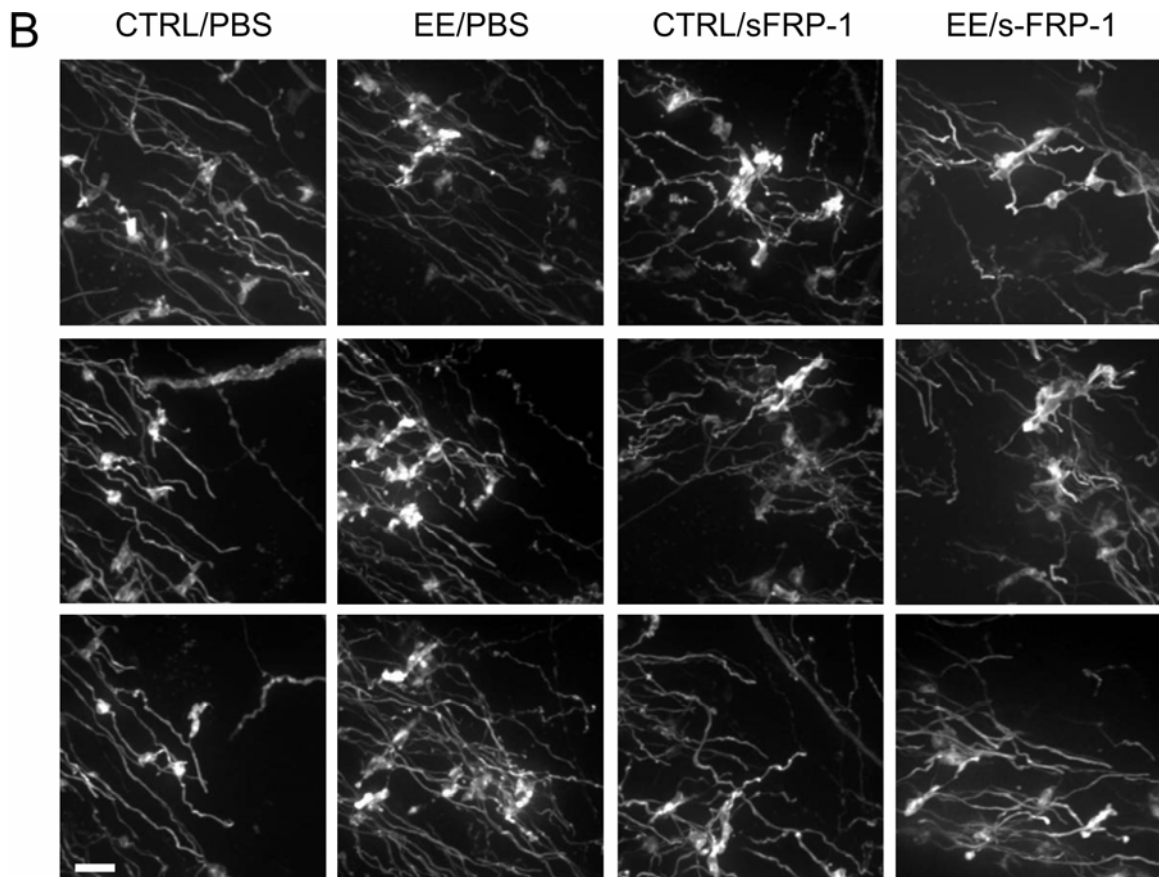


**Figure 3B. Inhibition of Wnt signaling by sFRP-1 suppresses experience-related rearrangements of mossy fiber terminal connectivity in the adult *in vivo***  
**(B)** High resolution images of randomly chosen crops in CA3b. EE induces the previously described increase in size and the addition of satellites (often many objects around a central one) in PBS injected animals. EE fails to exhibit similar increase in complexity and size when sFRP-1 is injected simultaneously. However, sFRP-1 treatment results in elongated and flattened shapes of LMTs under both, EE and CTRL, conditions.  
 Scale bar: 10  $\mu$ m.

### **Wnt7b expression in the adult hippocampus is regulated by experience and positive feedback.**

We next wondered whether and how expression of Wnt7b protein was influenced by inhibition of Wnt signaling. Comparison of Wnt7b staining intensities upon sFRP-1 treatment under EE and CTRL conditions revealed, that inhibition of Wnt signaling in animals housed under CTRL conditions led to a marked decrease in staining intensity compared to PBS injected animals housed under the same conditions. This decrease was almost totally rescued in sFRP-1 injected animals exposed to EE, as they exhibited similar staining intensities as the PBS injected EE group (Figure 3C). These results suggest that Wnt7b expression is dynamically regulated in the adult hippocampus. Experience, as well as Wnt signaling itself, seems to provide positive feedback loops that

boost Wnt7b expression, while decreased Wnt signaling leads to a marked decrease in levels of Wnt7b.

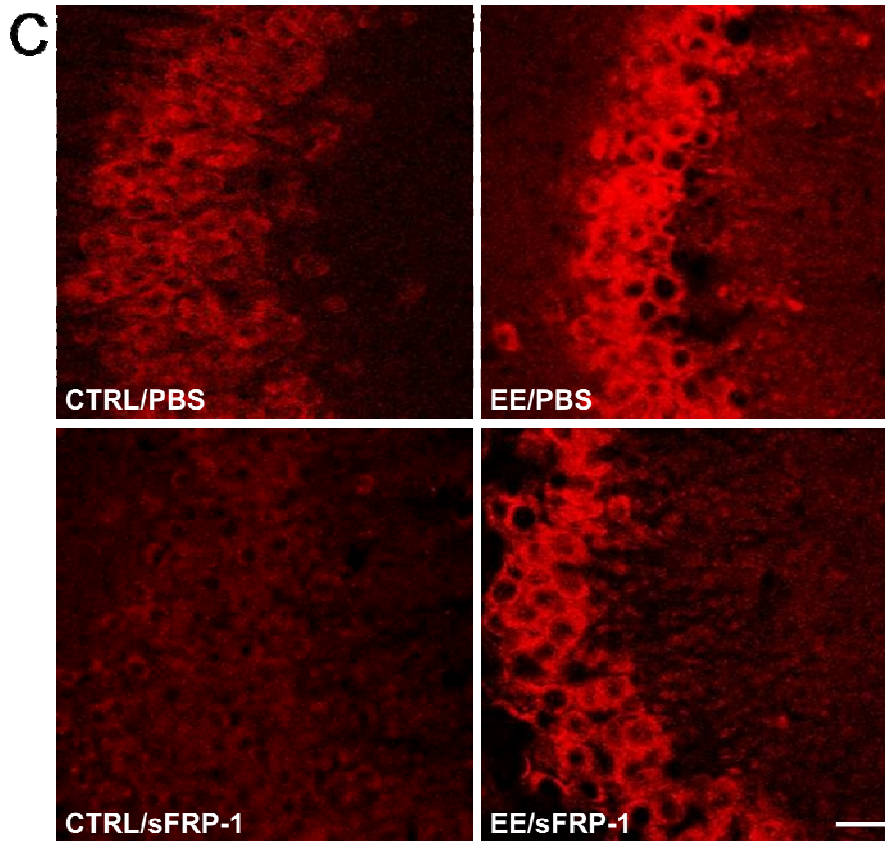


**Figure 3C. Inhibition of Wnt signaling by sFRP-1 suppresses experience-related rearrangements of mossy fiber terminal connectivity in the adult *in vivo***

(C) Wnt7b staining in mice housed under CTRL and EE conditions, with and without sFRP-1 treatment. Note the marked decrease of staining intensity upon sFRP-1 treatment and the almost complete rescue of this depression by EE. Scale bar: 20  $\mu$ m.

### **Wnt7b is expressed in mature hippocampal slice cultures**

We next determined whether long-term hippocampal slice cultures could be a valuable tool to investigate how Wnt signaling affects LMT-C rearrangements in an experimentally accessible system. As a prerequisite we investigated whether Wnt7b protein was expressed in mature hippocampal slice cultures. Staining of mature slices revealed that Wnt7b protein was present in granule and CA3 pyramidal cells in comparable patterns as *in vivo*. Remarkably, we observed similar Wnt7b positive lines of puncta in stratum lucidum as *in vivo*. In the slice, some of these Wnt7b accumulations colocalized with a small subset of GFP labeled LMTs, indicating that they might stain thorny excrescences that enwrap the LMTs. Interestingly, only a small subset of labeled

LMTs colocalized with Wnt7b accumulations, while the majority did not (Figure 4). Finally, and consistent with our observations *in vivo*, mossy fibers did not contain detectable amounts of Wnt7b although granule cells expressed Wnt7b (Figure 4).

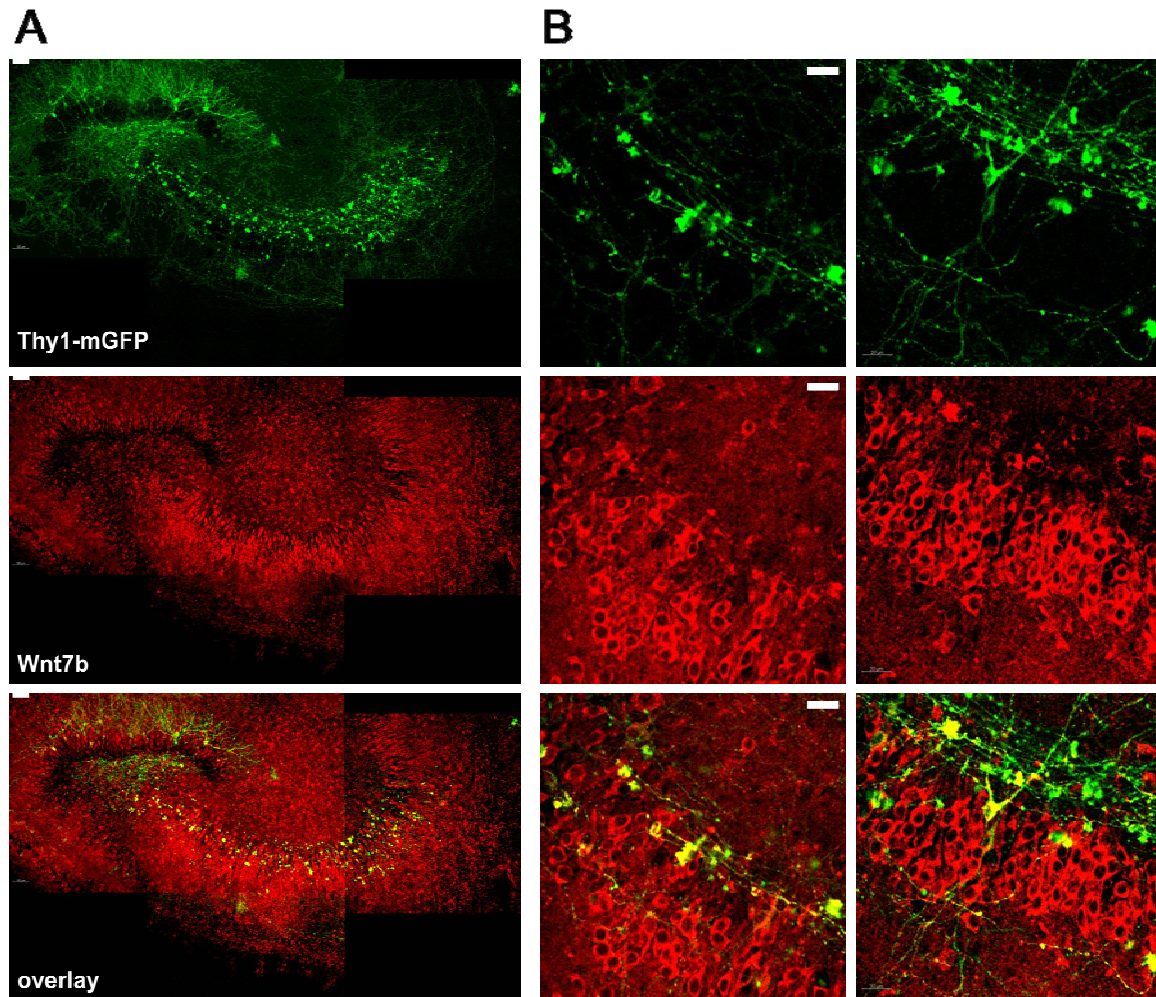


**Figure 4. Wnt7b is expressed in mature hippocampal slice cultures.**

Example of Wnt7b staining (Wnt7b = middle panels) of a mature (40DIV) hippocampal slice culture made from a Thy1-mGFP (GFP signal = top panels) transgenic mouse.

(A) Entire slice culture with labeled GFP positive granule cells in the dentate gyrus projecting their mossy fibers through the hilus into the CA3 region (top). Wnt7b is expressed weakly in granule cells and more strongly in CA3 pyramidal neurons (middle panel and overlay on the bottom).

(B) High magnification images in CA3b revealing the presence of Wnt7b accumulations or puncta in stratum lucidum, where they colocalize with a small subset of LMTs.

All images shown in this panel are MIPs. Colocalizations were confirmed in 3D analysis (not shown).

Scale bars 20  $\mu$ m.

### **Wnt signaling affects LMT sizes in slice culture**

In order to investigate the time course and the evolution of the effect of Wnt inhibition on LMT-C rearrangements observed *in vivo*, we treated slice cultures with the Wnt inhibitor sFRP-1 and with an activator of Wnt signaling, BIO, which specifically inhibits GSK3 $\beta$  and thus leads to activation of the canonical Wnt pathway similarly to Lithium.

We found that while 5 days of Wnt inhibition via sFRP-1 led to a general shrinkage of all LMTs, activation of the canonical Wnt pathway for the same time via BIO led to substantial growth of almost all LMTs (Figure 5). These results indicate that at short-term, Wnt signaling via the canonical pathway regulates LMT growth and maintenance.

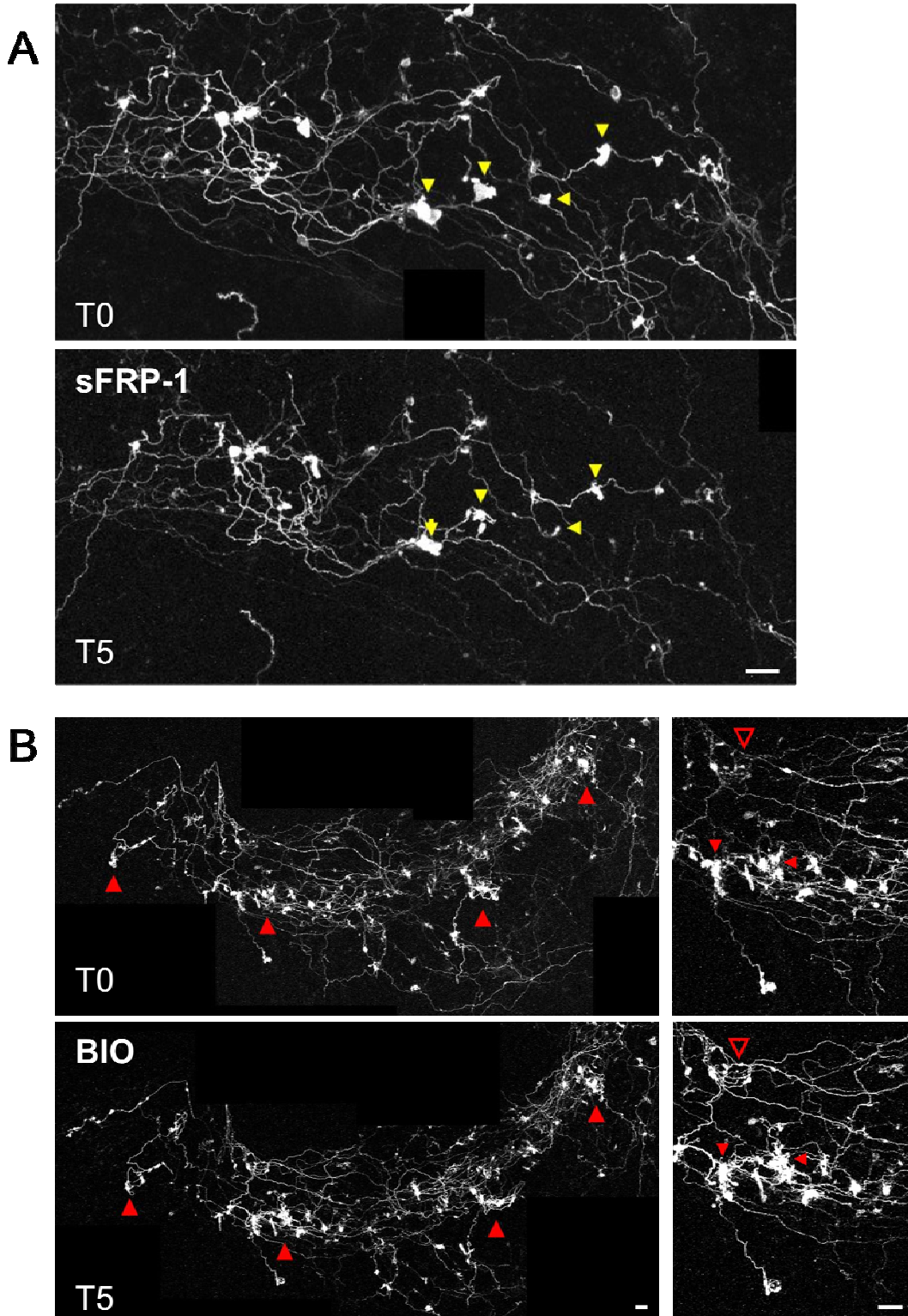


**Figure 5. Wnt signaling affects LMT sizes at short time scales**

Short term treatments affecting Wnt signaling in mature hippocampal slice cultures (DIV20-25).

**(A)** 5 days of Wnt inhibition via sFRP-1 result in a general decrease of LMT sizes.

**(B)** 5 days of activation of the canonical Wnt signaling pathway via the GSK3 $\beta$  inhibitor 'BIO' leads to marked increase in LMT sizes in mature hippocampal slice cultures.

Scale bars: 10  $\mu$ m.

### **Long-term Wnt inhibition in slice culture leads to remodeling of LMT shapes**

We next investigated the effects of long-term Wnt signaling inhibition in mature slices. We found that 20 days of sFRP-1 treatment yielded similar rearrangements of LMT shapes and mossy fiber terminal connectivity as described previously *in vivo*. LMTs adopted elongated and flat shapes. Notably, as *in vivo*, subsets of LMTs that were most affected laid in clusters together surrounded by less- or non-affected LMTs (Figure 6). Taken together, these results in slice cultures suggest that Wnt signaling exhibits a dynamic, at least 2-phasic role in regulating LMT remodeling.

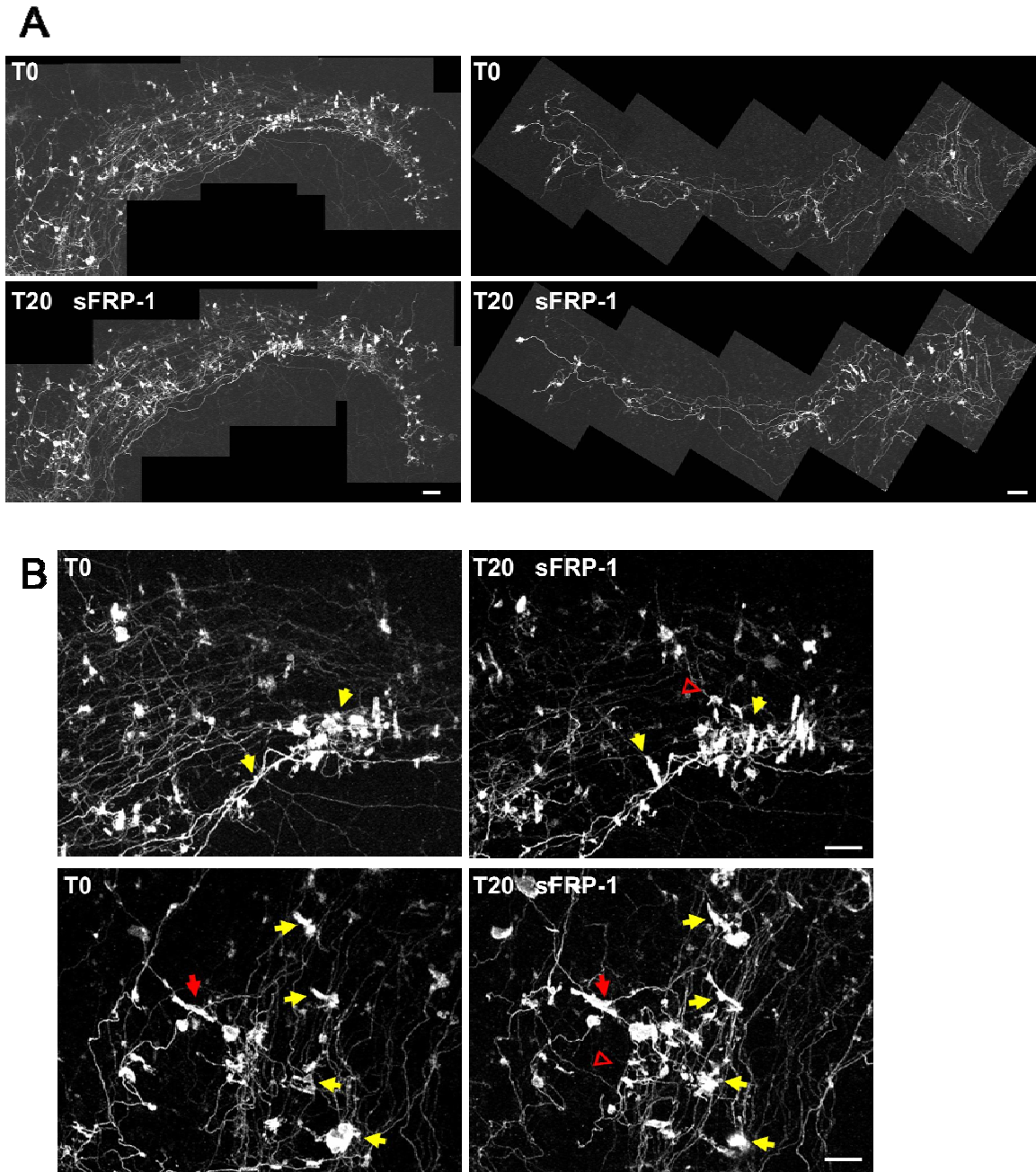


**Figure 6. Long-term Wnt inhibition in slice culture leads to remodeling of LMT shapes**

(A) Two examples of entire mossy fiber projections in slice culture treated for 20 days with sFRP-1. DIV20 slice culture before (T0, upper panels) and after 20 days of sFRP-1 treatment (T20, lower panels). (Left panels: Note the increase in elongated shapes of LMTs upon sFRP-1 treatment and the redistribution of large LMTs. The previously more homogeneously distributed LMTs grow bigger in some regions and shrink or remain the same size at other places leading to a “clustered” distribution of large, elongated LMTs. Right panels: A mossy fiber projection with less labeled axons to illustrate the reorganization of the mossy fiber projection by sFRP-1 treatment. While LMTs at the end of the projection remain largely unaffected, LMTs at the beginning of the projection, in CA3b, elongate and grow, shifting occurrence of the largest LMTs from the end (CA3a) of the projection before treatment to the beginning (CA3b) of the projection after the treatment.

(B) High magnification images of subregion of the upper left mossy fiber projection. Note the marked elongation of LMTs.

Scale bars: 20  $\mu$ m.

### 3.2.4. DISCUSSION

In this study we provide evidence that Wnt signaling plays important roles in the adult hippocampus in synapse maintenance and remodeling and in mediating experience-related rearrangements of neuronal circuit connectivity.

We show that Wnt7b is expressed in the adult hippocampus *in vivo*, as well as in mature hippocampal slice cultures and that inhibition of Wnt signaling by the secreted Frizzled related protein 1 (sFRP-1) results in marked remodeling of hippocampal large mossy fiber terminals (LMTs) in the adult *in vivo* and in mature slices.

We demonstrate that Wnt7b expression is substantially upregulated in CA3 pyramidal neurons upon enriched environment (EE) experience and that inhibition of Wnt signaling *in vivo* prevents the previously described effects of EE on mossy fiber terminal connectivity. The impact of these findings as well as important future directions will be subjects of the following discussion.

#### **Role for Wnt signaling in neuronal circuit plasticity in the adult**

Our results provide new insights into the regulation of synapse maintenance and remodeling *in vivo* and implicate Wnt signaling in experience-dependent structural plasticity in the adult. While the function of Wnt signaling in the establishment and remodeling of neuronal connectivity during development had been established in previous studies (Ciani & Salinas, 2005; Fradkin et al., 2005), we here revealed a novel and dynamically regulated role for Wnt signaling in controlling the rearrangements of neuronal connectivity occurring in the hippocampal mossy fiber pathway upon EE experience in the adult.

Inhibition of Wnt signaling via sFRP-1 in the hippocampi of three month old mice results in substantial remodeling of LMT shapes, resulting in elongation and flattening as well as an increase in the size heterogeneities of these presynaptic terminals. These shapes and arrangements of LMTs as well as the large heterogeneity in the LMT population are very similar to the changes that we described in relation to normal aging (Galimberti et al., 2006). Wnt inhibition for only two weeks results in rearrangements of the mossy fiber projection reminiscent of those observed in the oldest age group investigated previously,

namely 22 month. In our previous study, we observed that these changes in LMTs were accompanied by elongation of postsynaptic, thorny excrescence clusters on CA3 pyramidal dendrites, but not the elongation of individual thorns. Interestingly, it has been shown previously by others that, during development, Wnt signaling positively influences dendritogenesis of cultured hippocampal neurons via a pathway involving Dvl, Rac and JNK, an effect blocked by sFRP-1 (Yu & Malenka 2003, Rosso et al. 2005). It will therefore be interesting to analyze our data in more detail, to determine what impact sFRP-1 treatment has on the distribution and sizes of postsynaptic thorns on pyramidal cell dendrites.

We also show that upon sFRP-1 injections, Wnt7b protein levels are markedly decreased in CA3 pyramidal cell bodies and apical dendrites, the postsynaptic partners of LMTs. This finding is likely due to the interruption of a positive feedback mechanism by which Wnt signaling stimulates its own expression. This suggests that the effects of sFRP-1 might result from two cooperative mechanisms: the absence of Wnt signaling likely effects LMT growth and maintenance (see also short-term slice culture treatment), and at the same time inhibits or fails to stimulate further Wnt production. These two effects might act together and augment the effects of Wnt inhibition on LMT remodeling. It will be interesting to determine whether Wnt7b protein levels in CA3 display age-related changes, and could thus be implicated in the rearrangements of mossy fiber terminal connectivity upon ageing. One possibility is that Wnt7b expression decreases slowly with age, and that this is why we observe an “old” age phenotype of the mossy fiber projection in young animals treated with sFRP-1.

Earlier studies using dissociated cultured neurons have shown that manipulations that increase synaptic activity stimulate Wnt release (Yu & Malenka, 2003; Chen et al., 2006). Our results provide evidence, that EE, an *in vivo*- manipulation that involves increased motor, sensory as well as social activity, results in a marked increase in Wnt protein levels in hippocampal CA3 neurons and the specific accumulation of Wnt7b in subsets of dendritic thorns. We speculate that this specifically located Wnt7b might be released upon activity, and that it could thus lead to increased Wnt signaling at specific sites

within the mossy fiber to CA3 projection. This interpretation is consistent with studies in the developing CNS, which have provided strong evidence for Wnt proteins to function as retrograde signals to regulate axonal and presynaptic remodeling as well as presynaptic strengthening (Lucas & Salinas, 1997; Hall et al. 2000, Ahmad-Annur, 2006). Taken together with the specific localization of Wnt7b in a subset of thorny excrescences, these results could indicate that Wnt signaling might provide a means to induce growth and strengthening of specific subsets of synapses within the mossy fiber pathway upon altered experience. Such a specific shift of a subset of LMTs towards larger sizes and higher Basson contents per LMT have been described by us previously to occur in slice culture (Galimberti et al., 2006) and upon EE *in vivo* (my own unpublished results, not shown). Interestingly, in mature slice cultures we observed a small subset of LMTs colocalizing with Wnt7b positive puncta. Time-lapse imaging of slice cultures has previously revealed that only 1-2 LMTs per axon are highly dynamic and grow substantially over time (Galimberti et al., 2006). It would be interesting to reveal by staining at the end of such time-lapse experiments whether Wnt7b localizations in thorny excrescences correlate to especially large and plastic or rather to stabilized LMTs.

In order to reveal the precise impact of Wnt inhibition on mossy fiber terminal arrangements *in vivo*, it will be essential to reconstruct single axonal arbors and LMT-Cs upon sFRP-1 treatment, in mice housed under CTRL and EE conditions.

One limitation of our *in vivo* study is that sFRP-1 inhibits most Wnt signaling pathways. Despite the good correlation with our Wnt7b data, we can not exclude that the sFRP-1 effects are partly or entirely due to the inhibition of other Wnt pathways involving different Wnt proteins. In order to address this question, we could make use of our slice culture system. Mature hippocampal slice cultures could be treated with conditioned medium obtained from Wnt7b expressing cells (as used by Rosso et al., 2005) and the possibly induced rearrangements of mossy fiber terminal connectivity could be monitored at high temporal resolution and include the tracing of entire and individual axonal arbors. If Wnt7b treatment would be affective in slices, it could provide a convenient model system to investigate EE-like effects on synaptic connectivity *in vitro*.

The general effects of sFRP-1 could also lead to a reduction of granule cell neurogenesis, as neurogenesis was reported to be regulated by Wnt3a signaling (Lie et al., 2005) and is especially increased upon EE (Kempermann et al., 1997, 1998a, 1998b, 2002). Two lines of evidence argue that our results are likely not to be affected by a potential influence of sFRP-1 on dentate gyrus neurogenesis. First, we observe very similar results *in vivo* and *in vitro* with respect to LMT remodeling upon sFRP-1 treatment. We have previously observed that neurogenesis does not occur in our slice culture system (unpublished data). Secondly, our injection site is far away from the dentate gyrus above CA3a. Observations of surrounding hippocampal tissue in the septo-temporal extension of the hippocampus revealed that the characteristic effects of sFRP-1 on LMT shapes were not observed at marked distances from the injection site and thus argue for a local action of sFRP-1 restricted to a small region around the injection site, most likely not attaining the dentate gyrus. Therefore, our observations are unlikely to result from secondary effects caused by affecting granule cell neurogenesis.

Hippocampal slice cultures are an attractive system to unravel the molecular mechanisms of Wnt7b signaling in the adult hippocampus. We found that at short term, activation of the canonical Wnt pathway via the specific GSK3 $\beta$  inhibitor, BIO, results in a size increase of most LMTs within the mossy fiber projection, while sFRP-1 treatment for the same time, had opposite effects. These results are interesting with respect to the previously reported roles for Dvl and inhibited GSK3 $\beta$  in microtubule stabilization. Dvl has been reported to be localized to active zones and to signal locally to regulate the phosphorylation of GSK3 $\beta$  targets, such as microtubule-associated protein 1B (MAP1B), a protein that regulates microtubule dynamics and by this stabilizes microtubules (Ciani et al., 2004). It would be interesting to see whether and to what extent LMTs contain microtubules. Microtubules as well as their regulation could make up substantial differences between differently plastic LMTs, a hypothesis that could be tested experimentally.

Finally, it would be interesting to determine whether sFRP-1 injections *in vivo* during EE, in parallel to preventing mossy fiber connectivity rearrangements, might also prevent the well-characterized functional effects of EE, i.e. the improvements in learning and

memory capacities (Moser et al., 1997; Schrijver et al., 2002; Lee et al., 2003; see also the General Introduction). This could provide an opportunity to correlate experience-related changes in neuronal circuit connectivity to well characterized experience-related functional and behavioral alterations.

### **3.2.5. MATERIALS & METHODS**

We used the same mice and experimental procedures as described in a previous study (Galimberti et al. 2006). Methods specifically used in this study are briefly outlined below.

#### **Imaging**

High resolution imaging of fixed sections was performed on a VISITRON spinning disc microscope, using an 100x oil immersion objective

#### **sFRP-1 treatments**

*In vivo*: Mature recombinant sFRP-1 (R&D systems - cat-no. 1384-SF) was dissolved in PBS / 0.1% BSA (C = 50ug/ml) and 300nl of this sFRP-1 solution or vehicle (PBS / 0.1% BSA) alone were injected. In brief: canulas were implanted unilaterally into the left hemisphere above the CA3a-b region, using the following coordinates: (implantation 0.5 mm above injection site as the needle surpasses canula by 0.5 mm) Anterio-posterior (from Bregma): -2.06 mm, lateral 2.5 mm, dorso-ventral -1.4 mm. All mice were Thy-1 – mGFP transgenics (see previous chapters); mice used for individual experiments were littermates and the age at death was 3-4 months. Mice were injected repeatedly every 3-4 days for 14 days up to 1 month. For EE experiments, mice were injected during the entire month of the EE experience.

*In vitro*: see previous chapter for details, we used sFRP-1 at 1µg/ml, and BIO (Calbiochem, San Diego, CA) at 2µM.

#### **Antibodies**

Bassoon as before, Wnt7b antibody (R&D – cat-no. AF-3460).

**3.3. LACK OF RAB3A AFFECTS MOSSY FIBER TERMINAL MORPHOLOGY  
BUT NOT EXPERIENCE-RELATED REARRANGEMENTS  
OF THEIR CONNECTIVITY**

Nadine Gogolla & Pico Caroni  
*unpublished results*

### **3.3.1. SUMMARY**

We previously showed that hippocampal mossy fiber terminal connectivities are substantially rearranged in response to age and experience throughout life. Here we explored whether mossy fiber long-term potentiation (mfLTP) is necessary for experience related rearrangements of neuronal circuit connectivity in the adult. We investigated mossy fiber terminal arrangements in Rab3a knockout (KO) mice that lack mfLTP. We found that Rab3a-KO mice housed under CTRL conditions exhibited pronounced alterations in mossy fiber terminal morphologies and decreased active zone densities. Environmental enrichment in Rab3a-KO mice induced marked rearrangements of mossy fiber terminal connectivity and rescued the active zone phenotype.

### **3.3.2. INTRODUCTION**

Long-term potentiation (LTP) is a broadly accepted model for the cellular basis of memory formation. Interestingly, it has been reported previously by others that LTP can lead to structural alterations, e.g. electrical stimulations that induce LTP and LTD in brain slices result in dendritic spine formation and elimination, respectively (Toni et al., 1999; Nägerl et al., 2004).

While most forms of LTP are postsynaptic and depend on NMDA receptors, mossy fiber (mf) LTP is NMDA receptor independent and presynaptic (Harris & Cotman, 1986; Nicoll & Malenka, 1995). In contrast to the postsynaptic forms, mfLTP has been shown to depend on the presynaptic proteins Rim1 $\alpha$  and Rab3a, which are involved in the control of synaptic vesicle release (Castillo et al., 1997, 2002). Rim1 $\alpha$  and Rab3a knockout (KO) mice specifically lack presynaptic LTP at mossy fibers in the hippocampus and at parallel fibers in the cerebellum (Castillo et al., 1997, 2002). Mossy fiber LTP is an attractive candidate mechanism to mediate experience-related rearrangements of neuronal circuit connectivity in the adult hippocampus. To explore this possibility we analyzed LMT arrangements in mice lacking Rab3a.

Rab proteins are a family of small GTPases involved in intracellular trafficking. Rab3a is the most abundant family member in the brain, and the only detectable isoform of Rab3 in mossy fiber terminals (Geppert et al., 1994, 1997; Castillo et al., 1997).

It has been shown that Rab3a is not essential for synaptic vesicle fusion, but that calcium-dependent neurotransmitter release, e.g. upon repetitive stimulation critically depends on the presence of Rab3a (Geppert et al., 1994). Accordingly, Rab3a-KO mice specifically lack mfLTP (Castillo et al., 1997).

Interestingly, Rab3a-KO mice show impaired spatial reversal learning and increased explorative activity (D'Adamo et al., 2004) and it has been suggested that Rab3a-dependent plasticity might play a specific role in reactivity to novel stimuli (Geppert et al., 1994).

Here we report that Rab3a-KO mice exhibit substantially smaller LMTs, consisting of few subunits and displaying atypical circular and symmetrical shapes. We further found that active zone densities were reduced in KO mice, and that EE rescued this phenotype. The characteristic increase in LMT sizes upon EE observed in WT animals did not occur in Rab3a-KO mice. Instead, we observed a marked increase in LMT numbers. Time-lapse imaging of long-term slice cultures suggested that Rab3a-KO mossy fibers have smaller and less stable LMTs, which lack satellites.

Taken together these results provide strong evidence that mfLTP has a critical role in inducing and maintaining LMT growth. These results further suggest that EE induces mossy fiber terminal rearrangements through mfLTP-independent mechanisms and that mfLTP is specifically required to promote the growth new terminals not their increased complexity.

### 3.3.3. RESULTS

#### **Rab3a-knockout mice exhibit smaller and less complex LMTs than wildtype mice**

In order to investigate whether the ability to express mfLTP might influence the morphology of LMTs, we imaged LMTs of adult mice lacking Rab3a. As a prerequisite to allow the analysis of LMT morphologies at high resolution, we crossed Rab3a-KO and -WT mice with Thy1-mGFP transgenic mice, expressing mGFP in only a few neurons (De Paola et al., 2003).

We found that LMTs in three months old Rab3a-KO mice were strikingly small, and exhibited circular and smooth outlines that stood in sharp contrast to the irregular and asymmetrical LMT shapes observed in WT animals (Figures 1A and 1C). Additionally, WT LMTs were composed of several subunits, while Rab3a-KO LMTs showed much simpler compositions, mostly consisting of only a single and rarely of two subunits (Figure 1C). A quantitative analysis of LMT volumes revealed that LMTs in Rab3a-KO animals are on average significantly smaller, and that the overall size distributions are shifted towards smaller sizes in the entire LMT population (Figure 1B).

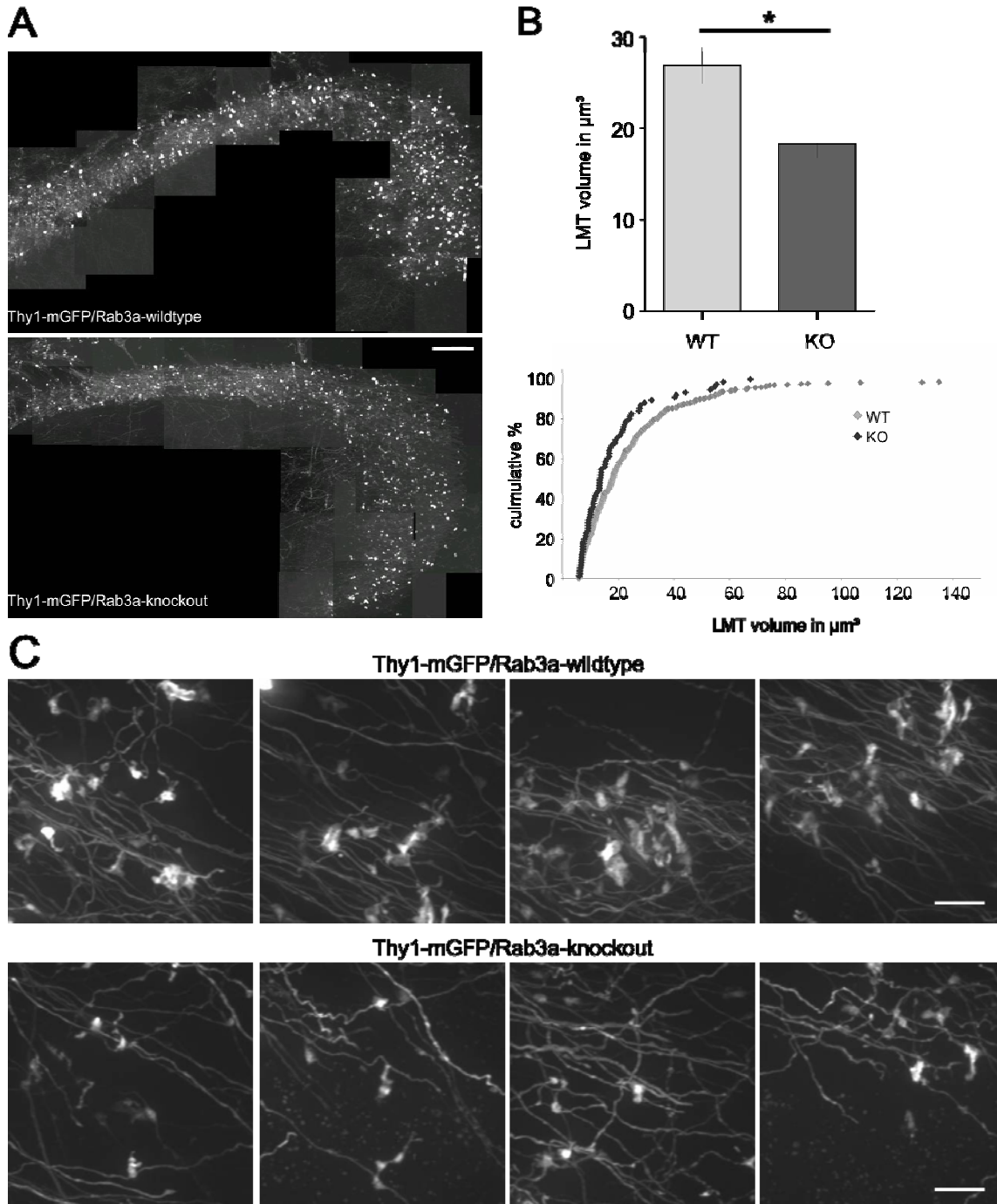


**Figure 1. Rab3a-knockout mice exhibit smaller and less complex LMTs than wildtype mice.**

(A) Entire mossy fiber projections of Rab3a-wildtype (upper panel) and -knockout (lower panel) Thy1-mGFP transgenic mice. Note that Rab3a KO mice exhibit substantially smaller LMTs throughout the entire CA3 region. (B) Quantitative analysis of LMT sizes in Rab3a-KO mice. Note that LMTs in Rab3a-KO are on average significantly smaller than in WT mice. Post-hoc student's t test:  $*p < 0.05$  (upper panel). A cumulative plot analysis showed that the size distribution curve is homogeneously shifted and that thus LMTs of all sizes are smaller in Rab3a-KO mice (lower panel). (C) High magnification images of Rab3a-KO and WT LMTs. Note the much larger and irregular shapes of WT LMTs (upper panels) compared to the small and circular outlines of Rab3a-KO LMTs. WT animals are composed of several subunits, while KO terminals are composed of only 1-2 subunits. Scale bars: 100 $\mu\text{m}$  (A); 10 $\mu\text{m}$  (C).

### **Experience-related increase in LMT numbers but not sizes in Rab3a KO mice**

In order to determine whether mFLTP is required for the experience-related rearrangements of mossy fiber terminal connectivity in the adult (Galimberti et al., 2006), we performed EE experiments with Rab3a-KO mice. Interestingly, although we did not observe a size shift towards larger LMTs under EE conditions, we found a pronounced increase in LMT numbers and especially an apparent increase in the number of very small LMTs upon EE (Figures 2A and 2B). Remarkably, also upon EE the Rab3a-KO LMTs conserved their small, circular and symmetrical shapes and did not adopt irregular, convoluted shapes as under control conditions.

### **EE rescues lower active zone densities in stratum lucidum of Rab3a KO mice**

We next wondered whether the marked increase in LMT numbers upon EE in Rab3a-KO mice was correlated to an increase in active zone numbers. We found that Rab3-KO mice housed under CTRL conditions exhibited dramatically reduced active zone densities in stratum lucidum compared to WT mice, as revealed by Bassoon immunostainings. Interestingly, EE markedly increased active zone densities in Rab3a-KO mice to levels comparable to those observed in WT mice, indicating that it rescued the Rab3a-KO phenotype with respect to active zone densities (Figure 2C).

### **EE rescues Wnt7b expression levels in CA3 pyramid cells of Rab3a-KO mice**

Having determined that Wnt signaling has a critical role for experience-dependent mossy fiber terminal rearrangements (see previous chapter), we wondered whether EE resulted in an increase of Wnt7b expression in Rab3a-KO comparable to that observed in WT mice. We found that Rab3a-KO mice housed under CTRL conditions exhibited dramatically reduced levels of Wnt7b protein in CA3 pyramidal neurons, and that EE rescued this phenotype by increasing the protein levels of Wnt7b to levels comparable to those in WT mice (Figure 2D).

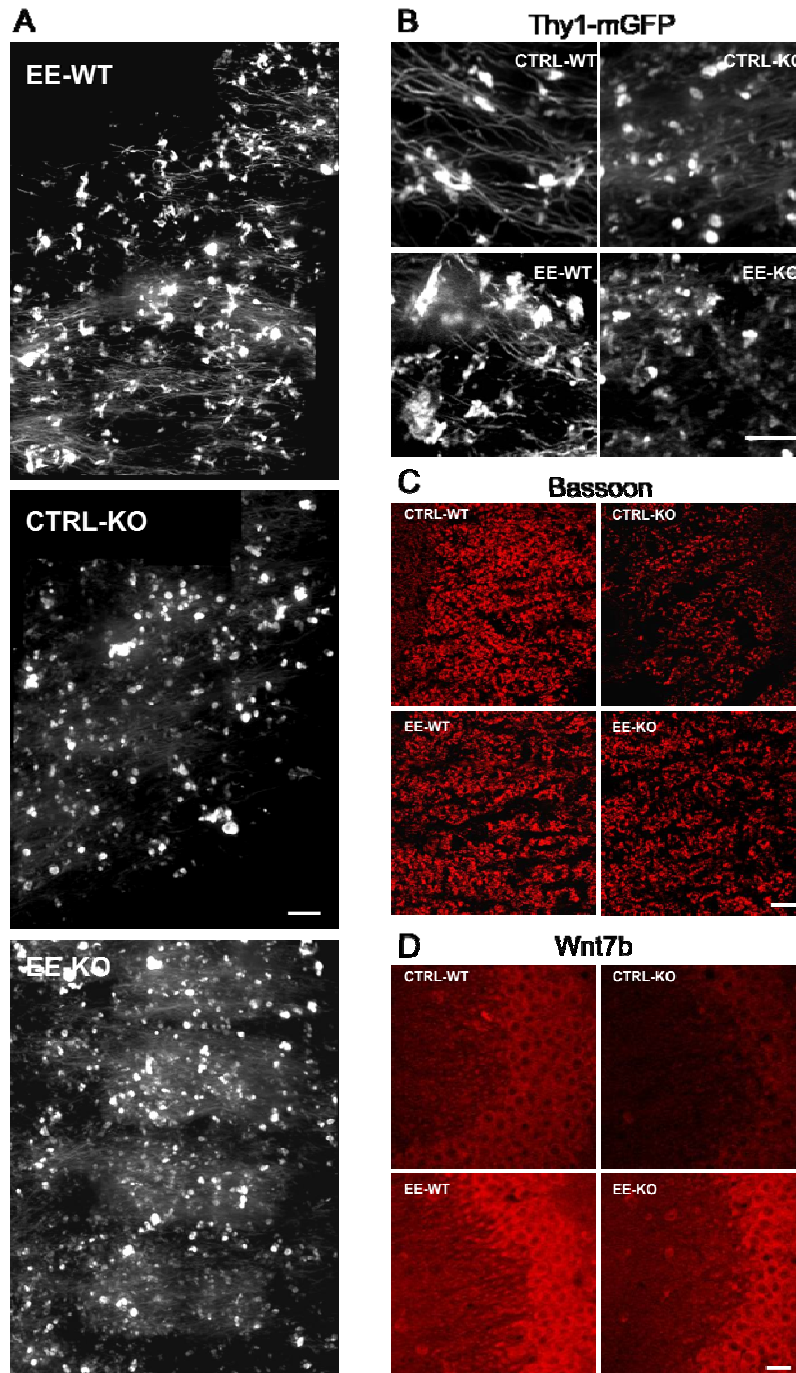


**Figure 2. Experience-related increase in LMT numbers but not sizes rescues lower active zone densities in stratum lucidum of Rab3a KO mice** (A) Images taken in CA3a of Rab3a WT and KO mice housed under EE conditions and KO mice housed under CTRL conditions. Note the marked increase in LMT numbers and especially of small LMTs in Rab3a KO mice housed in EE. While EE in WT mice causes increases in size and shape asymmetry of LMTs, in KO mice no change in shape or size of LMTs is detectable. (B) Higher magnifications of LMTs of KO and WT animals housed under CTRL or EE conditions. Note the circular and small shapes of LMTs in KO mice before and after EE; the increase in LMT numbers of especially small LMTs upon EE in KO, standing in sharp contrast to the irregular shapes of LMTs in WTs and the marked increase in size and complexities of WT LMTs upon EE. (C) Bassoon staining in KO and WT animals housed under CTRL or EE conditions. Note the markedly lower Bassoon densities in KO animals upon CTRL housing and the increase of densities upon EE. (D) Wnt7b staining in KO and WT animals housed under CTRL or EE conditions. Note the markedly lower Wnt7b levels in KO animals upon CTRL housing and the pronounced increase of intensity upon EE. Scale bars: 10µm (A, B, C); 20µm (D).

### **LMTs in hippocampal slice cultures made from Rab3a-KO mice exhibit substantially reduced sizes and stability**

In order to investigate the Rab3a-KO phenotype on LMT morphologies and their arrangements on mossy fibers in an experimentally more accessible system, we performed time-lapse imaging experiments in mature organotypic hippocampal slice cultures, made from a Rab3a-KO and WT mice crossed into Thy1-mGFP transgenic background. Analysis of single axons at different days *in vitro* (DIV) revealed that Rab3a-KO mossy fibers bore LMTs of substantially smaller sizes than WT axons (compare Figures 3A and 3B). The KO terminals exhibited circular shapes and were almost undistinguishable from the usually much smaller *en passant* varicosities. Slightly larger LMTs were only found at the very end of the mossy fiber in CA3a.

Interestingly, we also found that Rab3a-KO LMTs were less stable than those of WT mice (compare Figures 3A and 3B). We observed that within 20 days, a subset of terminals disappeared (Figure 3A, red star) while a few new ones appeared (Figure 3A, green star) whereas terminals in wild-type slices were predominantly stable (e.g. Figure 3B). Despite their instability, reduced size and atypical shapes, we found that LMTs in Rab3a-KO slices could still grow, and that one LMT seemed to be the largest and to grow the most, an observation we had previously made in WT slices (Galimberti et al., 2006). The numbers of LMTs per axon observed in Rab3a-KO mice seemed to be comparable to WT slices but KO LMTs did not bear satellites.

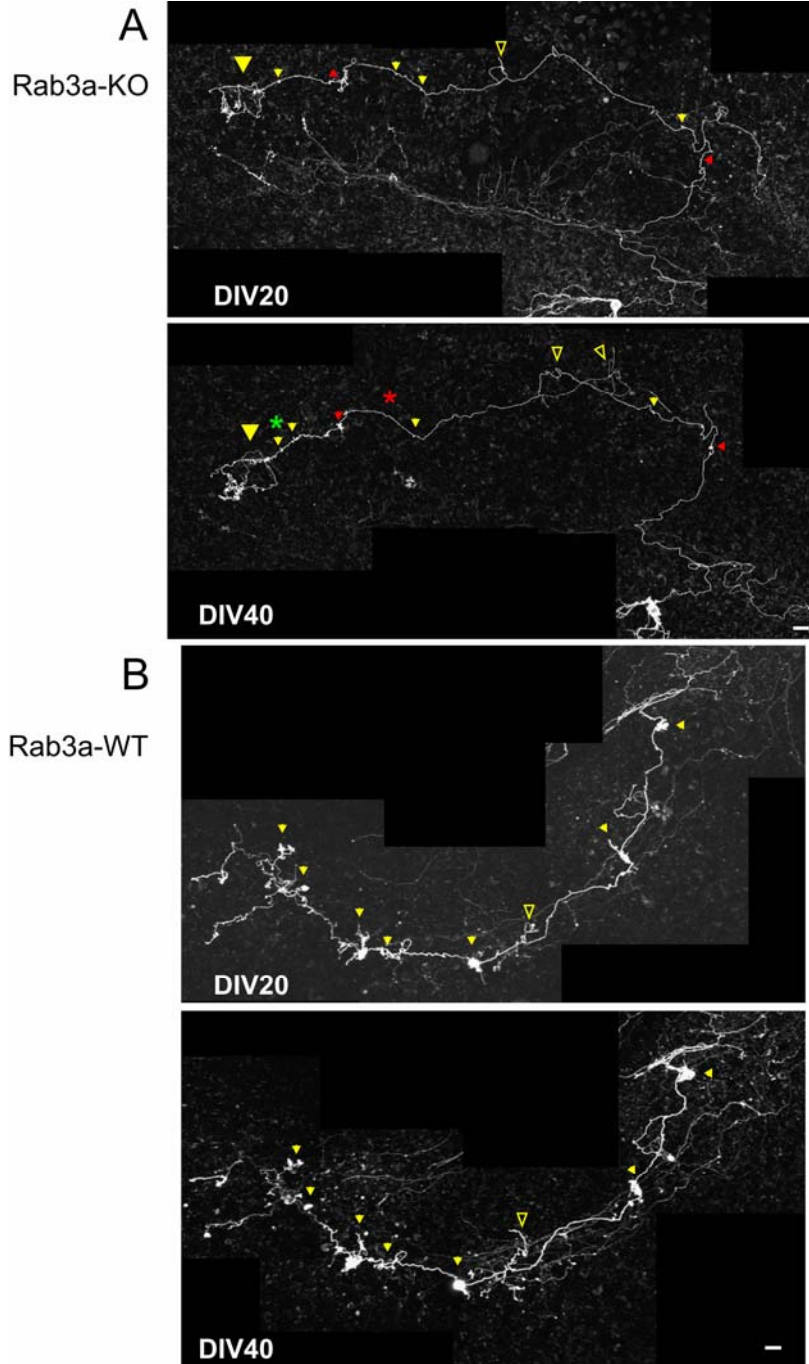


**Figure 3. LMTs in hippocampal slice cultures made from Rab3a-KO mice exhibit substantially reduced sizes and stability.** Examples of time-lapse images of mature organotypic hippocampal slice cultures, made from Rab3a-KO and WT/Thy1-mGFP transgenic mice, exhibiting one well labeled mossy fiber at DIV20 and DIV40 each. **(A)** Example from a Rab3a-KO mouse. Upper panel: Note that at DIV20 the LMTs (arrowheads) are largely reduced in size, most of them are undistinguishable from *en passant* varicosities. At the very end of the projection apparently larger LMTs can be seen (larger arrowhead, see text), as well as an axonal branch not bearing any LMTs (unfilled arrowhead). Lower panel: The same slice after 20 more days in culture (DIV40). Note that two LMTs grew over the period of 20 days (red arrowheads). All other LMTs remained unchanged or disappeared (red star). Occasionally, new, very small LMTs appeared at different places (green star). The axonal branch disappeared and another large axonal process was added at a different place (unfilled arrowhead). **(B)** Example from a Rab3a-WT mouse. Upper panel: Note that already at DIV20 the WT mossy fiber exhibits eight large LMTs (arrowheads) clearly distinguishable from the *en passant* varicosities (as big as the assumed LMTs in Rab3a KO). Lower panel: Note that after 20 more days in culture, many LMT grew or maintained their sizes and positions. The position and number of LMT does not change between DIV20 and 40. The axonal branch seen in DIV20 (unfilled arrowhead) remained its position and grew.

### 3.3.4. DISCUSSION

In this study, we provide evidence that the absence of Rab3a, a presynaptic protein essential for mfLTP, leads to marked alterations in LMT morphologies and stability. We further provide evidence that environmental enrichment rescues the decreased densities of active zones in the absence of Rab3a, presumably through the addition of new LMTs. The possible significance of these findings, remaining open questions, and possible directions for future work will be subjects of the following discussion.

#### **Rab3a-knockout mice exhibit smaller and less asymmetric LMTs than wildtype mice**

Our results provide novel insights into mechanisms governing LMT sizes and shapes. We demonstrate that in the absence of Rab3a and mfLTP, LMTs are smaller, less asymmetrical and composed of only very few subunits. These results are in agreement with our previous observations that inhibition of PKC, which inhibits mfLTP, leads to specific shrinkage especially of the larger LMTs, and to more equal size distributions of LMTs on single axons (Galimberti et al., 2006). Our results suggest that mfLTP has a critical role for LMT growth.

We show that active zone densities are markedly decreased in Rab3a-KO mice. This finding could result from two alternative scenarios. First, mossy fibers might establish less LMTs, resulting in less synaptic contacts and less active zones. Secondly, mossy fibers might establish equal numbers of LMTs as WT axons, but the Rab3a-KO LMTs might contain less active zones per terminal, and our own findings argue against the possibility that Rab3a-KO mice have less granule cells. Our slice culture data suggest that mossy fibers bear comparable numbers of LMTs per axon, but preliminary observations of single axons *in vivo* seem to hint at larger spacing of LMTs on single mossy fibers. One possible explanation for this discrepancy could be that some of the terminals counted *in vitro* as LMTs were in reality *en passant* varicosities. Thus, it remains unsolved whether Rab3a-KO mossy fibers bear less LMTs, LMTs bear less active zones or whether both is true. In order to address these questions it will be essential to trace individual axons *in vivo* and to follow single axons over longer times *in vitro*. Furthermore, Bassoon stainings and active zone quantifications per LMT could reveal the

relationship between LMT volume and active zone contents. In addition, electron microscopy could help to determine whether LMTs bear less or smaller active zones and whether the smaller LMT shapes are reflected by smaller postsynaptic thorny excrescences.

Moreover, it would be important to address in future studies whether Rab3a-KO LMTs lack the ability to grow. Our slice culture data seem to indicate that at least a subset of LMTs grew over 20 days *in vitro*. However the observed growth was very weak. Thus, it would be interesting to see how LMTs of Rab3a-KO mice evolve over longer time scales *in vivo*. We have previously shown that in WT animals, LMTs expand gradually along CA3 pyramidal dendrites and adopt more and more elongated shapes in the course of normal aging. The oldest animals we have looked at so far were four month old. No signs of asymmetrical, longer LMTs have been observed. However, this does not rule out that LMTs bear the capacity to grow at later ages.

### **Experience-related increase in LMT numbers but not sizes in Rab3a KO mice**

Having uncovered the marked impact of Rab3a and presumably mFLTP on LMT sizes, we investigated the impact of EE experience on mossy fiber terminal rearrangements in Rab3a-KO mice. Upon EE, we observed a marked increase specifically in the number of small LMTs and a concomitant increase in active zone densities. These results suggest that the active zone increase is due to the addition of new LMTs.

It will be particularly interesting to determine whether the newly formed LMTs upon EE are added on the main axon, or whether they are satellite LMTs. The formation of satellite LMTs would be consistent with our findings in WT animals that EE experience produces an increase in satellite numbers per core LMT-C (Galimberti et al., 2006). In addition, increased satellite numbers would provide additional evidence that mFLTP is not required for the increase in LMT-C complexity observed in our earlier study.

Finally, having observed partial anatomical rescue of the Rab3a-KO phenotype in LMTs of mice that experienced EE, it would be interesting to investigate whether EE might also be sufficient to rescue the behavioral deficits observed in Rab3a-KO mice (D'Adamo et al., 2004).

### **LMTs in hippocampal slice cultures made from Rab3a-KO mice exhibit substantially reduced sizes and stabilities**

As already observed in our previous studies, organotypic hippocampal slice cultures revealed remarkable consistency with results obtained from *in vivo* preparations, and thus provide an invaluable tool to study structural plasticity in an easy accessible system. Our results using slice cultures indicate that LMTs in Rab3a-KO mice are smaller and more symmetrical, grow much less and are less stable than WT LMTs *in vitro*. Additionally, they do not exhibit satellite LMTs. It will be interesting to determine in slice cultures, whether satellites or additional LMTs on the main axons will eventually appear with time or under conditions of enhanced activity, and whether these conditions would lead to LMT growth. Moreover, it would be most interesting to determine whether Wnt7b conditioned medium can lead to the addition of LMTs in the Rab3a-KO slice cultures (see previous Chapter).

Our *in vivo* data suggest that EE leads to an increase in LMT numbers but not sizes and to an increase in active zone numbers. The slice culture could help to determine by which mechanisms EE exerts these functions.

### **EE rescues lower Wnt7b expression in CA3 pyramid cells of Rab3a-KO mice**

Interestingly, our results reveal that CA3 pyramidal neurons of Rab3a-KO mice contain reduced levels of Wnt7b protein, a phenotype that is rescued by housing Rab3a-KO mice in EE. It is tempting to speculate that the increased levels of Wnt7b protein, that might be a result of increased activity in the hippocampus upon EE, lead to the observed increase in LMT numbers in Rab3a-KO mice. We show in a parallel study (see previous chapter) that inhibition of Wnt signaling largely prevents the effects of EE on mossy fiber terminal rearrangements. The observed upregulation of Wnt7b protein in CA3 pyramidal neurons together with the addition of LMTs upon EE in Rab3a-KO mice, could provide a further strong argument for the crucial role of Wnt signaling in mediating the effects of EE on mossy fiber connectivity in the adult, namely the increase of divergence through the addition of satellite LMTs, or possibly core LMTs in the case of Rab3a-KO mice.

In order to test this hypothesis it might be useful to treat hippocampal slice cultures made from Rab3a-KO mice with drugs that affect Wnt signaling. We have previously shown that BIO, an activator of canonical Wnt signaling, induces LMT growth in slice cultures upon short-term treatment. If the effects of EE on mossy fiber terminal connectivity are indeed largely mediated by Wnt signaling, we would predict that BIO treatment in Rab3a-KO slices might mimic the EE effects observed in Rab3a-KO mice *in vivo*, leading to the addition of many small LMTs. Similarly, one could address whether inhibition of Wnt signaling via sFRP-1 has any further effects in Rab3a-KO slices. Finally, it would be essential to investigate whether the addition of small LMTs upon EE in Rab3a-KO mice could be blocked by sFRP-1 application *in vivo*.

Our results in Rab3a-KO mice, combined with the evidence for a crucial role of Wnt signaling in experience-related connectivity rearrangements in the hippocampal mossy fiber pathway, may provide a means to disentangle the relative contributions of the factors that influence long-term rearrangements of mossy fiber connectivity in the hippocampus upon age and experience, leading to both, LMT growth, and an increase in LMT-C complexity.

Our results suggest that several factors contribute to mossy fiber rearrangements *in vivo*, and that among them Wnt signaling and mFLTP play distinct roles in mediating this plasticity.

### **3.3.5. MATERIALS & METHODS**

Rab3a KO mice were from Jackson laboratories (B6;129S-*Rab3a*<sup>tm1Sud</sup>/J) and were crossed into Thy1-mGFP lines (DePaola, 2003) as described. All other methods used as described in the previous sections.

## 4. GENERAL DISCUSSION

### *Overview*

The results presented in this work provide novel insights into structural rearrangements of neuronal circuit connectivity in the adult central nervous system with specific emphasis on the impact of experience and age upon these plasticity processes.

In brief, we provide evidence that: (1) Hippocampal mossy fiber terminals substantially rearrange their connectivity to CA3 pyramidal neurons in response to age and experience throughout life; (2) This form of experience-related neuronal circuit rearrangements is not specific to the hippocampal mossy fiber pathway, but does also occur at two different synaptic sites in the cerebellar cortex of adult mice; (3) Wnt signaling regulates experience-related rearrangements of hippocampal mossy fiber terminal connectivity in the adult; (4) Lack of Rab3a and mossy fiber LTP affect large mossy fiber terminal morphologies and sizes, but do not prevent experience-related increase in divergence of mossy fiber to CA3 connectivity.

These results have been presented in the previous four chapters and their relevance as well as critical points and future directions have been discussed in detail in the preceding sections.

Here, I would like to attempt to put our results into a shared general context, discuss possible implications as well as limitations of our findings and propose possible future directions of investigation to pursue the presented lines of research.

### **4.1. Rewiring of neuronal circuits in the adult CNS**

In the presented studies we provide evidence that neuronal circuits remodel their connectivities throughout life and in response to experience in different functional systems of the adult brain. The changes observed were found to be differently weighed and concerned some connections more than others. In addition, the changes related to

aging were qualitatively different from those observed upon changes in life style. These findings raise numerous questions pointing towards novel lines of research.

#### **4.1.1. Learning versus life-style**

One very important and yet unsolved question is whether general experience-dependent changes of neuronal connectivity are similar to those that might potentially occur upon a specific learning task. Several lines of research have indicated that both paradigms may induce structural changes in synapses (see Introduction). However, evidences that learning is laid down in a specific anatomical trace have not been reported in the adult yet. On the other hand, studies in the barn owl have shown the formation of an anatomical trace representing an adaptive and learned topographic map of the outside world during the critical period that persists in to adulthood (Linkenhoker et al. 2005). At the same time, similar learning and adaptation can still occur in the adult (Linkenhoker & Knudsen, 2002), but the potential underlying anatomical modifications have not been investigated. One important direction for future studies would thus be the attempt to disentangle the effects of a specific learning paradigm and those that occur upon changes in life-style or age. The cerebellum would be one very attractive candidate for studies of this kind due to its well-characterized anatomy and functional compartmentalization (see also Discussion in the Cerebellum Chapter) and would in addition offer the possibility to conduct such research in the living animals as the cerebellar cortex can be imaged by novel imaging techniques *in vivo*.

The results of similar studies on learning-induced anatomical circuit plasticity would certainly add to a better understanding of how memories and skills, as well as behaviors are laid down in the adult CNS.

#### **4.1.2. Aging versus experience**

Another interesting and yet poorly understood outcome of our studies is the life-long rearrangement of mossy fiber connectivity. Although it is generally accepted that old age results in cognitive decline and alterations of brain functions, our results provide evidence for a life-long modification of prominent circuit properties, such as divergence as well as the distribution of the mossy fiber output. Our interpretation of our own data is

that age leads to an increased focusing of the mossy fiber output, leading to fewer but more precise and stronger microcircuits, that might be preferentially recruited upon granule cell firing (see also Chklovskii et al., 2004; Ikegaya, 2004; and Discussion of the Mossy fiber Chapter). This might lead to changes in behavior that have not yet been investigated in very much detail. Thus, it would be interesting to see whether a precise analysis of the performance of differentially aged animals in behavioral tasks well-known to involve the hippocampus, e.g. the radial-arm maze or water maze test, would reveal gradual and age-related modifications. Furthermore, one could involve our findings on the regulation of mossy fiber rearrangements in such tests. For instance, inhibition of Wnt signaling *in vivo* resulted in obvious changes in mossy fiber terminal morphologies reminiscent to those observed in aged animals. It would be interesting to see whether sFRP-1 injected animals might behave different from control animals in the above mentioned or similar behavioral tests. It is tempting to speculate that the observed structural changes in the mossy fiber pathway could result in corresponding behavior, such as, e.g. a behavior typical for old animals in young, sFRP-1 injected mice. Similar studies could be conducted with animals that lack mossy fiber LTP.

In contrast to aging, experience-related changes of the mossy fiber projection resulted in increased divergence and concomitantly in the strengthening of connectivity (growth of LMTs). Interestingly, our data on single reconstructed cerebellar mossy fibers provide similar evidences, namely an increase in mossy fiber branching and MFT densities upon EE and thus argue that this might be a common effect of EE on brain circuitry.

Remarkably, inhibition of Wnt signaling concomitant to EE seemed to block this increase in divergence (data still to be quantified). Thus, it would be interesting to see whether the beneficial roles of EE on learning and memory performance (see Introduction) might be prevented by Wnt inhibition *in vivo*.

#### **4.1.3. Roles for Rab3a and Wnt in structural plasticity in the adult CNS**

Interestingly, both molecular mechanisms examined in the present work and found to affect hippocampal synaptic structure, are also effective in the cerebellar cortex. It would thus be interesting in future studies to investigate the roles of Rab3a, involved in parallel

fiber LTP, and Wnt7a, involved in formation of MFTs, in experience- and age-related structural plasticity of the cerebellar cortex. These studies could provide a means to generalize some of our findings in the hippocampus.

### ***Conclusion***

In the present work we have demonstrated the occurrence and analyzed the characteristics of neuronal circuit rearrangements in the adult CNS upon age and experience in two independent functional systems of the brain. Furthermore, we started to unravel the molecular mechanisms underlying the observed circuit plasticities. Our data provide several starting points for future studies that may reveal the anatomical modifications that underlie learning and memory.

## 5. SUPPLEMENTARY PROTOCOLS

### 5.1. Preparation of organotypic hippocampal slice cultures for long-term live imaging

Nadine Gogolla<sup>1,3</sup>, Ivan Galimberti<sup>1,3</sup>, Vincenzo DePaola<sup>2</sup> and Pico Caroni<sup>1</sup>

<sup>1</sup>Friedrich Miescher Institute, Maulbeerstrasse 66, CH-4058 Basel, Switzerland.

<sup>2</sup>Cold Spring Harbor Laboratories, Cold Spring Harbor, New York, USA.

<sup>3</sup>These authors contributed equally to this work.

*Nature Protocols*

2006 (1(3):1165-71)

## **ABSTRACT**

This protocol details a method to establish organotypic slice cultures from mouse hippocampus, which can be maintained for several months. The cultures are based on the interface method, which does not require special equipment, is easy to execute and yields slice cultures that can be imaged repeatedly – from when they are isolated at postnatal day 6–9, and up to 6 months *in vitro*. The preserved tissue architecture facilitates the analysis of defined hippocampal synapses, cells and entire projections. Monitoring of defined cellular and molecular components in the slices can be achieved by preparing slices from transgenic mice or by introducing transgenes through transfection or viral vectors. This protocol can be completed in 3 h.

## **INTRODUCTION**

Recent advances in gene delivery and live imaging technology have had a marked impact on the range of experimental tools that are available to life scientists<sup>1,2</sup>. For research in neuroscience, these developments have meant that studying the structure and function of biologically relevant neuronal circuits can now be approached in a non-invasive way and with unprecedented analytical power. To fully exploit these technological developments, adequate biological preparations to investigate neuronal circuits have to be established in parallel. Fortunately, preparations that were developed by physiologists more than a decade ago<sup>3,4,5</sup> could be readily adapted for live imaging studies of defined neuronal circuits<sup>6,7</sup>.

### ***Advantages of the method***

Key features of the hippocampal organotypic slice cultures<sup>4</sup> include: well-defined cellular architecture of the hippocampal circuit, which preserves the organization *in vivo*, and allows the identification and manipulation of defined neurons and synapses<sup>3,4,5,6,7</sup>; presence of axonal projections (mossy fiber axons extending from dentate gyrus granule cells to the distal end of CA3), which can largely be recovered in the slices in their

original state (that is, without lesioning) and which establish stereotypic numbers of readily identifiable presynaptic terminals onto excitatory and inhibitory neurons in the hilus and in CA3<sup>6-9</sup>; a long-term thickness of 100–150  $\mu\text{m}$ , preserving three-dimensional organizations of connectivity<sup>4, 5</sup>; maturation of the slice cultures, closely reflecting the corresponding schedule *in vivo*<sup>8, 9</sup>; option to prepare the slices from mice of any genetic background, including those of poor postnatal viability.

### ***Critical aspects***

The main critical issues relate to the extent to which organotypic slice cultures reproduce the properties of hippocampal circuits *in vivo*<sup>5</sup>. This information is important for deciding whether the approach is appropriate for addressing the particular experimental issues that might be in mind. These issues have been investigated in much detail by physiologists, who have demonstrated extensive similarities, but also a few discrepancies, to properties of the corresponding circuits in the adult brain<sup>5</sup>. With respect to development, the slice cultures exhibit a temporal profile of excitatory and inhibitory miniature synaptic events, which closely match, qualitatively and quantitatively, the corresponding times *in vivo*<sup>8</sup>. This indicates that features that are critical to hippocampal circuit development and maturation are well established at 1 week postnatally, and are stable under organotypic culture conditions. A further critical issue involves the unavoidable separation of the hippocampal slices from their natural inputs, outputs and neuromodulatory systems. It turns out that most neuronal excitability and network properties are well preserved, in spite of the fact that the actual activity in the slices must be significantly different from the *in vivo* situation<sup>5</sup>. Predictably, synaptic connectivity in the slice cultures is initially greatly reduced due to the isolation procedure but, during the first 2–3 weeks *in vitro*, synapse numbers recover to a level comparable to that *in vivo*<sup>5</sup>, and the cultures are stable with respect to total synapse numbers from about 3 weeks *in vitro*<sup>6</sup>. As a result, the degree of connectivity between some of the individual neurons that are present in the slices (e.g., pyramidal neurons in CA3) is higher than *in vivo*, a fact that facilitates the analysis of synaptically connected neurons<sup>5</sup>. With the exception of the molecular layer of the dentate gyrus, in which the occasional recurrent mossy fiber collaterals can produce an excitation level that is higher than that of normal granule cells, this higher connectivity

does not seem to produce aberrant patterns of activity<sup>5</sup>. The slices can, however, be electrically labile, and gentle handling is important to avoid epileptic-like discharges. One way to avoid higher excitability in granule cells is to prepare slices from P20-30 mice when the circuits are more stable<sup>10</sup>. Finally, attempts to investigate adult neurogenesis in hippocampal slice cultures have suggested that the phenomenon is much less frequent than *in vivo*. This might be influenced by the culture medium, but the issue requires further investigation.

### ***Possible results and outlook***

Organotypic slice cultures from ~1-week-old mouse hippocampus appear to reproduce most anatomical and functional properties of the corresponding hippocampal circuits *in vivo* for at least 6 months *in vitro* due to the intrinsic properties of their neurons. Accordingly, limitations to their applications might be confined to studies of hippocampal input–output relationships. This leaves an exciting range of possibilities for the exploration of mechanisms that control the assembly and function of neuronal circuits. Some of these include: time-lapse imaging from the sub-second to the months range, and from individual molecules to entire neuronal projections and circuits; imaging of neuronal<sup>6, 7, 11, 12</sup> and glial<sup>13</sup> subtypes; molecular manipulation using transfection<sup>14, 15</sup> or viral approaches<sup>16, 17</sup> to knock down or overexpress genes, silence or activate neurons, render neurons responsive to light or selective drugs and to highlight sub-circuits; combined physiology-imaging methods; manipulations to investigate lesion-induced plasticity and pathways of neurodegeneration and repair (e.g., amyloid- or epilepsy-related); following the insertion of new neurons, the development of axons and their connections, or the insertion of exogenously added stem cells; *post-hoc* analysis using, for example, tracers, electron microscopy and single-cell genomic methods.

## MATERIALS

### *Reagents*

- Animals: 6–9-day-old mouse pups. You can prepare slices from six pups within one session, but for the beginner it may be preferable to start with two or three pups

**! CAUTION** All animal experiments must comply with national regulations.

- Hand sterilizing solution, e.g., Sterilium (Bode) or equivalent
- Penicillin/streptomycin (Invitrogen, cat. no. 16050-122)
- HEPES
- Hank's balanced salt solution (HBSS; Invitrogen, cat. no. 24020-083)
- Horse serum
- 2 × MEM (liquid Eagle's with Hank's Salts and 25 mM HEPES; Gibco, cat. no. 04195120M)
- Tris-(hydroxymethyl)aminomethane

### *Equipment*

- Dissection microscope (e.g., ZEISS Stemi 2000-C binocular with 10 ×23 objectives, but any 5–10 ×magnifying dissection microscope is suitable)
- McIlwain tissue chopper (The Mickle Laboratory Engineering Co. Ltd.)
- Sterile dissection hood
- Razor blades that can be fixed in the McIlwain tissue chopper
- Filter paper (e.g., Schleicher & Schuell, cat. no. 300009, or Whatman paper)
- Small (35 mm ×10 mm) and large (100 mm ×20 mm) cell culture dishes (Corning, cat. no. 430165 and 430293, respectively)
- 6-well culture plates (Corning, cat. no. 3516)

- Culture plate inserts: 0.4  $\mu\text{m}$  Millicell membrane, 30 mm diameter (Millipore, cat. no. PICM03050)
- Vacuum filter sterilizer for medium (e.g., Vacuum-driven disposable filtration system, 0.22  $\mu\text{m}$  pore width; Millipore, cat. no. SCGPU02RE)
- Cell culture incubator at 35 °C, 95% air, 5% CO<sub>2</sub>

### *Equipment Setup*

- **Dissection tools** Scalpel, two round-ended spatulas, small scissors, large scissors, one pair of fine straight forceps, two pairs of curved fine forceps and two glass Pasteur pipettes that have to be custom designed as follows: one pipette is fire-polished at the tip so that it adapts a round shape, has no sharp edges, but still has a small opening; the second pipette is cut at the intersection of the fine and thick tube using a canula opener (glass cutter), and the resulting large opening of this pipette is fire-polished to smooth the edges.

### *Reagent Setup*

- **Penicillin/streptomycin solution** Dissolve 1.6 g penicillin G (100 U ml<sup>-1</sup>) and 2.5 g streptomycin (0.1 mg ml<sup>-1</sup>) in 200 ml H<sub>2</sub>O, filter-sterilize and store at -20 °C in 2-ml aliquots. Note that penicillin can reduce GABAergic neurotransmission in slices<sup>18</sup>. Signs of epileptic activity have, however, not been detected under these culture conditions.
- **Horse serum** Heat-inactivate the complement system of the horse serum at 56 °C for 30 min; aliquots can be stored at -20 °C for at least 1 year.

#### ?Troubleshooting

- **Dissecting medium** 50 ml MEM 2x, 1 ml penicillin/streptomycin solution, 120 mg Tris (hydroxymethyl)aminomethane (final concentration: 10 mM); add up to 100 ml with ddH<sub>2</sub>O.

▲ **CRITICAL** Prepare within 24 h of the experiment, filter-sterilize through a 0.22  $\mu\text{m}$  membrane and keep it at 4 °C until dissection.

- **Culture medium** 50 ml MEM 2x, 1 ml penicillin/streptomycin solution, 120 mg Tris (hydroxymethyl)aminomethane (final concentration: 10 mM), 910  $\mu$ l of a 7.5% NaHCO<sub>3</sub> aqueous solution, 50 ml heat-inactivated horse serum, 50 ml 1x HBSS; add up to 200 ml with ddH<sub>2</sub>O.  
**▲ CRITICAL** Filter-sterilize through a 0.22  $\mu$ m membrane and keep at 4 °C. Pre-heat only the medium that is needed for a medium change on the same day. Culture medium can be stored at 4 °C for at least 1 month.

### *Overview*

- Step 1 - 4 Preparation of membrane inserts and culture medium
- Step 5 - 9 Preparation of dissection medium and chambers
- Step 10 - 13 Preparation of dissection material
- Step 14 - 17 Hippocampus dissection and cutting of coronal sections
- Step 18 - 47 Dissection
- Step 48 Cold incubation
- Step 49 - 59 Selection and incubation of hippocampal slices

## **PROCEDURE**

### **Preparation of membrane inserts and culture medium • TIMING 10-30 min**

1. Prepare the culture medium and filter-sterilize it.
2. Add 1 ml culture medium per well of a 6-well plate; prepare 3–4 wells for each pup to be dissected (one pup should yield 6–8 usable hippocampal slices and about two slices are cultured on one membrane).
3. Add one culture plate insert into each prepared well, so that the insert membranes touch the medium, but are not covered by it.

4. To warm up the medium, put the prepared 6-well plates into the cell culture incubator.

**Preparation of dissection medium and chambers • TIMING 10-20 min preparation  
+ 15 min sterilization**

5. Prepare the dissection medium, filter-sterilize and keep it at 4 °C.
6. Cut a small triangle (about 4 x4 x4 cm) out of the filter paper, take the cover of a 100-mm cell culture dish and place the filter paper triangle into it. Prepare 1 cover + filter paper for each pup to be dissected.
7. Sterilize the covers containing the filter papers under ultraviolet light in the culture hood for 15 min.
8. Add 1 ml of cold dissection medium on top of each filter paper and cover with the bottom of the cell culture dish under sterile conditions.
9. Keep these 'dissection chambers' at 4 °C until dissection.

**Preparation of dissection material • TIMING 5-15 min**

10. Clean all dissection tools with 70% ethanol, fire-sterilize them inside the dissection hood and keep them there. Clean a fresh razor blade with a chloroform:isoamylalcohol (49:1) solution, followed by 100% ethanol and 70% ethanol and fix it in the McIlwain tissue chopper placed inside the dissection hood.

**! CAUTION** Chloroform is toxic; avoid inhalation, ingestion or contact with skin, eyes or mucous membranes.

11. Fix the plastic platform on the McIlwain tissue chopper and clean it with 70% ethanol; switch the chopper on and adjust the cutting thickness to 400 µm.
12. Keep the dissection medium on ice inside the dissection hood.
13. Put one 35-mm cell culture dish per pup to be dissected under the dissection hood.

**Hippocampus dissection and cutting of coronal sections • TIMING 15-30 min/pup**

14. Place one of the prepared, cold 'dissection chambers' under the dissection microscope and remove the top plate so that the filter paper covered with cold dissection medium is exposed.

**▲ CRITICAL STEP** Steps 14–38 are carried out under sterile conditions inside a dissection hood unless otherwise mentioned.

15. Decapitate one pup outside the dissection hood using large scissors. Note that anesthesia of pups is notoriously difficult (dry ice is one possibility), and that decapitation as described above is usually advised. Nevertheless, make sure that the procedure complies with local regulations.

16. Flush the head with 70% ethanol and transfer it into the hood.

**▲ CRITICAL STEP** The fur of the pup is a potential contamination source. [?Troubleshooting](#)

17. Sterilize your gloves with Sterilium or 70% ethanol before you proceed.

**▲ CRITICAL STEP** Proceed carefully for Steps 18–24. The delicate nervous tissue of the brain is easily damaged by the sharp dissection tools or the edges of the cut skull. [?Troubleshooting](#)

## Dissection

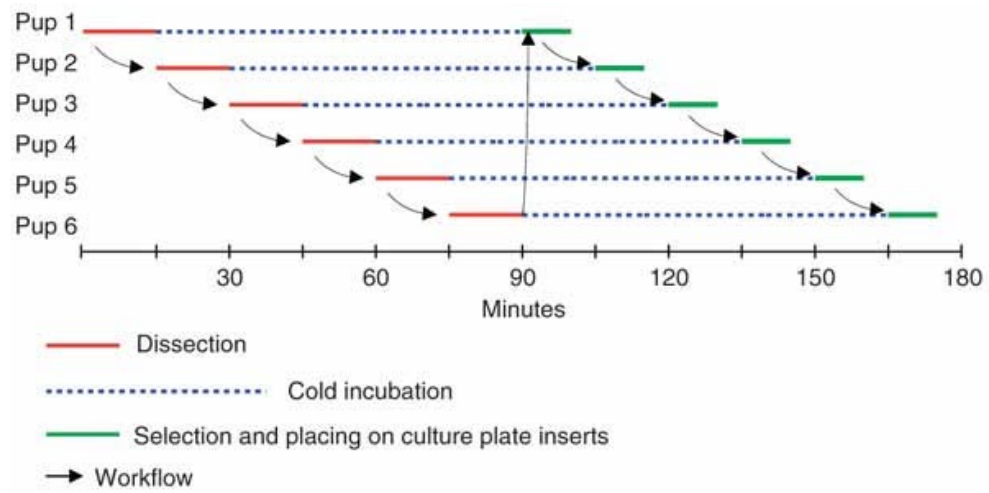


**Figure 1. Workflow diagram.** Slices from pups 1 to 6 are prepared sequentially: dissection, cold incubation and slice selection are performed in a staggered way.

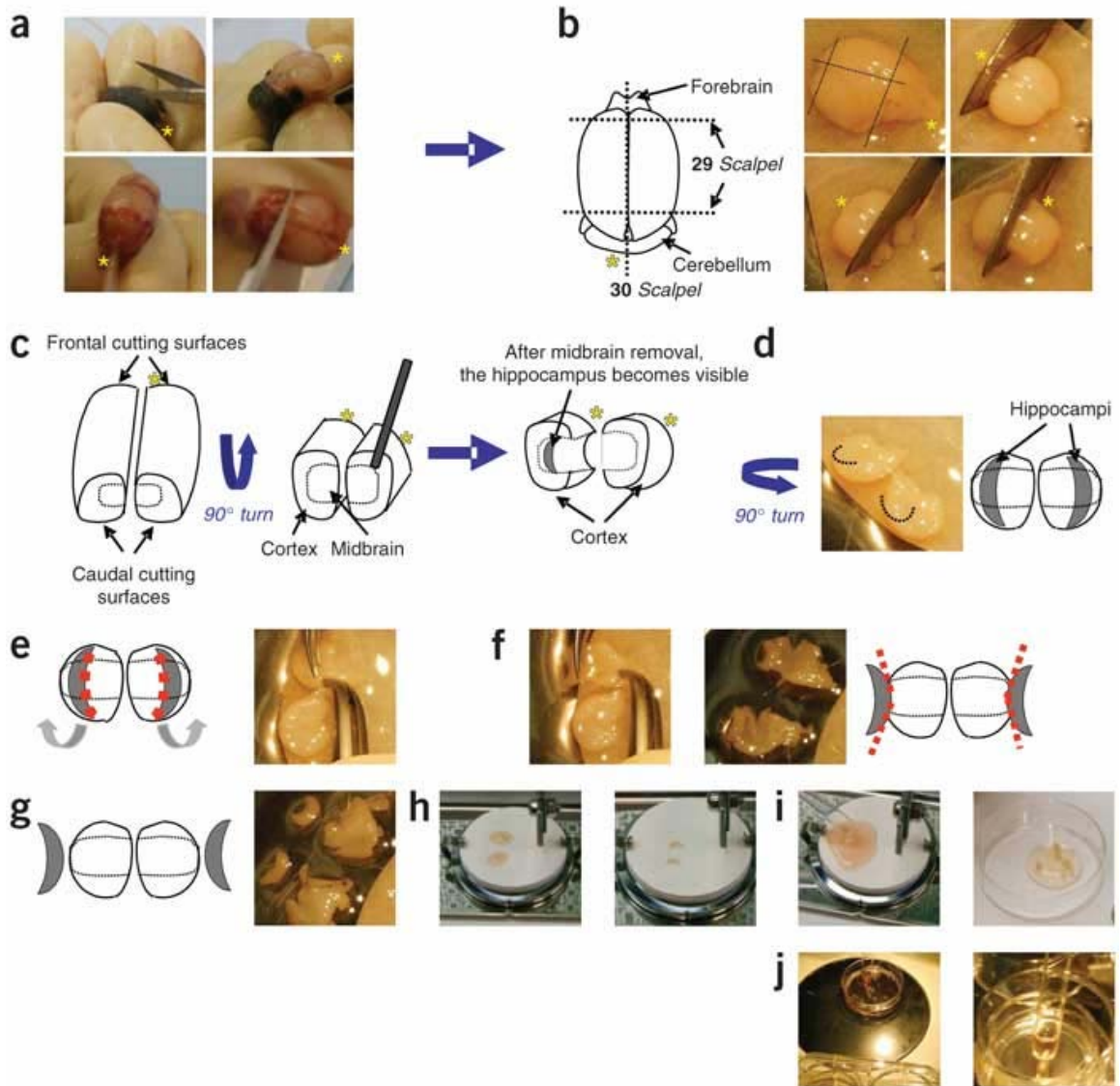


**Figure 2. Illustration of hippocampal slice preparation protocol** (Steps 18-53). (a) Steps 18-22; (b) Steps 28-30; (c) Steps 31-32; (d) Step 33; (e) Step 34; (f) Steps 35-36; (g) Step 38; (h) Steps 39-43; (i) Steps 44-46; (j) Steps 50-53. \* Back of the head (neck).

## Dissection

18. Make an incision into the skin along the midline of the head, starting at the neck up to between the eyes using the small scissors (see Figs. 1-3).
19. To hold the head more easily and to expose the skull, flip the skin around the head and pull it to the lower side, where you pinch it between your fingers.
20. Use the small scissors and the fine straight forceps to remove neck muscles and the first vertebrae.
21. Insert the lower part of the small scissors carefully into the foramen magnum and cut the skull along the midline from the foramen magnum to the front until you reach between the eyes.
22. Make two lateral cuts starting from the midline towards the sides.
23. Peel away the skull using the fine straight forceps.
24. Hold the head upside down above the prepared filter paper, which should be covered with cold dissection medium.
25. Introduce the spatula carefully between the brain and the skull and remove the brain from the skull, cut the cranial nerves and, if necessary, the olfactory bulbs with the spatulas.
26. Let the brain drop gently onto the filter paper covered with dissection medium.
27. Immediately put a few drops of cold dissection medium onto the exposed brain.
28. Put the brain upside up with the ventral side lying on the filter paper.
29. Use the scalpel to cut off the forebrain and the cerebellum by coronal cuts.
30. Using the scalpel, separate the two hemispheres cutting along the inter-hemispheric fissure.
31. Place one brain hemisphere on the frontal or caudal cutting surfaces; the intersection between cortex, midbrain and brainstem becomes visible.
32. Separate the cortex with the underlying hippocampus from the brainstem, midbrain and striatum using the two spatulas.  
**▲ CRITICAL STEP** Do not touch the hippocampus with the spatulas. [?Troubleshooting](#)

33. Place the cortex upside down, so that the hippocampus is exposed.
34. Use the curved forceps to cut the connections of the hippocampus to the ventral side (fimbria); leave it connected to the cortex by the subiculum.
35. Flip the hippocampus over and out.
36. Using the scalpel, cut the connection of the hippocampus to the enthorinal cortex (subiculum).
37. Flush the dissected hippocampus with ice-cold dissection medium.
38. Prepare the second hippocampus of the opposite hemisphere in the same way (see Fig. 2).
39. Use the wide-bore, custom-made Pasteur pipette to suck one hippocampus into the pipette along with some dissection medium and transfer it to the plastic platform on the McIlwain tissue chopper.
40. Repeat the same for the second hippocampus.
41. Using the narrow-bore pipette, align the two hippocampi perpendicularly to the chopper blade.
  - ▲ **CRITICAL STEP** Avoid touching the slices; instead, use medium to push and pull them into the right position. [?Troubleshooting](#)
42. Remove all dissection medium around the hippocampi.
43. Chop rapidly into 400 µm thick transverse sections.
44. Float the freshly cut sections immediately with cold dissection medium.
45. Use the wide-bore pipette to transfer the sections into a 35-mm cell culture dish.
46. Separate the sections by shaking the dish gently. If the sections stick together, remove all dissection medium and shake harshly but not for too long; alternatively, use the narrow-bore pipette and try to separate the sections by the flow of some dissection medium.
  - ▲ **CRITICAL STEP** Use great care as the sections are very easily damaged!
47. After separation, fill the 35-mm dish with cold dissection medium so that all sections are covered; push floating sections down to the bottom of the dish by dropping medium onto their tops.

### Cold incubation • **TIMING 30 min-1.5 h/pup**

48. Cover the 35-mm cell culture dish with its cover and label it with the number of the pup and the exact time. Incubate the separated slices for a minimum of 30 min at 4 °C (up to 1.5 h). Repeat Steps 14–48 for all pups (see Fig. 1).

▲ **CRITICAL STEP** After incubation of each pup, clean and fire-sterilize all dissection tools and the chopper platform; take a fresh and cold 'dissection chamber'; change and sterilize your gloves! [?Troubleshooting](#)

### Selection and incubation of hippocampal slices • **TIMING 10-20 min /pup**

49. After completing the dissection of the last pup, start the selection of slices from the first dissected pup (see label) and proceed with the selection in the same sequence as in the dissection (see Fig. 1).

▲ **CRITICAL STEP** Make sure that slices from each pup were cold incubated for at least 30 min (check the time on the label). Place the first 35-mm dish (slices of the first pup) under the dissection microscope in the dissection hood.

50. Remove the lid of the 35-mm dish and select the best slices for culturing according to the following criteria (see Fig. 3) Slices should have smooth margins and be clearly visible, have uniform and well-defined cell layers in the dentate gyrus and in CA1-3; the dentate gyrus should be tightly connected to the rest of the slice, and the fimbria should be intact. [?Troubleshooting](#)

51. Collect one pre-heated 6-well plate containing culture medium and a cell culture insert from the 35 °C incubator.

52. Using the wide-bore pipette, transfer the selected slices individually onto the membranes along with some dissection medium. Alternatively, some labs use thin spatulas for the transfer, but we have no direct experience with this alternative method.

53. Using the narrow-bore pipette, orientate the slices to the middle of the membrane by pushing and pulling them with the stream of dissection medium.

54. You can place up to four slices on one membrane but the number of slices on one membrane has to be adapted to the planned experiments.

**▲ CRITICAL STEP** For live imaging, you should only place one or two slices on each membrane. Place the slices as close to the center as possible, so that the plastic edge of the membrane insert will not hinder the microscope's access to the top of the slices. Adapt the slice number that you put on one membrane to the estimated time required for later imaging of all slices on one culture plate insert. The time you can keep one culture plate insert outside the incubator during imaging is restricted to a maximum of 30 min (see also Imaging Protocol<sup>19</sup>). Keep a minimal distance of 2 mm between the slices to avoid fusion when flattening out during the culture period.

55. Using the narrow-bore pipette, remove all dissection medium around the slices.

**▲ CRITICAL STEP** This is critical because any remaining dissection medium covering the slices hinders oxygen exchange.

56. To avoid cooling, put the 6-well culture plate back into the incubator immediately after having placed the slices.

57. After 3–4 d, remove all culture medium below the insert and replace it with 1 ml of fresh, 35 °C-warmed culture medium.

58. Replace the culture medium every 3–4 d.

59. The slice cultures can be maintained for several months. Criteria to verify viability: the slices must be transparent, firmly attached to the membrane and the dentate gyrus must be visible to the naked eye. In addition, if neurons are labeled with fluorescent markers, microscopic examination should reveal an absence of axonal and dendritic beading. If necessary, cell death in the slices can be assayed with propidium iodide<sup>6</sup>.

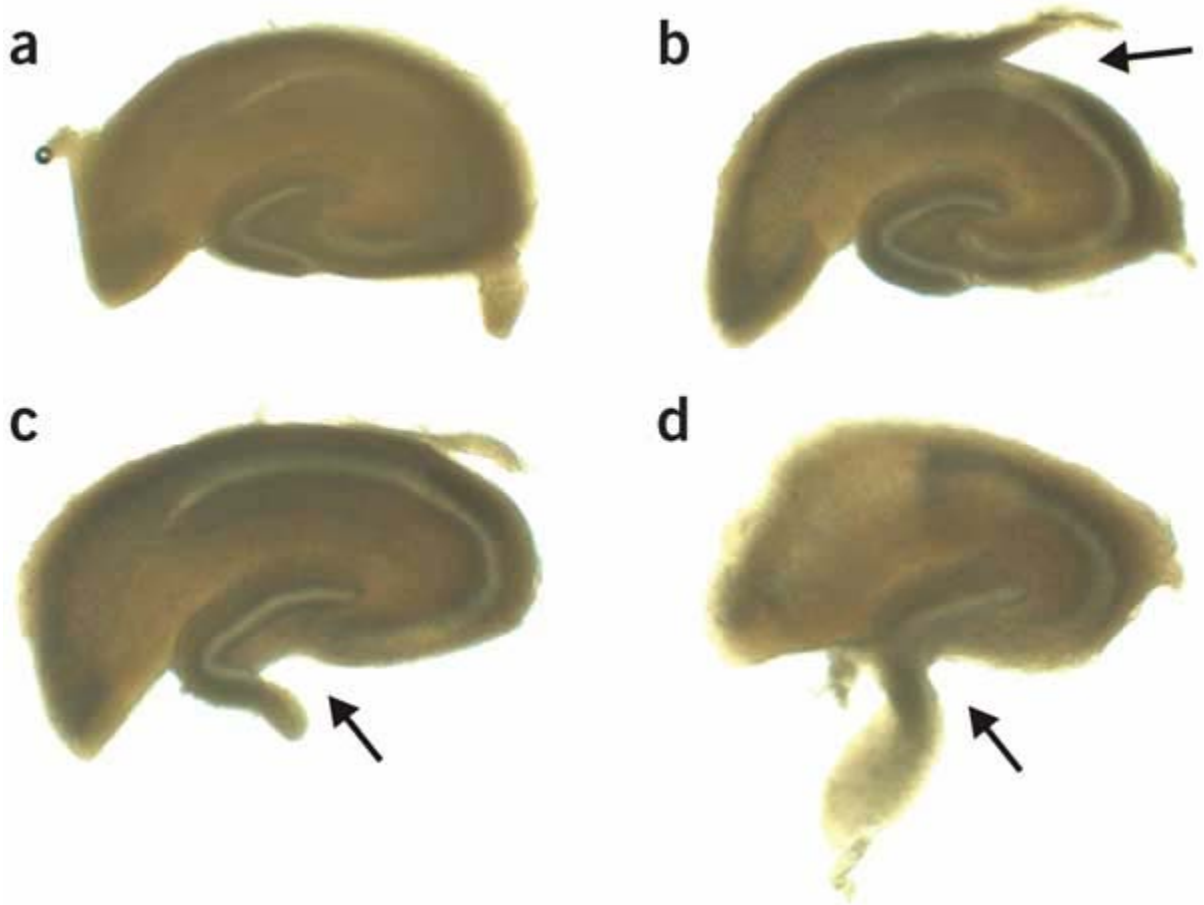


**Figure 3. Selection of slices for culturing.** (a) Optimal slice with nice cell layers in the dentate gyrus and CA1-3 and smooth margins (b) slice in which the CA1 region was lesioned during preparation (arrow); (c) slice in which the dentate gyrus was lesioned (arrow); (d) slice in which the dentate gyrus detached from the rest of the section (arrow). Only the slice in a should be selected for culturing.

## ? Troubleshooting

<b>Problem</b>	<b>Possible Reason</b>	<b>Solution</b>
Slices become contaminated soon after preparation	Contamination by the fur or blood of the pups	Use 70% ethanol to repeatedly flush the head after decapitation  Change and sterilize the gloves after having touched the pups' fur and blood
Slices detach from the membrane of the cell culture plate insert soon after preparation	Check for the correct composition and pH of the culture medium  Change the horse serum	Always adjust the pH of the culture medium to 7.2  Inactivate the horse serum carefully and note the batch number, if possible; keep using a batch that has worked as long as possible (make many aliquots)
Slices die prematurely during the culturing period	Slices can become epileptic if treated too harshly	Always move slices slowly and smoothly  Avoid strong vibrations
Axons and/or dendrites assume a beaded appearance	Wrong medium composition  Wrong pH of culture medium  Treatment during preparation too harsh  Slice preparation took too long  Media were not at the right temperature  Incubator at wrong temperature or atmosphere  The slices that were selected for culturing did not show the right morphology or were injured	Strictly follow the indications in the protocol concerning media and times during preparations and handling
Aberrant axonal projections		Select only slices in which the cell layers can be clearly seen and have the expected shape  Make sure that you do not touch the slices with any sharp tools  The cutting angle was not perpendicular to the long axis of the hippocampus Make sure that you cut and then select slices that were cut perpendicularly to the long axis of the hippocampus

## • TIMING

Steps 1–4:	10–15 min (For trained experts);	20–30 min (For beginners).
Steps 5–9:	10 + 15 min (For trained experts);	20 min (For beginners).
Steps 10–13:	5–10 min (For trained experts);	15 min (For beginners).
Steps 14–47:	15 min per pup (For trained experts);	30 min per pup (For beginners).
Step 48:	30–90 min (For trained experts);	30–90 min (For beginners).
Steps 49–56:	10 min per pup (For trained experts);	20 min per pup (For beginners).

### *Anticipated results*

Critical factors to reproducibly achieve good yields and quality of slice cultures are speed, avoiding physical damage of the hippocampus and avoiding contaminations during the preparation (see Figs. 1- 3). These requirements mainly depend on training and concentration. We therefore recommend that beginners practice repeatedly during the first 2–4 weeks, in order to become confident and to acquire good experimental skills. A trained user should produce 6–8 good quality slices per pup, which can be maintained and imaged for at least 6–10 weeks.

### *Acknowledgments*

We are very grateful to Dominique Muller (University of Geneva, Switzerland) for introducing us to his hippocampal slice culture method. We thank M. Abanto, E. Bednarek and S. Saxena (Friedrich Miescher Institut (FMI)) for comments on the manuscript. The FMI is part of the Novartis Research Foundation.

## References

1. Conchello, J.A. & Lichtman, J.W. Optical sectioning microscopy. *Nature Methods* 2, 920–931 (2005)
2. Yuste, R. Fluorescence microscopy today. *Nature Methods* 2, 902–904 (2005)
3. Gahwiler, B.H. Organotypic monolayer cultures of nervous tissue. *J. Neurosci. Methods* 4, 329–342 (1981)
4. Stoppini, L., Buchs, P.A. & Muller, D. A simple method for organotypic cultures of nervous tissue. *J. Neurosci. Methods* 37, 173–182 (1991)
5. Gahwiler, B.H. *et al.* Organotypic slice cultures: a technique has come of age. *Trends Neurosci.* 20, 471–477 (1997)
6. De Paola, V., Arber, S. & Caroni, P. AMPA receptors regulate dynamic equilibrium of presynaptic terminals in mature hippocampal networks. *Nature Neurosci.* 6, 491–500 (2003)
7. Galimberti, I. *et al.* Long-term rearrangements of hippocampal mossy fiber terminal connectivity in the adult regulated by experience. *Neuron* 50, 749–763 (2006)
8. De Simoni, A., Griesinger, C.B. & Edwards, F.A. Development of rat CA1 neurones in acute versus organotypic slices: role of experience in synaptic morphology and activity. *J. Physiol.* 550, 135–147 (2003)
9. Henze, D.A., Urban, N.N. & Barrionuevo, G. The multifarious hippocampal mossy fiber pathway: a review. *Neuroscience* 98, 407–427 (2000)
10. Xiang, Z. *et al.* Long-term maintenance of mature hippocampal slices *in vitro*. *J. Neurosci. Methods* 98, 145–154 (2000)
11. Caroni, P. Overexpression of growth-associated proteins in the neurons of adult transgenic mice. *J. Neurosci. Methods* 71, 3–9 (1997)
12. Feng, G. *et al.* Imaging neuronal subsets in transgenic mice expressing multiple spectral variants of GFP. *Neuron* 28, 41–51 (2000)
13. Dailey, M.E. & Waite, M. Confocal imaging of microglial cell dynamics in hippocampal slice cultures. *Methods* 18, 222–230 (1999)

14. Lo, D.C., McAllister, A.K. & Katz, L.C. Neuronal transfection in brain slices using particle-mediated gene transfer. *Neuron* 13, 1263–1268 (1994)
15. Benediktsson, A.M., Schachtele, S.J., Green, S.H. & Dailey, M.E. Ballistic labeling and dynamic imaging of astrocytes in organotypic hippocampal slice cultures. *J. Neurosci. Methods* 141, 41–53 (2005)
16. Ehrenguber, M.U. *et al.* Recombinant Semliki Forest virus and Sindbis virus efficiently infect neurons in hippocampal slice cultures. *Proc. Natl. Acad. Sci. USA* 96, 7041–7046 (1999)
17. Miyaguchi, K., Maeda, Y., Kojima, T., Setoguchi, Y. & Mori, N. Neuron-targeted gene transfer by adenovirus carrying neural-restrictive silencer element. *Neuroreport* 10, 2349–2353 (1999)
18. Andersen, P. Basic mechanisms of penicillin-induced epileptiform discharges. *Progr. Clin. Biol. Res.* 124, 3–13 (1983)
19. Gogolla, N., Galimberti, I., Depaola, V. & Caroni, P. Long-term live imaging of neuronal circuits in organotypic hippocampal slice cultures. *Nature Protocols* doi: doi: 10.1038/nprot.2006.169

## 5.2. Long-term live imaging of neuronal circuits in organotypic hippocampal slice cultures

Nadine Gogolla<sup>1,3</sup>, Ivan Galimberti<sup>1,3</sup>, Vincenzo DePaola<sup>2</sup> and Pico Caroni<sup>1</sup>

<sup>1</sup>Friedrich Miescher Institute, Maulbeerstrasse 66, CH-4058 Basel, Switzerland.

<sup>2</sup>Cold Spring Harbor Laboratories, Cold Spring Harbor, New York, USA.

<sup>3</sup>These authors contributed equally to this work.

*Nature Protocols*

2006 (1, - 1223 – 1226)

## ABSTRACT

This protocol details a method for imaging organotypic slice cultures from the mouse hippocampus. The cultures are based on the interface method, which does not require special equipment, is easy to execute, and yields slice cultures that can be imaged repeatedly after they are isolated on postnatal day 6–9 and for up to 6 months *in vitro*. The preserved tissue architecture facilitates the analysis of defined hippocampal synapses, cells and entire projections. Time-lapse imaging is based on transgenes expressed in the mice, or on constructs introduced through transfection or viral vectors; it can reveal processes that develop over time periods ranging from seconds to months. Imaging can be repeated at least eight times without detectable morphological damage to neurons. Subsequent to imaging, the slices can be processed for immunocytochemistry or electron microscopy, to collect further information about the structures that have been imaged. This protocol can be completed in 35 min.

## INTRODUCTION

Recent advances in live-imaging technology have had a dramatic impact on the range of experimental tools available to life scientists<sup>1,2</sup>. These include the following: microscopes with greatly improved sensitivity, temporal/spatial resolution and spectral versatility; powerful image-acquisition and image-processing software; and an ever growing repertoire of fluorescent reagents to monitor second messengers, and to identify macromolecules and their physiological modifications as well as subcellular structures *in situ*. For research in neuroscience, these developments have meant that studying the structure and function of biologically relevant neuronal circuits can now be approached in a noninvasive way, and with unprecedented analytical power. In order to fully exploit these technological developments, adequate biological preparations have to be established in parallel to investigate neuronal circuits. Fortunately, preparations developed by physiologists more than a decade ago<sup>3,4,5</sup> can be readily adapted for live-imaging studies of defined neuronal circuits<sup>6,7</sup>. Labeling subsets of neurons and their subcellular structures can be achieved using transgenic mice and a mouse Thy1-promoter cassette<sup>8,9</sup>. While cytosolic fluorescent proteins work well<sup>9</sup>, expression of membrane-

targeted GFP constructs provides optimal visualization of neuronal outlines<sup>6,7</sup>. Further constructs available for Thy1-transgenic mice include, for example, synaptopHluorin<sup>10</sup>. Alternatively, transgenes can be introduced directly into slice cultures using transfection methods<sup>11,12</sup> or viruses<sup>13,14</sup>.

### ***Advantages of the method***

Key features of the organotypic hippocampal slice cultures<sup>4</sup> include the following: (i) well-defined cellular architecture of the hippocampal circuit, which preserves the organization *in vivo*, and allows the identification and manipulation of defined neurons and synapses<sup>3,4,5,6,7</sup>; (ii) the presence of axonal projections (mossy fiber axons extending from dentate gyrus granule cells to the distal end of CA3), which can largely be recovered in the slices in their original state (i.e., without lesioning), and establish stereotypical numbers of readily identifiable presynaptic terminals onto excitatory and inhibitory neurons in the hilus and CA3<sup>6,7,15</sup>; (iii) a long-term thickness of 100–150  $\mu\text{m}$ , preserving the 3D organizations of connectivity<sup>4,5</sup>; (iv) maturation of the slice cultures closely reflecting the corresponding schedule *in vivo*<sup>16</sup>; and (v) the option to prepare the slices from mice of any genetic background, including those with poor postnatal viability.

### ***Critical aspects***

One set of critical issues relates to the extent to which organotypic slice cultures reproduce the properties of hippocampal circuits *in vivo*<sup>5</sup>. This information is important for deciding whether the approach is appropriate to address the particular experimental issues of interest. These issues have been investigated in detail by physiologists, who have demonstrated extensive similarities, but also a few discrepancies, with respect to the properties of the corresponding circuits in the adult brain<sup>5,16</sup>. Further critical issues relate to the manipulations involved in the imaging procedures. The slices can be electrically labile, and gentle handling is important in order to avoid epileptic-like discharges<sup>5</sup>. In addition, it is essential to minimize the times during which the slices are kept outside of the tissue-culture incubator, and to allow sufficient recovery times between single imaging sessions (see PROCEDURE). These factors must be balanced against the

requirements of the experimental questions. We recommend always optimizing and standardizing the particular experimental protocols, taking into account reproducibility and negative side-effects. By contrast, contaminations and phototoxicity can largely be avoided through appropriate precautions.

### ***Possible results and outlook***

Organotypic hippocampal slice cultures from mice aged ~1 wk appear to reproduce most anatomical and functional properties of the corresponding hippocampal circuits *in vivo* for at least 6 months *in vitro*, due to the intrinsic properties of their neurons. Accordingly, the slices provide an exciting range of possibilities for the exploration of mechanisms controlling the assembly and function of neuronal circuits. These include the following: (i) time-lapse imaging over periods ranging from sub-seconds to months, and of objects in the slices ranging from individual molecules to entire neuronal projections and circuits; (ii) imaging of neuronal<sup>6, 7, 9</sup> and glial<sup>12</sup> subtypes; (iii) molecular manipulation using transfection or viral approaches to knock down or overexpress genes, silence or activate neurons, render neurons responsive to light or selective drugs, and highlight sub-circuits; (iv) combined physiology and imaging methods; (v) manipulations to investigate lesion-induced plasticity, and pathways of neurodegeneration and repair (e.g., amyloid-related or epilepsy-related pathways); (vi) following the insertion of new neurons, the development of axons and their connections, or the insertion of exogenously added stem cells; and (vii) *post-hoc* analysis using, for example, tracers, electron microscopy and single-cell genomic methods.

## MATERIALS

### *Reagents*

- Mouse organotypic hippocampal slice cultures (see Reagent setup)
- Fungizone antimycotic, liquid (Gibco, cat. no. 15290-018)
- Tyrode salt solution (see Reagent setup)

### *Equipment*

- Single-point scanner upright confocal microscope with spectral detection (e.g., Olympus Bx61 LSM Fluoview or Zeiss LSM 510) equipped with a 40 $\times$ 0.75W water-immersion objective
- 35-mm Petri dishes (Corning, cat. no. 430165)

### *Reagent Setup*

- **Mouse organotypic hippocampal slice cultures** Prepared from mice aged 6–9 d (see PROCEDURE). We have imaged slices at times ranging from 5 d to 6 months *in vitro*. **! CAUTION** All procedures must adhere to local laws regulating handling of experimental animals.
- **Tyrode salt solution** 2.7 mM KCl, 0.5 mM MgCl<sub>2</sub>, 136.9 mM NaCl, 0.36 mM NaH<sub>2</sub>PO<sub>4</sub>, 1.4 mM Na<sub>2</sub>HPO<sub>4</sub>, 5.5 mM glucose, 1.8 mM CaCl<sub>2</sub> (pH 7.26)  
**▲ CRITICAL** Filter-sterilize through a 0.22- $\mu$ m membrane.

## PROCEDURE

### *Overview*

- Step 1           Set up of the confocal microscope
- Step 2 - 6       Imaging session

### **Set up of the confocal microscope • TIMING 10 min**

1. Optimal acquisition settings are adapted to the intensity of the labeled cells based on the following criteria: use the smallest laser intensity possible, and enhance the intensity by increasing the gain and photo-multiplier (PMT) strength and/or opening the pinhole; also, use the largest step size possible (adapted to the size of the imaged objects). We obtained the best results for mossy fiber terminals using a step size of 0.62  $\mu$ m. In order to allow fast acquisition (and, thus, cause minimal damage to the slice cultures), use a low-resolution mode, avoid using averaging functions (e.g., Kalman) and apply the fastest scanning rate available to the microscope. We imaged mossy fiber terminals at 512  $\times$ 512 pixels.

#### **!Troubleshooting**

### **Imaging session • TIMING 30 min maximum**

2. Working in the cell-culture hood, place the cell-culture insert into a 35-mm Petri dish and add 2 ml pre-warmed Tyrode salt solution at 37 °C (1 ml above and 1 ml below the membrane).
3. Move to the confocal microscope. Use the 40  $\times$ /0.75W water-immersion objective and the mercury lamp to look for labeled cells.
4. **▲ CRITICAL STEP** To avoid contaminations originating during the imaging sessions, we clean the objective with 70% (vol/vol) ethanol in water before imaging individual slices. By taking this simple precaution, and using Fungizone and antibiotics in the culture media (see slice-preparation protocol, Gogolla et al. (2006) Nat. Prot. 1, 1165-1171) we rarely experience contaminations upon imaging sessions.

5. In order to include all labeled structures in the 3D region of interest (ROI), set the start point of the z-stack slightly below the first labeled structure, and the stop point slightly above the last labeled structure. For example, acquisition of the entire mossy fiber projection required four or five 3D stacks of 40–60 confocal planes in 10–15 min.

**▲ CRITICAL STEP** The slices should not stay in the Tyrode salt solution and outside the incubator for more than 30 min.

6. After imaging, remove the Tyrode salt solution, return the culture-plate insert into the six-well plate and place it back in the incubator.

**▲ CRITICAL STEP** From now on, to avoid contaminations, the slices should be kept in culture medium supplemented with Fungizone ( $0.25 \mu\text{g ml}^{-1}$ ).

7. Repeat Steps 2–5 for the next imaging session, keeping the same settings. In most cases, slices can be imaged repeatedly at least eight times, although some precautions should be taken (see below).

**▲ CRITICAL STEP** Generally, we have observed that when the experiments require more than two or three imaging sessions, good results depend on allowing long recovery time intervals between individual imaging sessions (e.g., 10–20 d), and keeping slices outside of the incubator for no longer than 20 min during imaging sessions. Our observations suggest that, provided one adheres to the principles outlined above (also see TROUBLESHOOTING), phototoxicity is not the major limiting factor. Instead, most damage to the slices associated with the imaging sessions is due to the changes of medium, and the times when the slices are kept outside of the incubator. It is important to note that our protocol was optimized for imaging granule cells and their mossy fibers. We have noticed that pyramidal neurons in CA3 appear to be more vulnerable to repeated handling, and recommend that repeated imaging protocols should be initially tested and optimized. Characteristic signs of selective damage include major reductions in the intensity of the GFP signal

(Thy1-driven expression of membrane-targeted GFP), thinning of neuronal processes and losses of spines. [!Troubleshooting](#)

**!Troubleshooting** for imaging organotypic slice cultures.

Problem	Possible reason	Solution
<b>Phototoxicity</b> Possible signs include the following: abrupt weakening of fluorescence intensity; swellings and breakdowns of axons and dendrites into beaded chains; blurred GFP signal around membranes; formation of large blebs on cell bodies, dendrites or presynaptic terminals; loss of dendritic spines.	Too high and/or long exposure to UV light.	Use appropriate filters to reduce the intensity of the UV light when inspecting the fluorescent signal; reduce the exposure time to UV light to a minimum; search the ROI wherever possible using the live-scanning mode of the microscope avoiding using UV light; use fast and precise shutters.
	Too high laser intensity.	Adapt imaging settings to use the lowest laser intensity possible; optimize the imaging settings outside the ROI; acquire the images using the 16-bit mode, in order to be able to use low laser intensities; select the appropriate emission filter, in order to maximize signal intensity without increasing laser strength.
	Too long exposure to laser energy.	Use the fastest scan mode and the smallest amount of confocal images that still allow proper analysis; avoid time consuming averaging options during acquisition; instead, optimize image quality after acquisition (e.g., by applying deconvolution).
	Too high light energy (UV and/or laser).	Use the smallest magnification objective possible to resolve the structures of interest; choose a high numerical aperture objective; choose an objective lens that is optimized for your emission wavelength.

### *Anticipated results*

Critical factors for a successful imaging experiment are careful handling of the slices and rapid image acquisition. We strongly recommend always using the same confocal settings for comparable imaging sessions, and practicing the rapid identification of the orientation of labeled slices when first looking at a new type. It is also important to be able to rapidly re-identify the ROI within a given slice. This can be helped by making a schematic drawing, with landmarks of the particular slice, and using it for rapid orientation during the next imaging session (Fig.1).

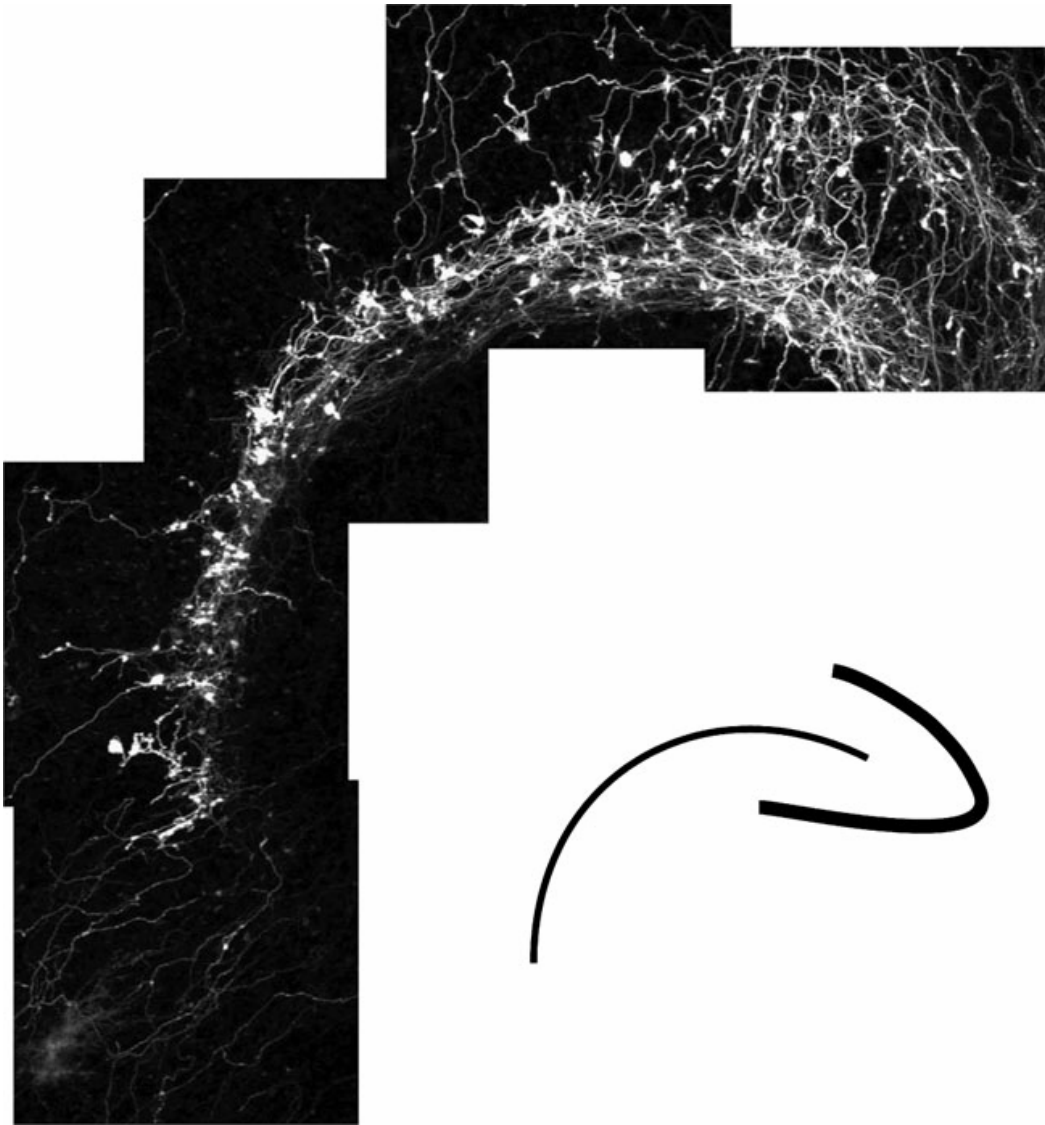


**Figure1. The five images were acquired with a 40 $\times$  objective and then tiled.** The schematic on the right indicates the orientation of the hippocampus (dentate gyrus on the right). The axons are labeled by a membrane-targeted GFP construct, as described in the text.

## References

1. Conchello, J.A. & Lichtman, J.W. Optical sectioning microscopy. *Nat. Methods* 2, 920–931 (2005)
2. Yuste, R. Fluorescence microscopy today. *Nat. Methods* 2, 902–904 (2005)
3. Gahwiler, B.H. Organotypic monolayer cultures of nervous tissue. *J. Neurosci. Meth.* 4, 329–342 (1981)
4. Stoppini, L., Buchs, P.A. & Muller, D. A simple method for organotypic cultures of nervous tissue. *J. Neurosci. Meth.* 37, 173–182 (1991)
5. Gahwiler, B.H. *et al.* Organotypic slice cultures: a technique has come of age. *Trends Neurosci.* 20, 471–477 (1997)
6. De Paola, V., Arber, S. & Caroni, P. AMPA receptors regulate dynamic equilibrium of presynaptic terminals in mature hippocampal networks. *Nat. Neurosci.* 6, 491–500 (2003)
7. Galimberti, I. *et al.* Long-term rearrangements of hippocampal mossy fiber terminal connectivity in the adult regulated by experience. *Neuron* 50, 749–763 (2006)
8. Caroni, P. Overexpression of growth-associated proteins in the neurons of adult transgenic mice. *J. Neurosci. Meth.* 71, 3–9 (1997)
9. Feng, G. *et al.* Imaging neuronal subsets in transgenic mice expressing multiple spectral variants of GFP. *Neuron* 28, 41–51 (2000)
10. Araki, R. Transgenic mouse lines expressing synaptotagmin in hippocampus and cerebellar cortex. *Genesis* 42, 53–60 (2005)
11. Lo, D.C., McAllister, A.K. & Katz, L.C. Neuronal transfection in brain slices using particle-mediated gene transfer. *Neuron* 13, 1263–1268 (1994)
12. Benediktsson, A.M., Schachtele, S.J., Green, S.H. & Dailey, M.E. Ballistic labeling and dynamic imaging of astrocytes in organotypic hippocampal slice cultures. *J. Neurosci. Meth.* 141, 41–53 (2005)
13. Ehrenguber, M.U. *et al.* Recombinant Semliki Forest virus and Sindbis virus efficiently infect neurons in hippocampal slice cultures. *Proc. Natl. Acad. Sci. USA* 96, 7041–7046 (1999)
14. Miyaguchi, K., Maeda, Y., Kojima, T., Setoguchi, Y. & Mori, N. Neuron-targeted gene transfer by adenovirus carrying neural-restrictive silencer element. *Neuroreport* 10, 2349–2353 (1999)
15. Henze, D.A., Urban, N.N. & Barrionuevo, G. The multifarious hippocampal mossy fiber pathway: a review. *Neuroscience* 98, 407–427 (2000)
16. De Simoni, A., Griesinger, C.B. & Edwards, F.A. Development of rat CA1 neurones in acute versus organotypic slices: role of experience in synaptic morphology and activity. *J. Physiol.* 550, 135–147 (2003)

### 5.3. Staining protocol for organotypic hippocampal slice cultures

Nadine Gogolla<sup>1,3</sup>, Ivan Galimberti<sup>1,3</sup>, Vincenzo DePaola<sup>2</sup> and Pico Caroni<sup>1</sup>

<sup>1</sup>Friedrich Miescher Institute, Maulbeerstrasse 66, CH-4058 Basel, Switzerland.

<sup>2</sup>Cold Spring Harbor Laboratories, Cold Spring Harbor, New York, USA.

<sup>3</sup>These authors contributed equally to this work.

*Nature Protocols*

2006 (1, 2452 – 2456)

## ABSTRACT

This protocol details a method to immunostain organotypic slice cultures from mouse hippocampus. The cultures are based on the interface method, which does not require special equipment, is easy to execute and yields slice cultures that can be imaged repeatedly, from the time of isolation at postnatal day 6–9 up to 6 months *in vitro*. The preserved tissue architecture facilitates the analysis of defined hippocampal synapses, cells and entire projections. Time-lapse imaging is based on transgenes expressed in the mice or on constructs introduced through transfection or viral vectors; it can reveal processes that develop over periods ranging from seconds to months. Subsequent to imaging, the slices can be processed for immunocytochemistry to collect further information about the imaged structures. This protocol can be completed in 3 d.

## INTRODUCTION

Recent advances in live imaging and transgenic technology have had a substantial impact on the range of experimental tools available to life scientists<sup>1, 2</sup>. These include microscopes with greatly improved sensitivity, temporal and spatial resolution and spectral versatility; powerful image acquisition and processing software; and an ever-growing repertoire of fluorescent reagents to monitor second messengers, identify macromolecules and their physiological modifications, and examine subcellular structures *in situ*. In the field of neuroscience, these developments have allowed studies of the structure and function of biologically relevant neuronal circuits to be approached in a noninvasive way and with unprecedented analytical power. To fully exploit these technological developments, adequate biological preparations must be adapted for live-imaging studies of defined neuronal circuits<sup>3, 4, 5, 6, 7</sup>. Subsequent immunostaining of the preparations allows retrospective definition of the cellular and molecular identity of the imaged structures and their local surroundings, as well as molecular correlation of the dynamic processes.

## Advantages of the method

Key features of the hippocampal organotypic slice cultures<sup>4</sup> from mice include (i) well-defined cellular architecture of the hippocampal circuit, which preserves the organization *in vivo* and allows for the identification and manipulation of defined neurons and synapses<sup>3, 4, 5, 6, 7</sup>; (ii) presence of axonal projections (mossy fiber axons extending from dentate gyrus granule cells to the distal end of CA3) that can largely be recovered in the slices in their original state (that is, without lesioning) and that establish stereotypic numbers of readily identifiable presynaptic terminals onto excitatory and inhibitory neurons in the hilus and CA3 (refs. <sup>6, 7, 8</sup>); (iii) a long-term thickness of 100–150 μm, preserving three-dimensional organizations of connectivity<sup>4, 5</sup>; (iv) maturation of the slice cultures closely reflecting the corresponding schedule *in vivo*<sup>9</sup>; (v) the option to prepare the slices from mice of any genetic background, including those expressing fluorescent transgenes in selected neurons<sup>6, 7, 10, 11</sup> and those of poor postnatal viability. Imaging coupled to retrospective immunocytochemistry allows the acquisition of information about unlabeled structures in the areas surrounding the imaged (fluorescent) structures, and the investigation of molecular mechanisms at the level of local identified structures within neuronal circuits.

## Critical aspects

The main critical issues relate to the extent to which organotypic slice cultures reproduce the properties of hippocampal circuits *in vivo*<sup>5</sup>. This information is important in deciding whether the approach is appropriate to address the particular experimental issues one has in mind. These issues have been investigated in much detail by physiologists, who have demonstrated extensive similarities, but also a few discrepancies, between properties of the corresponding circuits in the neonatal and adult mouse brains<sup>5, 9</sup>. Critical limitations of the immunocytochemistry protocol mainly involve issues of antibody penetration and antigen accessibility. Some of these problems can be solved by varying the fixation and permeabilization protocols or by cutting sections of the slices.

## Possible results and outlook

Organotypic slice cultures from approximately 1-week-old mouse hippocampus seem to reproduce most anatomical and functional properties of the corresponding hippocampal circuits *in vivo* for at least 6 months *in vitro* as a result of the intrinsic properties of their neurons. Imaging of the slices coupled to *post hoc* immunocytochemistry thus provides an exciting range of possibilities for the exploration of mechanisms controlling the assembly and function of neuronal circuits. Some of these possibilities include (i) time-lapse imaging and molecular analysis over periods ranging from sub-seconds to months, and from individual molecules to entire neuronal projections and circuits; (ii) imaging and analysis of neuronal<sup>6, 7, 10, 11</sup> and glial<sup>12</sup> subtypes; (iii) molecular manipulation using transfection<sup>12, 13</sup> or viral approaches<sup>14, 15</sup> to knock down or overexpress genes, silence or activate neurons, render neurons responsive to light or selective drugs, and highlight subcircuits; (iv) protocols that combine physiology, imaging and immunocytochemistry; (v) manipulations to investigate lesion-induced plasticity and pathways of neurodegeneration and repair (such as amyloid- or epilepsy-related pathways); (vi) the potential to follow and characterize the insertion of new neurons, the development of axons and their connections, or the insertion of exogenously added stem cells; and (vii) additional *post hoc* analysis using methods involving tracers, electron microscopy and single-cell genomics.

## MATERIALS

### *Reagents*

- Organotypic hippocampal slices
- Paraformaldehyde (PFA; Merck, cat. no. 1.04005.1000)
- Methanol (MeOH; Merck, cat. no. 1.06009.1000)
- Triton X-100 (Fluka Chemika, cat. no. 93420)
- BSA (Sigma, cat. no. A3912-100G)
- PBS (with or without magnesium and/or calcium)
- Primary and secondary antibodies suitable for immunohistochemistry
- 4% PFA in PBS (cooled to 4 °C)  
**! CAUTION** PFA is toxic. Avoid inhalation, ingestion or contact with skin, eyes or mucous membranes.
- 20% MeOH in PBS (cooled to 4 °C)
- Permeabilization solution: 0.5% Triton X-100 in PBS

### **? TROUBLESHOOTING**

- Blocking solution: 20% BSA in PBS
- Antibody solutions: 5% BSA in PBS + antibodies at specific dilution
- First washing solution: 5% BSA in PBS
- Second washing solution: PBS

### *Equipment*

- Scalpel or razor blade
- Fine straight forceps
- Microscope slides (e.g., 76 x 26 mm; Menzel-Gläser)
- Thin cover glasses (e.g., 40 x 24 mm, 170 nm thick; Assistant)
- Mounting medium (e.g., ProLong Gold antifade reagent, Invitrogen, cat. no. P36934)
- 12- or 24-well plates (Corning, cat. no. 3513)

## PROCEDURE

### *Overview*

- Step 1 - 8 Fixation of slice cultures (day 1)
- Step 9 - 10 Permeabilization of slice tissue (day 1)
- Step 11 - 12 Blocking (day 2)
- Step 13 - 15 Cutting slices off membrane of culture plate inserts (day 2)
- Step 16 - 19 Incubation with primary antibody (day 2)
- Step 20 - 23 Washing off primary antibody (day 3)
- Step 24 - 26 Incubation with secondary antibody (day 3)
- Step 27 Washing off secondary antibody
- Step 28 - 32 Mounting of stained slice cultures (day 3)

#### **Fixation of slice cultures (day 1) • TIMING 15 min**

1. Remove the culture medium beneath the membrane by suction.
2. Add 1 ml of cold 4% PFA solution above and 1 ml beneath the membrane insert.

**! CAUTION** Use gloves to handle PFA, and wear a mask.

3. Wait 5 minutes. **? TROUBLESHOOTING**
4. Remove the PFA solution completely.
5. Wash once briefly by adding 1 ml of cold PBS above and 1 ml beneath the insert and then removing by suction.
6. Add 1 ml of cooled 20% MeOH/PBS solution above and 1 ml beneath the insert.
7. Wait 5 minutes. **? TROUBLESHOOTING**
8. Wash once briefly with PBS as in Step 5.

#### **Permeabilization of slice tissue (day1) • TIMING Minimum 12 h**

9. Add 1 ml of permeabilization solution (0.5% Triton X-100 in PBS) above and 1 ml beneath the insert.

10. Incubate overnight, or for at least 12 h, at 4 °C.

■ **PAUSE POINT** Slices can be kept in the permeabilization solution for up to 18 h.

### ?TROUBLESHOOTING

#### **Blocking (day 2) • TIMING Minimum 4 h**

11. Remove permeabilization solution.

12. Add blocking solution (20% BSA in PBS).

■ **PAUSE POINT** Can be left for 4 h at room temperature (22–24 °C) or overnight at 4 °C. Sections can be kept in the blocking solution at 4 °C for at least 2–3 d.

#### **Cutting slices off membrane of culture plate inserts (day 2) • TIMING 5 min**

13. To reduce the volume of antibody solutions needed, the slices are cut off the membranes of the culture plate inserts. Place the culture plate insert on a plastic cover (preferably a transparent plastic cover lying on a dark background to make the tissue easily visible).

14. Use forceps and scalpel to carefully cut the membrane piece together with the hippocampal slice out of the surrounding membrane. Keep 1–2 mm of distance to the tissue to avoid damage. (Optional: the slices can already be cut off just after the fixation to further limit the amounts of permeabilization and blocking solutions required).

▲ **CRITICAL STEP** Always keep the top side of the membrane facing up, and do not flip it around.

15. Place the cut-off membrane pieces (top sides facing up) onto the lid of a culture plate.

▲ **CRITICAL STEP** To avoid drying, always keep a droplet of 5% BSA/PBS solution on top of each slice.

**Incubation with primary antibody (day 2) • TIMING Minimum 4 h or overnight**

16. To avoid drying of the slices during the antibody incubations, build a 'wet chamber' by putting wet paper tissues into a box that can be tightly closed and is large enough to hold the culture dish covers of Step 15.
17. Prepare the primary antibody solutions in 5% BSA/PBS (50  $\mu$ l per slice).
18. Drop 50  $\mu$ l of the antibody solution onto each slice.
19. Carefully place the lid holding the slices into the wet chamber and close it.

■ **PAUSE POINT** The primary antibody can be incubated overnight at 4 °C or for 3–4 h at room temperature.

**Washing off primary antibody (day 3) • TIMING 30 min**

20. Fill the wells of a 12- or 24- well plate with 5% BSA/PBS (fill three times as many wells as you have slices to stain).
21. Put each stained slice into one well containing the 5% BSA/PBS washing solution.

▲ **CRITICAL STEP** Always keep the top side of the slice facing up.

22. To wash off excess antibody, put the plate onto a horizontal shaker for 5–10 min at moderate speed (be careful that the fluid movement does not cause the slice to flip over).
23. Transfer the slices to the next unused wells and repeat this washing twice more.

**Incubation with secondary antibody (day 3) • TIMING Minimum 3 h**

24. Prepare the secondary antibody solution (50  $\mu$ l per slice).

▲ **CRITICAL STEP** If you use fluorescent secondary antibodies, perform the following steps whenever possible in the dark, and keep the antibody-containing solutions away from light.

25. Put the slices back onto a fresh plate lid (as in Step 15).

26. Proceed as for primary antibody (Steps 16–19).

■ **PAUSE POINT** The secondary antibody can be incubated for 3–4 h at room temperature or overnight at 4 °C.

**Washing off secondary antibody • TIMING 30 min**

27. Wash off the secondary antibody as for the primary antibody (Steps 20–23) but using simple PBS solution (no BSA required).

**Mounting of stained slice cultures (day 3) • TIMING 30 min**

28. Put the washed slices, top sides facing up, onto a glass microscope slide.

29. Put a droplet of mounting medium directly on the slice.

▲ **CRITICAL STEP** Avoid drying out the slices.

30. Cover the slice immediately with a thin cover glass.

31. Seal the cover glass with nail polish.

■ **PAUSE POINT**

32. Store at 4 °C in the dark. The labeled slices can be kept for several months.

• **TIMING**

Day 1: fixation, 5 min PFA + 5 min MeOH; permeabilization, minimum 12 h (overnight).

Day 2: blocking, minimum 3 h; incubation with primary antibody, minimum 4 h or overnight.

Day 3: washing off primary antibody, 30 min; incubation with secondary antibody, minimum 3 h; washing off secondary antibody, 30 min; mounting sections, 5 min; sealing cover glasses, 5 min.

## ?TROUBLESHOOTING

Table 1 Troubleshooting advice.

<b>Problem</b>	<b>Possible reason</b>	<b>Solution</b>
Transgenic GFP signal is beaded or very weak	Fixation can destroy GFP signal (Steps 3 and 7)	Reduce fixation times (e.g., 3 min each for PFA and MeOH)  Methanol fixation may not be required for each antibody. Try omitting methanol Use anti-GFP antibody to enhance the signal
Antibody does not penetrate deeply into the tissue	Permeabilization too weak (Step 10; especially in young slices, which are more dense)	Increase Triton X-100 concentration during the permeabilization step to 1–2% and/or prolong the incubation

## ANTICIPATED RESULTS

Critical factors are the fixation of the slices and penetration of antibodies and reagents. Penetration of reagents can be enhanced by double fixation followed by permeabilization overnight. Unfortunately, fixations are not entirely predictable, even when using the same protocol, so one should plan on processing several copies of crucial data. Suboptimal fixation can lead to a blurred appearance of small structures such as active zones. Optimization of protocols for special needs is recommended.

This protocol should produce good-resolution labeling of cellular and subcellular structures (Fig. 1) and unambiguous identification of regions of interest, such as those that had been followed with live imaging before fixation.

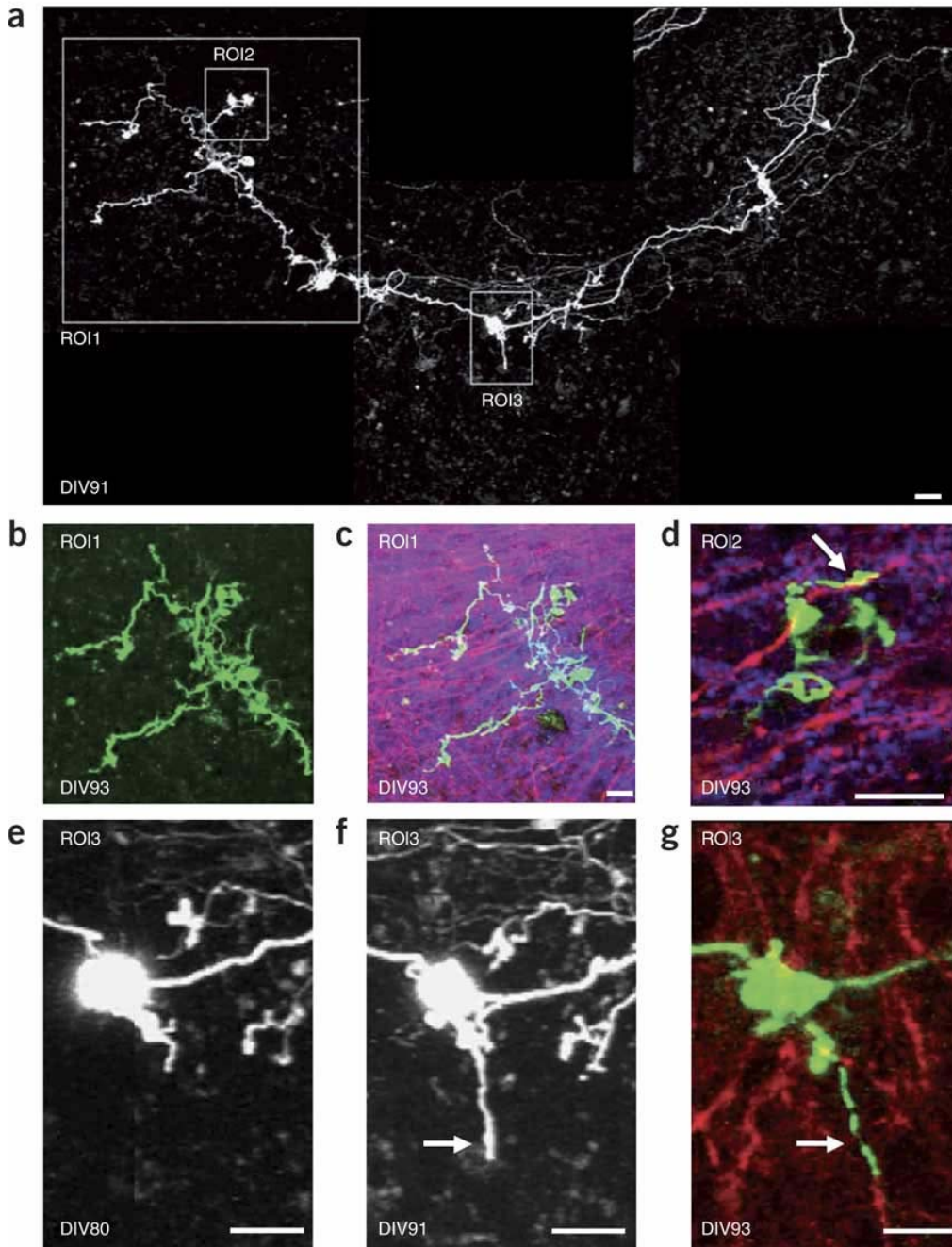


**Figure 1.** A slice from a Thy1-mGFP single-transgenic mouse shows mossy fiber projection expressing membrane-targeted GFP. After imaging, the slice was fixed and stained for Bassoon (active zone marker) and phospho-GluR1 (pyramidal neuron dendrite marker). Live imaging was done on *in vitro* day 80 (DIV80) and DIV91; fixation and staining were done on DIV93. (a) Low-magnification view of mossy fiber projection and regions of interest (mossy fiber terminal complexes; ROI1–3). (b) Maximum-intensity projection of the GFP signal in ROI1 after fixation. (c) Same as b, but with superimposed Bassoon (blue) and phospho-GluR1 (red) signals. (d) Single confocal plane of ROI2. Note process grown from the mossy fiber terminal between DIV91 and DIV93 (arrow), which exhibits a terminal bouton and contacts the same dendrite (phospho-GluR1) as its mossy fiber terminal of origin. (e,f) Live imaging of ROI3 (maximum-intensity projection). (g) Single confocal plane of ROI3 after fixation and staining (green, GFP; red, phospho-GluR1). Note process that grew from the mossy fiber terminal between DIV80 and DIV91 (arrows in f and g), extending along a phospho-GluR1-positive dendrite. Scale bars, 25  $\mu$ m.

## References

1. Conchello, J.A. & Lichtman, J.W. Optical sectioning microscopy. *Nat. Meth.* 2, 920–931 (2005)
2. Yuste, R. Fluorescence microscopy today. *Nat. Meth.* 2, 902–904 (2005)
3. Gahwiler, B.H. Organotypic monolayer cultures of nervous tissue. *J. Neurosci. Meth.* 4, 329–342 (1981)
4. Stoppini, L., Buchs, P.A. & Muller, D. A simple method for organotypic cultures of nervous tissue. *J. Neurosci. Meth.* 37, 173–182 (1991)
5. Gahwiler, B.H. *et al.* Organotypic slice cultures: a technique has come of age. *Trends Neurosci.* 20, 471–477 (1997)
6. De Paola, V., Arber, S. & Caroni, P. AMPA receptors regulate dynamic equilibrium of presynaptic terminals in mature hippocampal networks. *Nat. Neurosci.* 6, 491–500 (2003)
7. Galimberti, I. *et al.* Long-term rearrangements of hippocampal mossy fiber terminal connectivity in the adult regulated by experience. *Neuron* 50, 749–763 (2006)
8. Henze, D.A., Urban, N.N. & Barrionuevo, G. The multifarious hippocampal mossy fiber pathway: a review. *Neuroscience* 98, 407–427 (2000)
9. De Simoni, A., Griesinger, C.B. & Edwards, F.A. Development of rat CA1 neurons in acute versus organotypic slices: role of experience in synaptic morphology and activity. *J. Physiol.* 550, 135–147 (2003)
10. Caroni, P. Overexpression of growth-associated proteins in the neurons of adult transgenic mice. *J. Neurosci. Meth.* 71, 3–9 (1997) |
11. Feng, G. *et al.* Imaging neuronal subsets in transgenic mice expressing multiple spectral variants of GFP. *Neuron* 28, 41–51 (2000)
12. Benediktsson, A.M., Schachtele, S.J., Green, S.H. & Dailey, M.E. Ballistic labeling and dynamic imaging of astrocytes in organotypic hippocampal slice cultures. *J. Neurosci. Meth.* 141, 41–53 (2005).
13. Lo, D.C., McAllister, A.K. & Katz, L.C. Neuronal transfection in brain slices using particle-mediated gene transfer. *Neuron* 13, 1263–1268 (1994)
14. Ehrenguber, M.U. *et al.* Recombinant Semliki Forest virus and Sindbis virus efficiently infect neurons in hippocampal slice cultures. *Proc. Natl. Acad. Sci. USA* 96, 7041–7046 (1999)
15. Miyaguchi, K., Maeda, Y., Kojima, T., Setoguchi, Y. & Mori, N. Neuron-targeted gene transfer by adenovirus carrying neural-restrictive silencer element. *Neuroreport* 10, 2349–2353 (1999)

## 6. REFERENCES

- Acsady L, Kamondi A, Sik A, Freund T, Buzsaki G (1998) GABAergic cells are the major postsynaptic targets of mossy fibers in the rat hippocampus. *J Neurosci* 18(9):3386-403.
- Ahmad-Annuar A, Ciani L, Simeonidis I, Herreros J, Fredj NB, Rosso SB, Hall A, Brickley S, Salinas PC (2006) Signaling across the synapse: a role for Wnt and Dishevelled in presynaptic assembly and neurotransmitter release. *J Cell Biol* 174(1):127-39
- Allen CB, Celikel T, Feldman DE (2003) Long-term depression induced by sensory deprivation during cortical map plasticity in vivo. *Nat Neurosci* 6(3):291-9.
- Amaral DG & Witter MP (1989) The three-dimensional organization of the hippocampal formation: a review of anatomical data. *Neuroscience* 31(3):571-591.
- Anagnostaras SG, Maren S & Fanselow MS (1999) Temporally graded retrograde amnesia of contextual fear after hippocampal damage in rats: within-subjects examination. *J Neurosci* 19:1106-1114.
- Arellano JI, Espinosa A, Fairen A, Yuste R, DeFelipe J (2007) Non-synaptic dendritic spines in neocortex. *Neuroscience* 145(2):464-9.
- Artola A et al. (2006) Long-lasting modulation of the induction of LTD and LTP in rat hippocampal CA1 by behavioural stress and environmental enrichment. *Eur J Neurosci* 23:261–272.
- Barnes CA, McNaughton BL (1983) Excitability changes in hippocampal granule cells of senescent rat. *Prog Brain Res* 58:445-51.
- Benaroya-Milshtein N et al. (2004) Environmental enrichment in mice decreases anxiety, attenuates stress responses and enhances natural killer cell activity. *Eur J Neurosci* 20:1341–1347.
- Bennett EL, Rosenzweig MR & Diamond MC(1969) Rat brain: effects of environmental enrichment on wet and dry weights. *Science* 163, 825–826.
- Bennett MR (2000) The concept of long term potentiation of transmission at synapses. *Prog Neurobiol* 60(2):109-37.
- Bennett JC, McRae PA, Levy LJ & Frick KM (2006) Long-term continuous, but not daily, environmental enrichment reduces spatial memory decline in aged male mice. *Neurobiol Learn Mem* 85:139–152.

Berardi N, Pizzorusso T, Maffei L (2000) Critical periods during sensory development. *Curr Opin Neurobiol* 10:138–145.

Berardi N, Pizzorusso T, Maffei L (2004) Extracellular matrix and visual cortical plasticity: freeing the synapse. *Neuron* 44(6):905-8.

Black JE, Isaacs KR, Anderson BJ, Alcantara AA, Greenough WT (1990) Learning causes synaptogenesis whereas motor activity cause angiogenesis, in cerebellar cortex of adult rats. *Proc Natl Acad Sci* 87:5568–5572.

Blake DT, Heiser MA, Caywood M, Merzenich MM, (2006) Experiencedependent adult cortical plasticity requires cognitive association between sensation and reward. *Neuron* 52: 371–381.

Bliss TV, Gardner-Medwin AR (1973) Long-lasting potentiation of synaptic transmission in the dentate area of the unanaesthetized rabbit following stimulation of the perforant path. *J Physiol.* 232(2):357-74.

Bliss TV, Lomo T (1973) Long-lasting potentiation of synaptic transmission in the dentate area of the anaesthetized rabbit following stimulation of the perforant path. *J Physiol* 232(2):331-56.

Bliss TV, Collingridge GL (1993) A synaptic model of memory: long-term potentiation in the hippocampus. *Nature* 361(6407):31-9.

Bonhoffer T, Yuste R (2002) Spine motility. Phenomenology, mechanisms, and function. *Neuron* 35(6):1019-27.

Bontempi B, Laurent-Demir C, Destrade C, Jaffard R (1999) Time-dependent reorganization of brain circuitry underlying long-term memory storage. *Nature* 400(6745):671-5.

Bower JM, Woolston DC (1983) Congruence of spatial organization of tactile projections to granule cell and Purkinje cell layers of cerebellar hemispheres of the albino rat: vertical organization of cerebellar cortex. *J Neurophysiol* 49(3):745-66.

Brainard MS, Knudsen EI (1998) Sensitive periods for visual calibration of the auditory space map in the barn owl optic tectum. *J Neurosci* 18(10):3929-42.

Bruel-Jungerman E, Laroche S & Rampon C (2005) New neurons in the dentate gyrus are involved in the expression of enhanced long-term memory following environmental enrichment. *Eur J Neurosci* 21:513–521.

- Brunig I, Kaech S, Brinkhaus H, Oertner TG, Matus A (2004) Influx of extracellular calcium regulates actin-dependent morphological plasticity in dendritic spines. *Neuropharmacology* 47(5):669-76.
- Burke SN, Barnes CA (2006) Neural plasticity in the ageing brain. *Nat Rev Neurosci* 7(1):30-40.
- Buzsaki G (2002) Theta oscillations in the hippocampus. *Neuron* 33(3):325-40.
- Cadigan KM, Liu YI (2006) Wnt signaling: complexity at the surface. *J Cell Sci* 119:395-402.
- Calford MB, Tweedale R (1991a) Acute changes in cutaneous receptive fields in primary somatosensory cortex after digit denervation in adult flying fox. *J Neurophysiol* 65(2):178-87.
- Calford MB, Tweedale R (1991b) Immediate expansion of receptive fields of neurons in area 3b of macaque monkeys after digit denervation. *Somatosens Mot Res* 8(3):249-60.
- Castillo PE, Janz R, Sudhof TC, Tzounopoulos T, Malenka RC, Nicoll RA (1997) Rab3A is essential for mossy fibre long-term potentiation in the hippocampus. *Nature* 388(6642):590-3.
- Cancedda L, Putignano E, Sale A, Viegi A, Berardi N, Maffei L (2004) Acceleration of visual system development by environmental enrichment. *J Neurosci* 24(20):4840-8.
- Castillo PE, Schoch S, Schmitz F, Sudhof TC, Malenka RC (2002) RIM1 $\alpha$  is required for presynaptic long-term potentiation. *Nature* 415 (6869): 327–330.
- Cesa R, Strata P (2005) Axonal and synaptic remodeling in the mature cerebellar cortex. *Prog Brain Res* 148:45-56.
- Cesa R, Morando L, Strata P (2005) Purkinje cell spinogenesis during architectural rewiring in the mature cerebellum. *Eur J Neurosci* 22(3):579-86.
- Cesa R, Scelfo B, Strata P (2007) Activity-dependent presynaptic and postsynaptic structural plasticity in the mature cerebellum. *J Neurosci* 27(17):4603-11.
- Chapillon P, Manneche C, Belzung C & Caston J (1999) Rearing environmental enrichment in two inbred strains of mice: 1. Effects on emotional reactivity. *Behav Genet* 29:41–46.
- Chen J, Park CS, Tang SJ (2006) Activity-dependent synaptic Wnt release regulates hippocampal long term potentiation. *J Biol Chem* 281(17):11910-6

- Chicurel ME, Harris KM (1992). Three-dimensional analysis of the structure and composition of CA3 branched dendritic spines and their synaptic relationships with mossy fiber boutons in the rat hippocampus. *J Comp Neurol* 325:169-182.
- Chklovskii DB, Mel BW, Svoboda K (2004) Cortical rewiring and information storage. *Nature* 431:782-788.
- Ciani L, Krylova O, Smalley MJ, Dale TC, Salinas PC (2004) A divergent canonical WNT-signaling pathway regulates microtubule dynamics: dishevelled signals locally to stabilize microtubules. *J Cell Biol* 164(2):243-53.
- Ciani L, Salinas PC (2005) WNTs in the vertebrate nervous system: from patterning to neuronal connectivity. *Nat Rev Neurosci* 6(5):351-62.
- Clark SA, Allard T, Jenkins WM, Merzenich MM (1988) Receptive fields in the body-surface map in adult cortex defined by temporally correlated inputs. *Nature* 332(6163):444-5.
- Cohen D, Yarom Y (1998) Patches of synchronized activity in the cerebellar cortex evoked by mossy-fiber stimulation: questioning the role of parallel fibers. *Proc Natl Acad Sci U S A* 95(25):15032-6.
- Connor JR, Wang EC & Diamond MC (1982) Increased length of terminal dendritic segments in old adult rats' somatosensory cortex: an environmentally induced response. *Exp Neurol* 78:466-470.
- Crist RE, Li W, Gilbert CD (2001) Learning to see: experience and attention in primary visual cortex. *Nat Neurosci* 4(5):519-25.
- D'Adamo P, Wolfer D, Kopp C, Tobler I, Toniolo D, Lipp HP (2004) Mice deficient for the synaptic vesicle protein Rab3a show impaired spatial reversal learning and increased explorative activity but none of the behavioral changes shown by mice deficient for the Rab3a regulator Gdi1. *Eur J Neurosci* 19(7): 1895-90.
- Dan Y, Poo MM (2004) Spike timing-dependent plasticity of neural circuits. *Neuron* 44(1):23-30.
- Dan Y & Poo MM (2006) Spike timing-dependent plasticity: from synapse to perception. *Physiol Rev* 86(3):1033-48.
- Danzer SC, McNamara JO (2004) Localization of brain-derived neurotrophic factor to distinct terminals of mossy fiber axons implies regulation of both excitation and feedforward inhibition of CA3 pyramidal cells. *J Neurosci* 15:11346-11355.
- Darian-Smith C, Gilbert CD (1994) Axonal sprouting accompanies functional reorganization in adult cat striate cortex. *Nature* 368(6473):737-40.

Datwani A, Iwasato T, Itohara S, Erzurumlu RS (2002) NMDA receptor-dependent pattern transfer from afferents to postsynaptic cells and dendritic differentiation in the barrel cortex. *Mol Cell Neurosci* 21(3):477-92.

Debanne D, Gahwiler BH, Thompson SM (1998) Long-term synaptic plasticity between pairs of individual CA3 pyramidal cells in rat hippocampal slice cultures. *J Physiol* 507:237-47.

De Paola V, Arber S, Caroni P (2003) AMPA receptors regulate dynamic equilibrium of presynaptic terminals in mature hippocampal networks. *Nat Neurosci* 6(5):491-500.

De Paola v, Holtmaat A, Knott G, Song S, Wilbrecht L, Caroni P, Svoboda K (2006) Cell type-specific structural plasticity of axonal branches and boutons in the adult neocortex. *Neuron* 49: 861-875.

Diamond MC, Rosenzweig MR, Bennett EL, Lindner B & Lyon L (1972) Effects of environmental enrichment and impoverishment on rat cerebral cortex. *J Neurobiol* 3: 47–64.

Diamond MC, Ingham CA, Johnson RE, Bennett EL & Rosenzweig MR (1976) Effects of environment on morphology of rat cerebral cortex and hippocampus. *J Neurobiol* 7:75–85.

Doupe AJ, Kuhl PK (1999) Birdsong and human speech: common themes and mechanisms. *Annu Rev Neurosci* 22:567–631.

Dudai Y (1996) Consolidation: fragility on the road to the engram. *Neuron* 17:367–370.

Dudai Y (2004) The neurobiology of consolidations, or, how stable is the engram? *Annu Rev Psychol.* 2004;55:51-86.

Dudek & Bear (1993) Bidirectional long-term modification of synaptic effectiveness in the adult and immature hippocampus. *J Neurosci* 13(7):2910-8.

Duffy SN, Craddock KJ, Abel T & Nguyen PV (2001) Environmental enrichment modifies the PKA-dependence of hippocampal LTP and improves hippocampus-dependent memory. *Learn Mem* 8:26–34.

Ehlers MD (2003) Activity level controls postsynaptic composition and signaling via the ubiquitin-proteasome system. *Nat Neurosci* 6:231–242.

Eichenbaum H (2000) A cortical-hippocampal system for declarative memory. *Nat Rev Neurosci* 1(1):41-50

Engel D, Jonas P (2005) Presynaptic action potential amplification by voltage-gated Na<sup>+</sup> channels in hippocampal mossy fiber boutons. *Neuron* 45:405–417.

Engert F, Bonhoeffer T (1999) Dendritic spine changes associated with hippocampal long-term synaptic plasticity. *Nature* 399(6731):66–70.

Faherty CJ, Kerley D & Smeyne RJ (2003) A Golgi-Cox morphological analysis of neuronal changes induced by environmental enrichment. *Brain Res Dev Brain Res* 141:55–61.

Feng G, Mellor RH, Bernstein M, Keller-Peck C, Nguyen QT, Wallace M, Nerbonne JM, Lichtman JW, Sanes JR (2000) Imaging neuronal subsets in transgenic mice expressing multiple spectral variants of GFP. *Neuron* 28:41–51.

Fischer QS, Beaver CJ, Yang Y, Rao Y, Jakobsdottir KB, Storm DR, McKnight GS, Daw NW (2004) Requirement for the RIIbeta isoform of PKA, but not calcium-stimulated adenylyl cyclase, in visual cortical plasticity. *J Neurosci* 24(41):9049–58.

Foster TC, Gagne J & Massicotte G (1996) Mechanism of altered synaptic strength due to experience: relation to long-term potentiation. *Brain Res* 736:243–250.

Foster TC & Dumas TC (2001) Mechanism for increased hippocampal synaptic strength following differential experience. *J Neurophysiol* 85:1377–1383.

Fox K, Zahs K (1994) Critical period control in sensory cortex. *Curr Opin Neurobiol* 4:112–119.

Fradkin LG, van Schie M, Wouda RR, de Jong A, Kamphorst JT, Radjkoemar-Bansraj M, Noodermeer JN (2004) The *Drosophila* Wnt5 protein mediates selective axon fasciculation in the embryonic central nervous system. *Dev Biol* 272(2):362–75.

Fradkin LG, Garriga G, Salinas PC, Thomas JB, Yu X, Zou Y (2005) Wnt signaling in neural circuit development. *J Neurosci* 25(45):10376–8.

Frankland PW, Josselyn SA, Anagnostaras SG, Kogan JH, Takahashi E, Silva AJ (2004) Consolidation of CS and US representations in associative fear conditioning. *Hippocampus* 14(5):557–69.

Frenkel MY, Sawtell NB, Diogo AC, Yoon B, Neve RL, Bear MF (2006) Instructive effect of visual experience in mouse visual cortex. *Neuron* 51(3):339–49.

Frick KM & Fernandez SM (2003) Enrichment enhances spatial memory and increases synaptophysin levels in aged female mice. *Neurobiol Aging* 24:615–626.

Friske JE & Gammie SC (2005) Environmental enrichment alters plus maze, but not maternal defense performance in mice. *Physiol Behav* 85:187–194.

- Fu YX, Djupsund K, Gao H, Hayden B, Shen K, Dan Y (2002) Temporal specificity in the cortical plasticity of visual space representation. *Science* 296(5575):1999-2003.
- Furmanski CS, Schluppeck D, Engel SA (2004) Learning strengthens the response of primary visual cortex to simple patterns. *Curr Biol* 14(7):573-8.
- Gahwiler BH, Capogna M, Debanne D, McKinney RA, Thompson SM (1997) Organotypic slice cultures: a technique has come of age. *Trends Neurosci* 20:471-477.
- Galimberti I, Gogolla N, Alberi S, Santos AF, Muller D, Caroni P (2006) Long-term rearrangements of mossy fiber terminal connectivity in the adult regulated by experience. *Neuron* 50(5): 749-63
- Gan WB, Kwon E, Feng G, Sanes JR, Lichtman JW (2003) Synaptic dynamism measured over minutes to months: age-dependent decline in an autonomic ganglion. *Nat Neurosci* 6(9):956-60.
- Geiger JR, Jonas P (2000) Dynamic control of presynaptic Ca(2+) inflow by fast-inactivating K(+) channels in hippocampal mossy fiber boutons. *Neuron* 28:927-939.
- Geppert M, Bolshakov VY, Siegelbaum SA, Takei K, De Camilli P, Hammer RE, Südhof TC (1994) The role of Rab3A in neurotransmitter release *Nature* 369(6480):493-7.
- Geppert M, Goda Y, Stevens CF, Südhof TC (1997) Rab3A regulates a late step in synaptic vesicle fusion. *Nature* 387:810-814.
- Gilbert CD (1998) Adult cortical dynamics. *Physiol Rev* 78(2):467-85.
- Glazewski S, Chen CM, Silva A, Fox K (1996) Requirement for alpha-CaMKII in experience-dependent plasticity of the barrel cortex. *Science* 272(5260):421-3.
- Glazewski S, Giese KP, Silva A, Fox K (2000) The role of alpha-CaMKII autophosphorylation in neocortical experience-dependent plasticity. *Nat Neurosci* 3(9):911-8.
- Glazewski S, Bejar R, Mayford M, Fox K (2001) The effect of autonomous alpha-CaMKII expression on sensory responses and experience-dependent plasticity in mouse barrel cortex. *Neuropharmacology* 41(6):771-8.
- Globus A, Scheibel AB (1967) The effect of visual deprivation on cortical neurons: a Golgi study. *Exp Neurol* 19(3):331-45.
- Globus A, Rosenzweig MR, Bennett EL, Diamond MC (1973) Effects of differential experience on dendritic spine counts in rat cerebral cortex. *J Comp Physiol Psychol* 82(2):175-81.

Goda Y, Stevens CF (1996) Long-term depression properties in a simple system. *Neuron* 16(1):103-11.

Gonzales RB, DeLeon Galvan CJ, Rangel YM, and Claiborne BJ (2001). Distribution of thorny excrescences on CA3 pyramidal neurons in the rat hippocampus. *J Comp Neurol* 430:357-368.

Gordon MD, Nusse R (2006) Wnt signaling: multiple pathways, multiple receptors, and multiple transcription factors. *J Biol Chem* 281(32):22429-33.

Graf W, Gerrits N, Yatim-Dhiba N, Ugolini G (2002) Mapping the oculomotor system: the power of transneuronal labelling with rabies virus. *Eur J Neurosci* 15:1557–1562.

Gray NW, Weimer RM, Bureau I, Svoboda K (2006) Rapid redistribution of synaptic PSD-95 in the neocortex in vivo. *PLoS Biol* 4(11):e370.

Green EJ & Greenough WT (1986) Altered synaptic transmission in dentate gyrus of rats reared in complex environments: evidence from hippocampal slices maintained in vitro. *J Neurophysiol* 55:739–750.

Greenough WT & Volkmar FR (1973a) Pattern of dendritic branching in occipital cortex of rats reared in complex environments. *Exp Neurol* 40:491–504.

Greenough WT, Volkmar FR & Juraska JM (1973b) Effects of rearing complexity on dendritic branching in frontolateral and temporal cortex of the rat. *Exp Neurol* 41:371–378.

Greenough WT, Hwang HM & Gorman C (1985) Evidence for active synapse formation or altered postsynaptic metabolism in visual cortex of rats reared in complex environments. *Proc Natl Acad Sci USA* 82:4549–4552.

Grutzendler J, Kasthuri N, Gan WB (2002) Long-term dendritic spine stability in the adult cortex. *Nature* 420(6917):812-6.

Hall AC, Lucas FR, Salinas PC (2000) Axonal remodeling and synaptic differentiation in the cerebellum is regulated by WNT-7a signaling. *Cell* 100(5): 525-35

Hardingham N, Glazewski S, Pakhotin P, Mizuno K, Chapman PF, Giese KP, Fox K (2003) Neocortical long-term potentiation and experience-dependent synaptic plasticity require alpha-calcium/calmodulin-dependent protein kinase II autophosphorylation. *J Neurosci* 23(11):4428-36.

Harris EW, Cotman CW (1986) Long-term potentiation of guinea pig mossy fiber responses is not blocked by N-methyl D-aspartate antagonists. *Neurosci Lett* 70(1): 132-7

Hebb DO (1949) *The Organization of Behavior: A neuropsychological theory* (Wiley, New York).

- Hensch TK (2003) Controlling the critical period. *Neurosci Res* 47(1):17-22.
- Hensch TK (2005) Critical period plasticity in local cortical circuits. *Nat Rev Neurosci* 6(11):877-88.
- Henze DA, Urban NN, Barrionuevo G (2000) The multifarious hippocampal mossy fiber pathway: a review. *Neuroscience* 98:407–427.
- Henze DA, Wittner L, Buzsaki G (2002) Single granule cells reliably discharge targets in the hippocampal CA3 network in vivo. *Nat Neurosci* 5:790-795.
- Hofer SB, Mrsic-Flogel TD, Bonhoeffer T, Hubener M (2006) Prior experience enhances plasticity in adult visual cortex. *Nat Neurosci* 9(1):127-32.
- Hoffman KL, McNaughton BL (2002) Coordinated reactivation of distributed memory traces in primate neocortex. *Science* 297(5589):2070-3.
- Holtmaat AJ, Trachtenberg JT, Wilbrecht L, Shepherd GM, Zhang X, Knott GW, Svoboda K (2005) Transient and persistent dendritic spines in the neocortex in vivo. *Neuron* 45(2):279-91.
- Holtmaat A, Wilbrecht L, Knott GW, Welker E, Svoboda K (2006) Experience-dependent and cell-type-specific spine growth in the neocortex. *Nature* 441(7096):979-83.
- Hopfield JJ (1982) Neural networks and physical systems with emergent collective computational abilities. *Proc Natl Acad Sci USA* 79:2554–2558.
- Huang YY, Zakharenko SS, Schoch S, Kaeser PS, Janz R, Südhof TC, Siegelbaum SA, Kandel ER (2005) Genetic evidence for a protein-kinase-A-mediated presynaptic component in NMDA-receptor-dependent forms of long-term synaptic potentiation. *Proc Natl Acad Sci U S A* 102(26):9365-70.
- Huang CM, Wang L, Huang RH (2006) Cerebellar granule cell: ascending axon and parallel fiber. *Eur J Neurosci* 23(7):1731-7.
- Hutchinson S, Lee LH, Gaab N, Schlaug G (2003) Cerebellar volumes of musicians. *Cereb Cortex* 13(9):943-9.
- Ickes BR et al. (2000) Long-term environmental enrichment leads to regional increases in neurotrophin levels in rat brain. *Exp Neurol* 164:45–52.
- Ikegaya Y, Aaron G, Cossart R, Aronov D, Lampl I, Ferster D, Yuste R (2004) Synfire chains and cortical songs: temporal modules of cortical activity. *Science* 304:559-564.

Ishida M, Saitoh T, Shimamoto K, Ohfuné Y, Shinozaki H (1993). A novel metabotropic glutamate receptor agonist: marked depression of monosynaptic excitation in the newborn rat isolated spinal cord. *Br J Pharmacol* 109:1169-1177.

Ito M (1984) *The Cerebellum and Neural Control*. Raven Press, New York.

Ito M (2001) Cerebellar long-term depression - characterization, signal transduction and functional roles. *Physiol Rev* 81:1143–1195.

Ito M (2006) Cerebellar circuitry as a neuronal machine. *Progress in Neurobiology* 78 (2006) 272–303

Jarrard LE (1995) What does the hippocampus really do? *Behav Brain Res* 71:1-10.

Jiang CH, Tsien JZ, Schultz PG, Hu Y (2001) The effects of aging on gene expression in the hypothalamus and cortex of mice. *Proc Natl Acad Sci U S A* 98(4):1930-4.

Johnston D, Amaral DG (1998) Hippocampus in „The synaptic organization of the brain“ (ed. Shepherd G.M.) Oxford Univ Press, N.Y.:417-458.

Johnston & Amaral (2004) *Synaptic organization of the brain*, 5<sup>th</sup> edition, Oxford University press.

Kalaska J, Pomeranz B (1979) Chronic paw denervation causes an age-dependent appearance of novel responses from forearm in "paw cortex" of kittens and adult cats. *Neurophysiol* 42(2):618-33.

Kamiya H, Shinozaki H, Yamamoto C (1996) Activation of metabotropic glutamate receptor type 2/3 suppresses transmission at rat hippocampal mossy fibre synapses. *J Physiol* 493:447-455.

Kavalali ET, Klingauf J, Tsien RW (1999) Activity-dependent regulation of synaptic clustering in a hippocampal culture system. *Proc Natl Acad Sci U S A* 96:12893-12900.

Kelahan AM, Doetsch GS (1984) Time-dependent changes in the functional organization of somatosensory cerebral cortex following digit amputation in adult raccoons. *Somatosens Res.* 1984;2(1):49-81.

Kempermann G, Kuhn HG & Gage FH (1997) More hippocampal neurons in adult mice living in an enriched environment. *Nature* 386:493–495.

Kempermann G, Kuhn HG & Gage FH (1998a) Experience-induced neurogenesis in the senescent dentate gyrus. *J Neurosci* 18:3206–3212.

Kempermann G, Brandon EP & Gage FH (1998b) Environmental stimulation of 129/SvJ mice causes increased cell proliferation and neurogenesis in the adult dentate gyrus. *Curr Biol* 8:939–942.

Kempermann G, Gast D & Gage FH (2002) Neuroplasticity in old age: sustained fivefold induction of hippocampal neurogenesis by long-term environmental enrichment. *Ann Neurol* 52:135–143.

Keuroghlian AS, Knudsen EI (2007) Adaptive auditory plasticity in developing and adult animals. *Prog Neurobiol.* (april 2007, Epub ahead of print).

Kirov SA, Harris KM (2000) Dendrites are more spiny on mature hippocampal neurons when synapses are inactivated. *Nat Neurosci* 2(10):878-83.

Kleim JA, Swain RA, Czerlanis CM, Kelly JL, Pipitone MA, Greenough WT (1997) Learning dependent dendritic hypertrophy of cerebellar stellate cells: plasticity of local circuit neurons. *Neurobiol Learn Mem* 67:29–33.

Knierim JJ (2003) Hippocampus and memory. Can we have our place and fear it too? *Neuron.* 2003 Feb 6;37(3):372-4.

Knott GW, Quairiaux C, Genoud C, Welker E (2002) Formation of dendritic spines with GABAergic synapses induced by whisker stimulation in adult mice. *Neuron* 34:265-273.

Knott GW, Holtmaat A, Wilbrecht L, Welker E, Svoboda K (2006) Spine growth precedes synapse formation in the adult neocortex in vivo. *Nat Neurosci* 9(9):1117-24.

Kobayashi K, Poo MM (2004) Spike train timing-dependent associative modification of hippocampal CA3 recurrent synapses by mossy fibers. *Neuron* 41:445-454.

Konur S, Yuste R (2004) Developmental regulation of spine and filopodial motility in primary visual cortex: reduced effects of activity and sensory deprivation. *J Neurobiol* 59(2):236-46.

Korkotian E, Segal M (1999) Release of calcium from stores alters the morphology of dendritic spines in cultured hippocampal neurons. *Proc Natl Acad Sci U S A* 96(21):12068-72.

Kozorovitskiy Y, Gross CG, Kopil C, Battaglia L, McBreen M, Stranahan AM, Gould E (2005) Experience induces structural and biochemical changes in the adult primate brain. *Proc Natl Acad Sci U S A* 102(48):17478-82

Kozorovitskiy Y, Hughes M, Lee K, Gould E (2006) Fatherhood affects dendritic spines and vasopressin V1a receptors in the primate prefrontal cortex. *Nat Neurosci* 9(9):1094-5.

- Krylova O, Herreros J, Cleverley KE, Ehler E, Henriquez JP, Hughes SM, Salinas PC (2002) WNT-3, expressed by motoneurons, regulates terminal arborization of neurotrophin-3-responsive spinal sensory neurons. *Neuron* 35(6):1043-56.
- Kuhl PK (2004) Early language acquisition: cracking the speech code. *Nat Rev Neurosci* 5:831–843.
- Lambert TJ, Fernandez SM & Frick KM (2005) Different types of environmental enrichment have discrepant effects on spatial memory and synaptophysin levels in female mice. *Neurobiol Learn Mem* 83:206–216.
- Lamprecht R, LeDoux J (2004) Structural plasticity and memory. *Nat Rev Neurosci* 5(1):45-54.
- Laurienti PJ, Burdette JH, Maldjian JA, Wallace MT (2006) Enhanced multisensory integration in older adults. *Neurobiol Aging* 27(8):1155-63.
- Lawrence JJ, McBain CJ (2003) Interneuron diversity series: containing the detonation--feedforward inhibition in the CA3 hippocampus. *Trends Neurosci* 26:631-640.
- Lee CK, Weindruch R, Prolla TA (2000) Gene-expression profile of the ageing brain in mice. *Nat Genet* 25(3):294-7.
- Lee DH, Strittmatter SM, Sah DW (2003) Targeting the Nogo receptor to treat central nervous system injuries. *Nat Rev Drug Discov* 2:872–878.
- Lee EH, Hsu WL, Ma YL, Lee PJ & Chao CC (2003) Enrichment enhances the expression of sgk, a glucocorticoid-induced gene, and facilitates spatial learning through glutamate AMPA receptor mediation. *Eur J Neurosci* 18, 2842–2852.
- Lee WC, Huang H, Feng G, Sanes JR, Brown EN, So PT, Nedivi E (2006). Dynamic remodeling of dendritic arbors in GABAergic interneurons of adult visual cortex. *PLoS Biol* 4:e29.
- Lee SM, Tole S, Grove E, McMahon AP (2006) A local Wnt-3a signal is required for development of the mammalian hippocampus. *Development* 127(3):457-67.
- Leggio MG et al. (2005) Environmental enrichment promotes improved spatial abilities and enhanced dendritic growth in the rat. *Behav Brain Res.* 163:78–90.
- Lendvai B, Stern EA, Chen B, Svoboda K (2000). Experience-dependent plasticity of dendritic spines in the developing rat barrel cortex in vivo. *Nature* 404:876-881.
- Levy WB, Steward O (1983) Temporal contiguity requirements for long-term associative potentiation/depression in the hippocampus. *Neuroscience* (4):791-7.

- Li W, Piech V, Gilbert CD (2004) Perceptual learning and top-down influences in primary visual cortex. *Nat Neurosci* 7(6):651-7.
- Li W, Luxenberg E, Parrish T, Gottfried JA (2006) Learning to smell the roses: experience-dependent neural plasticity in human piriform and orbitofrontal cortices. *Neuron* 21;52(6):1097-108.
- Lichtman JW, Colman H (2000). Synapse elimination and indelible memory. *Neuron* 25:269-278.
- Lie DC, Colamarino SA, Song HJ, Desire L, Mira H, Consiglio A, Lein ES, Jessberger S, Lansford H, Dearie AR, Gage FH (2005) Wnt signalling regulates adult hippocampal neurogenesis. *Nature* 437(7063):1370-5.
- Linkenhoker BA, Knudsen EI (2002). Incremental training increases the plasticity of the auditory space map in adult barn owls. *Nature* 419:293-296.
- Linkenhoker BA, von der Ohe CG, Knudsen EI (2005). Anatomical traces of juvenile learning in the auditory system of adult barn owls. *Nat. Neurosci* 8:93-98.
- Logan CY, Nusse R (2004) The Wnt signaling pathway in development and disease. *Annu Rev Cell Dev Biol* 20:781-810.
- Lucas FR, Salinas PC (1997) WNT-7a induces axonal remodeling and increases synapsin I levels in cerebellar neurons. *Dev Biol* 192(1): 31-44.
- Luo ZG, Wang Q, Zhou JZ, Wang J, Luo Z, Liu M, He X, Wynshaw-Boris A, Xiong WC, Lu B, Mei L (2002) Regulation of AChR clustering by Dishevelled interacting with MuSK and PAK1. *Neuron* 35(3):489-505.
- Lyuksytova AI, Lu CC, Milanesio N, King LA, Guo N, Wang Y, Nathans J, Tessier-Lavigne M, Zou Y (2003) Anterior-posterior guidance of commissural axons by Wnt-frizzled signaling. *Science* 302(5652):1984-8.
- Maffei L, Galli-Resta L (1990) Correlation in the discharges of neighboring rat retinal ganglion cells during prenatal life. *Proc Natl Acad Sci U S A* 87(7):2861-4.
- Majdan M, Shatz CJ (2006) Effects of visual experience on activity-dependent gene regulation in cortex. *Nat Neurosci* 9(5):650-9.
- Majewska AK, Newton JR, Sur M (2006) Remodeling of synaptic structure in sensory cortical areas in vivo. *J Neurosci* 26(11):3021-9.
- Malenka RC, Nicoll RA (1999) Long-term potentiation – a decade of progress. *Science* 285(5435):1870-4.

- Malenka RC & Bear MF (2004) LTP and LTD: an embarrassment of riches. *Neuron* 44(1):5-21.
- Markram H, Lubke J, Frotscher M, Sakmann B (1997) Regulation of synaptic efficacy by coincidence of postsynaptic APs and EPSPs. *Science* 275(5297):213-5.
- Markham JA, Juraska JM (2002) Aging and sex influence the anatomy of the rat anterior cingulate cortex. *Neurobiol Aging* 23(4):579-88.
- Mataga N, Nagai N, Hensch TK (2002) Permissive proteolytic activity for visual cortical plasticity. *Proc Natl Acad Sci U S A* 99(11):7717-21.
- Mataga N, Mizuguchi Y, Hensch TK (2004) Experience-dependent pruning of dendritic spines in visual cortex by tissue plasminogen activator. *Neuron* 44(6):1031-41.
- McEwen BS (1999) Stress and hippocampal plasticity. *Annu Rev Neurosci* 22:105-122.
- McGaugh JL (2000) Memory--a century of consolidation. *Science* 287(5451):248-51.
- McGee AW, Yang Y, Fischer QS, Daw NW, Strittmatter SM (2005) Experience-driven plasticity of visual cortex limited by myelin and Nogo receptor. *Science* 309(5744):2222-6.
- McNaughton BL & Morris RG (1987) Hippocampal synaptic enhancement and information. *Trends Neurosci* 10:408-415.
- Merzenich MM, Kaas JH, Wall JT, Sur M, Nelson RJ, Felleman DJ (1983a) Progression of change following median nerve section in the cortical representation of the hand in areas 3b and 1 in adult owl and squirrel monkeys. *Neuroscience* 10(3):639-65.
- Merzenich MM, Kaas JH, Wall J, Nelson RJ, Sur M, Felleman D (1983b) Topographic reorganization of somatosensory cortical areas 3b and 1 in adult monkeys following restricted deafferentation. *Neuroscience* 8(1):33-55.
- Merzenich MM, Nelson RJ, Stryker MP, Cynader MS, Schoppmann A, Zook JM (1984) Somatosensory cortical map changes following digit amputation in adult monkeys. *J Comp Neurol* 224(4):591-605.
- Meshi D, Drew MR, Saxe M, Ansorge MS, David D, Santarelli L, Malapani C, Moore H, Hen R (2006) Hippocampal neurogenesis is not required for behavioral effects of environmental enrichment. *Nature Neurosci* 9:729-731.
- Milner B, Squire LR, Kandel ER (1998) Cognitive neuroscience and the study of memory. *Neuron* 20(3):445-68.

- Moita MA, Rosis S, Zhou Y, LeDoux JE, Blair HT (2003) Hippocampal place cells acquire location-specific responses to the conditioned stimulus during auditory fear conditioning. *Neuron* 37(3):485-97.
- Morando L, Cesa R, Harvey RJ, Strata P (2005) Spontaneous electrical activity and structural plasticity in the mature cerebellar cortex. *Ann N Y Acad Sci* 1048:131-40.
- Mori M, Abegg MH, Gahwiler BH, Gerber U (2004) A frequency-dependent switch from inhibition to excitation in a hippocampal unitary circuit. *Nature* 431:453-456
- Moser MB, Trommald M, Andersen P (1994) An increase in dendritic spine density on hippocampal CA1 pyramidal cells following spatial learning in adult rats suggests the formation of new synapses. *Proc Natl Acad Sci U S A* 91(26):12673-5.
- Moser MB, Trommald M, Egeland T & Andersen P (1997) Spatial training in a complex environment and isolation alter the spine distribution differently in rat CA1 pyramidal cells. *J Comp Neurol* 380:373-381.
- Mower GD (1991) The effect of dark rearing on the time course of the critical period in cat visual cortex. *Brain Res Dev Brain Res* 58(2):151-8.
- Mulkey RM, Malenka RC (1992) Mechanisms underlying induction of homosynaptic long-term depression in area CA1 of the hippocampus. *Neuron* 9(5):967-75.
- Muller D, Toni N, Buchs PA (2000). Spine changes associated with long-term potentiation. *Hippocampus* 10:596-604.
- Nägerl UV, Eberhorn N, Cambridge SB, Bonhoeffer T (2004) Bidirectional activity-dependent morphological plasticity in hippocampal neurons. *Neuron* 44(5):759-67.
- Naka F, Narita N, Okado N & Narita M (2005) Modification of AMPA receptor properties following environmental enrichment. *Brain Dev* 27:275-278.
- Napper RM, Harvey RJ (1988a) Quantitative study of granule and Purkinje cells in the cerebellar cortex of the rat. *J Comp Neurol* 274(2):151-7.
- Napper RM, Harvey RJ (1988b) Quantitative study of the Purkinje cell dendritic spines in the rat cerebellum. *J Comp Neurol* 274(2):158-67.
- Napper RM, Harvey RJ (1988c) Number of parallel fiber synapses on an individual Purkinje cell in the cerebellum of the rat. *J Comp Neurol* 274(2):168-77.
- Napper RM, Harvey RJ (1991) Quantitative studies on the mammalian cerebellum. *Prog Neurobiol* 36(6):437-63.

- Nicoll RA, Malenka RC (1995) Contrasting properties of two forms of long-term potentiation in the hippocampus. *Nature* 377(6545): 115-8
- Nicoll RA & Schmitz D (2005) Synaptic plasticity at hippocampal mossy fiber synapses. *Nat Rev Neurosci* 6:863–876.
- Nithianantharajah J, Levis H & Murphy M (2004) Environmental enrichment results in cortical and subcortical changes in levels of synaptophysin and PSD-95 proteins. *Neurobiol Learn Mem* 81:200–210.
- Nithianantharajah J, Hannan AJ (2006) Enriched environments, experience-dependent plasticity and disorders of the nervous system. *Nat Rev Neurosci* 7(9):697-709.
- Nusse R (2005) Wnt signaling in disease and in development. *Cell Res* 15(1):28-32.
- O'Keefe J, Dostrovsky J (1971) The hippocampus as a spatial map. Preliminary evidence from unit activity in the freely-moving rat. *Brain Res* 34(1):171-5.
- O'Keefe J, Nadel L (1978) *The Hippocampus as a Cognitive Map* (Clarendon, Oxford).
- O'Keefe J & Recce ML (1993) Phase relationship between hippocampal place units and the EEG theta rhythm. *Hippocampus* 3:317–330.
- Oray S, Majewska A, Sur M (2004) Dendritic spine dynamics are regulated by monocular deprivation and extracellular matrix degradation. *Neuron* 44(6):1021-30.
- Oscarsson O (1976) Spatial distribution of climbing and mossy fibre inputs into the cerebellar cortex. In: Creutzfeldt, O. (Ed.), *Afferent and Intrinsic Organization of Laminated Structures in the Brain*. Springer-Verlag, Berlin, pp. 34–42.
- Ossipow V, Pellissier F, Schaad O, Ballivet M (2004) Gene expression analysis of the critical period in the visual cortex. *Mol Cell Neurosci* 27(1):70-83.
- Palkovits M, Magyar P, Szentagothai J (1971) Quantitative histological analysis of the cerebellar cortex in the cat. 3. Structural organization of the molecular layer. *Brain Res* 34(1):1-18.
- Parnavelas JG, Globus A, Kaups P (1973) Continuous illumination from birth affects spine density of neurons in the visual cortex of the rat. *Exp Neurol* 40(3):742-7.
- Penttonen M, Kamondi A, Sik A, Acsady L, Buzsaki G (1997) Feed-forward and feed-back activation of the dentate gyrus in vivo during dentate spikes and sharp wave bursts. *Hippocampus* 7:437-450.

Pham TM et al. (1999) Changes in brain nerve growth factor levels and nerve growth factor receptors in rats exposed to environmental enrichment for one year. *Neuroscience* 94, 279–286.

Pham TA, Graham SJ, Suzuki S, Barco A, Kandel ER, Gordon B, Lickey ME (2004) A semi-persistent adult ocular dominance plasticity in visual cortex is stabilized by activated CREB. *Learn Mem* 11(6):738-47.

Pichitpornchai C, Rawson JA, Rees S (1994) Morphology of parallel fibres in the cerebellar cortex of the rat: an experimental light and electron microscopic study with biocytin. *J Comp Neurol* 342(2):206-20

Pizzorusso T, Medini P, Berardi N, Chierzi S, Fawcett JW, Maffei L (2002) Reactivation of ocular dominance plasticity in the adult visual cortex. *Science* 298(5596):1248-51.

Pizzorusso T, Medini P, Landi S, Baldini S, Berardi N, Maffei L (2006) Structural and functional recovery from early monocular deprivation in adult rats. *Proc Natl Acad Sci USA* 103(22):8517-22.

Pleskacheva MG, Wolfer DP, Kupriyanova IF, Nikolenko DL, Scheffrahn H, Dell'Omo G, Lipp HP (2000). Hippocampal mossy fibers and swimming navigation learning in two vole species occupying different habitats. *Hippocampus* 10:17-30.

Poirazi P, Mel BW (2001). Impact of active dendrites and structural plasticity on the memory capacity of neural tissue. *Neuron* 29:779-796.

Polley DB, Steinberg EE, Merzenich MM (2006) Perceptual learning directs auditory cortical map reorganization through top-down influences. *J Neurosci* 26: 4970–4982.

Polster MR, Nadel L, Schacter DL (1991) Cognitive neuroscience analysis of memory: a historical perspective. *J Cogn Neurosci* 3:95–116.

Putignano E, Lonetti G, Cancedda L, Ratto G, Costa M, Maffei L, Pizzorusso T (2007) Developmental downregulation of histone posttranslational modifications regulates visual cortical plasticity. *Neuron* 53(5):747-59.

Qin L, Marrs GS, McKim R, Dailey ME (2001). Hippocampal mossy fibers induce assembly and clustering of PSD95-containing postsynaptic densities independent of glutamate receptor activation. *J Comp Neurol* 440:284-298.

Ramirez-Amaya V, Balderas I, Sandoval J, Escobar ML, Bermudez-Rattoni F (2001). Spatial long-term memory is related to mossy fiber synaptogenesis. *J Neurosci* 21:7340-7348.

- Rampon C et al. (2000a) Enrichment induces structural changes and recovery from nonspatial memory deficits in CA1 NMDAR1-knockout mice. *Nature Neurosci* 3:238–244.
- Rampon, C. et al. (2000b) Effects of environmental enrichment on gene expression in the brain. *Proc. Natl Acad Sci USA* 97:12880–12884.
- Rassmusson DD (1982) Reorganization of raccoon somatosensory cortex following removal of the fifth digit. *J Comp Neurol* 205(4):313-26.
- Rassmusson DD, Nance DM (1986) Non-overlapping thalamocortical projections for separate forepaw digits before and after cortical reorganization in the raccoon. *Brain Res Bull* 16(3):399-406.
- Rassmusson DD (1988) Projections of digit afferents to the cuneate nucleus in the raccoon before and after partial deafferentation. *J Comp Neurol* 277(4):549-56.
- Recanzone GH, Merzenich MM, Jenkins WM, Grajski KA, Dinse HR (1992) Topographic reorganization of the hand representation in cortical area 3b owl monkeys trained in a frequency-discrimination task. *J Neurophysiol* 67(5):1031-56.
- Recanzone GH, Schreiner CE, Merzenich MM (1993) Plasticity in the frequency representation of primary auditory cortex following discrimination training in adult owl monkeys. *J Neurosci* 13(1):87-103.
- Reid CA, Fabian-Fine R, Fine A (2001) Postsynaptic calcium transients evoked by activation of individual hippocampal mossy fiber synapses. *J Neurosci* 21(7):2206-14.
- Rollenhagen A, Bischof HJ (1994) Spine morphology of neurons in the avian forebrain is affected by rearing conditions. *Behav Neural Biol* 62(2):83-9.
- Ross RS, Eichenbaum H (2006) Dynamics of hippocampal and cortical activation during consolidation of a nonspatial memory. *J Neurosci* 26(18):4852-9.
- Rosso SB, Sussman D, Wynshaw-Boris A, Salinas PC (2005) Wnt signaling through Dishevelled, Rac and JNK regulates dendritic development. *Nat Neurosci* 8(1): 34-42
- Roy V, Belzung C, Delarue C & Chapillon P (2001) Environmental enrichment in BALB/c mice: effects in classical tests of anxiety and exposure to a predatory odor. *Physiol Behav* 74:313–320.
- Sandi C, Davies HA, Cordero MI, Rodriguez JJ, Popov VI, Stewart MG (2003). Rapid reversal of stress induced loss of synapses in CA3 of rat hippocampus following water maze training. *Eur J Neurosci* 17:2447-2456.

- Sawtell NB, Frenkel MY, Philpot BD, Nakazawa K, Tonegawa S, Bear MF (2003) NMDA receptor-dependent ocular dominance plasticity in adult visual cortex. *Neuron* 38(6):977-85.
- Schopke R, Wolfer DP, Lipp HP, Leisinger-Trigona MC (1991) Swimming navigation and structural variations of the infrapyramidal mossy fibers in the hippocampus of the mouse. *Hippocampus* 1:315-328.
- Schoups A, Vogels R, Qian N, Orban G (2001) Practising orientation identification improves orientation coding in V1 neurons. *Nature* 412(6846):549-53.
- Schuett S, Bonhoeffer T, Hubener M (2001) Pairing-induced changes of orientation maps in cat visual cortex. *Neuron* 32(2):325-37.
- Schwegler H, Crusio WE, Lipp HP, Brust I, Mueller GG (1991) Early postnatal hyperthyroidism alters hippocampal circuitry and improves radial-maze learning in adult mice. *J Neurosci* 11:2102-2106.
- Schwegler H, Crusio WE (1995) Correlations between radial-maze learning and structural variations of septum and hippocampus in rodents. *Behav Brain Res* 67(1):29-41.
- Schrijver NC, Bahr NI, Weiss IC & Wurbel H (2002) Dissociable effects of isolation rearing and environmental enrichment on exploration, spatial learning and HPA activity in adult rats. *Pharmacol Biochem Behav* 73:209-224.
- Scoville WB, Milner B (1957) Loss of recent memory after bilateral hippocampal lesions. *J Neurol Neurosurg Psychiat* 20:11-21.
- Segal M (2005) Dendritic spines and long-term plasticity. *Nat Rev Neurosci* 6(4):277-84.
- Shapiro ML, Eichenbaum H (1999) Hippocampus as a memory map: Synaptic plasticity and memory encoding by hippocampal neurons. *Hippocampus* 9:365-384.
- Silva-Gomez AB, Rojas D, Juarez I, Flores G (2003) Decreased dendritic spine density on prefrontal cortical and hippocampal pyramidal neurons in postweaning social isolation rats. *Brain Res* 983(1-2):128-36.
- Sin WC, Haas K, Ruthazer ES, Cline HT (2002) Dendrite growth increased by visual activity requires NMDA receptor and Rho GTPases. *Nature* 419(6906):475-80.
- Skaggs WE, McNaughton BL (1996) Replay of neuronal firing sequences in rat hippocampus during sleep following spatial experience. *Science* 271(5257):1870-3.
- Skeberdis VA, Chevaleyre V, Lau CG, Goldberg JH, Pettit DL, Suadicani SO, Lin Y, Bennett MV, Yuste R, Castillo PE, Zukin RS. (2006) Protein kinase A regulates calcium permeability of NMDA receptors. *Nat Neurosci* 9(4):501-10.

Smith DM, Mizumori SJ (2006) Hippocampal place cells, context, and episodic memory. *Hippocampus*. 2006;16(9):716-29.

Song S, Sjöström PJ, Reigl M, Nelson S, Chklovskii DB (2005) Highly nonrandom features of synaptic connectivity in local cortical circuits. *PLoS Biol* 3:e68.

Squire LR, Alvarez P (1995) Retrograde amnesia and memory consolidation: a neurobiological perspective. *Curr Opin Neurobiol* 5:169–177.

Stettler DD, Yamahachi H, Li W, Denk W, Gilbert CD (2006). Axons and synaptic boutons are highly dynamic in adult visual cortex. *Neuron* 49, 1-11.

Stewart MG, Davies HA, Sandi C, Kraev IV, Rogachevsky VV, Peddie CJ, Rodriguez JJ, Cordero MI, Donohue HS, Gabbott PL, Popov VI (2005) Stress suppresses and learning induces plasticity in CA3 of rat hippocampus: a three-dimensional ultrastructural study of thorny excrescences and their postsynaptic densities. *Neuroscience* 131(1):43-54.

Stickgold R (2005) Sleep-dependent memory consolidation. *Nature* 437(7063):1272-8.

Stoppini L, Buchs PA, Müller D (1991) A simple method for organotypic cultures of nervous tissue. *J Neurosci Methods* 37:173-182.

Sutherland GR, McNaughton B (2000) Memory trace reactivation in hippocampal and neocortical neuronal ensembles. *Curr Opin Neurobiol* 10(2):180-6.

Suzuki S, al-Noori S, Butt SA, Pham TA (2004) Regulation of the CREB signaling cascade in the visual cortex by visual experience and neuronal activity. *J Comp Neurol* 479(1):70-83.

Tailby C, Wright LL, Metha AB, Calford MB (2005) Activity-dependent maintenance and growth of dendrites in adult cortex. *Proc Natl Acad Sci U S A* 102(12):4631-6.

Tan J, Gerrits NM, Nanhoe R, Simpson JI, Voogd J (1995a) Zonal organization of the climbing fiber projection to the flocculus and nodulus of the rabbit: a combined axonal tracing and acetylcholinesterase histochemical study. *J Comp Neurol* 356:23–50.

Tan J, Epema AH, Voogd J (1995b) Zonal organization of the flocculovestibular nucleus projection in the rabbit: a combined axonal tracing and acetylcholinesterase histochemical study. *J Comp Neurol* 356:51–71.

Tang YP, Wang H, Feng R, Kyin M & Tsien JZ (2001) Differential effects of enrichment on learning and memory function in NR2B transgenic mice. *Neuropharmacology* 41, 779–790.

Tashiro A, Dunaevsky A, Blazeski R, Mason CA, Yuste R (2003) Bidirectional regulation of hippocampal mossy fiber filopodial motility by kainate receptors: a two-step model of synaptogenesis. *Neuron* 38(5):773-84.

Teng E, Squire LR (1999) Memory for places learned long ago is intact after hippocampal damage. *Nature* 400(6745):675-7.

tom Dieck S, Sanmarti-Vila L, Langnaese K, Richter K, Kindler S, Soyke A, Wex H, Smalla KH, Kampf U, Franzer JT, Stumm M, Garner CC, Gundelfinger ED (1998) Bassoon, a novel zinc-finger CAG/glutamine-repeat protein selectively localized at the active zone of presynaptic nerve terminals. *J Cell Biol* 142:499-509.

Toni N, Buchs PA, Nikonenko I, Bron CR, Muller D (1999) LTP promotes formation of multiple spine synapses between a single axon terminal and a dendrite. *Nature* 402(6760):421-5.

Torashdotter M, Metsis M, Henriksson BG, Winblad B & Mohammed AH (1998) Environmental enrichment results in higher levels of nerve growth factor mRNA in the rat visual cortex and hippocampus. *Behav Brain Res* 93:83-90.

Trachtenberg, JT, Chen BE, Knott GW, Feng G, Sanes JR, Welker E, Svoboda K (2002) Long-term in vivo imaging of experience-dependent synaptic plasticity in adult cortex. *Nature* 420:788-794.

Turnbull BG, Rasmusson DD (1990) Acute effects of total or partial digit denervation on raccoon somatosensory cortex. *Somatosens Mot Res* 7(4):365-89.

Turnbull BG, Rasmusson DD (1991) Chronic effects of total or partial digit denervation on raccoon somatosensory cortex. *Somatosens Mot Res* 8(3):201-13.

Turner AM & Greenough WT (1985) Differential rearing effects on rat visual cortex synapses. I. Synaptic and neuronal density and synapses per neuron. *Brain Res.* 329:195-203.

Turner DA, Deupree DL (1991) Functional elongation of CA1 hippocampal neurons with aging in Fischer 344 rats. *Neurobiol Aging* 12(3):201-10.

Van Praag H, Kempermann G, Gage FH (2000) Neural consequences of environmental enrichment. *Nat Rev Neurosci.* 1(3):191-8.

von der Ohe CG, Garner CC, Darian-Smith C, Heller HC (2007) Synaptic protein dynamics in hibernation. *J Neurosci* 27(1):84-92.

Voogd J, Glickstein M (1998) The anatomy of the cerebellum. *Trends Neurosci* 21(9):370-5

- Vyas A, Jadhav S, Chattarji S (2006) Prolonged behavioral stress enhances synaptic connectivity in the basolateral amygdala. *Neuroscience* 143(2):387-93.
- Wilson RS, Barnes LL, Krueger KR, Hoganson G, Bienias JL, Bennett DA (2005) Early and late life cognitive activity and cognitive systems in old age. *J Int Neuropsychol Soc* 11(4):400-7.
- Wood ER, Dudchenko PA, Eichenbaum H (1999) *Nature* 397:613–616.
- Xia Z, Storm DR (2005) The role of calmodulin as a signal integrator for synaptic plasticity. *Nat Rev Neurosci* 6(4):267-76.
- Yang Y, Fischer QS, Zhang Y, Baumgartel K, Mansuy IM, Daw NW (2005) Reversible blockade of experience-dependent plasticity by calcineurin in mouse visual cortex. *Nat Neurosci* 8(6):791-6.
- Yoshikawa S, McKinnon RD, Kokel M, Thomas JB (2003) Wnt-mediated axon guidance via the Drosophila Derailed receptor. *Nature* 422(6932):583-8.
- Yoshimura Y, Dantzer JL, Callaway EM (2005) Excitatory cortical neurons form fine-scale functional networks. *Nature* 433:868-873.
- Yu X, Malenka RC (2003) Beta-catenin is critical for dendritic morphogenesis. *Nat Neurosci* 6(11):1169-77.
- Yuste R, Bonhoeffer T (2001) Morphological changes in dendritic spines associated with long-term synaptic plasticity. *Annu Rev Neurosci* 24:1071-89.
- Yuste R, Bonhoeffer T (2004) Genesis of dendritic spines: insights from ultrastructural and imaging studies. *Nat Rev Neurosci* 5(1):24-34.
- Zhou Q, Homma KJ, Poo MM (2004) Shrinkage of dendritic spines associated with long-term depression of hippocampal synapses. *Neuron* 44:749-57.
- Zola-Morgan SM & Squire LR (1990) The primate hippocampal formation: evidence for a time-limited role in memory storage. *Science* 250:288-290.
- Zuo Y, Lin A, Chang P, Gan WB (2005) Development of long-term dendritic spine stability in diverse regions of cerebral cortex. *Neuron* 46:181-189.

# Nadine Gogolla

Born the 17<sup>th</sup> August, 1977  
Place of birth: Hamm, Germany  
Nationality: German

## **Work address**

Friedrich Miescher Institute for Biomedical Research  
86Maulbeerstrasse 66  
4058 Basel  
Switzerland  
tel: +41 616 97 66 99  
fax : +41 61 697 39 76

## **Personal address**

Breisacherstrasse  
4057 Basel  
Switzerland  
tel.: +41 616 83 07 80  
mobile: +41 764 81 35 18  
e-mail: nadine@fmi.ch

## **Research interests**

The brain has a remarkable capacity to adapt in response to experience and changes in its environment. One of the main sites that express adaptation in the central nervous system is the synapse, and synaptic plasticity is the basis for most models of learning and memory. My major research interest lies in the nature of changes that occur in response to experience and age, as well as in the mechanisms that regulate such modifications. I am particularly interested in how learning in the juvenile animal, where plasticity is enhanced, compares to adult learning, and why plasticity is restricted in the adult. Furthermore, I am fascinated by the fact that training can enhance plasticity. Is this enhancement restricted to the trained synapse and/or circuit or does it extend to other synapses or circuits? How can stable memories be formed in an environment of constant change? Can the capacity for plasticity be influenced by past experience? I believe that better understanding of the mechanisms underlying plasticity of the CNS may provide us with new insights into brain function, such as memory or even consciousness.

## **Education and research experience**

- |                        |   |
|------------------------|---|
| <b>11/2002-present</b> | <i>FRIEDRICH MIESCHER INSTITUTE</i> (Basel, Switzerland)<br><b>Graduate studies</b> with <b>Dr. Pico Caroni</b><br><i>Morphological plasticity in the CNS regulated by experience and aging</i>   |
| <b>9/2001-9/2002</b>   | <i>INSERM U546, UNIVERSITY OF PARIS VI</i> (France) and<br><i>UNIVERSITY OF MARBURG</i> (Germany)<br><b>Diploma thesis</b> with <b>Prof. Roland Liblau</b> (Paris) and <b>Prof. Britta Engelhardt</b> (Marburg)<br><i>CNS specific autoimmunity in MOG-HA transgenic mice</i> |
| <b>1/2001-7/2002</b>   | <i>INSERM U546, UNIVERSITY OF PARIS VI</i> (France)<br><b>Project work</b> supervised by <b>Prof. Roland Liblau</b><br><i>Development of a new transgenic mouse model for CNS specific autoimmunity</i>   |
| <b>10/1997-9/2002</b>  | <i>PHILIPPS-UNIVERSITY OF MARBURG</i> (Germany)<br>Studies of Human Biology (Theoretical medicine), Diploma in Human Biology  |
| <b>10/1998-1/2001</b>  | <i>PHILIPPS-UNIVERSITY OF MARBURG</i> (Germany)<br>Studies of Human Medicine (Preclinical part of the studies)  |

## **Publications**

- Galimberti, I.<sup>1</sup> Gogolla, N.<sup>1</sup>, Alberi, S., Santos, A.F., Muller, D., Caroni, P. (2006). Long-term rearrangements of hippocampal mossy fiber terminal connectivity in the adult regulated by experience. *Neuron* 50 (5):749-763  
<sup>1</sup>equal contribution
- Gogolla, N.<sup>1</sup>, Galimberti, I.<sup>1</sup>, De Paola, V., Caroni, P. (2006). Preparation of organotypic hippocampal slice cultures for long-term live imaging. *Nature Protocols* 1: 1165 - 1171  
<sup>1</sup>equal contribution
- Gogolla, N.<sup>1</sup>, Galimberti, I.<sup>1</sup>, De Paola, V., Caroni, P. (2006). Long-term live imaging of neuronal circuits in organotypic slice cultures. *Nature Protocols* 1: 1223 - 1226  
<sup>1</sup>equal contribution
- Gogolla, N.<sup>1</sup>, Galimberti, I.<sup>1</sup>, De Paola, V., Caroni, P. (2006). Staining protocol for organotypic hippocampal slice cultures. *Nature Protocols* 1: 2452 – 2456  
<sup>1</sup>equal contribution

## **Scientific communications**

### ***Abstracts***

- Gogolla, N., Galimberti, I. and Caroni, P. (2005). Topographically selective and experience-dependent expansion of hippocampal mossy fiber outputs in the adult. *Neural circuit meeting, Ascona, Abstract*
- Gogolla, N., Galimberti, I., and Caroni, P. (2006) Life-long rearrangements of hippocampal mossy fiber terminal connectivity in the adult regulated by experience. *FENS Forum, Vienna, Abstract, vol.3, A225.8*
- Gogolla, N., Galimberti, I., and Caroni, P. (2006). Long-term rearrangements of hippocampal mossy fiber terminal connectivity in the adult regulated by experience. *SfN, Atlanta, Abstract*

### ***Poster Presentations***

- Society for Neuroscience meeting (2006), Atlanta, USA
- FENS Forum (2006), Vienna, Austria
- Neuronal Circuit meeting, (2005), Ascona, Switzerland

## **Fellowships and grants**

10/1997-11/2002

**German National Merit foundation** (Studienstiftung des deutschen Volkes) Long-term student fellowship

## **Language skills**

**German** *Native language*

**English, French** *Fluent*

**Spanish, Latin** *Basic knowledge*

## **General interests**

Sports (Triathlon, mountain hiking), drawing, guitar playing

Ich erkläre, dass ich die Dissertation, *Experience-dependent structural rearrangements of synaptic connectivity in the adult central nervous system*, nur mit der darin angegebenen Hilfe verfasst und bei keiner anderen Fakultät eingereicht habe.